DISSSERTATION ZU ERLANGUNG DES DOKTORGRADES

DER FAKULTÄT FÜR CHEMIE UND PHARMAZIE DER

LUDWIG-MAXIMILIANS-UNIVERSITÄT MÜNCHEN

SYNTHESIS AND INVESTIGATION OF NEW PHOSPHORUS-CHALCOGEN CATIONS

Maximilian Josef Poller

aus

München, Deutschland

2019

Erklärung

Diese Dissertation wurde im Sinne von § 7 der Promotionsordnung vom 28. November 2011 von Herrn Prof. Dr. Konstantin Karaghiosoff betreut.

Eidesstattliche Versicherung

Diese Dissertation wurde eigenständig und ohne unerlaubte Hilfe erarbeitet.

München, 11. April 2019

Maximilian J. Poller

Dissertation eingereicht am	21. Februar 2019
1. Gutachter:	Prof. Dr. Konstantin Karaghiosoff
2. Gutachter:	Prof. Dr. Neil Burford
Mündliche Prüfung am	2. April 2019

Acknowledgement

While I was working on this dissertation in Victoria and in Munich, I was supported by many people. In particular I would like to thank…

… Prof. Neil Burford, for welcoming me into his research group, for providing me with a stipend through his research grant, for his mentorship, for his advice in weekly meetings during my time in Victoria, and for the opportunities to present my results at conferences.

… Prof. Konstantin Karaghiosoff, for his mentorship not only in Munich but also in Victoria *via* many skype conversations that often extended late into his evening, for his advice on chemistry and NMR spectroscopy, and for measuring my crystals.

… the members of the Burford research group, Chris Frazee, Hannah Sinclair, Paul Gray, Riccardo Suter, and Saurabh Chitnis, for welcoming me in their midst, for advice, not only on chemistry but also on many other issues, and for great times at the Grad House.

… my research interns, Johanna Frickel and Tanja Huber, for their contributions to the experimental work of this thesis.

… Chris Barr, for training my on the NMR spectrometers and for his extensive advice on NMR spectroscopy.

… Andrew Macdonald, for his help with all kinds of instrument and glove box issues, often on short notice.

… Dr. Brian Patrick, for measuring some of my crystals.

… Chris, Jess, Luna, and Van Anh, for proofreading this dissertation.

… my family, for their constant support throughout all these years.

… my girlfriend Luna, for her patience, for many sleepless nights on skype, and for putting up with a three year long-distance relationship.

To all of them:

Thank you very much.

Table of Contents

Abbreviations

CCDC	Cambridge Crystallographic Data Centre
Cy	cyclohexyl-
DCM	dichloromethane
Dipp	diisopropylphenyl
dmap	N,N-dimethylaminopyridine
EA	elemental analysis
e.g.	*exempli gratia,* Latin “for example”
Et	ethyl-
eqv.	equivalent
et al.	*et alii,* Latin “and others” (and coworkers)
i.e.	*id est*, Latin “that is”
^{i}Pr	isopropyl-
IR	infrared spectroscopy
Me	methyl-
MeCN	acetonitrile
MP or m.p.	melting point
Mes	mesityl-
n.a.	not available/not applicable
NMR	nuclear magnetic resonance (spectroscopy)
n.r.	not resolved
OTf	trifluoromethanesulfonate (triflate)
Ph	phenyl-
R (R’)	organic alkyl- or aryl groups
RT	room temperature
SI	Supporting Information/Supplementary Information
^{t}Bu	tert-butyl-
XRD	(single crystal) x-ray diffraction

Introduction

A Personal Comment on the Importance of Fundamental Research

"We must not forget that when radium was discovered no one knew that it would prove useful in hospitals. The work was one of pure science. And this is a proof that scientific work must not be considered from the point of view of the direct usefulness of it. It must be done for itself, for the beauty of science, and then there is always the chance that a scientific discovery may become like the radium a benefit for humanity."

Marie Curie, Lecture at Vassar College, Poughkeepsie, New York (14 May 1921).[1]

As Marie Curie pointed out in the above statement, scientific progress is often made without a specific goal in mind, but emerges out of the fundamental discoveries a scientist makes in the pursuits driven by his curiosity.

The research of organic chemistry, which started almost 200 years ago with Friedrich Wöhlers synthesis of urea, has since provided us with a wealth of organic compounds and materials. However, Friedrich Wöhlers goal was not the synthesis of urea. In fact, at first he didn't even know he had synthesised it, it is first described as "eine eigenthümliche krystallisirte Materie" – a peculiar crystallised substance[2] and wasn't identified until several years later[3]. His initial interest was the reaction of "cyan" with liquid ammonia and his approach must have been something along the lines of "What will happen if I mix those things?". He did not know or anticipate the wealth of synthetic organic compounds, that were developed in his footsteps and that we use nowadays in our everyday lives. Friedrich Wöhlers discovery, for which he is credited as the father of organic chemistry, was made in the pursuit of his curiosity, in the pursuit of science for itself, for its beauty, as Marie Curie called it.

In the same fashion, the work presented in this thesis is not intended to reveal industrially valuable processes or useful compounds. It is a pursuit of science without any consideration of usefulness, for the beauty of science itself.

Cations based on a Polyphosphorus Framework

Cations based on a phosphorus framework are quite rare. In fact, only one molecular cation consisting purely of phosphorus atoms has been reported so far. It has been synthesised by the group of Ingo Krossing by reacting an excess of white phosphorus (P_4) with $[NO][Al(OR^F)_4]$ (Scheme Intro.1).[4]

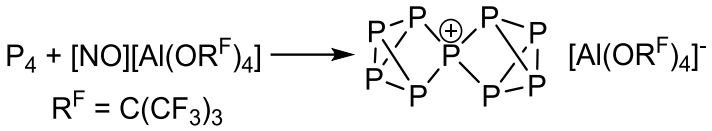

Scheme Intro.1: Molecular Cation consisting only of phosphorus atoms.

The structure of the P_9^+ cation can be described as two P_4 units joined by a phosphonium centre.

Several more cations are known in which the phosphorus framework is joined with other elements. Cations composed of a combination of phosphorus and chalcogen atoms are discussed below. Another group is the combination of phosphorus and halogen atoms, such as the $P_5X_2^+$ (X = Br, I) cations, which can be understood as the formal extension of the P_4 framework by a PX_2^+ fragment (Scheme Intro.2).[5]

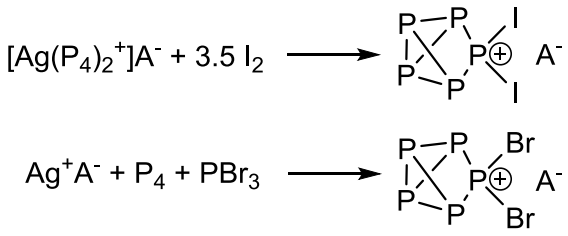

Scheme Intro.2: Synthesis of the $P_5X_2^+$ cations (X = Br, I).

Analogous organo-phosphorus cations ($P_5R_2^+$) have been reported by Jan Weigand *et al.* who also investigated their reaction with chalcogens which are presented in the subchapter below.[6]

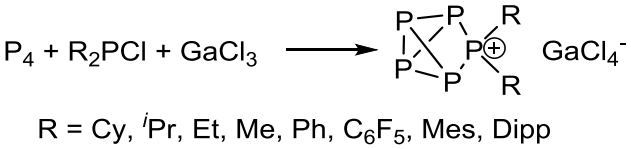

Scheme Intro.3: Organo-phosphorus cation $P_5R_2^+$.

The $P_5R_2^+$ cations are synthesised by inserting an *in-situ* generated R_2P^+ unit into the framework of white phosphorus, P_4 (Scheme Intro.3). Inserting multiple R_2P^+ units into the P_4 tetrahedron results in di- and tri-cations (Scheme Intro.4).[7] The structure of the trication resembles the nortricyclene cage which is also a recurring motif in phosphorus-chalcogen cations.

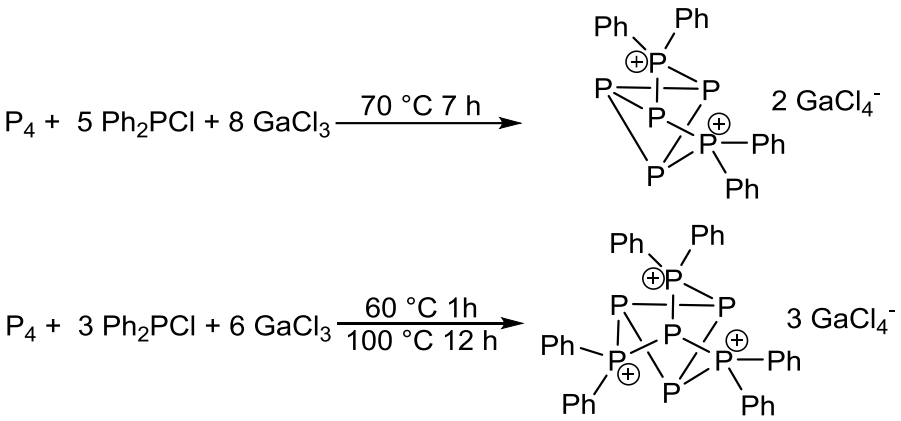

Scheme Intro.4: Organo-phosphorus di- and trications.

Another phosphorus halogen cation is $P_2I_5^+$ which is known as a salt with EI_4^- (E = Al, Ga, In) anions. It can be synthesised from PI_3 and a group 13 metal triiodide (AlI_3, GaI_3, InI_3). (Scheme Intro.5 a)[8]

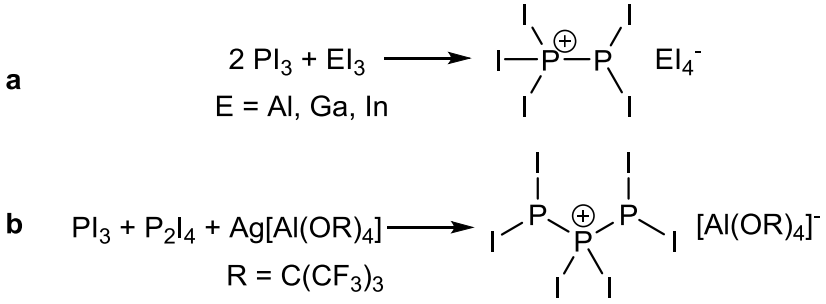

Scheme Intro.5: Synthesis of $P_2I_5^+$ (a) and $P_3I_6^+$ (b) salts.

A similar cation, featuring a chain of three phosphorus atoms can be synthesised by reacting PI_3, P_2I_4 and the halide abstracting agent $Ag[Al(OR)_4]$ (Scheme Intro.5b).[9]

The $P_2I_5^+$ cation is a structural analogue to the phosphinophosphonium cations (Scheme Intro.6a)[10,11] which are introduced in greater detail in the introduction to Chapter 1.

In $P_2I_5^+$, $P_3I_6^+$ and in the phosphinophosphonium cations, multiple phosphorus atoms are catenated, which mimics the behaviour of carbon which is well known for forming catenated chains reaching from alkanes up to polymers. Therefore, this is one reason for calling phosphorus the “carbon copy”.[12] In fact, the tetra-coordinate phosphonium center, which is found in $P_2I_5^+$ and in phosphinophosphonium cations, is isovalent to a neutral carbon atom.

Catenation of two phosphonium centers leads to diphosphonium cations (Scheme Intro.6b) [13], which can be synthesised by oxidising two phosphines (R_3P) with triphenyantimony bistriflate.[14] Longer *catena*-phosphorus cations, containing chains of three (Scheme Intro5b, Intro.6c, and Intro.6d) and of four (Scheme Intro.6e) phosphorus atoms, are also known.[15–17] These cations are typically synthesised by halide abstraction from R_2PCl or $RPCl_2$ in the presence of a phosphine ligand (R_3P).

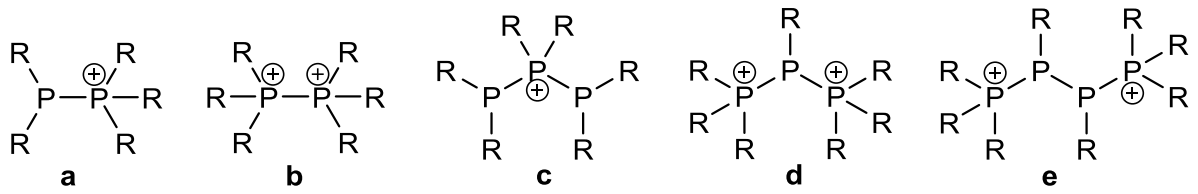

Scheme Intro.6: ***a*** *phosphinophosphonium cation*[10,11]*,* ***b*** *diphosphonium cation*[13]*,* ***c*** *1,3-diphosphino-2-phosphonium cation*[15]*,* ***d*** *2-phosphino-1,3-diphosphonium cation*[16]*,* ***e*** *2,3-diphosphino-1,4-diphosphonium cation*[17]*.*

Aside from these linear *catena*-phosphorus cations, there are also several cyclic derivatives. Surprisingly, three- and four-membered phosphinophosphonium rings are fairly stable. The three- and four-membered phosphinophosphonium rings can be created by oxidative addition of a methyl group to the respective cyclophosphine using methyltriflate (Scheme Intro.7a and Intro.7b).[18]

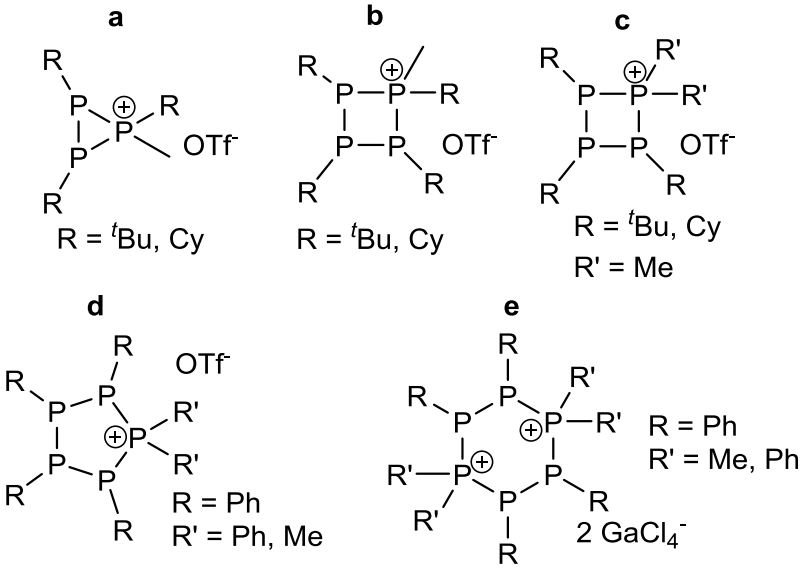

Scheme Intro.7: Cyclic catena-phosphorus cations.

Alternatively, the four-membered cyclo-phosphinophosphonium cations can be synthesised by expanding a cyclo-triphosphine with an *in-situ* generated R_2P^+ unit as described above for the polycyclic phosphorus cations ($P_5R_2^+$ Scheme Intro.3 and $P_6R_4^{2+}$ and $P_7R_6^{3+}$ in Scheme Intro.4). This method results in a different pattern of substituents (Scheme Intro.7c).[18] The same method applied to $(PhP)_5$ surprisingly does not result in a six-membered ring but in a five-membered ring in which one of the original PhP groups has been substituted with an R_2P^+ group (Scheme Intro.7d).[15] Nevertheless, a six-membered tetraphosphino-1,4-diphsophonium ring (SchemeIntro.7e) is accessible by reacting $(PhP)_5$ with R_2PCl and $GaCl_3$ in a melt.[19]

These linear and cyclic *catena*-phosphorus cations give an impression on how far the similarities between carbon and phosphorus can go. However, in carbon chemistry - organic chemistry - the large variety of compounds exists not only due to catenation, it is the

incorporation of non-carbon atoms - heteroatoms - that provides us with a wealth of organic molecules such as: alcohols, thiols, aldehydes, ketones, carboxylic acids, and many more. The question is whether the chemistry of catena phosphorus cations can be enriched in a similar fashion *e.g.* by the introduction of chalcogen atoms.

Cations based on Phosphorus-Chalcogen Frameworks

As with the polyphosphorus cations above, cations based on phosphorus-chalcogen frameworks are quite rare. So far no binary phosphorus-oxygen, phosphorus-sulfur or phosphorus-tellurium cation has been discovered. There is only one binary molecular phosphorus-selenium cation known so far. $P_3Se_4^+$ (Scheme Intro.8) has only been reported recently (in 2015), after being independently discovered by three different research groups who reported it in a joined publication.[20]

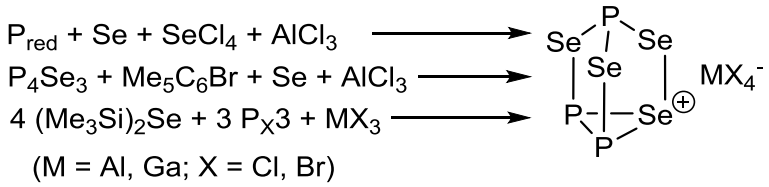

Scheme Intro.8: Synthesis and structure of $P_3Se_4^+$.[20]

The $P_3Se_4^+$ cation can be understood as a structural analogue to the neutral P_4Se_3 with one Se^+ replacing one P atom. The cage-like nortricyclene structure is known for its inherent stability and is a recurring feature for phosphorus-chalcogen cations.

There are more phosphorus-chalcogen based cations that also include other elements, such as halogens. A series of ternary phosphorus-sulfur-halogen cations has been reported by Ingo Krossing *et al.* (Scheme Intro.9). They can be synthesised by reacting P_4S_3 with PX_3 (X = Br, I) and the silver salt of a weakly coordinating anion.[21]

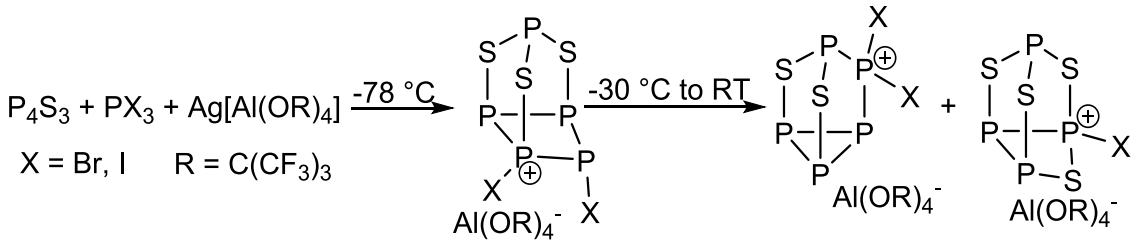

Scheme Intro.9: Synthesis of ternary P-S-X cations (X = Br, I).

Similar to the $P_3Se_4^+$ cation the structures of these P-S-X cations are derivatives of the nortricyclene cage, which is likely to contribute to their stability.

Another cation based on a phosphorus-sulfur-iodine framework, $P_7S_6I_2^+$ (Scheme Intro.10), has been reported shortly after the three shown in Scheme Intro.8, by the same researchers.[22]

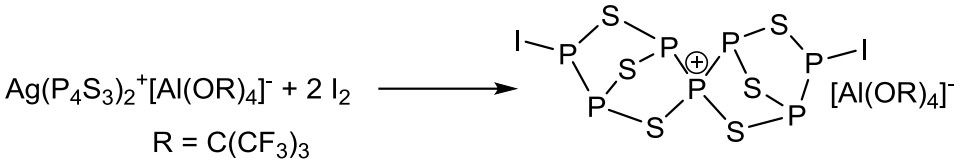

Scheme Intro.10: Synthesis of the spirocyclic $P_7S_6I_2^+$ cation.

The structure of $P_7S_6I_2^+$ deviates more from the nortricyclene structure, but is also polycyclic, similar to two norbornane units sharing one corner atom.

Aside from the ternary P-S-X cations, there are some phosphorus chalcogen cations with organic substituents in lieu of the halogen atoms. One method to achieve such compounds was demonstrated by J. Weigand *et al.* who reacted chalcogens (sulfur and selenium) with the above presented $P_5R_2^+$, $P_6R_4^+$, and $P_7R_6^+$ cations (Scheme Intro.11). This resulted in the insertion of the chalcogen into the cage structure, completing the nortricyclene cage.[6]

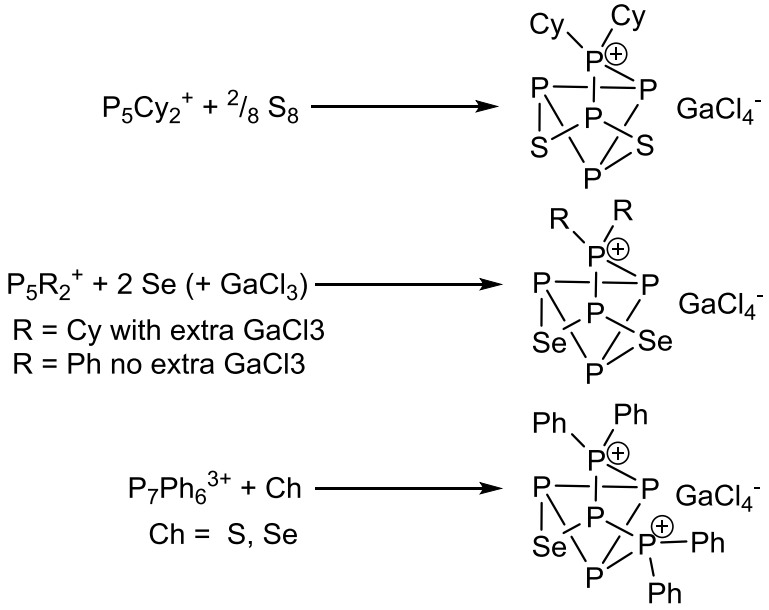

Scheme Intro.11: Synthesis of phosphorus-chalcogen cations.

A different approach has been employed by O. Schön in the Karaghiosoff research group. Starting with neutral P_4S_3 and P_4Se_3, he oxidatively added organic substituents in a reaction analogous to the classical Friedel-Crafts alkylation (Scheme Intro.12).[23]

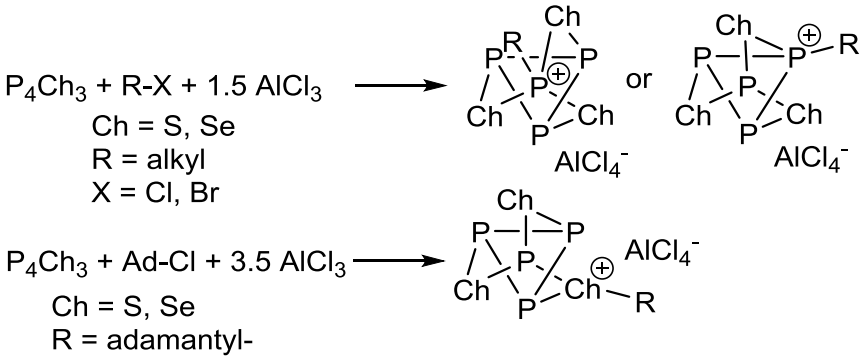

Scheme Intro.12: Friedel-Crafts alkylation of P_4S_3 and P_4Se_3.

By additionally adding sulfur or selenium respectively to the reaction mixture of the Friedel-Crafts alkylation, O. Schön also managed to synthesise cations of the composition $RP_4S_4^+$, $RP_4Se_4^+$ and $RP_4S_5^+$ (Scheme Intro.13).[23]

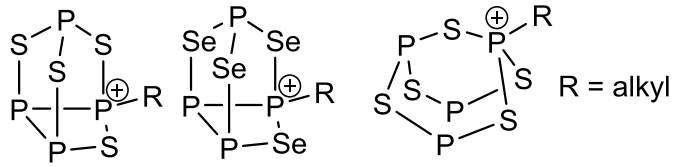

Scheme Intro.13: Phosphorus Chalcogen cations reported by O. Schön.

All of these phosphorus-sulfur and phosphorus-selenium are based on polycyclic cages, mostly structural analogues of nortricyclene, which may contribute to their stability. There are few cations with phosphorus-sulfur or phosphorus-selenium frameworks without these structural features. An example are the four-membered $R_4P_2S_2^{2+}$ and $R_4P_2Se_2^{2+}$ rings discovered by Neil Burford *et al.* (Scheme Intro.14)[24,25] These cations are formed after the halide abstraction from a diamino-chloro-phosphine and a formal dimers of R_2PCh^+ (Ch = S, Se).

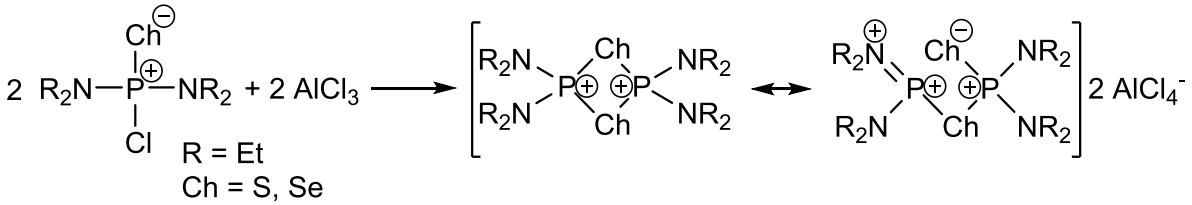

Scheme Intro.14: Synthesis of $(R_2N)_4P_2S_2^{2+}$ and $(R_2N)_4P_2Se_2^{2+}$.

The stability of these cations seems to stem from the electron donating amine substituents rather than from a polycyclic structural motive (Scheme Intro.14). Nevertheless, they are only known to be stable in their dimeric form as four-membered rings, which can be seen as structural analogues to Lawessons Reagent and Woollins Reagent (Scheme Intro.15).

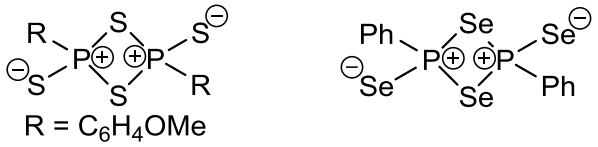

Scheme Intro.15: Lawessons Reagent (left) and Woollins Reagent (right).

There are a few cations which resemble the monomers and rely on donating and bulky substituents or additional ligands for stabilisation. A three-coordinate seleno-phosphonium cation has been reported by A. Schmidpeter *et al*.[26] A similar thiosphosphonium cation has been reported by Neil Burford *et al*. in conjunction with a stabilising ligand.[27] A three-coordinate oxophosphonium cation has been reported recently by F. Dielmann *et al*.[28] These chalcogeno-phosphonium cations are presented in greater detail in the introductions of Chapter 1 and Chapter 3.

This overview shows how limited the range of known phosphorus-chalcogen cations is. Especially considering the range of *catena*-phosphorus cations presented above, as most phosphorus-chalcogen cations rely on polycyclic cage structures rather than open chains or larger monocycles.

Research Objectives

The main objective of this work is the synthesis and investigation of cations based on a phosphorus-sulfur or phosphorus-selenium framework, in order to increase the general knowledge of such molecules. This investigation should diversify phosphorus chemistry by exploring synthetic strategies that can be applied to known phosphorus based cations, thereby finding new structural motifs based on phosphorus in conjunction with sulfur or selenium.

Synthetic strategies for this goal include the oxidation of phosphorus cations with elemental sulfur or selenium as it is known for the synthesis of phosphine sulfides or selenides (Scheme Intro.16).

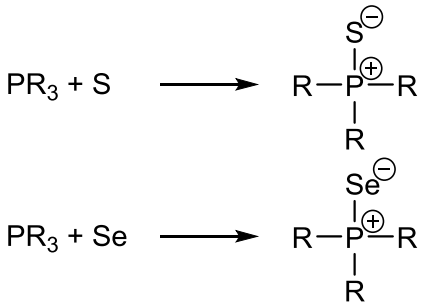

Scheme Intro.16: Oxidation of phosphines to form phosphine sulfides or selenides.

Another strategy will be the abstraction of a halide from a phosphorus-chalcogen compound to create cation, as it has been shown for examples above (*e.g.* Scheme Intro.5 and Scheme Intro.14). Lastly, neutral phosphorus-chalcogen compounds can be oxidised to form diphosphonium diselenides, using an oxidation agent such as Ph_3SbOTf_2 which has previously been used successfully to oxidise phosphines to diphosphonium cations.[14]

Newly formed compounds are mainly identified by ^{31}P NMR spectroscopy in solution. Due to the 100 % natural abundance of the ^{31}P isotope as well as its good NMR sensitivity, ^{31}P NMR spectra provide valuable information about the structure of new compounds. For molecules containing selenium, the ^{77}Se isotope provides an additional NMR observable nucleus. Although only approximately 7.5 % abundant and less NMR sensitive than ^{31}P, the ^{77}Se satellite signals in the ^{31}P NMR spectra provide useful information about connectivity in the molecules.

Additionally, successfully crystallised samples are investigated by x-ray diffraction, providing a complete image of the new compound in solid state and confirming interpretations of NMR spectroscopic results.

The underlying goal of these investigations is the discovery of new compounds and reactions that may serve as a basis for future researchers who are in the pursuit of materials based on phosphorus-sulfur and phosphorus-selenium frameworks.

References

[1] "Wikiquote" can be found under https://en.wikiquote.org/wiki/Marie_Curie, **n.d.**

[2] F. Wöhler, *Ann. der Phys. und Chemie* **1825**, *79*, 177–182.

[3] F. Wöhler, *Ann. der Phys. und Chemie* **1828**, *87*, 253–256.

[4] T. Köchner, T. A. Engesser, H. Scherer, D. a. Plattner, A. Steffani, I. Krossing, *Angew. Chem. Int. Ed.* **2012**, *51*, 6529–6531.

[5] I. Krossing, I. Raabe, *Angew. Chem. Int. Ed.* **2001**, *40*, 4406–4409.

[6] M. H. Holthausen, A. Hepp, J. J. Weigand, *Chem. Eur. J.* **2013**, *19*, 9895–9907.

[7] J. J. Weigand, M. Holthausen, R. Fröhlich, *Angew. Chem. Int. Ed.* **2009**, *48*, 295–298.

[8] C. Aubauer, G. Engelhardt, T. M. Klapötke, A. Schulz, *J. Chem. Soc. Dalt. Trans.* **1999**, *9*, 1729–1734.

[9] I. Krossing, *J. Chem. Soc. Dalt. Trans.* **2002**, 500.

[10] N. Burford, T. S. Cameron, P. J. Ragogna, E. Ocando-Mavarez, M. Gee, R. McDonald, R. E. Wasylishen, *J. Am. Chem. Soc.* **2001**, *123*, 7947–7948.

[11] C. A. Dyker, N. Burford, *Chem. – An Asian J.* **2008**, *3*, 28–36.

[12] K. B. Dillon, F. Mathey, J. F. Nixon, *Phosphorus: The Carbon Copy*, Wiley, **1998**.

[13] J. J. Weigand, S. D. Riegel, N. Burford, A. Decken, *J. Am. Chem. Soc.* **2007**, *129*, 7969–7976.

[14] A. P. M. Robertson, N. Burford, R. McDonald, M. J. Ferguson, *Angew. Chem. Int. Ed.* **2014**, *53*, 3480–3483.

[15] N. Burford, C. A. Dyker, A. Decken, *Angew. Chem. - Int. Ed.* **2005**, *44*, 2364–2367.

[16] P. A. Gray, Y. Y. Carpenter, N. Burford, R. McDonald, *Dalton Trans.* **2016**, *45*, 2124–2129.

[17] Y. Y. Carpenter, C. A. Dyker, N. Burford, M. D. Lumsden, A. Decken, *J. Am. Chem. Soc.* **2008**, *130*, 15732–15741.

[18] C. A. Dyker, N. Burford, G. Menard, M. D. Lumsden, A. Decken, *Inorg. Chem.* **2007**, *46*, 4277–4285.

[19] J. J. Weigand, N. Burford, M. D. Lumsden, A. Decken, *Angew. Chem. Int. Ed.* **2006**, *45*, 6733–6737.

[20] K.-O. Feldmann, T. Wiegand, J. Ren, H. Eckert, J. Breternitz, M. F. Groh, U. Müller, M. Ruck, B. Maryasin, C. Ochsenfeld, et al., *Chem. Eur. J.* **2015**, *21*, 9697–9712.

[21] M. Gonsior, I. Krossing, E. Matern, *Chem. Eur. J.* **2006**, *12*, 1703–1714.

[22] M. Gonsior, I. Krossing, E. Matern, *Chem. Eur. J.* **2006**, *12*, 1986–1996.

[23] O. Schön, Organophosphorchalkogenide Erste Phosphor-Chalkogen-Kationen Neue Heterocyclen Und Selenophosphonate, Ludwig-Maximilians-Universität München, **2007**.

[24] N. Burford, R. E. V. H. Spence, R. D. Rogers, *J. Am. Chem. Soc.* **1989**, *111*, 5006–5008.

[25] N. Burford, R. E. v. H. Spence, R. D. Rogers, *J. Chem. Soc. Dalton Trans.* **1990**, 3611–3619.

[26] A. Schmidpeter, G. Jochem, K. Karaghiosoff, C. Robl, *Angew. Chem. Int. Ed.* **1992**, *31*, 1350–1352.

[27] J. J. Weigand, N. Burford, D. Mahnke, A. Decken, *Inorg. Chem.* **2007**, *46*, 7689–7691.

[28] M. A. Wünsche, T. Witteler, F. Dielmann, *Angew. Chem. Int. Ed.* **2018**, *57*, 7234–7239.

Summary

Diversifying Catena-Phosphorus Cations with Sulfur and Selenium

As mentioned in the introduction, the diversification of *catena*-phosphorus cations with chalcogen atoms was a major goal of this dissertation. In Chapter 1 phosphinophosphonium triflates were allowed to react with elemental sulfur or grey selenium. As a result, several new types of cations based on phosphorus-sulfur and phosphorus-selenium frameworks were discovered and described for the first time (Scheme S.1).

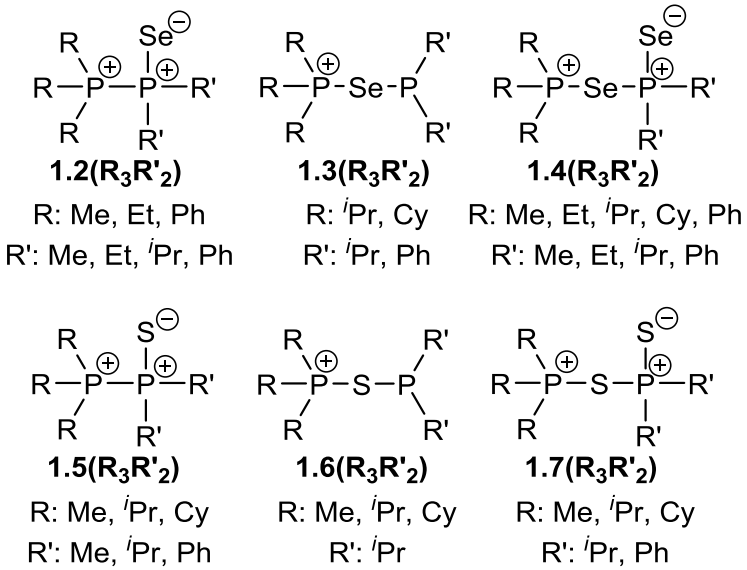

Scheme S.1: Types of phosphorus-sulfur and phosphorus-selenium based cation presented in Chapter 1.

Out of the newly discovered cations, only one derivative of **1.2** was known previously, several new derivatives have been discovered. Cations **1.3**, **1.4**, **1.5**, **1.6** and **1.7** were described for the first time.

The phosphorus selenium based cations were identified by their characteristic signal pattern in the $^{31}P\{^{1}H\}$ NMR spectra of the reaction mixtures. The ^{77}Se satellite signals and P-Se coupling constants (Table S.1) in the $^{31}P\{^{1}H\}$ spectra were instrumental in determining the structures of these new cations.

Table S.1: NMR spectroscopic coupling constants of cations presented in Chapter 1.

	P-P	**R'_2P-$Se_{terminal}$**	**R'_2P-$Se_{bridging}$**	**R_3P-$Se_{bridging}$**
1.2	36 Hz – 126 Hz	759 Hz – 875 Hz	n.a.	n.a.
1.3	22 Hz – 32 Hz	n.a.	115 Hz – 163 Hz	431 Hz – 448 Hz
1.4	11 Hz – 14 Hz	776 Hz – 826 Hz	258 Hz – 305 Hz	400 Hz – 451 Hz
1.5	46 Hz – 160 Hz	n.a.	n.a.	n.a.
1.6	27 Hz – 37 Hz	n.a.	n.a.	n.a.
1.7	11 Hz – 15 Hz	n.a.	n.a.	n.a.

The phosphorus-sulfur based cations were identified based on their P-P coupling constants (Table S.1) which are similar to those of the respective selenium derivatives. Notable is the relatively wide range of the $^{1}J_{PP}$ coupling in cations **1.2** and **1.3** compared to the ranges of other coupling constants, the reason for which is unclear.

In addition to the NMR spectroscopic identification, some compounds were also successfully crystallised and investigated with single crystal x-ray diffraction experiments (Figure S.1).

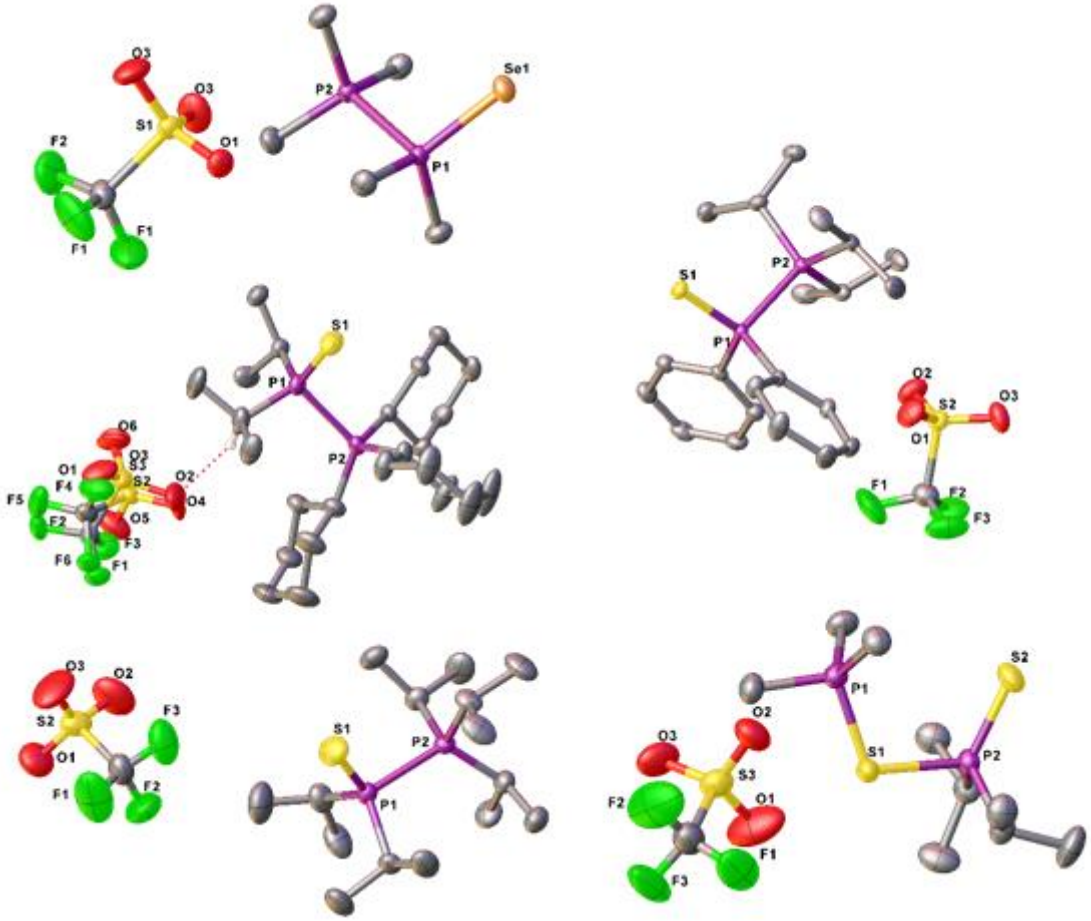

Figure S.1: Solid state structures of newly discovered phosphorus-chalcogen triflates, hydrogen atoms are omitted for clarity, thermal ellipsoids are drawn at 50 % probability level.

The results of these structural investigations confirm the interpretation of the $^{31}P\{^{1}H\}$ NMR spectra. Notable structural features of the investigated compounds are the distorted tetrahedral environment of the phosphorus atoms and the unusually long P-P distances in the investigated derivatives of cations **1.5**.

Aside from the discovery of new phosphorus-sulfur and phosphorus-selenium based cations, these investigations allow us an insight into the reactivity of the phosphinophosphonium cations. Phosphinophosphonium cations with phenyl substituents on the R_3P side do not yield any of the above described products. Although the respective phosphorus-selenium cations have been observed in reaction mixtures, only Ph_3PSe has been isolated along with unidentified byproducts. This leads to the conclusion that the inductive effect of the alkyl

substituents on the R_3P- side of the phosphinophosphonium cations is essential to the stability of the resulting phosphorus-chalcogen cation.

It appears that in the reactions with selenium, the bulkiness of the substituents determines whether the first selenium atom is inserted into the P-P bond (cations **1.3**) or added onto the PR'_2 unit in a terminal position (cations **1.2**). Bulkier substituents, such as isopropyl or cyclohexyl lead to cations **1.3** whereas smaller substituents such as methyl lead to cations **1.2**. The conversion of **1.2** into **1.3** has not been observed.

In contrast, in the reaction with sulfur, both derivatives (**1.5** and **1.6**) have been observed side by side. However, only cations **1.5** were successfully crystallised. The conversion of one into the other has not been directly observed. It is possible, that the better solubility of sulfur in dichloromethane (compared to selenium in dichloromethane) leads to a higher reactivity which is in turn responsible for the more diverse product distributions. In either case, addition of excess of the chalcogen leads mainly to cations **1.4** and **1.7** respectively. The addition of more than two chalcogen atoms, e.g. in the form of a diselenide or disulfide bridge between the two phosphorus atoms has not been observed. With tellurium, the phosphinophosphonium cations show no reaction.

Overall, this project not only contributed to the knowledge of the reactivity of phosphinophosphonium cations, it also established several new kinds of cations based on phosphorus-sulfur and phosphorus-selenium frameworks.

Reversible oxidative coupling of two phosphine selenides

After the successful introduction of sulfur and selenium into phosphinophosphonium cations, the attempted next step was to introduce these elements into diphosphonium cations. However, diphosphonium cations were found to be unreactive towards elemental sulfur and selenium. Therefore, a different approach was applied: instead of oxidising two phosphines with Ph_3SbOTf_2 to form a diphosphonium dication, the phosphines were oxidised to their respective selenide first and were then allowed to react with the antimony compound.

Low temperature $^{31}P\{^1H\}$ NMR spectra of the reaction mixture with triisopropylphosphine selenide showed three distinct signals, which were assigned to the starting material, a phosphine selenide-antimony complex (**2.1**) and a diphosphonium diselenide (**2.2**) respectively (Scheme S.2). The three components are in a dynamic equilibrium that is observed as a single broad peak in the $^{31}P\ \{^1H\}$ NMR spectrum at room temperature. The $^{31}P\{^1H\}$ NMR signals of the methyl derivatives were identified separately at room temperature.

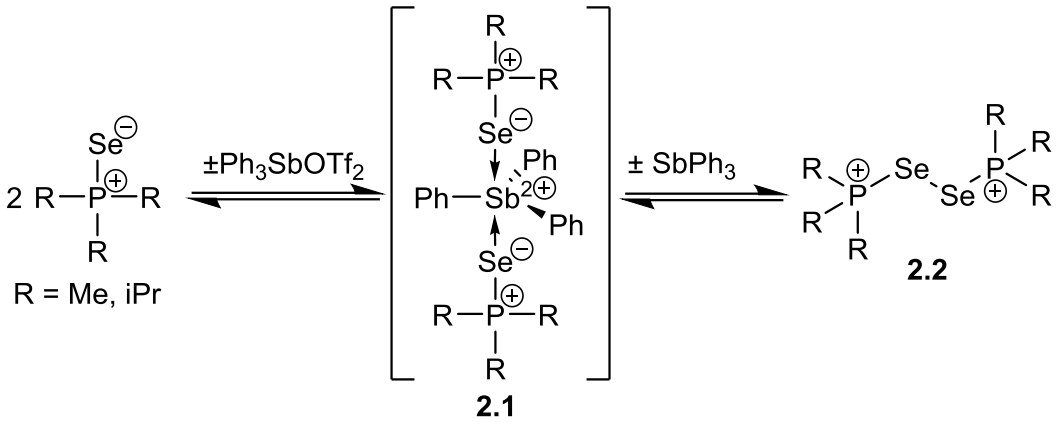

*Scheme S.2: Equilibrium between **2.1** and **2.2** and the starting material (i.e. R_3PSe and Ph_3SbOTf_2).*

In order to prove the reversibility in the dynamic equilibrium, the products of the reaction, **2.2**OTf_2 and Ph_3Sb mixed in solution, resulting in the same equilibrium that was initially observed, thereby proving the reversibility of the oxidative coupling of two phosphine selenides (Scheme S.2).

This kind of reversible oxidative coupling/reductive elimination involving a main group cation has been reported for the first time and is a significant step forward in the research on reactivity of main group cations. Additionally, this reaction presents a new synthetic pathway to cations with a phosphorus-selenium framework. The methyl and isopropyl derivatives of **2.2**OTf_2 are new examples of rare diphosphonium diselenide cations. They were successfully isolated and characterised by NMR spectroscopy and single crystal x-ray diffraction.

New cationic phosphorus-selenium rings

Results of the project presented in Chapter 1 as well as previous investigations by N. Burford *et al.*[1] inspired the research of Chapter 3, in which new phosphorus-selenium based heterocycles are presented.

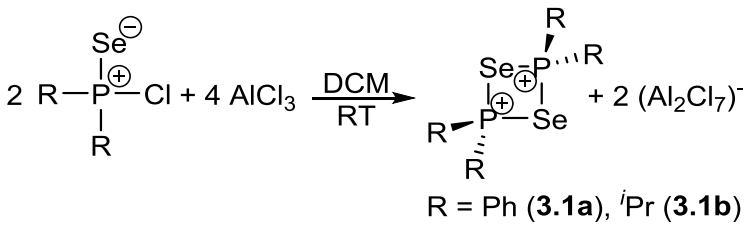

Scheme S.3: Synthesis of new cationic phosphorus-selenium heterocycles.

By reacting chlorodiphenylphosphine selenide and chlorodiisopropylphosphine selenide with aluminum trichloride, two new derivatives of four-membered cationic phosphorus-selenium heterocycles (**3.1a** and **3.1b**) have been discovered (Scheme S.3). Attempts to synthesise the sulfur analogues of cations **3.1** were unsuccessful. The bis-heptachlorodialuminate salts of the new cations (**3.1**) were characterised by NMR spectroscopy and single crystal x-ray diffraction (Figure S.2).

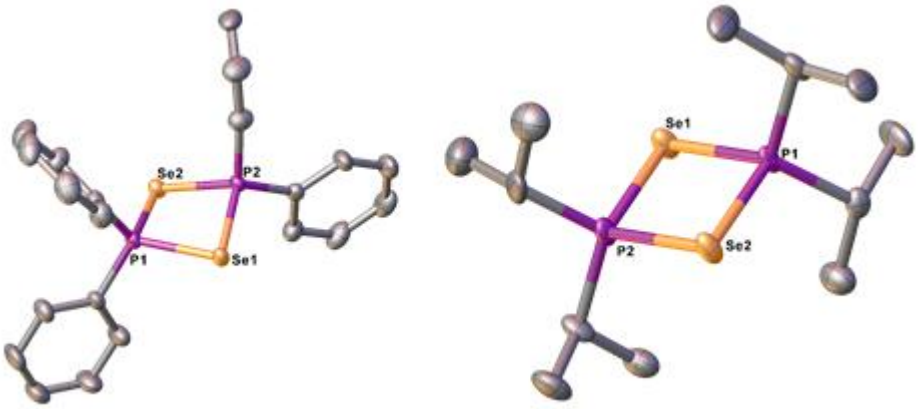

*Figure S.2: Solid state structures of cations **3.1a** (left) and **3.1b** (right), hydrogen atoms and $(Al_2Cl_7)^-$ anions are omitted for clarity, thermal ellipsoids are drawn at 50 % probability level.*

Investigations of the reactivity of these newly discovered cations resulted in the discovery of two five-membered cationic phosphorus-selenium based heterocycles, **3.2** and **3.3**.

Cation **3.2** (Figure S.3) was discovered unexpectedly and has only been identified by single crystal x-ray diffraction. It has been formed by the formal insertion of a $-CH_2-$ group, presumably from the solvent (dichloromethane), into the ring of cation **3.1a**. The contribution of the solvent to its formation emphasises the difficulty of choosing a suitable solvent for such reactive cations.

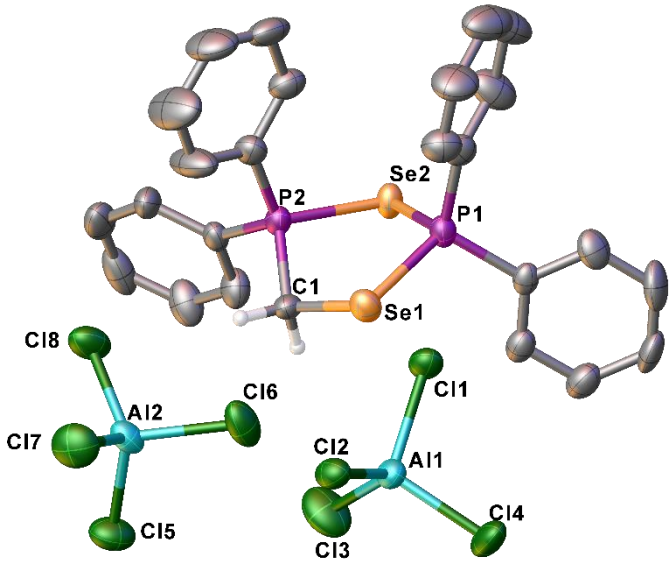

*Figure S.3: Solid state structure of **3.2**$(AlCl_4)_2$, phenyl hydrogen atoms are omitted for clarity, thermal ellipsoids are drawn at 50 % probability level.*

Cation **3.3** was the intended result of the solvent-free reaction of **3.1a**$(Al_2Cl_2)_2$ with elemental selenium. It has been conclusively identified by its $^{31}P\{^1H\}$ and $^{77}Se\{^1H\}$ NMR spectra with the help of a spin system simulation using gNMR. (Figure S.4)[2]

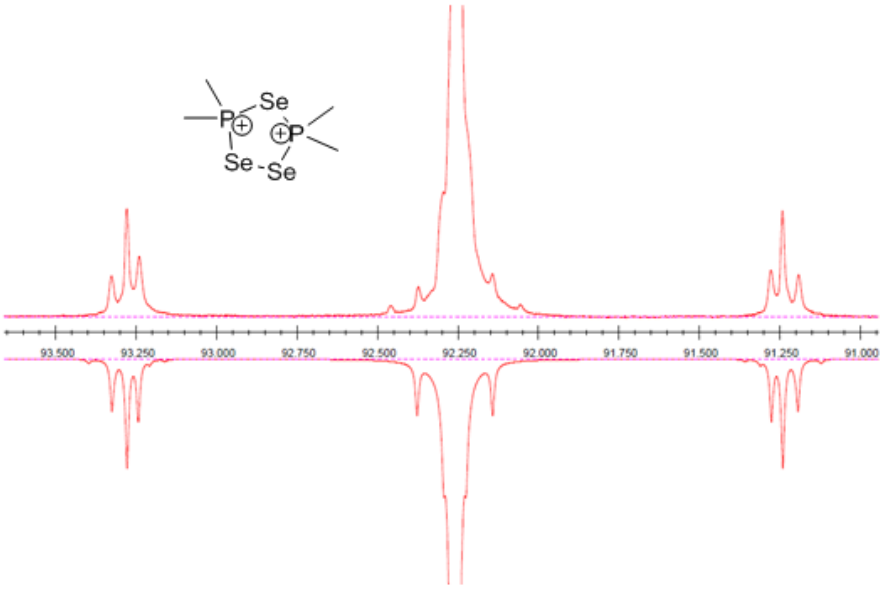

*Figure S.4: Proposed structure and $^{31}P\{^{1}H\}$ NMR spectrum (top experimental, bottom simulated) of cation **3.3**.*

The discovery of these new cationic phosphorus-selenium based heterocycles not only extend our knowledge of such molecules. The synthetic principles of the ring extensions shown in the discoveries of **3.2** and **3.3** also offer a way for the potential diversification of such compounds and may lead to many more new molecules.

Unexpected Compounds

Oftentimes reactions don't go as planned, however sometimes the outcome can still be scientifically valuable. Several of such results are presented in Chapter 4 of this thesis. Compounds **4.1** and **4.2** (Figure S.5) give us potential insights in the decomposition pathways of phosphorus-selenium cations of Chapter 1 (**1.2**, **1.3**, **1.4**).

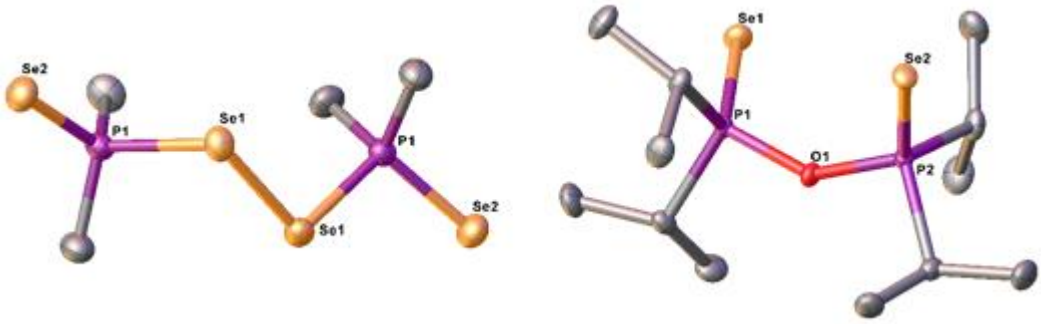

*Figure S.5: Solid state structures of **4.1**(left) and **4.2** (right), hydrogen atoms are omitted for clarity, thermal ellipsoids are drawn at 50 % probability level.*

While compound **4.1** can be explained by the probable instability of its precursor, the formation of **4.2** must have required the contamination with water, in order to introduce the oxygen atom. Therefore, cation **4.2** is testament to the moisture sensitivity of the cations presented in Chapter 1.

Cation **4.3** (Figure S.6) has also been discovered in the investigations of Chapter 1, specifically in the attempt to crystallise **1.4(Ph$_3$Pr$_2$)**OTf from a solution in acetonitrile layered with diethyl ether.

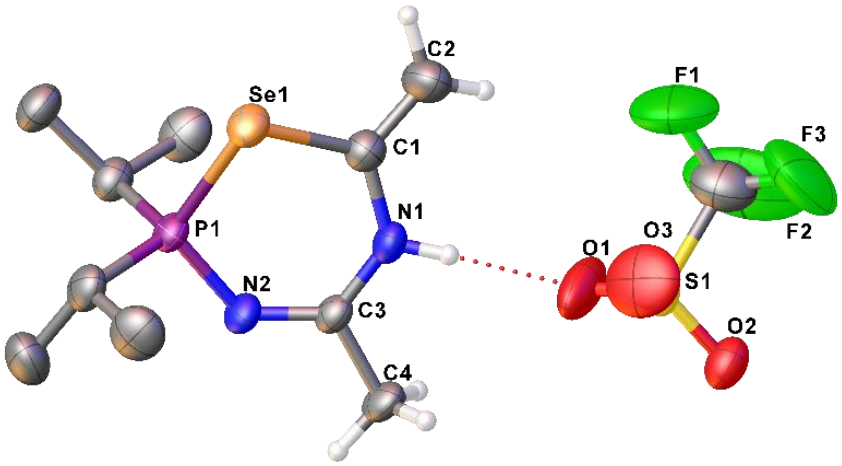

*Figure S.6: Solid state structure of **4.3**OTf, isopropyl hydrogen atoms are omitted for clarity, thermal ellipsoids are drawn at 50 % probability level.*

Cation **4.3** was presumably formed from the dissociation of **1.4(Ph$_3$Pr$_2$)**OTf and subsequent reaction of $^{i}Pr_2PSe^+$ with the solvent (acetonitrile). Its discovery is a valuable result because it provides an insight into the potential reactivity of an R_2PSe^+ cation, which could potentially be generated *in situ* from cations **1.4**.

An attempt to reproduce the formation of **4.3** through a slightly different route unexpectedly yielded compound **4.4**OTf (Figure S.7).

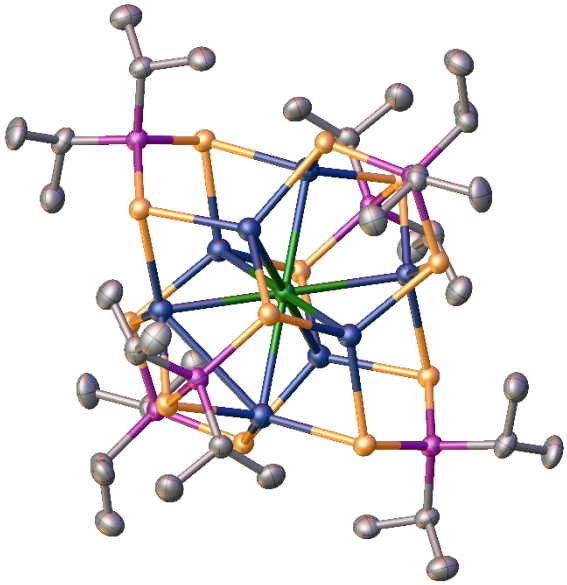

*Figure S.7: Solid state structure of **4.4**OTf, hydrogen atoms and triflate anion are omitted for clarity, thermal ellipsoids are drawn at 50 % probability level.*

4.4 consists of a cubic arrangement of silver cations, held together by a central chloride anion and six phosphorus-selenium based ligands. The formation of the ligand is speculated to be induced by contamination with moisture, which led to the formation of H_2Se and subsequent

formation of the ligand. This kind of self-assembly has only been reported once before for a similar copper based structure.[3] It has been observed for the first time with silver cations.

Lastly, an otherwise unsuccessful project yielded an unexpected interesting result: $[OPS(DMAP)_2]^+OTf^-$ (**4.5**OTf) (Figure S.8).

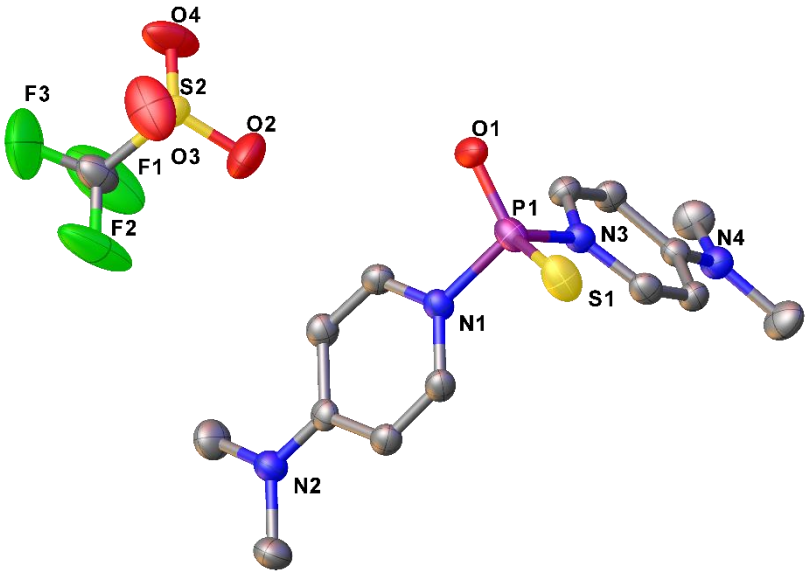

*Figure S.8: Solid state structure of **4.5**OTf, hydrogen atoms are omitted for clarity, thermal ellipsoids are drawn at 50 % probability level.*

4.5 can be seen as an OPS^+ cation, which is stabilised by two 4-dimethylaminopyridine ligands. The OPS^+ can be regarded as a heavy analogue of NO^+. As such it is an interesting small molecule and fills the gap in the row of heavier analogues between NO_2^+ and PS_2^+.[4][5]

Overall, these unexpected results should be taken as starting points for future research on phosphorus-chalcogen compounds.

References

[1] N. Burford, R. E. V. H. Spence, R. D. Rogers, *J. Am. Chem. Soc.* **1989**, *111*, 5006–5008.

[2] P. H. M. Budzelaar, **2006**.

[3] P.-K. Liao, D.-R. Shi, J.-H. Liao, C. W. Liu, A. V. Artem'ev, V. A. Kuimov, N. K. Gusarova, B. A. Trofimov, *Eur. J. Inorg. Chem.* **2012**, *2012*, 4921–4929.

[4] M. Meisel, P. Lönnecke, A.-R. Grimmer, D. Wulff-Molder, *Angew. Chem. Int. Ed.* **1997**, *36*, 1869–1870.

[5] F. D. Henne, F. A. Watt, K. Schwedtmann, F. Hennersdorf, M. Kokoschka, J. J. Weigand, *Chem. Commun.* **2016**, *52*, 2023–2026.

Chapter 1: Reactions of Phosphinophosphonium Cations with S_8 and Se

Abstract

The reactions of phosphinophosphonium triflate salts ($R_3P\text{-}PR'_2OTf$, R = Me, Et, ^{i}Pr, Cy, Ph; R' = Me, Et, ^{i}Pr, Ph) with sulfur and selenium were investigated by $^{31}P\{^1H\}$ NMR spectroscopy. The products of these reactions are new types of phosphorus-sulfur and phosphorus-selenium cations. In reactions with one equivalent of the respective chalcogen, it was found that, depending on the substituents, the chalcogen atom is either incorporated terminally ($R_3P\text{-}P(Ch)R'_2OTf$) or bridging between the two phosphorus atoms ($R_3P\text{-}Ch\text{-}PR'_2OTf$). In reactions with more than one equivalent of sulfur/selenium, the chalocgen atoms were incorporated in both positions ($R_3P\text{-}Ch\text{-}P(Ch)R'_2OTf$). Isolated compounds have additionally been studied by single crystal x-ray diffraction, confirming the interpretation of the $^{31}P\{^1H\}$ NMR spectroscopic data.

Introduction

The pnictogen elements mainly adopt oxidation state III, usually tri-coordinate with a lone pair such as amines or phosphines, or oxidation state V often tetra-coordinate such as the phosphate anion, sometimes penta-coordinate (*e.g.* PF_5). There are also molecules with a tri-coordinated pnictogen (V) center such as the nitrate anion (Scheme 1.1a) and its heavier analogues monomeric trithiometaphosphate (Scheme 1.1b)[1] and monomeric triselenometaphosphate (Scheme 1.1c)[2].

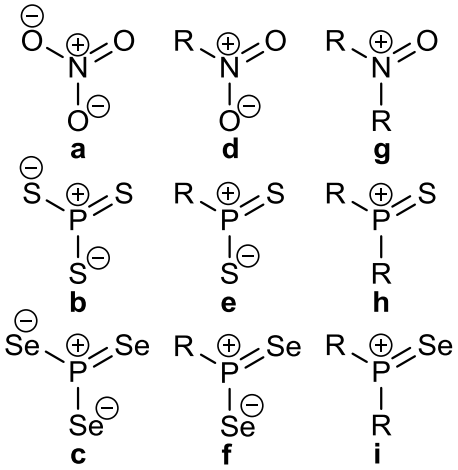

Scheme 1.1: Molecules containing a three coordinated pnictogen(V) atom.

Replacing one of the chalcogen atoms with a neutral substituent such as an alkyl- or aryl-group makes the molecule overall neutral. For the $–NO_2$ moiety, these types of compounds are well known as organic nitrates (Scheme 1.1d) and are easily synthesised with the use of a mixture of nitric acid and sulfuric acid. The heavier homologues of these compounds (Scheme 1.1e[3] and 1.1f[4]) are much rarer and more difficult to synthesise, but have been isolated successfully by M. Yushifuji *et al*.[3,4]

Replacing a second chalcogen atom with a neutral substituent would result in a cationic molecule. There is no record of the respective N-O-cation (Scheme 1.1g). However, rare examples of the P-S (Scheme 1.1h) and P-Se (Scheme 1.1i) derivatives are known to exist and a similar P-O cation has been reported recently.[7] These molecules rely on additional stabilising effects, such as mesomeric delocalisation of the positive charge or electron donation from substituents with lone pairs or additional Lewis basic ligands (Scheme 1.2).[5–7]

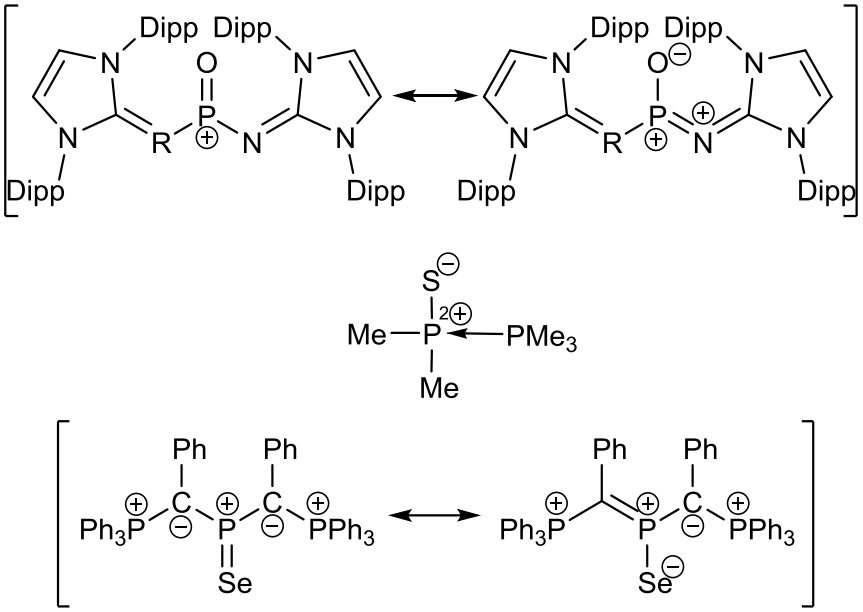

Scheme 1.2: Three coordinate chalcogenophosphonium cations, stabilised by mesomeric effects or electron donation from a ligand.[5–7]

This work shows a systematic way to synthesise such cations, stabilised by a phosphine ligand, by oxidising phosphinophosphonium cations.

Phosphinophosphonium cations ($R_3P\text{-}PR'_2^+$) involving a P-P bond between a tri-coordinate phosphorus center and a tetra-coordinate phosphonium center were first reported from reactions of a trialkyl- or triaryl-phosphine with a halophosphine in the presence of a halide abstracting agent such as $AlCl_3$, $GaCl_3$ or TMSOTf (trimethylsilyltriflate) (Scheme 1.3).[8,9] For the more basic phosphines, the reaction proceeds in the absence of a halide abstractor.[10–13]

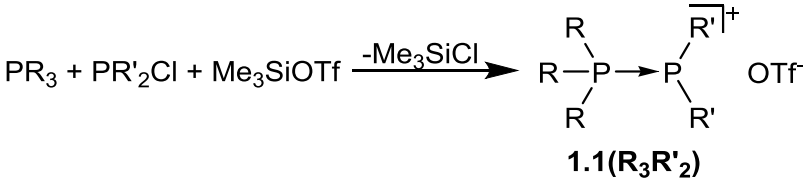

Scheme 1.3: Formation of phosphinophosphonium cations.

Initially, they were only characterised by their $^{31}P\{^1H\}$ NMR spectra, which exhibit a characteristic pattern of two doublets with strong P-P coupling constants of 336-506 Hz[8,9] (see also Chapter 5 – Synthesis of Phosphinophosphonium Cations) with chemical shifts that are at a significantly lower frequency of those expected for phosphonium or phosphenium cations.[8,9] The first single crystal x-ray structure determination of an acyclic phosphinophosphonium cation was published in 2001 and confirmed the previous structure determinations by ^{31}P NMR spectroscopy.[14]

The P-P bond can be described as a coordinate interaction between a phosphine donor and a phosphenium cation acceptor,[15–17] as implicated in many of the reactions of phosphinophosphonium cations.[18] Ligand exchange reactions have enabled the synthesis of

longer *catena*-phosphorus cations[10,19–22] as well as the formation of P-E bonds for a variety of donor element centers (E).[22–25]

This project now examined reactions of phosphinophosphonium cations with elemental sulfur and selenium to discover a variety of new phosphorus-chalcogen cations that expand the previously reported examples of cationic phosphorus-chalcogen compounds. [6,26–28]

Reactions with Selenium

The typical procedure of the investigated reactions involved adding elemental sulfur or elemental (grey) selenium to a solution of the respective phosphinophosphonium triflate (**1.1**) in dry acetonitrile or dry dichloromethane. Dichloromethane turned out to be the more suitable solvent for these reactions, which is probably in part due to the higher solubility of sulfur in dichloromethane compared to acetonitrile. Additionally, the reactions with selenium in dichloromethane lead to a single product more often. In some instances the reactions in acetonitrile were heated to temperatures between 50°C and 70°C. However, this usually led to a larger variety of unidentified by-products in comparison to reactions performed at ambient temperature. Detailed information about the experimental procedures is available in Chapter 5. Reactions of phosphinophosphonium cations with one equivalent of selenium usually resulted in a mixture of products (Scheme 1.4).

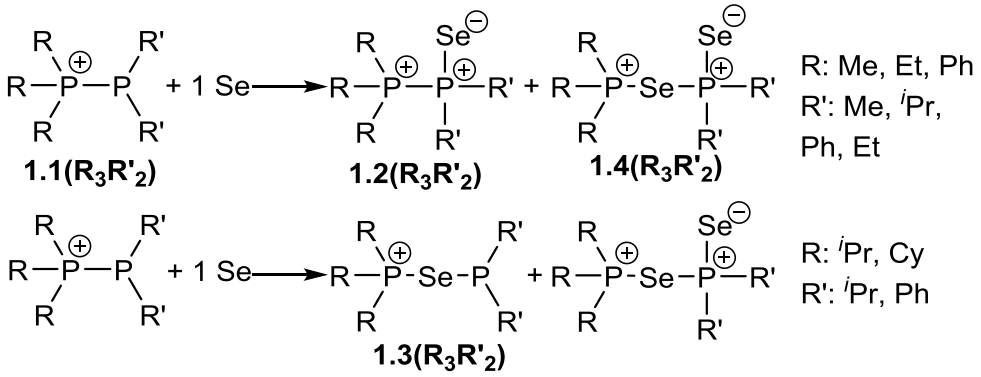

Scheme 1.4: Reactions of phosphinophosphonium cations with one equivalent of selenium.

For phosphinophosphonium cations with sterically less demanding substituents, the reactions yield mostly the expected product with one terminal selenium atom (cations **1.2**). Aside from the main product, some of cation **1.4** was observed which contains one terminal and one bridging selenium atom. Aside from these, some of the starting material (cations **1.1**) remained in the reaction mixture and a small amount of unidentified byproducts occurred. Reactions of

selenium with phosphinophosphonium cations with sterically more demanding substituents (*e.g* ^{i}Pr, Cy) result in the fewest by-products, in some case yielding a single product.

Reactions of phosphinophosphonium cations with two equivalents of selenium yielded cations **1.4** as main products along with phosphine selenides and some unidentified byproducts. Small amounts of cations **1.2** and **1.3** were also observed in the reaction mixtures (Scheme 1.5).

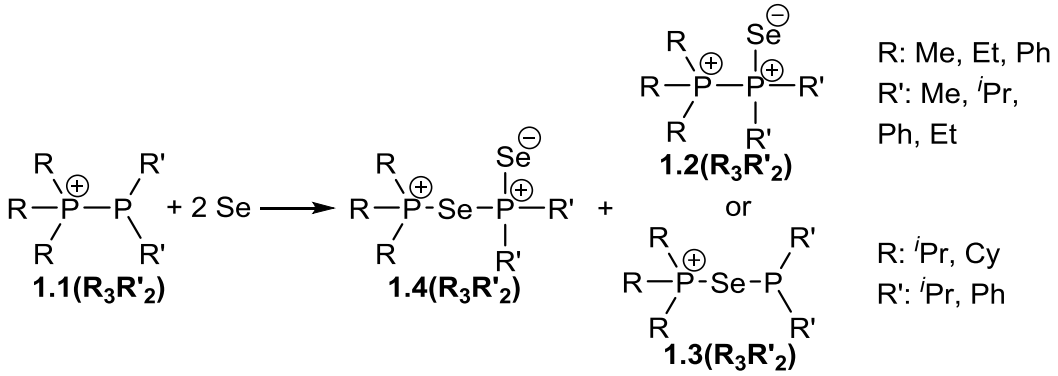

Scheme 1.5: Reactions of phosphinophosphonium cations with two equivalents of selenium.

Reactions of phosphinophosphonium cations with more than two equivalents of selenium resulted in similar outcomes as reactions with two equivalents.

Reaction of **1.1(Ph$_3$R'$_2$)** cations usually yielded triphenylphosphine selenide as the major product. Byproducts of all reactions include the respective hydrophosphonium cations (R_3PH^+) and the respective phosphine selenide (R_3PSe).

Reactions with Sulfur

Compared to the reactions with selenium, the reactions of phosphinophosphonium cations with sulfur are much less selective. Whereas cations **1.2** and **1.3** occur, depending on the R and R' groups, the corresponding sulfur cations **1.5** and **1.6** occur side by side in the same reactions along with the twofold sulfurized cation **1.7** (Scheme 1.6). Depending on the stoichiometry (n = 1), some of the starting material can also be found in the reaction mixture.

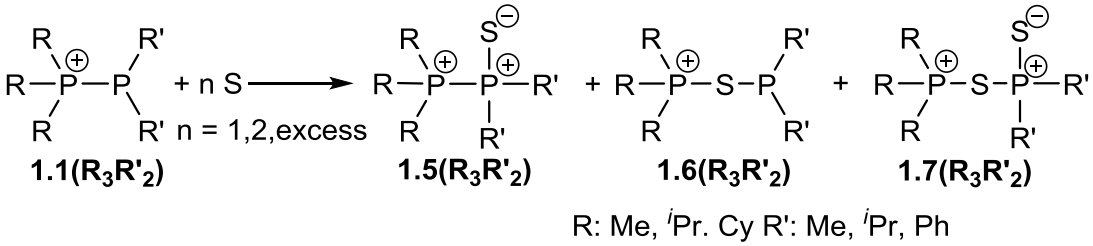

Scheme 1.6: Reactions of phosphino-phosphonium cations with sulfur.

Compound **1.5(Me$_3$Me$_2$)**OTf has been reported previously and was identified by its ^{31}P NMR spectroscopic data.[6] The other cations have been identified by comparison of their P-P coupling constants to the respective selenium analogues.

Interpretation of the $^{31}P\{^{1}H\}$ NMR spectra

The identification of the products is based on $^{31}P\{^{1}H\}$ NMR spectroscopic investigations of the reaction mixtures. The $^{31}P\{^{1}H\}$ NMR spectra of each reaction can be found in Appendix I. The NMR spectroscopic sensitivity of the ^{77}Se isotope is low, therefore, direct observation of ^{77}Se NMR spectra is difficult and requires concentrated samples. Nevertheless, the ^{77}Se isotope provided additional information through the satellite signals in the $^{31}P\{^{1}H\}$ NMR spectra. The characteristic signal patterns of different products were used to identify their specific connectivities. This is exemplified in Figure 1.1, Figure 1.2 and Figure 1.3, which show $^{31}P\{^{1}H\}$ NMR spectra of selected reactions that resulted in mainly one compound.

The $^{31}P\{^{1}H\}$ NMR spectrum for **1.2(Me$_3$^{i}Pr$_2$)**, shown in Figure 1.1, contains a doublet centered at 69.3 ppm with ^{77}Se satellites (doublets at 72.4 ppm and 66.2 ppm, $^{1}J_{PSe}$= 755 Hz, $^{1}J_{PP}$ = 121 Hz) that integrate to 6.6 % of the main signal. The $^{1}J_{PSe}$ coupling is typical for a terminal P-Se "double" bond in phosphine selenides, implicating a $^{i}Pr_2P(Se)^{+}$ fragment so that the reaction can be considered analogous to the oxidation of phosphines by selenium.

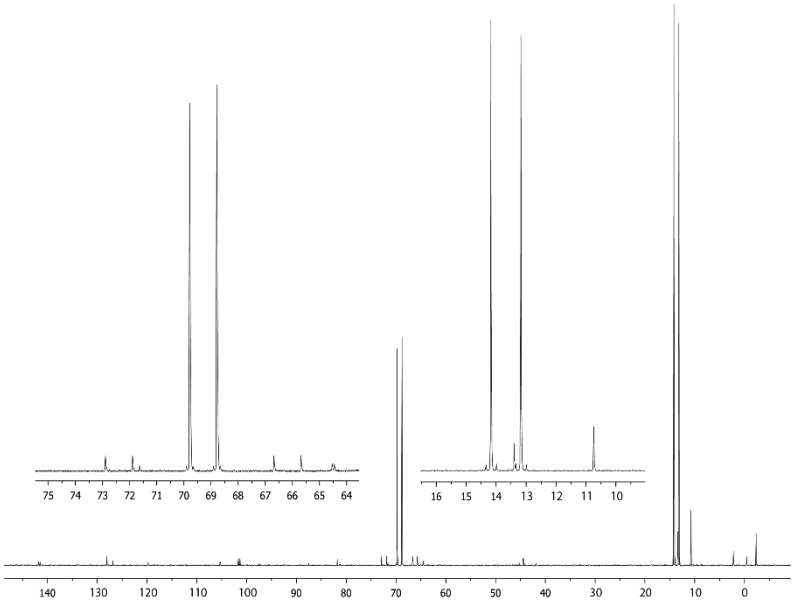

*Figure 1.1: $^{31}P\{1H\}$NMR spectrum for **1.2(Me$_3$^{i}Pr$_2$)**, showing the characteristic pattern for cations **1.2**.*

A second doublet centered at 13.7 ppm ($^{1}J_{PP}$ = 121 Hz) is assigned to a Me_3P- fragment which couples to the aforementioned $^{i}Pr_2P(Se)^{+}$. This second doublet does not have any ^{77}Se satellite signals.

Cations **1.3** exhibits two doublets in the $^{31}P\{^{1}H\}$ NMR spectrum both of which have one set of ^{77}Se satellites. One of the phosphorus-selenium coupling constants is larger than the other. The $^{31}P\{^{1}H\}$ NMR spectrum for **1.3(^{i}Pr$_3$^{i}Pr$_2$)** is shown in Figure 1.2, it has doublets centered at 80.0 ppm and at 72.9 ppm with a P-P coupling constant of 31 Hz. The smaller P-P coupling constant indicates that it is a $^{2}J_{PP}$ coupling instead of the $^{1}J_{PP}$ coupling in cations **1.1** and **1.2**. The doublet centered at 72.9 ppm has a set of ^{77}Se satellite signals with a $^{1}J_{PSe}$ coupling of 446 Hz, whereas the satellite signals of the doublet centered at 80.0 ppm exhibit a $^{1}J_{PSe}$

coupling constant of 165 Hz. This indicates that both phosphorus nuclei couple to one selenium atom, as well as to each other.

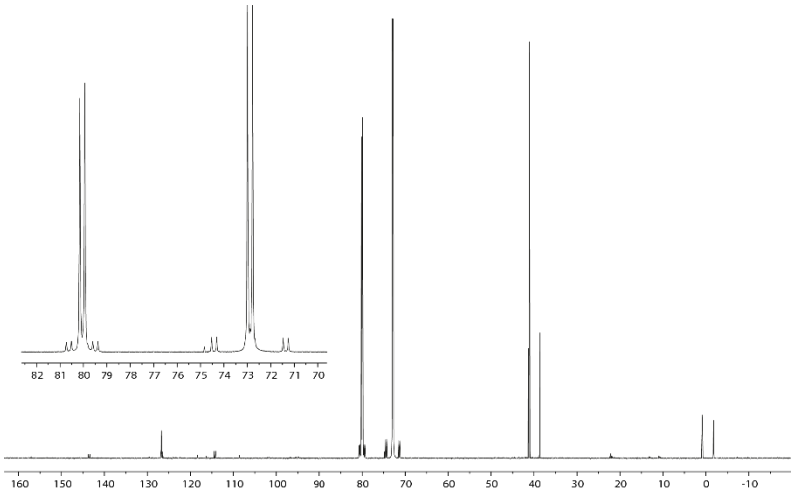

*Figure 1.2: $^{31}P\{^{1}H\}$ NMR spectrum for **1.3($^{i}Pr_3$$^{i}Pr_2$)**, showing the characteristic pattern for cations **1.3**.*

The $^{1}J_{PSe}$ coupling of 446 Hz is smaller than the coupling to a terminal Se atom as in cations **1.2** or as is typical for phosphine selenides. This supports the interpretation of a bridging (two coordinate) Se atom in the fashion of a phosphine selenide coordinating to a phosphenium cation. Similar P-Se coupling constants (478 Hz) have been found for $^{i}Pr_3P$-Se-Se-P$^{i}Pr_3^{2+}$ and for $^{i}Pr_3PSe$ coordinating to Ph_3Sb^{2+}.[29]

The $^{31}P\{^{1}H\}$ NMR spectrum for cations **1.4**, exemplified by the spectrum for **1.4(Cy_3Ph_2)** in Figure 1.3, shows two doublets with a small P-P coupling constant (centered at 75.8 ppm and at 46.2 ppm $^{2}J_{PP}$ = 13 Hz).

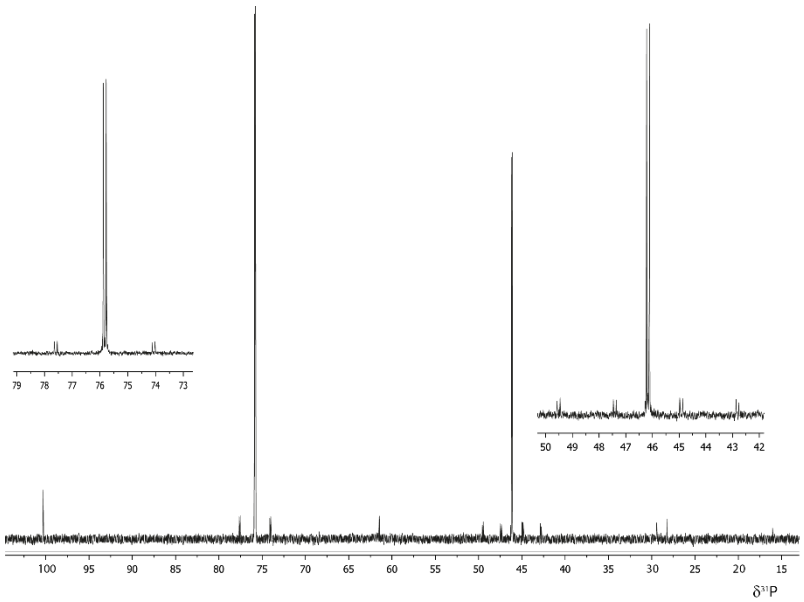

*Figure 1.3: $^{31}P\{^{1}H\}$ NMR spectrum for **1.4(Cy_3Ph_2)**, showing the characteristic pattern for cations **1.4**.*

The doublet centered at 75.8 ppm has only one set of ^{77}Se satellite signals ($^{1}J_{PSe}$ = 428 Hz, the other doublet (46.2 ppm) has two sets of ^{77}Se satellite signals (47.4 ppm d, 44.9 ppm d, $^{2}J_{PP}$ = 13 Hz, $^{1}J_{PSe}$ = 302 Hz; 49.5 ppm d, 42.8 ppm d, $^{2}J_{PP}$ = 13 Hz, $^{1}J_{PSe}$ = 815 Hz), indicating

coupling to two different ^{77}Se nuclei. Since ^{77}Se has a relatively low natural abundance, the visible satellite signals represent the molecules in which only either one of the Se atoms is NMR active. Therefore, they can be interpreted separately as ABX and ABY spin systems instead of one ABXY spin system. The interpretation of the signal pattern is analogous to the interpretation of the ^{31}P{^{1}H} NMR spectra of cations **1.2** and **1.3** above. The ^{31}P{^{1}H} NMR signals of cations **1.4** can be assigned to a structure with one terminal (mono-coordinate) Se atom ($^{1}J_{PSe}$ = 815 Hz) and one bridging (two-coordinate) Se atom ($^{1}J_{PSe}$ = 428 Hz, $^{1}J_{PSe}$ = 302 Hz).

In case of the reactions with sulfur, the products were mainly identified by their P-P coupling constants which were comparable to the respective P-Se cations. This was confirmed by the results of single crystal x-ray diffraction experiments presented below.

NMR spectroscopic data of reactions with selenium

The range of values for the $^{1}J_{PSe}$ coupling constants of the terminal Se atom in cations **1.2** and **1.4** as well as the $^{1}J_{PSe}$ coupling constants of the R_3P- phosphorus to the bridging selenium atom in cations **1.3** and **1.4** are fairly consistent within their ranges. The coupling on the other side of the bridging selenium atom differs between cations **1.3** (155 Hz to 168 Hz) and **1.4** (258 Hz to 305 Hz) which conforms to the different oxidation state of the phosphorus atoms involved.

Table 1.1: Overview of identified phosphinophosphonium selenide cations. (n.a.: not available/ n.r.: not resolved)

	δ [ppm]		**Coupling constants [Hz]**			
	R_3P-	R'_2P-	P-P	$R'_2P(Se)$-	R'_2P-Se-	R_3P-Se-
1.2(Me_3Me_2)	14.7	17.6	68	759	n.a.	n.a.
1.2($Me_3{}^{i}Pr_2$)	12.3	68.0	126	760	n.a.	n.a.
1.2(Me_3Ph_2)	18.9	31.0	62	785	n.a.	n.a.
1.2(Et_3Et_2)	21.4	42.4	117	762	n.a.	n.a.
1.2(Ph_3Ph_2)	60.9	93.8	36	875	n.a.	n.a.
1.3($^{i}Pr_3{}^{i}Pr_2$)	72.8	80.3	31	n.a.	163	448
1.3($^{i}Pr_3Ph_2$)	76.5	28.6	n.r.	n.a.	n.r.	439
1.3($Cy_3{}^{i}Pr_2$)	58.7	77.6	32	n.a.	168	442
1.3(Cy_3Ph_2)	65.3	27.3	22	n.a.	155	431
1.4(Me_3Me_2)	42.9	34.8	13	776	258	400
1.4($Me_3{}^{i}Pr_2$)	43.6	104.5	11	778	272	408
1.4(Et_3Et_2)	71.1	73.7	11	780	268	414
1.4($^{i}Pr_3{}^{i}Pr_2$)	88.9	108.6	13	790	298	444
1.4($^{i}Pr_3Ph_2$)	89.0	44.2	14	813	305	431
1.4($Cy_3{}^{i}Pr_2$)	75.5	106.3	13	787	300	436

1.4(Cy_3Ph_2)	75.1	44.7	13	814	304	427
1.4(Ph_3Ph_2)	35.9	51.8	10	826	282	451

Table 1.1 provides an overview over all newly discovered phosphinophosphonium selenide cations from the reactions of phosphinophosphonium cations with selenium. The spectra are displayed in Appendix I.

Of particular interest is the trend in the P-P coupling constants, which can be extrapolated to the sulfur containing analogues. It is notable that the P-P coupling in compounds **1.2** varies significantly with different R groups, whereas the P-P coupling in cations **1.3** and **1.4** are consistent throughout the various substituents. The $^2J_{PP}$ coupling in compounds **1.3** is not always resolved indicating that the coordination of the R_3PSe fragment to the R'_2P^+ fragment is weak and competes with the triflate anion. In order to test this hypothesis, cation **1.3(^{i}Pr_3Ph_2)** was prepared by reacting ^{i}Pr_3PSe, Ph_2PCl and two equivalents of $AlCl_3$ to yield **1.3(^{i}Pr_3Ph_2)(Al_2Cl_7)**. While the $^{31}P\{^1H\}$ NMR spectrum of the triflate salt did not show the P-P coupling or the Ph_2P-Se coupling, both were clearly resolved in the spectrum of the $(Al_2Cl_7)^-$ salt ($^2J_{PP}$ = 29 Hz, $^1J_{PSe}$ = 162 Hz, 438 Hz) with matching chemical shifts (75.6 ppm, 30.2 ppm). In the case of **1.3(Cy_3Ph_2)**, the P-P coupling as well as the P-Se coupling of the Ph_2P^+-Se-fragment could be resolved at low temperature.

NMR spectroscopic data of reactions with sulfur

Products of the reactions of phosphinophosphonium cations with sulfur do not have the benefit of satellite signals in the $^{31}P\{^1H\}$ NMR spectra. They were therefore identified based on their P-P coupling constants in comparison to the respective selenium compounds. The identified products are shown in Table 1.2, the spectra can be found in Appendix I.

Table 1.2: Identified products from reactions of phosphinophosphonium cations with sulfur.

	δ [ppm]		**P-P coupling constants [Hz]**
1.5(Me_3Me_2)	38.2	16.4	46
1.5($Me_3^{i}Pr_2$)	75.0	14.5	106
1.5(^{i}$Pr_3^{i}Pr_2$)	86.0	38.4	152
1.5(^{i}Pr_3Ph_2)	39.8	33.5	102
1.5($Cy_3^{i}Pr_2$)	84.9	26.5	160
1.5(Cy_3Ph_2)	43.1	24.14	103
1.6($Me_3^{i}Pr_2$)	135.5	98.9	37
1.6(^{i}$Pr_3^{i}Pr_2$)	77.2	67.7	27
1.6($Cy_3^{i}Pr_2$)	66.8	63.0	29
1.7($Me_3^{i}Pr_2$)	115.5	56.3	11

1.7(Me_3Ph_2)	66.2	56.7	11
1.7($^iPr_3{}^iPr_2$)	119.7	89.5	15
1.7($^iPr_3Ph_2$)	88.1	66.8	15
1.7($Cy_3{}^iPr_2$)	118.4	76.1	15
1.7(Cy_3Ph_2)	75.6	66.9	15

This interpretation has then been confirmed by the solid state structures that were determined by single crystal x-ray diffraction.

Structural investigations of new cations by single crystal x-ray diffraction

In order to obtain crystalline samples of the products, the reaction mixtures were layered with diethylether or hexanes and stored at -35 °C. Successfully crystallised compounds were then structurally characterised using single crystal x-ray diffraction.

Compound **1.2(Me_3Me_2)**OTf crystallises in the space group Pnma, cation and anion are well separated and show no interaction in the solid state.

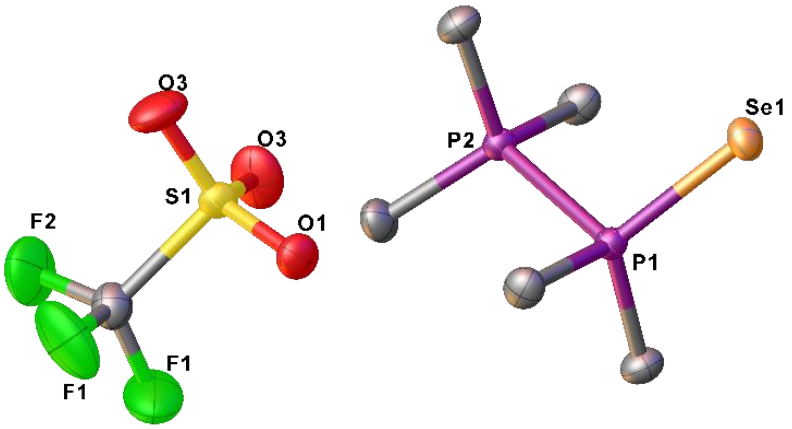

*Figure 1.4: Solid state structure of **1.2(Me_3Me_2)**OTf, hydrogen atoms are omitted for clarity, thermal ellipsoids are drawn at 50 % probability level, CCDC 1813379.*

The cation (Figure 1.4) has the expected staggered conformation with a P-P bond length that is longer than the P-P bond in **1.1(Me_3Me_2)**OTf[13] or the P-P bond of tetramethyl-diphosphine-monoselenide[28], and similar to the P-P bonds of the hexamethly-diphosphonium cation[11] and tetramethyl-diphosphine disulfide[30], both of which contain two phosphorus atoms with fourfold coordination. (Table 1.3)

*Table 1.3: Selected structural parameters for the cation **1.2(Me_3Me_2)** in comparison to those in similar compounds.*

Distances		
1.2(Me_3Me_2)	P1-P2	2.203(1) Å
1.1(Me_3Me_2)[13]	P-P	2.177(1) Å
Me_2P(Se)-PMe_2[28]	P-P	2.191(1) Å

Me_3P-PMe_3^{2+}[11]	P-P	2.198(2) Å
$Me_2P(S)$-$P(S)Me_2$[30]	P-P	2.211(1) Å
1.2(Me_3Me_2)	Se1-P1	2.095(1) Å
$Me_2P(Se)$-PMe_2[28]	Se-P	2.119(1) Å
Me_3PSe	Se-P	2.113(1) Å

The P-Se distance in **1.2(Me_3Me_2)** is slightly shorter than the P-Se distances reported for trimethylphosphine-selenide (structural data is provided in supporting information) and tetramethyl-diphosphine-monoselenide[31].

Some of the attempts to crystallise cations **1.2**, **1.3** or **1.4** yielded unexpected compounds (Scheme 1.7), which are presumed to be decomposition products.

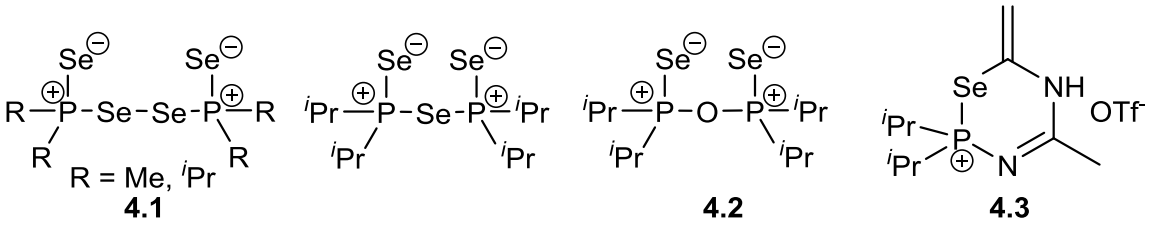

Scheme 1.7: Other compounds isolated from crystallisation attempts.

They are either byproducts of the initial reactions or decomposition products formed in the crystallisation experiments by reactions with the solvent or contamination with water or oxygen. Some of them (^{i}Pr $_2$P(Se)-Se-Se-P(Se)^{i}Pr$_2$ and ^{i}Pr$_2$P(Se)-Se-P(Se)^{i}Pr$_2$) have been reported previously.[32] The structures of the new compounds (**4.1(Me)**, **4.2** and **4.3**) are discussed in detail in Chapter 4.

Attempts to crystallise the sulfur derivatives were more successful, yielding structural data on several derivatives of cations **1.5** and **1.7**.

From reactions with sulfur, compounds **1.5(^{i}Pr$_3$^{i}Pr$_2$)**OTf (Figure 1.5), **1.5(^{i}Pr$_3$Ph$_2$)**OTf (Figure 1.6), **1.5(Cy$_3$^{i}Pr$_2$)**OTf (Figure 1.7) and **1.7(Me_3^{i}Pr$_2$)**OTf (Figure 1.8) have been successfully crystallised. The structures confirm the interpretation of the $^{31}P\{^1H\}$ NMR spectroscopic data which identified the compounds mainly on their P-P coupling constants.

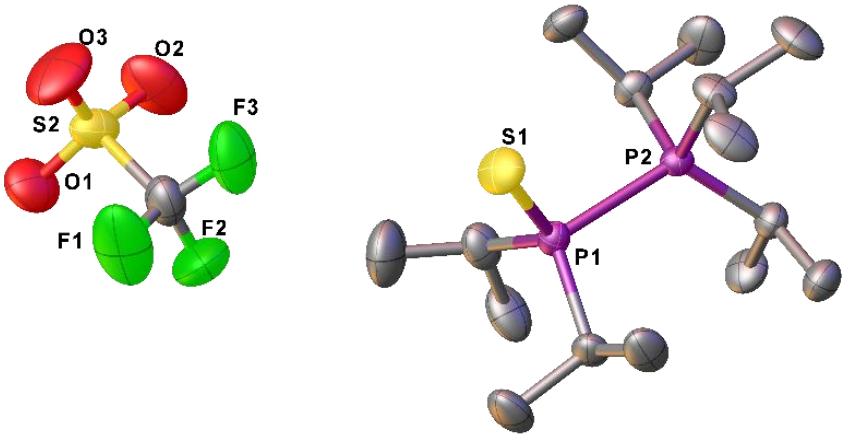

Figure 1.5: Solid state structure of ***1.5(^{i}Pr$_3$^{i}Pr$_2$)****OTf, hydrogen atoms are omitted for clarity, thermal ellipsoids are drawn at 50 % probability level, CCDC 1813380.*

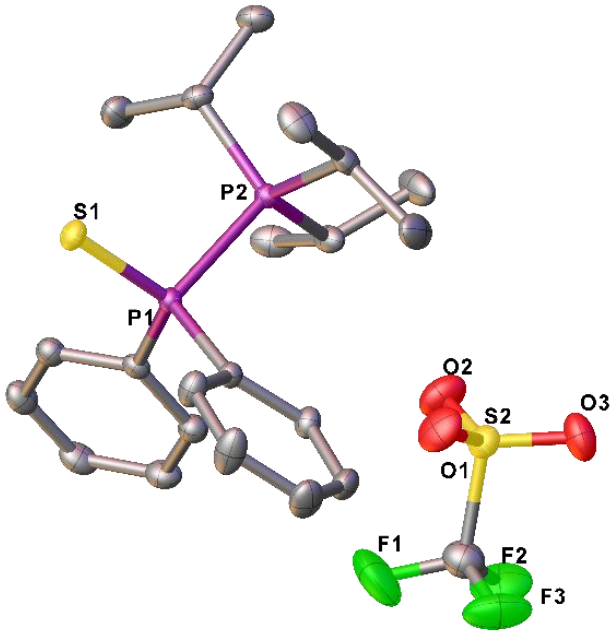

Figure 1.6: Solid state structure of ***1.5(^{i}Pr$_3$Ph$_2$)****OTf, hydrogen atoms are omitted for clarity, thermal ellipsoids are drawn at 50 % probability level, CCDC 1813381.*

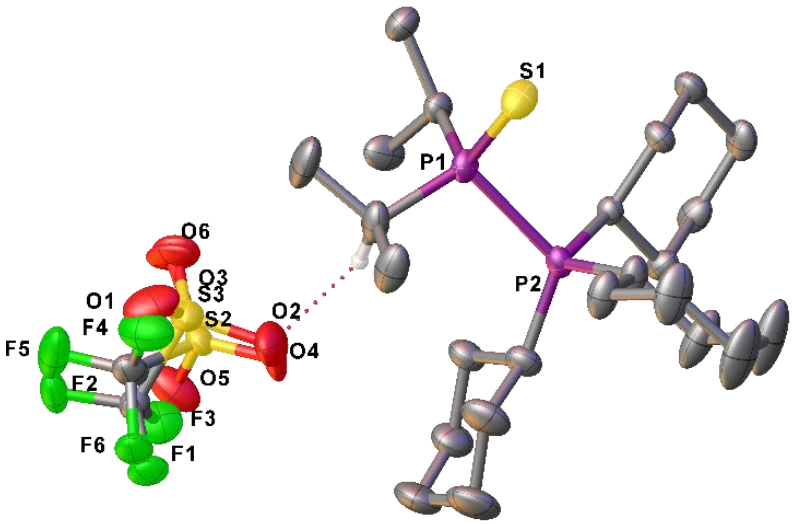

*Figure 1.7: Solid state structure of **1.5(Cy$_3$^{i}Pr$_2$)**OTf, hydrogen atoms are omitted for clarity, thermal ellipsoids are drawn at 50 % probability level.*

Compound **1.5(^{i}Pr$_3$^{i}Pr$_2$)**OTf crystallised in the space group $P2_12_12_1$, compound **1.5(^{i}Pr$_3$Ph$_2$)**OTf and compound **1.5(Cy$_3$^{i}Pr$_2$)**OTf crystallised in space group $P2_1/c$. In the cases of **1.5(^{i}Pr$_3$^{i}Pr$_2$)**OTf and **1.5(^{i}Pr$_3$Ph$_2$)**OTf, cation and anion are well separated and show no interaction. In **1.5(Cy$_3$^{i}Pr$_2$)**OTf there is a short contact between the triflate anion and one of the isopropyl hydrogen atoms with a H-O distance of 2.18(1) Å (Figure 1.7). However, the triflate anion is disordered, therefore this distance is quite inaccurate.

A notable feature of the structures of cations **1.5** is the unusually long P-P bond, which is longer than the P-P bond observed in **1.1(Me$_3$Me$_2$), 1.2(Me$_3$Me$_2$) and Me$_2$P(S)-P(S)Me$_2$**.This might be caused by the larger steric demand of the substituents in the crystallised examples. In contrast, the P-S bonds of cations **1.5** are slightly shorter than the P-S bonds of phosphine sulfides, but similar between derivatives of cations **1.5**.[30,33–35] The structural data of the new phosphorus-sulfur cations is summarized in Table 1.2.

Table 1.2: Selected structural parameters of new phosphorus-sulfur cations in comparison to structurally similar neutral compounds.

Distances		
1.5(^{i}Pr$_3$^{i}Pr$_2$)	P-P	2.310(2) Å
1.5(^{i}Pr$_3$Ph$_2$)	P-P	2.265(1) Å
1.5(Cy$_3$^{i}Pr$_2$)	P-P	2.3284(8) Å
Me$_2$P(S)-PMe$_2$[33]	P-P	2.202(1) Å
Me$_2$P(S)-P(S)Me$_2$[30]	P-P	2.211(1) Å
1.5(^{i}Pr$_3$^{i}Pr$_2$)	P-S	1.951(2) Å
1.5(^{i}Pr$_3$Ph$_2$)	P-S	1.944(1) Å
1.5(Cy$_3$^{i}Pr$_2$)	P-S	1.9526(9) Å
Me$_2$P(S)-PMe$_2$[33]	P-S	1.970(1) Å
Me$_2$P(S)-P(S)Me$_2$[30]	P-S	1.958(1) Å 1.959(1) Å
^{i}Pr$_3$PS[34]	P-S	1.962(2) Å
Ph$_3$PS[35]	P-S	1.9571(5) Å 1.9586(5) Å
1.7(Me$_3$^{i}Pr$_2$)	P1-S1	2.065(1) Å
1.7(Me$_3$^{i}Pr$_2$)	S1-P2	2.158(1) Å
^{t}Bu$_2$P-S-P^{t}Bu$_2$[28]	P-S	2.131(2) Å 2.135(2) Å
1.7(Me$_3$^{i}Pr$_2$)	P2-S2	1.937(1) Å
Angles		
1.7(Me$_3$^{i}Pr$_2$)	P1-S1-P2	106.33(4)°
^{t}Bu$_2$P-S-P^{t}Bu$_2$[28]	P-S-P	103.28(8)°

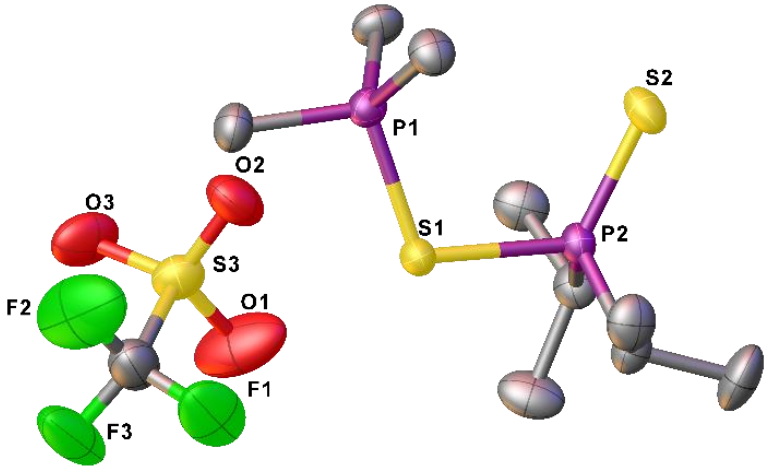

*Figure 1.8: Solid state structure of **1.7(Me$_3$^{i}Pr$_2$)**OTf, hydrogen atoms are omitted for clarity, thermal ellipsoids are drawn at 50 % probability level, CCDC 1813382.*

The solid state structure of **1.7(Me$_3$^{i}Pr$_2$)**OTf also confirms the interpretation of the $^{31}P\{^1H\}$ NMR spectroscopic assignment. Its terminal P-S bond is shorter than the P-S bond of triisopropylphosphine sulfide. The P-S bonds to the bridging sulfur atom are significantly longer, with the S1-P2 bond being the longest. The S1-P2 bond is slightly longer than the P-S bond in the neutral ^{t}Bu$_2$P-S-P^{t}Bu$_2$, whereas the P1-S1 bond is substantially shorter. This supports the interpretation of a trimethylphosphine sulfide ligand on a diisopropyl-thioxophosphonium (^{i}Pr$_2$P(S)$^+$) cation.

The P-S-P angle is with 106.33(4)° closer to the ideal tetrahedral angle than the P-S-P angle of ^{t}Bu$_2$P-S-P^{t}Bu$_2$.

Conclusion

In direct comparison to the reactions with selenium, the reactions of phosphinophosphonium cations with sulfur are less specific, *i.e.* they result in a larger variety of products. Under optimised conditions (DCM/ambient temperature/exact stoichiometry), some reactions with selenium yielded a single product, whereas reactions with sulfur always resulted in a multitude of products. Also, the addition of the first selenium atom occurs on the terminal position for small substituents and on the bridging position for bulkier substituents. In contrast, in reactions with sulfur, both may occur for the same substituents, although the cations with terminal sulfur atom (**1.5**) are evidently more stable, whereas the cations with bridging sulfur atoms were impossible to isolate. This is conclusive with the NMR spectroscopic observations we made for **1.3(^{i}Pr$_3$Ph$_2$)** which led to the assumption that the chalcogen-phosphenium bond is weak and leads to decomposition by reactions with the solvent or other byproducts.

Overall the sulfur cations crystallised more readily than the selenium containing cations, which mitigated the lack of structural information caused by the lack of satellite signals in the ^{31}P NMR spectra and confirmed our interpretation based on the P-P coupling constants. Whereas the

selenium containing compounds were identified by the ^{77}Se satellite signals in the $^{31}P\{^1H\}$ NMR spectra.

In conclusion, this chapter presents several new classes of phosphorus-sulfur (**1.5**, **1.6,** and **1.7**) and phosphorus-selenium (**1.2**, **1.3,** and **1.4**) cations, which have been derived from phosphino-phosphonium cations. A large number of new phosphorus-sulfur and phosphorus-selenium based cations were identified and characterised for the first time, using $^{31}P\{^1H\}$ NMR spectroscopy. Additionally five of them (**1.2(Me$_3$Me$_2$)**OTf, **1.5(^{i}Pr$_3$^{j}Pr$_2$)**OTf, **1.5(^{i}Pr$_3$Ph$_2$)**OTf, **1.5(Cy$_3$^{j}Pr$_2$)**OTf, and **1.7(Me$_3$^{j}Pr$_2$)**OTf) were structurally characterised by single crystal x-ray diffraction experiments. The structural characterisation confirmed the interpretation of the $^{31}P\{^1H\}$ NMR spectroscopic data.

Aside from the discovery of these new cations, these investigations also show an up-to-now unknown aspect of the reactivity of phosphino-phosphonium cations.

References

[1] H. W. Roesky, R. Ahlrichs, S. Brode, *Angew. Chemie* **1986**, *98*, 91–93.

[2] K. Karaghiosoff, M. Schuster, *Phosphorus. Sulfur. Silicon Relat. Elem.* **2001**, *168*, 117–122.

[3] M. Yoshifuji, K. Toyota, K. Ando, N. Inamoto, *Chem. Lett.* **1984**, *13*, 317–318.

[4] M. Yoshifuji, K. Shibayama, N. Inamoto, *Chem. Lett.* **1984**, *13*, 603–606.

[5] A. Schmidpeter, G. Jochem, K. Karaghiosoff, C. Robl, *Angew. Chem. Int. Ed.* **1992**, *31*, 1350–1352.

[6] J. J. Weigand, N. Burford, D. Mahnke, A. Decken, *Inorg. Chem.* **2007**, *46*, 7689–7691.

[7] M. A. Wünsche, T. Witteler, F. Dielmann, *Angew. Chem. Int. Ed.* **2018**, *57*, 7234–7239.

[8] C. W. Schultz, R. W. Parry, *Inorg. Chem.* **1976**, *15*, 3046–3050.

[9] A. H. Cowley, R. A. Kemp, *Chem. Rev.* **1985**, *85*, 367–382.

[10] N. Burford, P. J. Ragogna, R. McDonald, M. J. Ferguson, *J. Am. Chem. Soc.* **2003**, *125*, 14404–14410.

[11] J. J. Weigand, S. D. Riegel, N. Burford, A. Decken, *J. Am. Chem. Soc.* **2007**, *129*, 7969–7976.

[12] M. Gonsior, I. Krossing, L. Müller, I. Raabe, M. Jansen, L. van Wüllen, *Chem. Eur. J.* **2002**, *8*, 4475–4492.

[13] S. S. Chitnis, E. MacDonald, N. Burford, U. Werner-Zwanziger, R. McDonald, *Chem. Commun.* **2012**, *48*, 7359.

[14] N. Burford, T. S. Cameron, P. J. Ragogna, E. Ocando-Mavarez, M. Gee, R. McDonald, R. E. Wasylishen, *J. Am. Chem. Soc.* **2001**, *123*, 7947–7948.

[15] D. Himmel, I. Krossing, A. Schnepf, *Angew. Chem. Int. Ed.* **2014**, *53*, 6047–6048.

[16] D. Himmel, I. Krossing, A. Schnepf, *Angew. Chem. Int. Ed.* **2014**, *53*, 370–374.

[17] G. Frenking, *Angew. Chem. Int. Ed.* **2014**, *53*, 6040–6046.

[18] A. P. M. Robertson, P. A. Gray, N. Burford, *Angew. Chem. Int. Ed.* **2014**, *53*, 6050–6069.

[19] C. A. Dyker, N. Burford, *Chem. – An Asian J.* **2008**, *3*, 28–36.

[20] N. Burford, P. J. Ragogna, R. McDonald, M. J. Ferguson, *Chem. Commun.* **2003**, 2066–2067.

[21] N. Burford, D. E. Herbert, P. J. Ragogna, R. McDonald, M. J. Ferguson, *J. Am. Chem. Soc.* **2004**, *126*, 17067–17073.

[22] N. Burford, P. J. Ragogna, *J. Chem. Soc. Dalton Trans.* **2002**, 4307–4315.

[23] N. Burford, P. J. Ragogna, K. N. Robertson, T. S. Cameron, N. J. Hardman, P. P. Power, *J. Am. Chem. Soc.* **2002**, *124*, 382–383.

[24] N. Burford, P. Losier, A. D. Phillips, P. J. Ragogna, T. S. Cameron, *Inorg. Chem.* **2003**, *42*, 1087–1091.

[25] N. Burford, C. A. Dyker, A. Decken, *Angew. Chem. Int. Ed.* **2005**, *44*, 2364–2367.

[26] O. Schön, Organophosphorchalkogenide Erste Phosphor-Chalkogen-Kationen Neue Heterocyclen Und Selenophosphonate, Ludwig-Maximilians-Universität München, **2007**.

[27] K.-O. Feldmann, T. Wiegand, J. Ren, H. Eckert, J. Breternitz, M. F. Groh, U. Müller, M. Ruck, B. Maryasin, C. Ochsenfeld, et al., *Chem. Eur. J.* **2015**, *21*, 9697–9712.

[28] S. Yogendra, S. S. Chitnis, F. Hennersdorf, M. Bodensteiner, R. Fischer, N. Burford, J. J. Weigand, *Inorg. Chem.* **2016**, *55*, 1854–1860.

[29] M. J. Poller, N. Burford, K. Karaghiosoff, *Chem. Eur. J.* **2018**, *24*, 85–88.

[30] S. S. Chitnis, J. M. Whalen, N. Burford, *J. Am. Chem. Soc.* **2014**, *136*, 12498–12506.

[31] A. Cogne, A. Grand, J. Laugier, J. B. Robert, L. Wiesenfeld, *J. Am. Chem. Soc.* **1980**, *102*, 2238–2242.

[32] C. Q. Nguyen, A. Adeogun, M. Afzaal, M. a Malik, P. O'Brien, *Chem. Commun.* **2006**, *274*, 2179.

[33] M. Gruber, P. G. Jones, R. Schmutzler, *Chem. Ber.* **1990**, *123*, 1313–1317.

[34] R. J. Staples, B. M. Segal, *Acta Crystallogr. Sect. E Struct. Reports Online* **2001**, *57*, o432–o433.

[35] N. de Silva, F. R. Fronczek, **2016**, DOI 10.5517/ccdc.csd.cc1lq93q.

Chapter 2: Reversible Oxidative Se-Se Coupling of Phosphine Selenides by $Ph_3Sb(OTf)_2$

In accordance with § 8 (3) of the “Promotionsordnung für die Fakultät für Chemie und Pharmazie der Ludwig-Maximilians-Universität München” this chapter has been previously published in: M. J. Poller, N. Burford, K. Karaghiosoff, *Chem. Eur. J.* **2018**, *24*, 85–88. and is presented here with permission of the publisher. The text has been reformatted and the numbering scheme has been adapted to fit the rest of this dissertation.

Abstract

Salts of diphosphoniumdiselenide dications ($[R_3PSeSePR_3][OTf]_2$) have been isolated from reactions of trialkylphosphine selenides with triphenylantimony bistriflate. The redox process is speculated to proceed via a cationic coordination complex $[Ph_3SbL_2][OTf]_2$ (L = Me_3PSe, $^{i}Pr_3PSe$), which is also formed in the reaction of $[R_3PSeSePR_3][OTf]_2$ with Ph_3Sb. The observations indicate that the reductive elimination of $[R_3PSeSePR_3]^{2+}$ from $[Ph_3Sb(SePR_3)_2]^{2+}$ is reversible through the oxidative addition of $[R_3PSeSePR_3]^{2+}$ to Ph_3Sb.

[Main Article]

The coordination chemistry of p-block centers as Lewis acceptors has evolved significantly in recent years,[1–6] with many analogies to the coordination chemistry of transition metal elements. In this context, we have recently reported complexes of $Ph_3Sb(OTf)_2$ with classical O- and N-donor ligands (Scheme 2.1a). In contrast, attempts to isolate the corresponding complexes of $Ph_3Sb(OTf)_2$ with Me_3P as a ligand result in reduction of the antimony(V) center to Ph_3Sb(III) and oxidation of the phosphine to $[Me_3PPMe_3][OTf]_2$ (Scheme 2.1b), illustrating an oxidative P-P coupling process or reductive elimination of a diphosphonium dication from antimony.[7]

a) $Ph_3Sb(OTf)_2 + 2L \longrightarrow [Ph_3SbL_2][OTf]_2$
2.1(L) L = dmap, Ph_3PO

b) $Ph_3Sb(OTf)_2 + 2\ PMe_3 \longrightarrow Ph_3Sb + [Me_3PPMe_3][OTf]_2$

c) $Ph_3Sb(OTf)_2 + 2\ R_3PSe \longrightarrow [Ph_3SbL_2][OTf]_2 \rightleftharpoons Ph_3Sb + [R_3PSeSePR_3][OTf]_2$
2.1(L) L = R_3PSe **2.2(R)** R = Me, ^{i}Pr

d) $Ph_3Sb + [R_3PSeSePR_3][OTf]_2 \rightleftharpoons [Ph_3SbL_2][OTf]_2$
2.2(R) R = Me, ^{i}Pr **2.1(L)** L = R_3PSe

Scheme 2.1: Redox reactions involving Ph_3Sb and $Ph_3Sb(OTf)_2$.

We have now discovered that in an analogous reaction $Ph_3Sb(OTf)_2$ effects oxidative Se-Se coupling of trialkylphosphine selenides to give salts of **2.2** (Scheme 2.1c). $^{31}P\{^1H\}$ NMR spectra of the respective reaction mixtures indicate that these reactions proceed via the coordination complexes **2.1(R_3PSe)** (Scheme 2.1c). Interestingly, NMR studies of the reactions of **2.2** with Ph_3Sb (Scheme 2.1d) indicate that this redox process is reversible, demonstrating the versatility of this redox behaviour of antimony. Similar redox behaviour has only been reported for antimony in conjunction with a gold center, for which Gabbai *et al.* reported a reversible umpolung of the Sb-Au bond upon reduction/oxidation.[8]

Mixtures of two equivalents of $^i Pr_3PSe$ with $Ph_3Sb(OTf)_2$ in dichloromethane at RT show a broad signal in the $^{31}P\{^1H\}$ NMR spectrum (70.4 ppm, $^1J_{PSe}$ = 663 Hz). The difference in chemical shift relative to the sharp signal for $^i Pr_3PSe$ (68.9 ppm)[9] is small, but when cooled to 187 K, three separate signals are observed. (Figure 2.1)

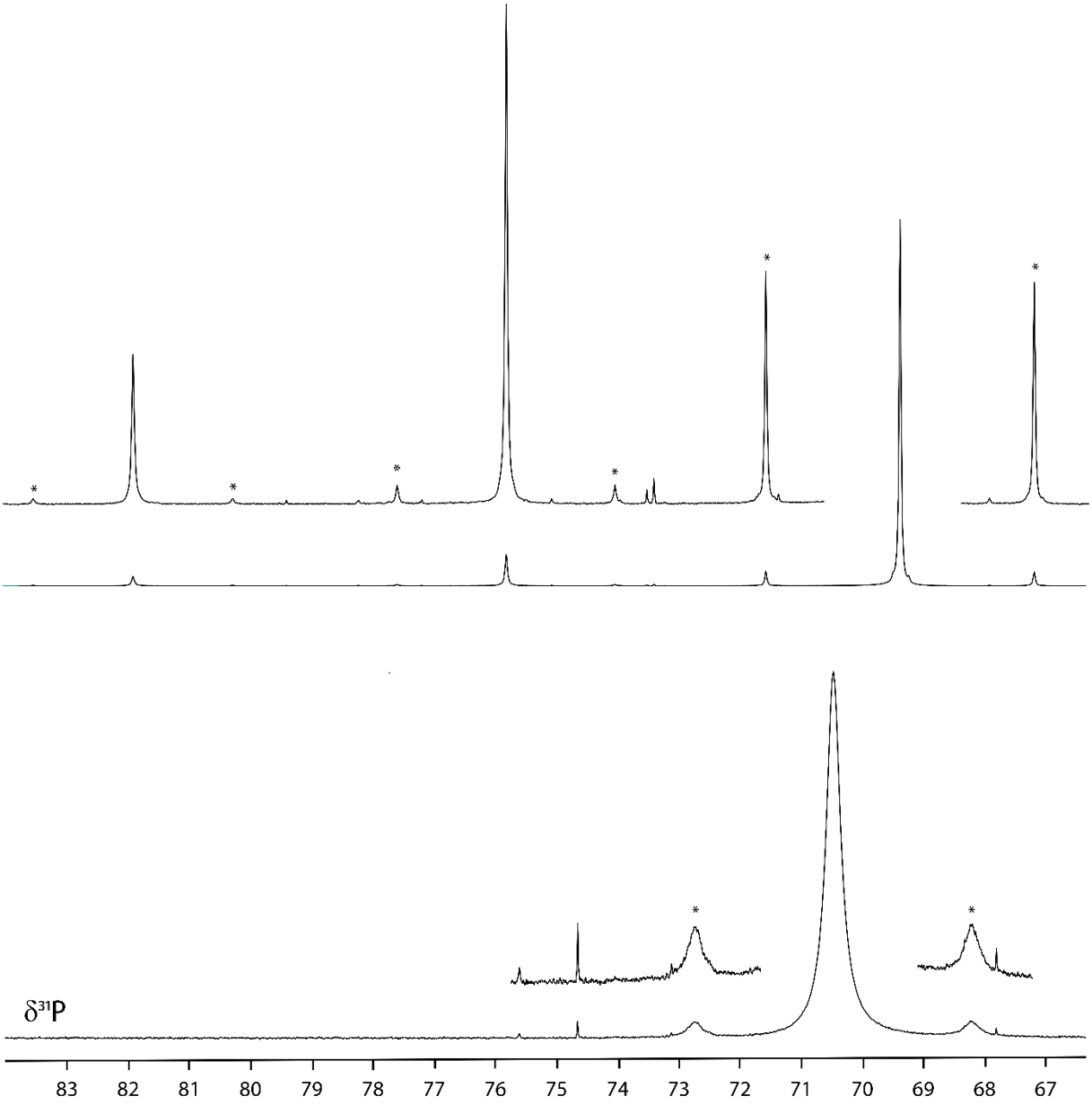

*Figure 2.1: $^{31}P\{^{1}H\}$ NMR spectra of a solution of 2 $^{i}Pr_3PSe$ + Ph_3SbOTf_2 at 298 K (bottom) and at 187 K (top), the ^{77}Se satellites are marked with *.*

The most intense signal at 69.4 ppm ($^{1}J_{PSe}$ = 641 Hz) corresponds to free $^{i}Pr_3PSe$[9], the signal at 81.9 ppm ($^{1}J_{PSe}$ = 478 Hz) is assigned to **2.2(^{i}Pr)**, which has been successfully isolated and characterised, and the signal at 75.8 ppm ($^{1}J_{PSe}$ = 519 Hz) is assigned to the coordination complex **2.1(^{i}Pr$_3$PSe)**. The phosphorus-selenium coupling constants support this assignment. The ^{31}P NMR data and assignments for **2.1(^{i}Pr$_3$PSe)** are summarized in Table 2.1.

Table 2.1: Overview of $^{31}P\{^1H\}$ NMR data for the reactions of $^{i}Pr_3PSe$ with Ph_3SbOTf_2

	δ [ppm]	$^1J_{PSe}$ [Hz]	solvent	assignment
Scheme 2.1c R = ^{i}Pr (298 K)	70.4	663	$[D_2]$DCM	equilibrium
Scheme 2.1c R = ^{i}Pr (298 K)	74.4	583	$[D_3]$MeCN	equilibrium
Scheme 2.1c R = ^{i}Pr (187 K)	81.9	478	$[D_2]$DCM	**2.2(^{i}Pr)**
	75.8	519		**2.1($^{i}Pr_3PSe$)**
	69.4	641		$^{i}Pr_3PSe$
2.2(^{i}Pr) (298 K)	83.2	467	$[D_3]$MeCN	**2.2(^{i}Pr)**
$^{i}Pr_3PSe$ (300 K)[9]	68.9	711	$[D_2]$DCM	
Scheme 2.1d R = ^{i}Pr (298 K)	76.9	572	$[D_3]$MeCN	equilibrium
Scheme 2.1d R = ^{i}Pr (298 K)	70.3	677	$[D_2]$DCM	equilibrium

Mixtures of **2.2(^{i}Pr)** with Ph_3Sb, as in Scheme 2.1d, exhibit $^{31}P\{^1H\}$ NMR signals that are consistent with those observed for **2.1($^{i}Pr_3PSe$)** in Scheme 2.1c, indicating that this process is reversible. We conclude that mixtures of $Ph_3Sb(OTf)_2$ with $^{i}Pr_3PSe$ form **2.1($^{i}Pr_3PSe$)** which adopts an equilibrium with Ph_3Sb and **2.2(^{i}Pr)** (Scheme 2.1c). At 298 K the exchange rate of the equilibrium leads to a single broad signal in the $^{31}P\{^1H\}$ NMR spectrum, but at low temperatures the exchange is slower and individual signals for each component are observed. In acetonitrile, mixtures of $^{i}Pr_3PSe$ and $Ph_3Sb(OTf)_2$ exhibit a chemical shift of 74.4 ppm, which we interpret as the formation of **2.1($^{i}Pr_3PSe$)** being more favoured in acetonitrile than in dichloromethane, due to the higher basicity of acetonitrile in comparison to dichloromethane. Although acetonitrile is a better solvent for the synthesis of **2(^{i}Pr),** acetonitrile is not suitable for low temperature NMR investigations.

Independent of temperature, the reaction of Me_3PSe with $Ph_3Sb(OTf)_2$, as illustrated in Scheme 2.1c, exhibits a $^{31}P\{^1H\}$ NMR chemical shift at 32 ppm ($^1J_{PSe}$ = 466 Hz), representing a significant difference in chemical shift (trimethylphosphine selenide: 8.8 ppm, $^1J_{PSe}$ = 682 Hz)[10]. This signal is assigned to the respective coordination complex **2.1(Me_3PSe)**. Compound **2.2(Me)** has been isolated from the reaction mixture and solutions of the pure compound exhibit a ^{31}P chemical shift of 40.0 ppm with $^1J_{PSe}$ = 412 Hz. As in the isopropyl derivatives, the $^1J_{PSe}$ coupling constants are consistent with the assignment to the coordination complex and diphosphoniumdiselenide dication, respectively. The NMR data and assignments for the methyl derivatives are summarized in Table 2.2. The $^{31}P\{^1H\}$ NMR spectrum for the reaction of **2.2(Me)** with Ph_3Sb (Scheme 2.1d) includes a broad signal at 34 ppm, confirming the reversibility of the reductive elimination of **2.2(Me)** from **2.1(Me_3PSe)**.

Table 2.2: Overview of $^{31}P\{^1H\}$ NMR data for the reactions of Me_3PSe with Ph_3SbOTf_2

	δ [ppm]	$^1J_{PSe}$ [Hz]	solvent	assignment
Scheme 2.1c R = Me (298 K)	32	466	$[D_3]$MeCN	**2.1(Me_3PSe)**
Me_3PSe[10]	8.8	682	$CDCl_3$	
Scheme 2.1d R = Me (298 K)	34	445	$[D_3]$MeCN	**2.1(Me_3PSe)**
2.2(Me)	40.0	412	$[D_3]$MeCN	**2.2(Me)**

Compounds **2.2(Me)** and **2.2(^{i}Pr)** have been structurally characterised by X-ray diffraction. While **2.2(Me)** crystallises in the space group C2/c, **2.2(^{i}Pr)** crystallises in the space group $P2_1/c$ and both contain well separated cations and anions. Selected structural features of the cations are compared with features of related cations in Table 2.3. The cation in **2.2(Me)** (Figure 2.2) adopts a gauche conformation with a P-Se-Se-P dihedral angle of 92.1(1)°, similar to that in cations **2.3**[11] and **2.4**[12]. While the Se-Se bond in **2.2(Me)** is bisected by a twofold axis, an inversion center on the Se-Se bond of **2.2(^{i}Pr)** (Figure 2.3) defines a trans-conformation similar to that in compound **2.6**[13]. The trans-conformation observed for **2.2(^{i}Pr)** is surprising as cation **2.4**[12] exhibits a gauche-conformation[12] despite accommodating sterically similar substituents. The cyclic framework of **2.5**[14] enforces an almost cis-conformation, with a P-Se-Se-P angle of 29.1°.

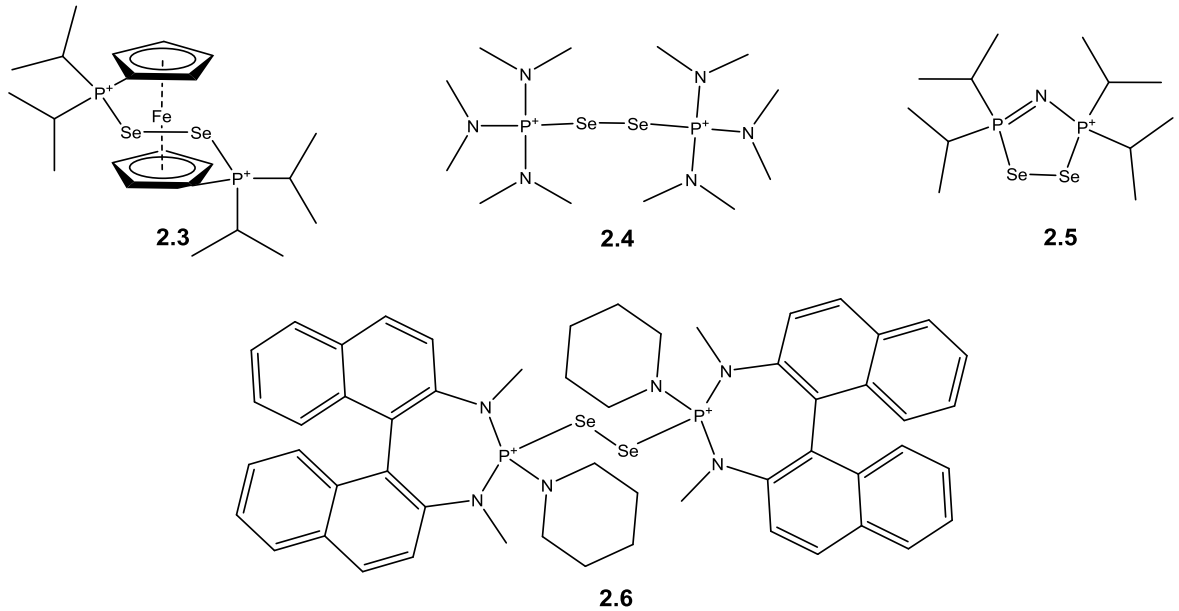

2.3 **2.4** **2.5**

2.6

[Scheme 2.2: Other diphosphonium diselenide cations.]

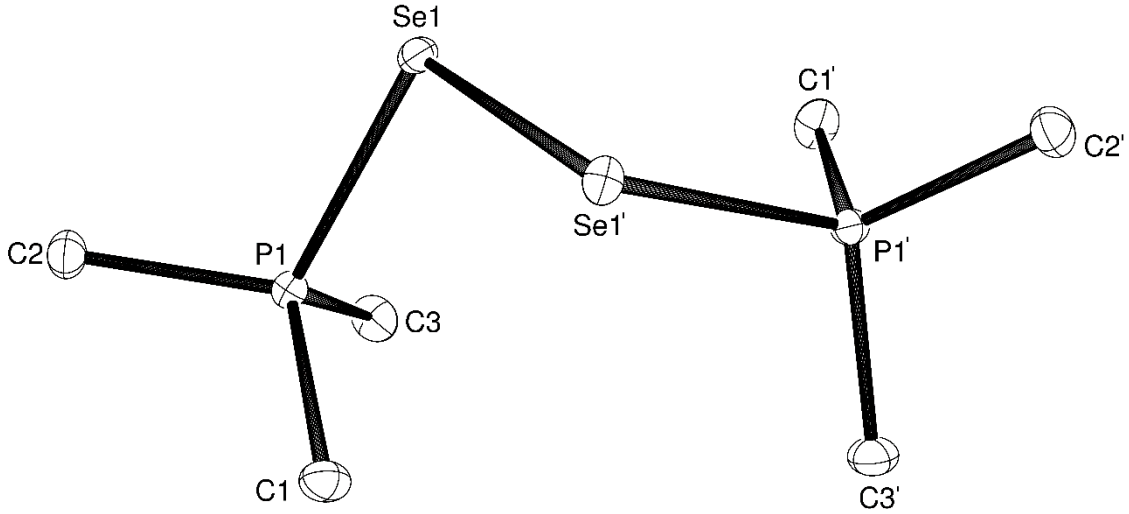

*Figure 2.2: Molecular structure of the dication of **2**(Me) in the crystal; ORTEP representation, thermal ellipsoids are drawn at 50 % probability level. H atoms are omitted for clarity.*
Symmetry code for half the molecule: 1-x, y, 0.5-z.

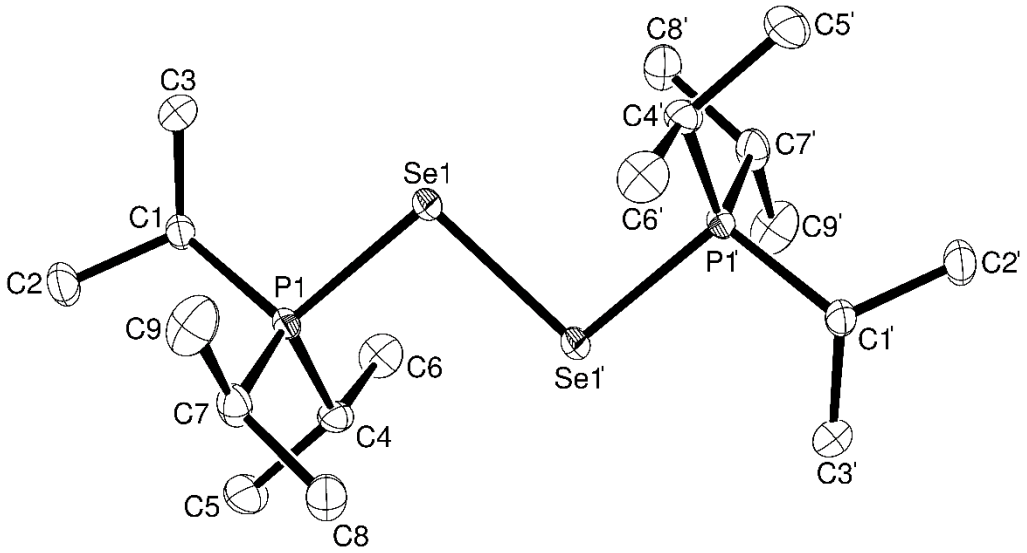

*Figure 2.3: Molecular structure of the dication of **2**(ⁱPr) in the crystal; ORTEP representation, thermal ellipsoids are drawn at 50 % probability level. H atoms are omitted for clarity. Symmetry code for half the molecule: 1-x, 1-y, 1-z.*

*Table 2.3: Selected structural features of compounds **2.2(Me)** and **2.2(ⁱPr)** in comparison to previously reported diphosphoniumdiselenide cations. Dihedral angles of cyclic compounds are given in ().*

	space group	P-Se [Å]	Se-Se [Å]	P-Se-Se-P [°]
2.2(Me)	C2/c	2.260(1)	2.339(1)	92.1(1)
2.2(*i*Pr)	$P2_1/c$	2.235(1)	2.392(1)	180
2.3[11]	$P2_12_12_1$	2.279(1)	2.333(1)	(96.2)
		2.272(1)		
2.4[12]	P-1	2.233(8)	2.309(5)	112.8
		2.227(9)		
2.5[14]	P-1	2.273(1)	2.348(1)	(29.1)
		2.263(1)		
2.6[13]	P-1	2.244(1)	2.373(1)	180

The Se-Se bonds of *trans*-conformers **2.2(*i*Pr)** and **2.6**[13] are slightly longer than the Se-Se bonds of *gauche*-conformers **2.2(Me)**, **2.3**[11] and **2.4**[12] and are comparable to the Se-Se bond length for grey selenium, 2.37 Å[15]. The mean Se-Se bond length for diselenides (CCDC database) is 2.35 Å, which is closer to the value observed in the *gauche*-conformers. The P-Se bonds in derivatives of **2.2** are significantly longer (2.23 Å – 2.28 Å) than that of a phosphine selenide (mean value of 2.121 Å, CCDC database), consistent with the greater coordination number of the selenium atom in derivatives of **2.2**. The compounds in the *trans*-conformation (**2.2(*i*Pr)** and **2.6**[13]) have similar values for their respective P-Se bonds (2.24 Å). Compared to **2.2(Me)**, **2.3**[11] and **2.4**[12] exhibit values between 2.23 Å and 2.28 Å with **2.4**[12] having lower values (2.23 Å) than **2.2(Me)** (2.26 Å) and **2.3**[11] (2.27 Å – 2.28 Å). With values of 2.26 Å and 2.27 Å the P-Se bonds in **2.5**[14] are in a similar range as the values of **2.2(Me)** and **2.3**[11].

Conclusion

Redox reactions of R_3PSe with $Ph_3Sb(OTf)_2$ are speculated to proceed via cationic coordination complexes $[Ph_3Sb(SePR_3)_2][OTf]_2$ (**2.1**), which undergo reductive elimination of $[R_3PSeSePR_3][OTf]_2$ (**2.2**), representing an oxidative Se-Se coupling. Remarkably reactions of (**2.2**) with Ph_3Sb result in an oxidative addition to give **2.1**, demonstrating the reversibility of this redox process.

Acknowledgment

We thank the Natural Sciences and Engineering Research Council of Canada (NSERC) for funding and Dr. Brian Patrick (University of British Columbia) for the XRD measurement (data collection) of **2.2(Me)**.

References

[1] A. P. M. Robertson, P. A. Gray, N. Burford, *Angew. Chem. Int. Ed.* **2014**, *53*, 6050–6069.

[2] D. W. Stephan, *Angew. Chem. Int. Ed.* **2017**, *56*, 5984–5992.

[3] J. S. Jones, F. P. Gabbaï, *Acc. Chem. Res.* **2016**, *49*, 857–867.

[4] J. L. Dutton, P. J. Ragogna, *Coord. Chem. Rev.* **2011**, *255*, 1414–1425.

[5] P. P. Power, *Nature* **2010**, *463*, 171–177.

[6] E. Rivard, *Dalton Trans.* **2014**, *43*, 8577–8586.

[7] A. P. M. Robertson, S. S. Chitnis, H. a. Jenkins, R. McDonald, M. J. Ferguson, N. Burford, *Chem. Eur. J.* **2015**, *21*, 7902–7913.

[8] C. R. Wade, F. P. Gabbaï, *Angew. Chem. Int. Ed.* **2011**, *50*, 7369–7372.

[9] N. Kuhn, G. Henkel, H. Schumann, R. Fröhlich, *Zeitschrift für Naturforsch.* **1990**, *45b*, 1010–1018.

[10] R. García-Rodríguez, H. Liu, *J. Am. Chem. Soc.* **2012**, *134*, 1400–3.

[11] F. N. Blanco, L. E. Hagopian, W. R. Mcnamara, J. A. Golen, A. L. Rheingold, C. Nataro, *Organometallics* **2006**, *2*, 4292–4300.

[12] G. R. Willey, J. R. Barras, M. D. Rudd, M. G. B. Drew, *J. Chem. Soc. Dalton Trans.* **1994**, 3025–3029.

[13] S. E. Denmark, E. Hartmann, D. J. P. Kornfilt, H. Wang, *Nat. Chem.* **2014**, *6*, 1056–1064.

[14] J. Konu, T. Chivers, H. M. Tuononen, *Inorg. Chem.* **2006**, *45*, 10678–10687.

[15] P. Cherin, P. Unger, *Inorg. Chem.* **1967**, *6*, 1589–1591.

Chapter 3: New Cyclic Phosphorus-Selenium Cations

Abstract

This work reports two new examples of rare selenophosphonium dimers which are characterised by single crystal x-ray diffraction and NMR spectroscopy. An unexpected reaction of these four-membered P-Se-rings with $SbPh_3$ and the solvent yielded a dicationic five-membered ring, containing an additional CH_2 group, which has been identified by single crystal x-ray diffraction. Another ring extension reaction with grey selenium led to a cationic five-membered phosphorus-selenium ring, which has been conclusively identified by ^{31}P and ^{77}Se NMR spectroscopy (Scheme 3.1).

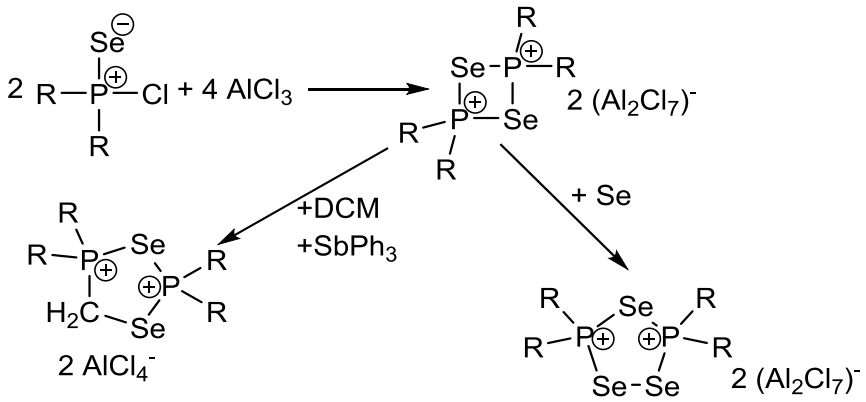

Scheme 3.1: Reactions presented in this chapter.

Introduction

The investigations presented in this chapter were inspired by an unexpected result of the project presented in Chapter 1: It can be assumed that the formation of cation **4.3** (presented in Chapter 4) was the result of the reaction of a tri-coordinate selenophosphonium cation with the solvent (acetonitrile) (Scheme 3.2).

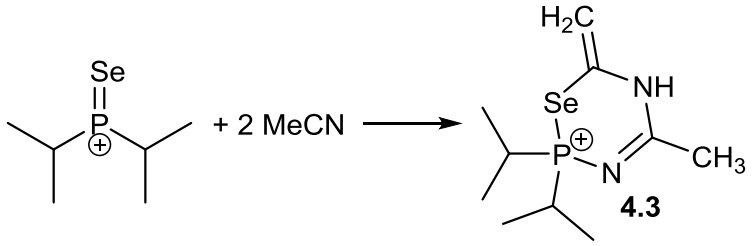

Scheme 3.2: Proposed reaction of $^{i}Pr_2PSe^{+}$ with MeCN.

Tri-coordinate chalcogenophosphonium cations have been studied previously by A. Schmidpeter,[1] N. Burford,[2,3] and most recently F. Dielmann[4]. The first tri-coordinate selenophosphonium cation, which was presented by A. Schmidpeter *et al.*, was synthesised via oxidation of the respective phosphorus-III compound. The chalcogenophosphonium cations presented by N. Burford *et al.* and F. Dielmann *et al.* were synthesised via halide abstraction. All these previously reported tri-coordinate chalcogenophosphonium cations rely on the stabilisation by mesomeric delocalisation of the positive charge or stabilisation by a donating moiety *i.e.* a nitrogen ligand (Scheme 3.3).

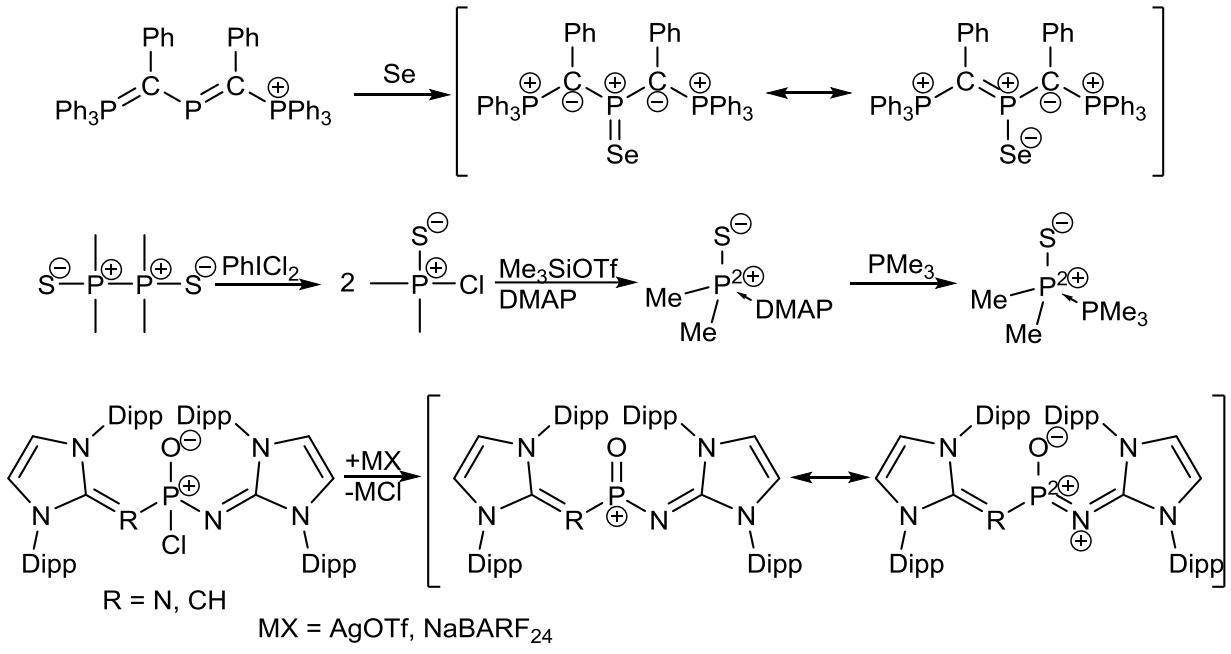

Scheme 3.3: Selected examples of three coordinate chalcogenophosphonium cations.[1,2,4]

Beside these 'monomeric' tri-coordinate chalcogenophosphonium cations, N. Burford *et al.* reported the dimeric chalcogenophosphonium cations of the composition $((R_2N)_2PCh)_2^{2+}$ (with Ch = S, Se; R = Et, ^{i}Pr). These dimers were the result of the chloride abstraction from $R_2P(Ch)Cl$ with $AlCl_3$ (Scheme 3.4).[3,5]

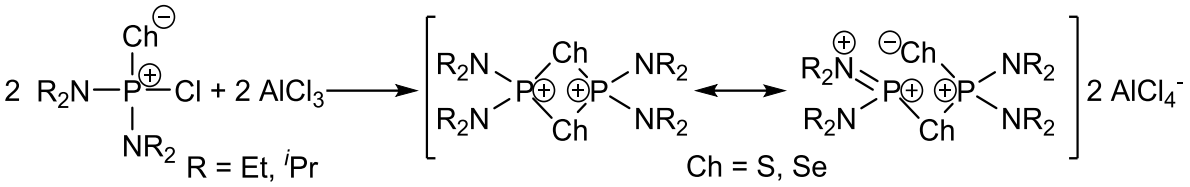

Scheme 3.4: Cyclic chalcogenophosphonium cation dimer.[3]

The structure of these dimers also allows for stabilisation by electron donation from the lone pair on the amine substituents (Scheme 3.4). The respective monomeric tri-coordinate chalcogenophosphonium cations have not been reported, which leads to the assumption that the electron donation from the amine substituents is insufficient to stabilise the monomeric form.

Interestingly, N. Burford *et al.* also reported a competing reaction in which the diaminochlorophosphine sulfide coordinates to aluminium trichloride *via* the sulfur atom, instead of transferring a chloride ion (Scheme 3.5).[5]

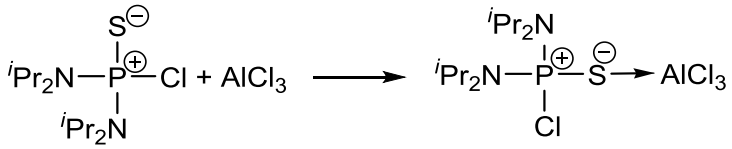

Scheme 3.5: Competing reaction of($^{i}Pr_2N)_2P(S)Cl$ with $AlCl_3$.[5]

The cyclic dimers are also of interest because cationic phosphorus-chalcogen rings are quite rare. Cyclic compounds containing phosphorus and selenium are well known. However, they are mostly neutral compounds.[6–8] Aside from the above mentioned selenophosphonium dimer, cationic rings composed of phosphorus and chalcogens are known as part of cationic clusters as presented in the introduction[9–11], or in conjunction with other elements, such as some of the cations referred to in Chapter 2.[12]

The goal of this chapter was the synthesis of tri-coordinate chalcogenophosphonium cations, or the respective dimeric dications, without any donating substituents, as implied in the above mentioned reaction (Scheme 3.2). Additionally, this chapter seeks to extend the knowledge about cyclic phosphorus-selenium cations by using the chalcogenophosphonium cations as starting materials for the synthesis of new examples of such compounds.

Results and Discussion

In order to isolate a selenophosphonium cation, chlorophosphonium selenides were allowed to react with two equivalents of aluminium trichloride in dichloromethane (Scheme 3.6). (The addition of only one equivalent aluminum trichloride did not induce any reaction.) The solution was layered with hexanes to precipitate the products, which were identified as **3.1a**$(Al_2Cl_7)_2$ and **3.1b**$(Al_2Cl_7)_2$ by $^{31}P\{^{1}H\}$ and $^{77}Se\{^{1}H\}$ NMR spectroscopy as well as single crystal x-ray diffraction. The phenyl derivative, **3.1a**$(Al_2Cl_7)_2$, formed large yellow crystals, whereas, the isopropyl derivative, **3.1b**$(Al_2Cl_7)_2$, precipitated as small powdery needles with a more orange

colour. Both compounds are soluble in dichloromethane but they decompose in coordinating solvents such as acetonitrile and diethyl ether, and they are insoluble in hexanes. When exposed to air, both compounds decompose quickly, indicated by a colour change to red.

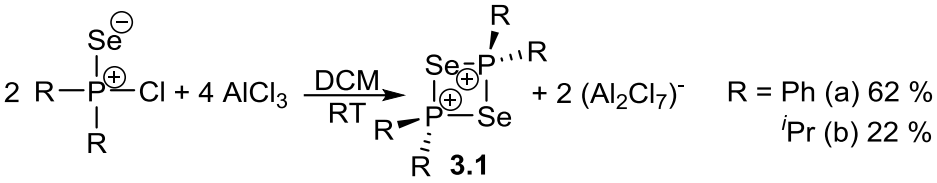

*Scheme 3.6: Reaction of $R_2P(Se)Cl$ with $AlCl_3$ leads to compound **3.1**.*

The $^{31}P\{^1H\}$ NMR spectra of cations **3.1** (Figure 3.1) show one singlet at a significantly lower frequency than the starting material. The singlet has a set of ^{77}Se satellite signals with coupling constants of 263 Hz and 248 Hz respectively, which are much smaller than the respective $^1J_{PSe}$ coupling constants in the starting materials.

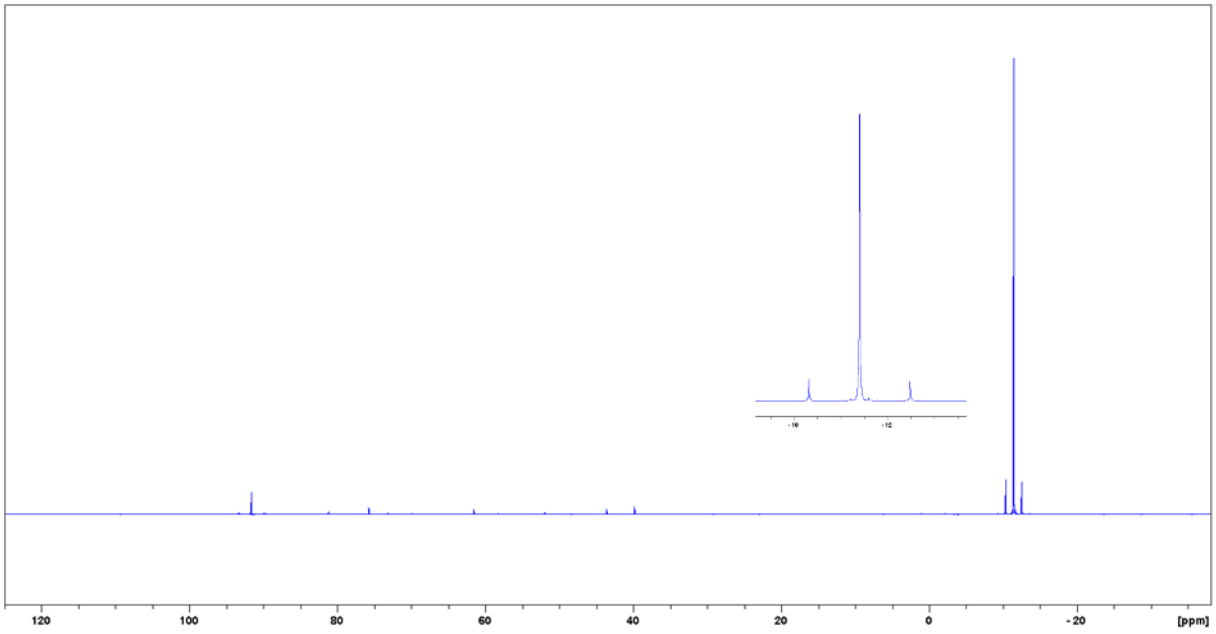

*Figure 3.1: $^{31}P\{^1H\}$ NMR spectrum of **3.1a**, spectra of **3.1b** are in Appendix III.*

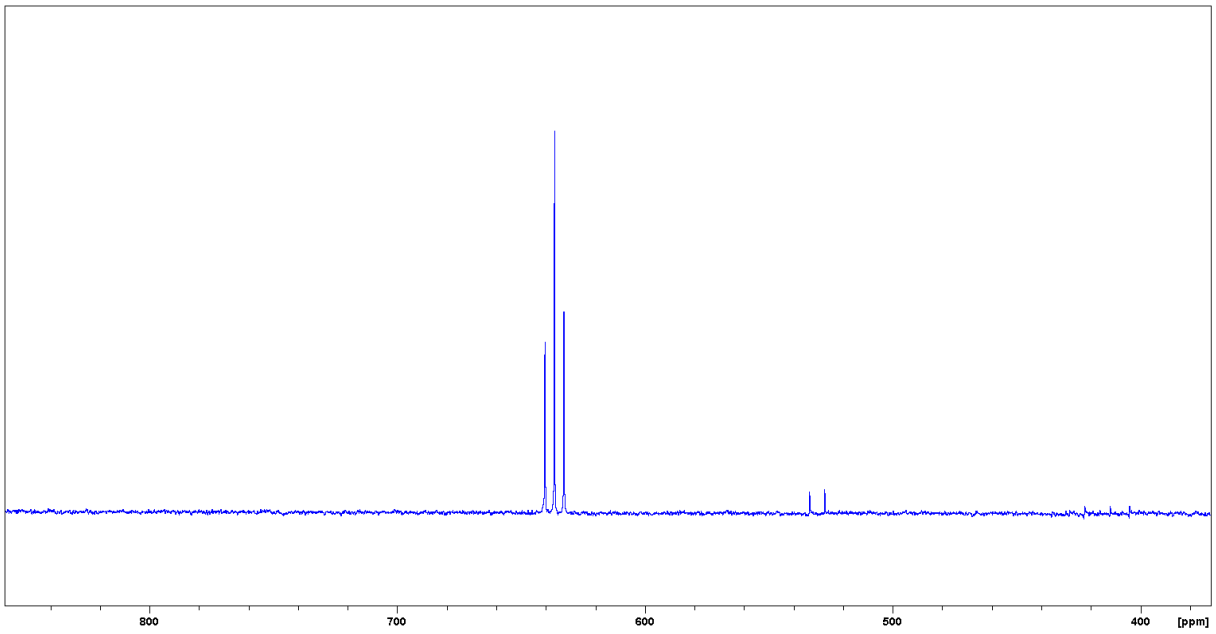

*Figure 3.2: $^{77}Se\{^{1}H\}$ NMR spectrum of **3.1a**, spectra of **3.1b** are in Appendix III.*

The $^{77}Se\{^{1}H\}$ NMR spectra (Figure 3.2) show triplet signals with matching P-Se coupling constants, confirming the connectivity of a Se atom to two equivalent ^{31}P nuclei. The ^{31}P and ^{77}Se NMR spectroscopic data is summarized in Table 3.1.

*Table 3.1: Selected NMR parameters of **3.1a** and **3.1b** in comparison to their respective starting materials*

	δ $^{31}P\{^{1}H\}$ [ppm]	J_{PSe} [Hz]	δ $^{77}Se\{^{1}H\}$ [ppm]
$Ph_2P(Se)Cl$	71.8	852	-63[13]
3.1a	-10.5	263	633
$^{i}Pr_2P(Se)Cl$	125.9	825	-232
3.1b	58.5	248	201

The $^{31}P\{^{1}H\}$ NMR spectrum of the reaction mixture from the synthesis of the isopropyl derivative (**3.1b**) explains the difference in yield (62 % for **3.1a** vs. 22 % for **3.1b**). Aside from the product, there is a signal at 127.0 ppm with a P-Se coupling constant of 515 Hz. The integral ratio of this signal to the product signal is 3:2. A larger excess of aluminum trichloride or longer reaction time did not lead to a more complete reaction.

A possible explanation for this new peak would be the formation of an adduct, in which the phosphine selenide coordinates to the aluminium trichloride (Scheme 3.7). Such adducts are known with triphenylphosphine selenide.[14]

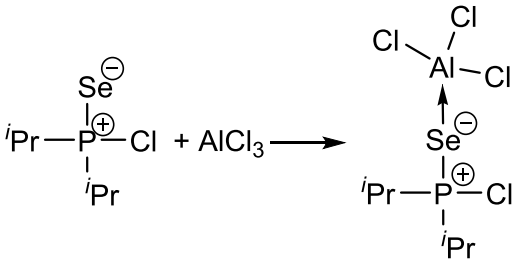

Scheme 3.7: Competing reactions of $^{i}Pr_2P(Se)Cl$ with $AlCl_3$.

The fact that the P-Se coupling constant is smaller than that of the free diisopropyl-chlorophosphine selenide supports this interpretation. This phenomenon (Scheme 3.7) is not observed with the diphenylchlorophosphine selenide, presumably because the phenyl substituents make this chlorophosphine selenide a weaker donor compared to the isopropyl substituents.

Single crystals of **3.1a**$(Al_2Cl_7)_2$ suitable for single crystal x-ray diffraction were easily obtained during the initial crystallisation from the reaction mixture by layering with hexanes. In the case of **3.1b**$(Al_2Cl_7)_2$, several crystallisation attempts were necessary to obtain crystals suitable for single crystal x-ray diffraction because the usual result were very fine needle shaped crystals. The phenyl derivative, **3.1a**$(Al_2Cl_7)_2$ crystallised in the $P2_1/n$ spacegroup with one cation and two anions in the asymmetric unit (figure 3.3) and four formula units in the unit cell. The closest distance between cation and anion occurs between Se1 and Cl14 with 3.120(1) Å, which is slightly shorter than the sum of the respective van der Waals radii (1.82 Å + 1.82 Å = 3.64 Å)[15].

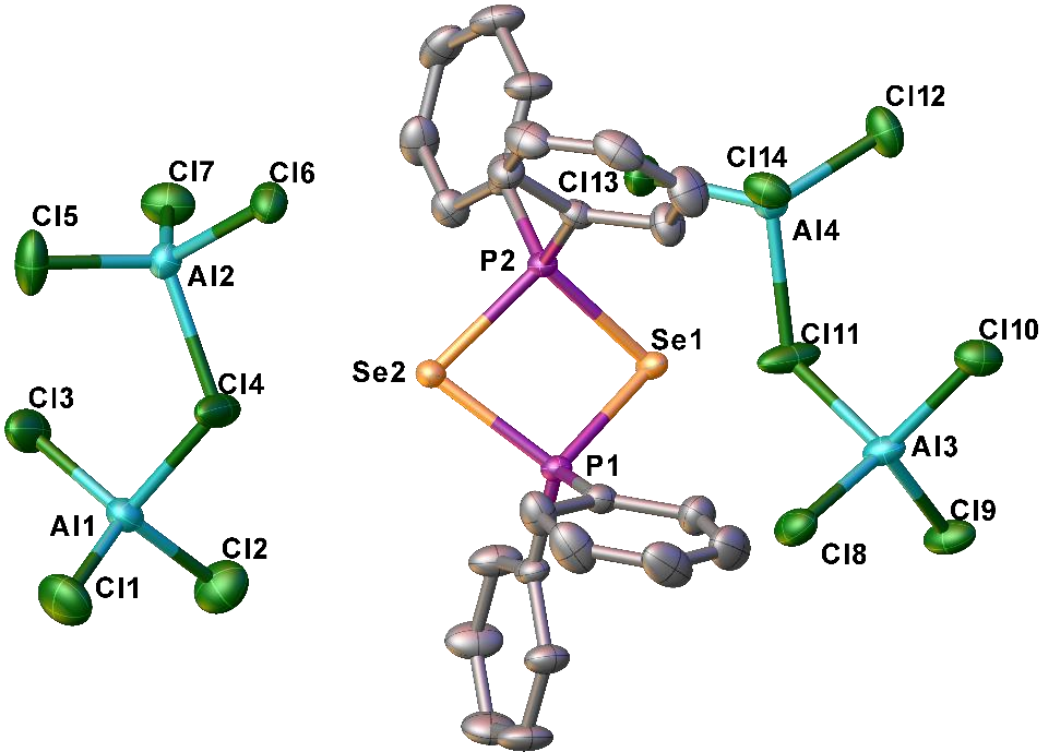

*Figure 3.3: Solid state structure of **3.1a**$(Al_2Cl_7)_2$, hydrogen atoms are omitted for clarity, thermal ellipsoids are drawn at 50 % probability level.*

3.1b$(Al_2Cl_7)_2$, the isopropyl derivative, crystallised in the $P2_12_12_1$ space group with two formula units in the asymmetric unit (Figure 3.4) and eight formula units in the unit cell. The closest cation anion distance occurs between Se3 and Cl17 with 3.38(1) Å.

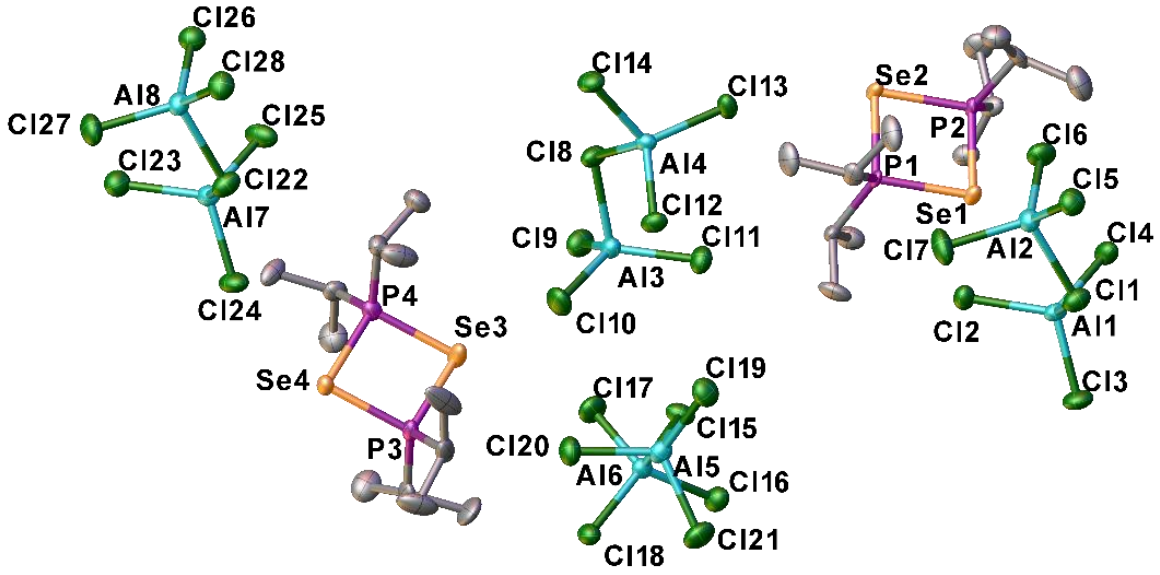

*Figure 3.4: Solid state structure of **3.1b**$(Al_2Cl_7)_2$, hydrogen atoms are omitted for clarity, thermal ellipsoids are drawn at 50 % probability level.*

Table 3.2 shows an overview of structural parameters of cations **3.1** in comparison to the previously reported derivative with the diethlyamine substituents (**3.1c**).[3]

*Table 3.2: Selected structural data of compounds **3.1**.*

	Bond length		**Angle**	
3.1a$(Al_2Cl_7)_2$	P1-Se1	2.2468(6) Å	P1-Se1-P2	80.92(2)°
	P2-Se1	2.2495(6) Å	Se1-P2-Se2	95.84(2)°
	P1-Se2	2.2387(6) Å	P2-Se2-P1	81.11(2)°
	P2-Se2	2.2485(6) Å	Se2-P1-Se1	96.19(2)°
3.1b$(Al_2Cl_7)_2$	P1-Se1	2.262(3) Å	P1-Se1-P2	83.2(1)°
	P2-Se1	2.235(4) Å	Se1-P2-Se2	97.0(1)°
	P1-Se2	2.241(3) Å	P2-Se2-P1	83.3(1)°
	P2-Se2	2.251(3) Å	Se2-P1-Se1	96.5(2)°
	P3-Se3	2.250(3) Å	P3-Se3-P4	83.1(1)°
	P4-Se3	2.230(3) Å	P3-Se4-P4	83.2(1)°
	P3Se4	2.228(3) Å	Se3-P3-Se4	96.9(1)°
	P4-Se4	2.250(3) Å	Se3-P4-Se4	96.8(1)°
3.1c$(AlCl_4)_2$[3]	P1-Se1	2.257(3) Å	P1-Se1-P2	82.9(1)°
	P2-Se1	2.238(3) Å	Se1-P2-Se2	97.3(1)°
	P1-Se2	2.249(3) Å	P2-Se2-P1	82.6(1)°
	P2-Se2	2.262(3) Å	Se2-P1-Se1	97.2(1)°

The P-Se-four membered rings of **3.1b** and **3.1c** are planar, with the sum of the angles in the ring being very close to 360°. The ring structure in **3.1a** is slightly distorted, with the angles adding up to 354.1(1)°. In each cation, the angles at the selenium atoms are smaller (80.9(1)° – 83.3(1)°) than the angles at the phosphorus atom (95.8(1)° – 97.3(1)°). The opposing angles in each ring are almost equal. The coordination sphere of the phosphorus atoms is distorted tetrahedral. The structures of the diphenyl- and diisopropylchlorophosphine selenide are not known , but a comparison of the P-Se distances with a typical trialkylphosphine selenide (mean value of 2.121 Å, CCDC database) shows that the P-Se bond lengths in cations **3.1** are significantly longer (Table 3.2). They are comparable to the P-Se bond lengths in the diphosphonium diselenides (2.26-2.28 Å) (Chapter 2)[12,16–19] which also contain a phosphonium moiety connected to a selenium atom via a formal single bond.

Reactions of **3.1a** with Lewis bases and coordinating solvents such as acetonitrile or diethyl ether yielded the original diphenylchlorophosphineselenide.

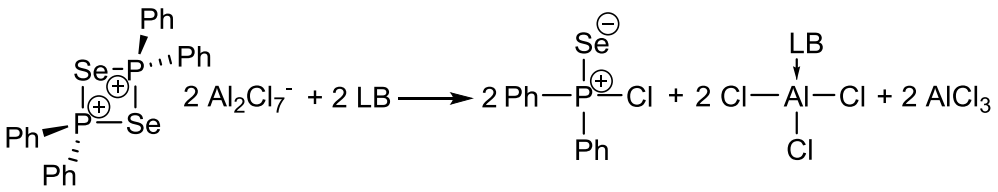

*Scheme 3.8: Decomposition of **3.1a** upon addition of a Lewis Base (LB).*

It appears that a solvent-aluminium chloride complex is formed, thereby setting free the chloride form the $Al_2Cl_7^-$ anion which in turn breaks up the P-Se-ring (Scheme 3.8). Attempts at exchanging the anion with $NaPF_6$ or NaBARF[24] resulted in the decomposition of **3.1a**, with the $^{31}P\{^1H\}$ NMR spectrum showing multiple unidentified peaks.

In contrast, the reaction of **3.1a** with triphenylantimony, which despite its lone pair is hardly Lewis basic, led to surprising results. The $^{31}P\{^1H\}$ NMR spectrum of the reaction mixture (Figure 3.5) contains, aside from many unidentified peaks, an AB_2 spin system, which does not appear to have any ^{77}Se satellite signals.

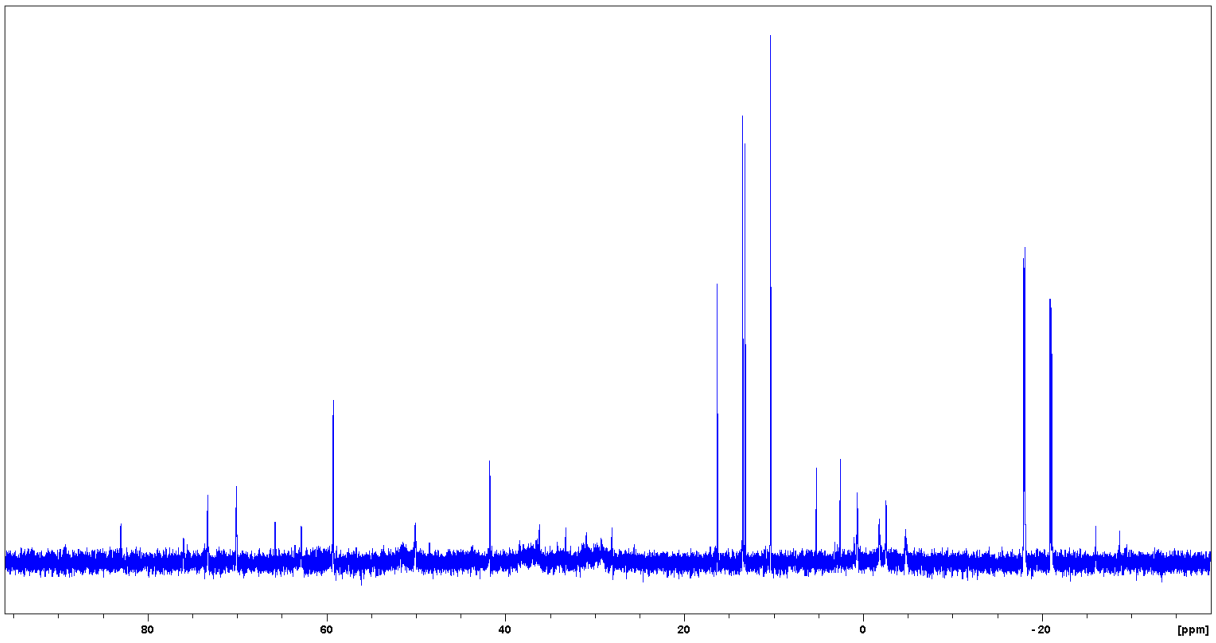

*Figure 3.5: $^{31}P\{^{1}H\}$ NMR spectrum of the reaction of **3.1a** with Ph_3Sb.*

An iterative simulation of the AB_2 system with gNMR[20] (Figure 3.6) provided the following values: δ(A) = 13.2 ppm, δ(B) = -19.4 ppm and J_{AB} = 362 Hz.

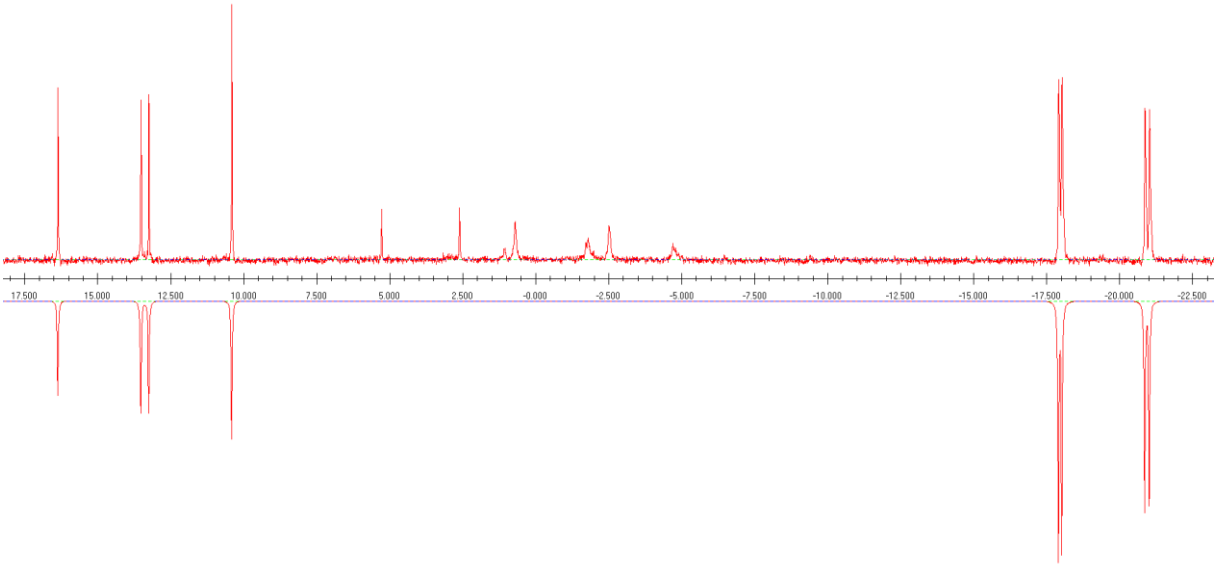

*Figure 3.6: Simulated (bottom) and experimental (top) $^{31}P\{^{1}H\}$ NMR spectra of the reaction mixture of **3.1a** with $SbPh_3$.*

These NMR spectroscopic values are in the range of a diphosphinophosphonium cation, examples of which have been reported previously.[21] The values for the hexaphenyl diphosphinophosphonium cation (Scheme 3.9) have been reported as 18 ppm, -22 ppm and J_{PP} = 365 Hz.[21]

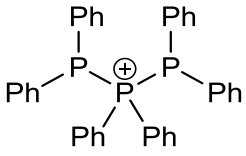

Scheme 3.9: Hexaphenyl diphosphinophosphonium cation.[21]

However, upon standing for several weeks, a crystal formed from the reaction solution and was identified as compound **3.2**$(AlCl_4)_2$ (Figure 3.7) by single crystal x-ray diffraction. The salt crystallised in the P-1 space group. Its asymmetric unit contains one cation (**3.2**) accompanied by two $AlCl_4^-$ anions. The closest contact between cation and anion occurs between Cl2 and one of the C1 protons (2.532(2) Å).

*Table 3.3: Selected structural parameters of cation **3.2**.*

Distances		Angles	
P1-Se1	2.238(2) Å	P1-Se1-C1	98.0(2)°
Se1-C1	1.934(8) Å	Se1-C1-P2	113.4(3)°
C1-P2	1.816(7) Å	C1-P2-Se2	103.8(2)°
P2-Se2	2.223(2) Å	P2-Se2-P1	91.7(1)°
Se2-P1	2.255(2) Å	Se2-P1-Se1	107.3(1)°

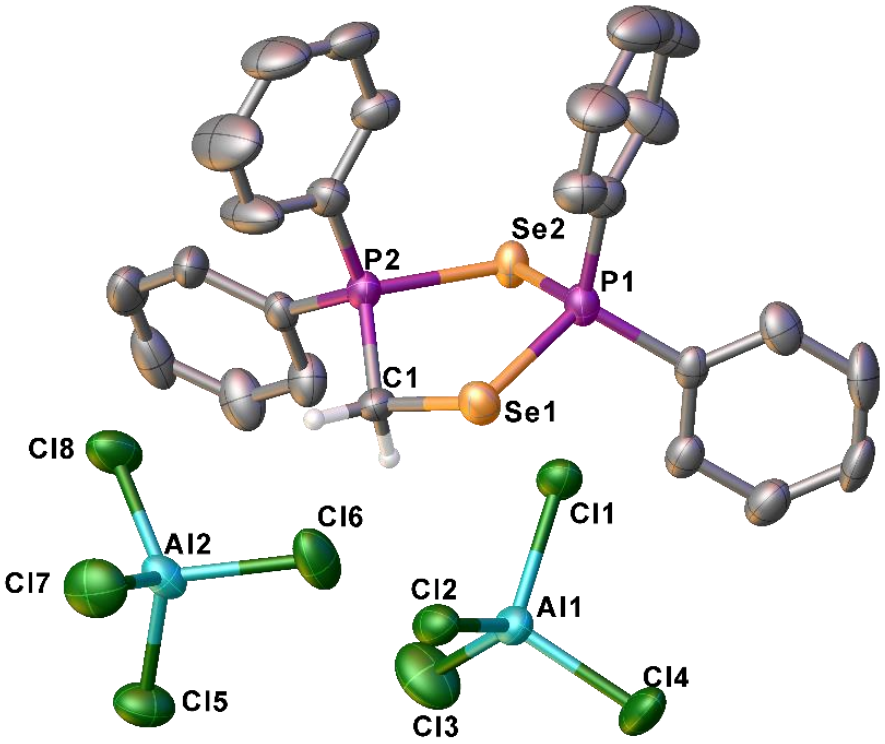

*Figure 3.7: Solid state structure of **3.2**$(AlCl_4)_2$, phenyl hydrogen atoms are omitted for clarity, ellipsoids at 50 % probability level.*

The P-Se bonds in **3.2** are marginally shorter than the P-Se bonds in cations **3.1**, but still longer than the typical bond of a phosphine selenide (see above). The P2-C1 bond (1.934(8) Å) is longer than the distances between the P atoms and the exocyclic C atoms (1.767(6) Å – 1.788(7) Å). The Se1-C1 bond is 1.934(8) Å long, which is close to the sum of the covalent radii (1.16 Å + 0.75 Å = 1.91 Å).[22] The angles at the Se atoms remain close to 90° with the angle at the Se2 atom being significantly smaller than the angle at the Se1 atom. The angles around the P atoms approach the tetrahedral optimum, which leads to an out-of-plane

distortion of the ring. The Se1-C1-P2 angle is the largest within the ring with 113.4(3)°. Selected structural parameters are summarised in Table 3.3.

The exact mechanism for the formation of cation **3.2** is unknown, but it appears as if by a redox reaction the solvent (dichloromethane) was reduced by triphenylantimony and formally a CH_2 carbene was inserted into the ring of cation **3.1a**.

The discovery of cation **3.2**, provided the inspiration to investigate further possible ring extensions of cation **3.1a**. Therefore **3.1a** was allowed to react with an additional equivalent of grey selenium at 140 °C in a melt (Scheme 3.10).

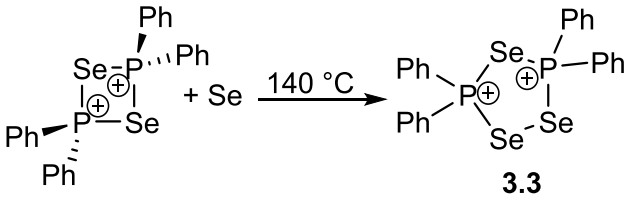

*Scheme 3.10: Reaction of **3.1a** with grey selenium, resulting in **3.3**.*

The result was an oily red substance which appeared to consist of a single product based on the $^{31}P\{^{1}H\}$ NMR spectrum. The spectrum shows one large singlet peak with a rather complex pattern of satellite signals (Figure). The large singlet peak indicates that there is only one type of ^{31}P environment in the molecule, indicating either a single nucleus or a symmetric product.

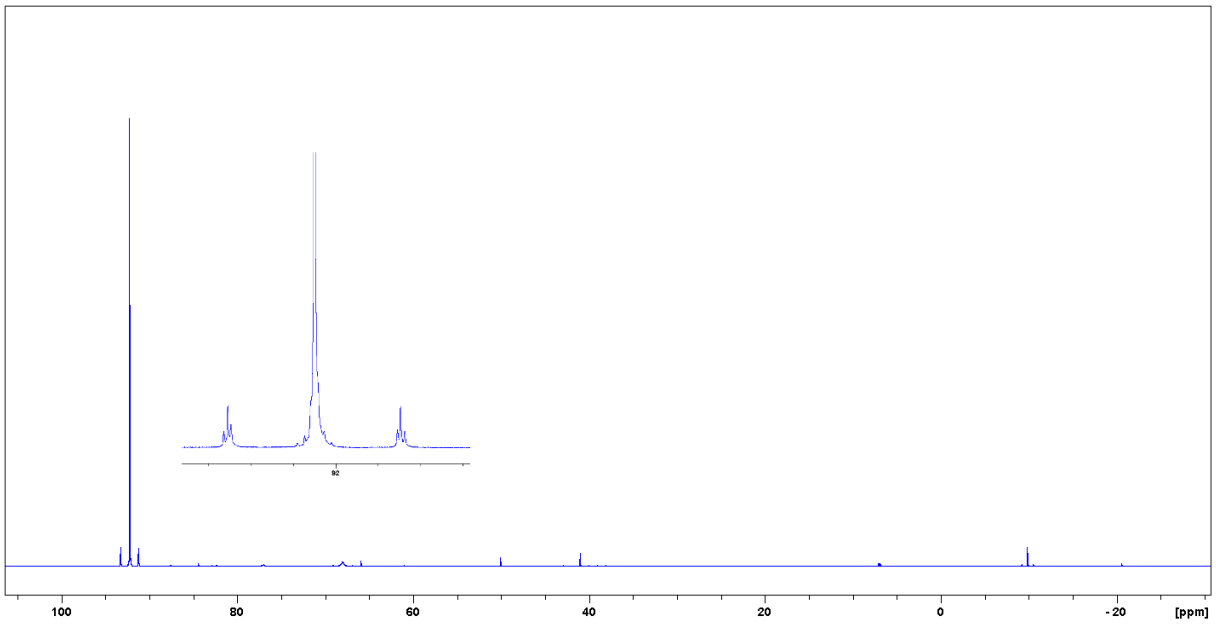

*Figure 3.8: $^{31}P\{^{1}H\}$ NMR spectrum of the product from the reaction of **3.1a**$(Al_2Cl_7)_2$ with grey selenium.*

The pattern of the ^{77}Se satellite signals correspond to the overlapping A parts of an AA'X (eight lines, some of which overlap with the main peak) and an A_2Y spin system (two lines) (Figure 3.10). This indicates multiple different ^{77}Se nuclei, at least one of which couples differently to two otherwise identical ^{31}P nuclei resulting in the AA'X spin system. Whereas the ^{77}Se nucleus responsible for the A_2Y spin system couples equally to the two ^{31}P nuclei. Based on these observations the structure of cation **3.3** was derived.

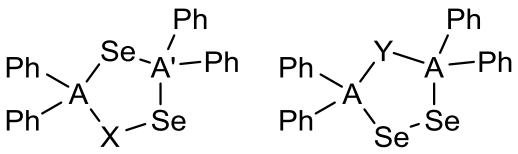

*Scheme 3.11: Spin systems of **3.3:** AA'X (left) and A_2Y (right).*

The ^{31}P NMR spectrum of 3.3 was then simulated using gNMR[20] and iteratively fitted to the experimental spectrum (Figure 3.9), yielding the coupling constants presented in Table 3.4.

*Table 3.4: NMR spectroscopic coupling constants for **3.3**.*

$^2J_{AA'}$	16.66 Hz
$^1J_{AX}$	-414.54 Hz
$^2J_{A'X}$	30.28 Hz
$^1J_{AY}$	412.75 Hz

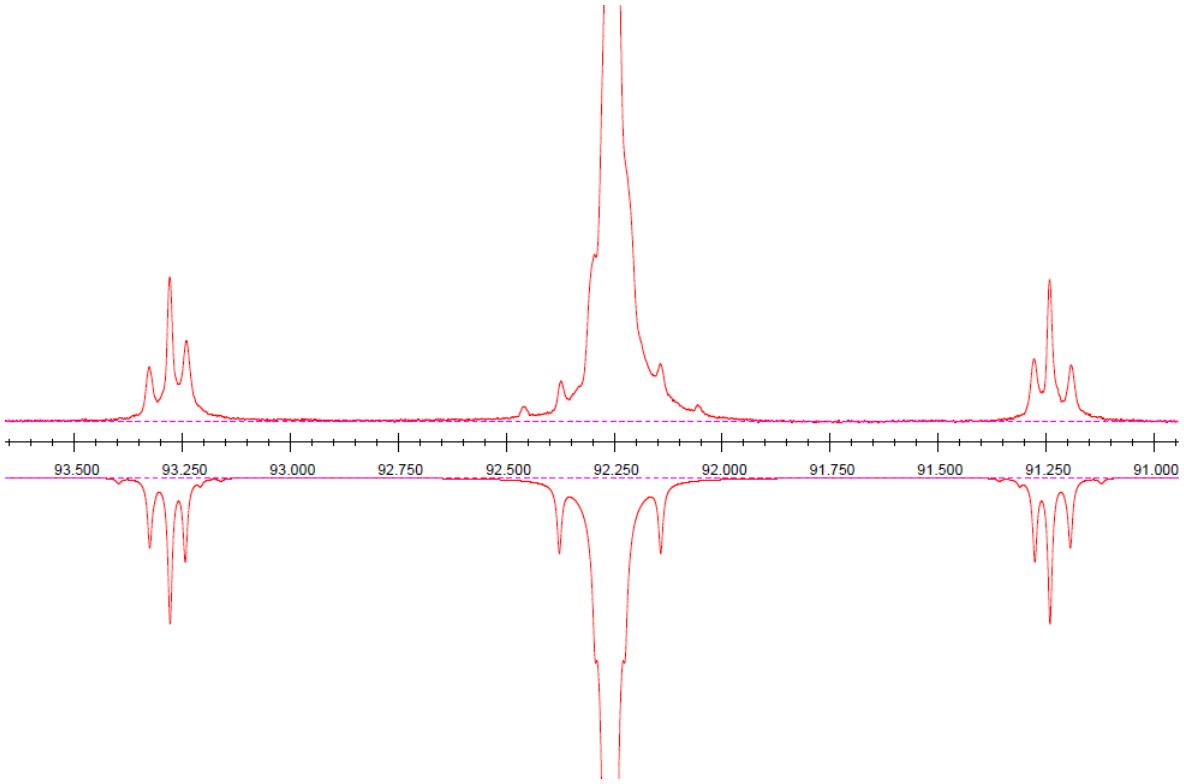

*Figure 3.9: Experimental (top) and simulated (bottom) $^{31}P\{^1H\}$ NMR spectra of **3.3**, the ^{13}C nuclei were not included in this simulation, therefore their satellite signals are not visible in the simulated spectrum, although they appear in the experimental spectrum.*

A $^{77}Se\{^{1}H\}$ NMR spectrum of the product (Figure 3.10) further supports the structure deducted from the $^{31}P\{^{1}H\}$ spectrum.

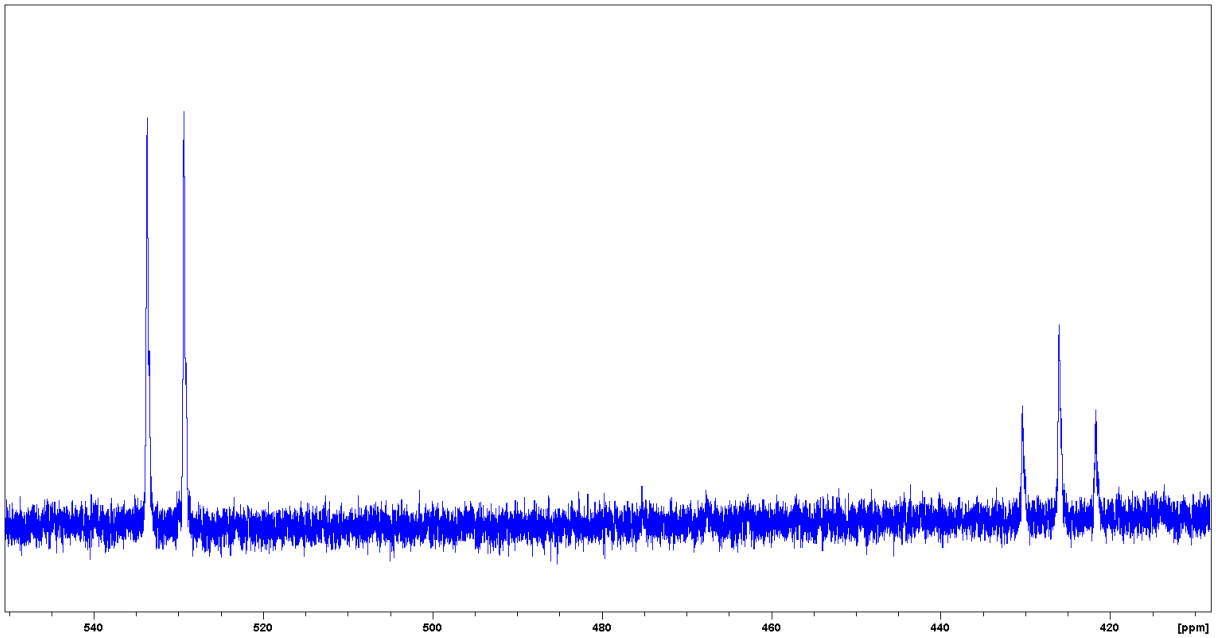

*Figure 3.10: $^{77}Se\{^{1}H\}$ NMR spectrum of **3.3**.*

It exhibits a triplet signal (426 ppm $^{1}J_{PSe}$ = 412 Hz), corresponding to the Y part of the A_2Y spin system, and a doublet signal (531 ppm, $^{1}J_{PSe}$ = 414 Hz) corresponding to the X part of the AA'X spin system.

Reactions of **3.1a** with more than one equivalent of selenium led to different products which are assumed to be six-membered and larger cyclic cations, however, none of these could be isolated or conclusively identified. Due to the symmetry of a six-membered ring, which makes all nuclei equivalent, this ring cannot be readily identified by NMR spectroscopy.

Conclusion

In conclusion, this chapter presents two derivatives of the dimer of an unstabilised three coordinate selenophosphonium cation (cations **3.1a** and **3.1b**) as heptachlorodialuminate salts. Experiments with Lewis bases led to the conclusion, that their monomeric form is not readily accessible. However, their cyclic structure can be extended to form larger rings, as is evident by the two examples (cations **3.2** and **3.3**) identified by single crystal x-ray diffraction (**3.2**) or $^{31}P\{^{1}H\}$ and $^{77}Se\{^{1}H\}$ NMR spectroscopy (**3.3**). The mechanism of these ring extension reactions remains unknown.

References

[1] A. Schmidpeter, G. Jochem, K. Karaghiosoff, C. Robl, *Angew. Chem. Int. Ed.* **1992**, *31*, 1350–1352.

[2] J. J. Weigand, N. Burford, D. Mahnke, A. Decken, *Inorg. Chem.* **2007**, *46*, 7689–7691.

[3] N. Burford, R. E. V. H. Spence, R. D. Rogers, *J. Am. Chem. Soc.* **1989**, *111*, 5006–

5008.

[4] M. A. Wünsche, T. Witteler, F. Dielmann, *Angew. Chem. Int. Ed.* **2018**, *57*, 7234–7239.

[5] N. Burford, R. E. v. H. Spence, R. D. Rogers, *J. Chem. Soc. Dalton Trans.* **1990**, 3611–3619.

[6] P. Bhattacharyya, A. M. Z. Slawin, J. D. Woollins, *J. Chem. Soc. Dalt. Trans.* **2001**, *2*, 300–303.

[7] J. D. Woollins, *Synlett* **2012**, *23*, 1154–1169.

[8] S. Parveen, P. Kilian, A. M. Z. Slawin, J. D. Woollins, *Dalton Trans.* **2006**, *59*, 2586–2590.

[9] K.-O. Feldmann, T. Wiegand, J. Ren, H. Eckert, J. Breternitz, M. F. Groh, U. Müller, M. Ruck, B. Maryasin, C. Ochsenfeld, et al., *Chem. Eur. J.* **2015**, *21*, 9697–9712.

[10] M. Gonsior, I. Krossing, E. Matern, *Chem. Eur. J.* **2006**, *12*, 1703–1714.

[11] O. Schön, Organophosphorchalkogenide Erste Phosphor-Chalkogen-Kationen Neue Heterocyclen Und Selenophosphonate, Ludwig-Maximilians-Universität München, **2007**.

[12] J. Konu, T. Chivers, H. M. Tuononen, *Inorg. Chem.* **2006**, *45*, 10678–10687.

[13] A. V. Il'Yasov, I. A. Nuretdinov, *Phosphorus. Sulfur. Silicon Relat. Elem.* **1998**, *136*, 479–482.

[14] N. Burford, B. W. Royan, R. E. v. H. Spence, R. D. Rogers, *J. Chem. Soc. Dalton Trans.* **1990**, 2111–2117.

[15] S. Alvarez, *Dalton Trans.* **2013**, *42*, 8617.

[16] M. J. Poller, N. Burford, K. Karaghiosoff, *Chem. Eur. J.* **2018**, *24*, 85–88.

[17] F. N. Blanco, L. E. Hagopian, W. R. Mcnamara, J. A. Golen, A. L. Rheingold, C. Nataro, *Organometallics* **2006**, *2*, 4292–4300.

[18] G. R. Willey, J. R. Barras, M. D. Rudd, M. G. B. Drew, *J. Chem. Soc. Dalton Trans.* **1994**, 3025–3029.

[19] S. E. Denmark, E. Hartmann, D. J. P. Kornfilt, H. Wang, *Nat. Chem.* **2014**, *6*, 1056–1064.

[20] P. H. M. Budzelaar, **2006**.

[21] N. Burford, C. A. Dyker, A. Decken, *Angew. Chem. Int. Ed.* **2005**, *44*, 2364–2367.

[22] P. Pyykkö, M. Atsumi, *Chem. Eur. J.* **2009**, *15*, 186–197.

Chapter 4: Unexpected Results

Introduction

This chapter presents several new compounds that have been discovered during the work for this dissertation. However, these compounds were not planned or synthesised on purpose, but discovered accidentally in the pursuit of other goals. They are presented here either because their discoveries provide us insights in the potential reactivity of cations from Chapter 1 or because they can be considered starting points for interesting research in other directions.

The majority of the compounds presented here were discovered in crystallisation attempts of the reaction mixtures of Chapter 1 (**4.1**, **4.2**, **4.3**OTf). They provide an insight in the potential reactivity and decomposition pathways of the cations presented in Chapter 1. Other compounds (*i.e.* **4.4**OTf and **4.5**OTf) are the result of different reactions that are not part of any project presented in this dissertation. They are presented in this Chapter because they are interesting new molecules that should be the topic of future investigations. Experimental details for all the discoveries are presented in the respective section of Chapter 5.

All the here presented compounds have in common, that they were only encountered in small quantities, usually a single crystal. Therefore they were mainly characterised by single crystal x-ray diffraction.

These discoveries show that these compounds can be synthesised, although they do not provide a specific synthetic procedure. Therefore this chapter is also meant as an inspiration for future research with the possible goal of finding a synthetic route and further investigating the properties and reactivity of these molecules.

$Me_2P(Se)$-Se-Se-$P(Se)Me_2$ – 4.1

The isopropyl derivative of compound **4.1** (**4.1(*i*Pr)**) was found in the crystallisation experiments of several reactions of phosphinophosphonium cations with selenium. **4.1(*i*Pr)** has previously been reported as the result of the reaction of $(^iPr)_2PSiCl_3$ with selenium (Scheme 4.1).[1]

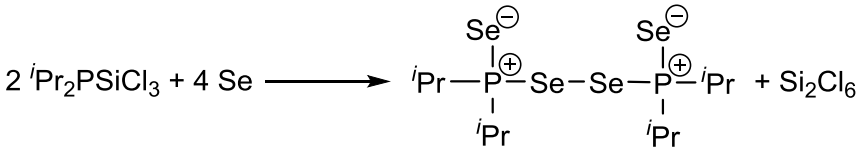

*Scheme 4.1: Synthesis of $^iPr_2P(Se)$-Se-Se-$P(Se)^iPr_2$ (**4.1(*i*Pr)**).[1]*

Although it is likely that the methyl derivative can be synthesised in the same way, it has not been reported yet and is therefore presented here. The presented structure is the result of the attempt to crystallise products of the reaction of **1.1(Me_3Me_2)**OTf with 2.5 equivalents of selenium by vapor diffusion of diethyl ether into the acetonitrile solution of the reaction products.

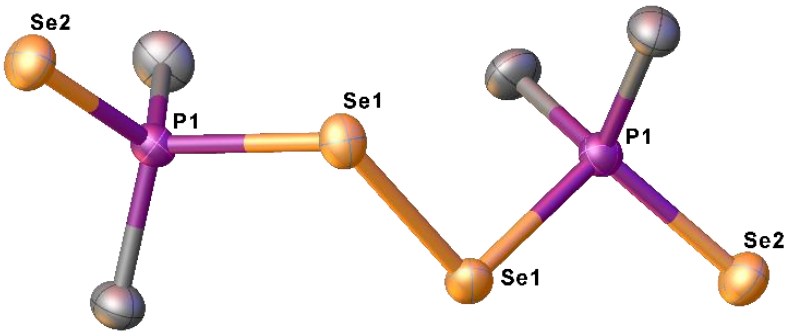

*Figure 4.1: Solid state structure of **4.1(Me)**, hydrogen atoms are omitted for clarity, thermal ellipsoids are drawn at 50 % probability level.*

4.1(Me) crystallised in the space group I2/a, with the asymmetric unit composed of half the molecule (Figure 4.1). Selected structural features of **4.1(Me)** and its ^{i}Pr derivative are shown in Table 4.1.

*Table 4.1: Selected structural features of **4.1(Me)** in comparison with the ^{i}Pr derivative.*

	4.1(Me)	**4.1(^{i}Pr)[1]**
Space Group	I2/a	C2/c
Distances		
P1-Se1	2.241(2) Å	2.243(1) Å
P1-Se2	2.111(3) Å	2.116(1) Å
Se1-Se1	2.351(2) Å	2.384(1) Å
Angles		
Se2-P1-Se1	104.0(1) °	100.91(3) °
P1-Se1-Se1	104.8(1) °	107.65(3) °
P1-Se1-Se1-P1	106.8(1) °	118.43(1) °

The phosphorus-selenium distances of **4.1(Me)** are very similar to the distances of the ^{i}Pr derivative, with the P1-Se2 distance being significantly shorter than the P1-Se1 distance. The Se1-Se1 distance is slightly longer in the ^{i}Pr derivative. The P1-Se1-Se1 angle of **4.1(Me)** is smaller than the respective angle in the ^{i}Pr derivative, which is closer to the ideal tetrahedral angle. The P1-Se1-Se1-P1 torsion is larger in the ^{i}Pr derivative.

Overall the structure of **4.1(Me)** is very similar to its ^{i}Pr derivative and it is likely that it can be synthesised via the same route. Nevertheless it is new, previously unreported compound and its discovery may be the incentive for further investigations of the reactivity or decomposition pathways of cations **1.2**, **1.3** and **1.4**.

Phosphinoselenoic Anhydride – 4.2

The air and moisture sensitive nature of phosphorus selenium compounds is well known and is readily evident by the smell of H_2Se or the formation of elemental selenium every time a sample is exposed to air. However, the intermediate compounds between the original phosphorus selenium compound and the products of total decomposition usually are not easily available to be studied. In this respect, compound **4.2** (Figure 4.2) is a fortunate discovery. The original reaction was between **1.1(Me$_3$^{i}Pr$_2$)**OTf and one eqv. of grey selenium in acetonitrile. However, over the course of several weeks, the sample must have been contaminated with moisture, leading to the formation of crystals of **4.2** (Scheme 4.2).

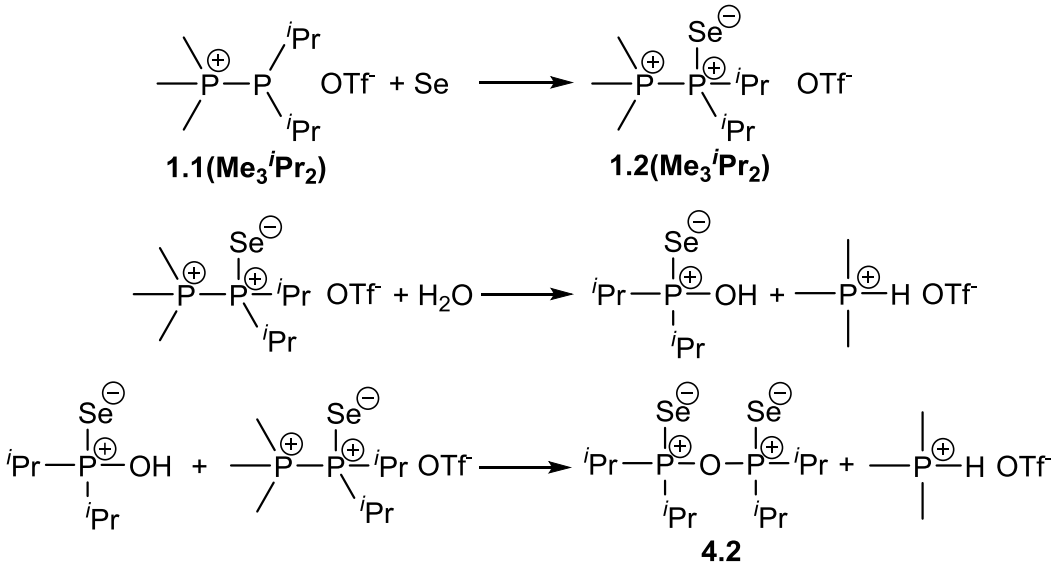

*Scheme 4.2: Proposed mechanism for the formation of **4.2**.*

4.2 is a neutral compound with two ^{i}Pr$_2$P(Se) moieties bridged by an oxygen atom. While several examples of similar compounds are known, they do not usually contain two different chalcogen elements. It has been identified and characterised by single crystal x-ray diffraction (Figure 4.2).

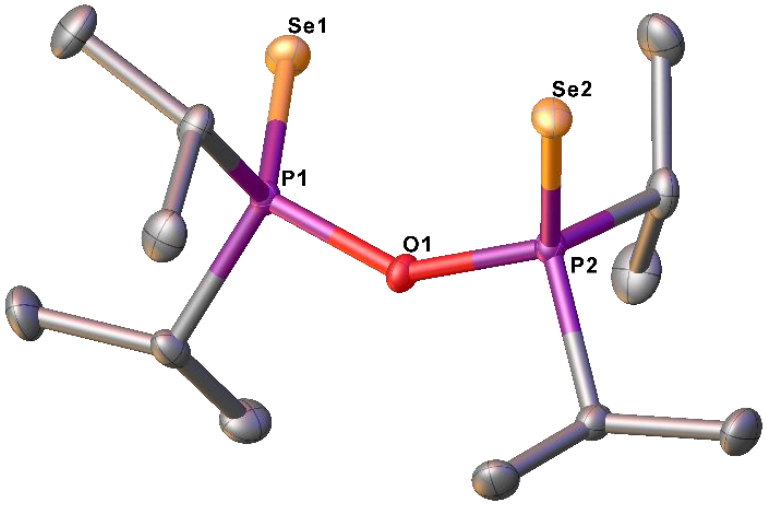

*Figure 4.2: solid state structure of **4.2**, hydrogen atoms are omitted for clarity, thermal ellipsoids are drawn at 50 % probability level.*

This is only the second derivative with two terminal selenium atoms and one bridging oxygen atom that has been structurally characterised. The structure of the phenyl derivative was reported in 1994 by P.G. Jones *et al.*[2] A comparison of selected structural parameters is shown in Table 4.2.

*Table 4.2: Selected structural parameters of **4.2** in comparison with diphenylphosphinoselenoic anhydride ($Ph_2P(Se)$-O-$P(Se)Ph_2$)[2].*

Distances	**4.2**	**$Ph_2P(Se)$-O-$P(Se)Ph_2$**[2]
P-Se	2.085(1) Å 2.091(1) Å	2.071(1) Å
P-O	1.625(2) Å	1.624 Å
Angles		
P-O-P	143.3(1)°	134.9 °

The structural parameters of **4.2** and Jones' diphenylphosphoinoselenoic anhydride are quite similar in respect to the bond length. However, the P-O-P angle is significantly larger in **4.2**. It is also worth noting, that in both compounds the P-O-P angle is much larger than the P-S-P angle reported for **1.7($Me_3^{i}Pr_2$)** (Table 1.4 Chapter 1) and **^{t}Bu_2P-S-P^tBu_2**[3] (106.3° and 103.3° respectively) which is in line with the common understanding that heavier atoms have a tendency for smaller (closer to 90°) angles.

In conclusion, **4.2** is a new derivative of a rare class of compounds. It is likely that the procedure used by P. G. Jones et al. is also applicable for the synthesis of compound **4.2**.

This new compound is of interest in this context, because it gives an insight into the reactivity of the products presented in Chapter 1.

Unexpected Reaction with Acetonitrile – 4.3OTf

This compound has been discovered in the crystallisation attempt of the reaction mixture of **1.1(Ph$_3$Pr$_2$)**OTf with two equivalents of grey selenium in acetonitrile. After stirring the reaction mixture for over a week, it was layered with diethyl ether and cooled to -35 °C. Over the time of several weeks, additional diethyl ether was added repeatedly while the mixture was stored at -35 °C, until eventually crystals formed. One of the crystals was suitable for x-ray diffraction and was identified as the triflate salt of **4.3** (Figure 4.3).

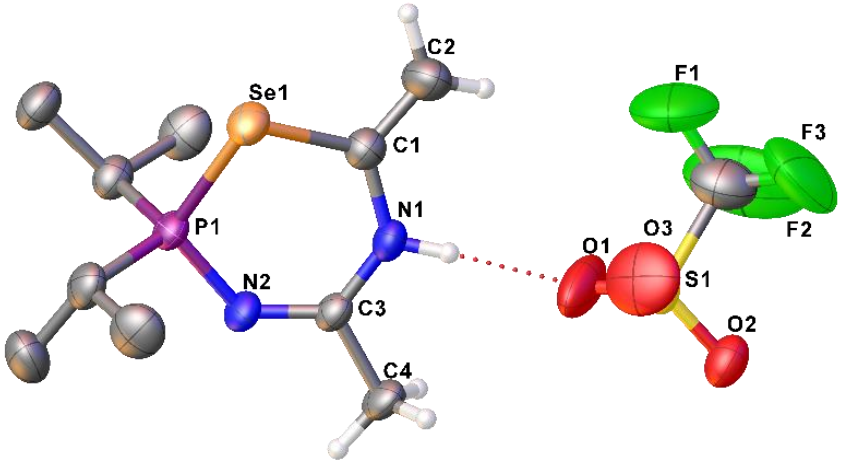

*Figure 4.3: Solid state structure of **4.3**OTf, isopropyl hydrogen atoms are omitted for clarity, thermal ellipsoids are drawn at 50 % probability level.*

Cation **4.3** appears to be the result of the reaction of a diisopropyl-selenophosphonium (^{i}Pr$_2$PSe$^+$) cation with acetonitrile. This was likely facilitated by the weak donor properties of Ph$_3$PSe, which in turn led to the separation of **1.4(Ph$_3$^{i}Pr$_2$)** into the aforementioned diisopropyl-selenophosphonium cation and free Ph$_3$PSe (Scheme 4.3).

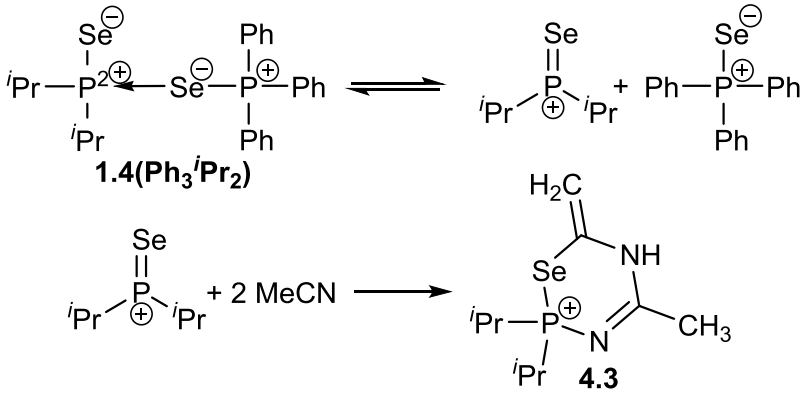

*Scheme 4.3: proposed formation of **4.3**OTf.*

Ph$_3$PSe was identified in the ^{31}P{^{1}H} NMR spectra of the reaction mixture and in the precipitate, from which the crystal was taken. However, the exact mechanism of the formation of **4.3**OTf remains unknown.

In the solid state structure, one of the O atoms of the triflate anion is situated close to the N1 proton (O-H = 1.966 Å), suggesting a hydrogen bond. In the cation, the C1-C2 bond is

significantly shorter than the C3-C4 bond indicating a double bond between C1 and C2 with C2 being a CH_2 group rather than a CH_3 moiety. The ring is not quite planar due to the small angle at the Se atom, which is close to 90°, and the almost tetrahedral environment of the P atom. The torsion between the atoms N2-P-Se-C1 makes any π interaction of the Se atom with the rest of the ring unlikely. The C1-N1-C3-N2 torsion on the other hand is very small, making this fragment almost planar. Selected structural features are presented in Table 4.3.

*Table 4.3: Selected structural parameters of cation **4.3**.*

Distances	
P-Se	2.218(1) Å
C1-C2	1.323(5) Å
C3-C4	1.490(4) Å
Angles	
N2-P-Se	109.7(1)°
P-Se-C1	93.3(1)°
N2-P-Se-C1	26.3(1)°
C1-N1-C3-N2	2.9(5)°

Cationic heterocycles containing a phosphonium center and a selenium atom are fairly rare, therefore it is difficult to find a comparison to this structure. Two examples of such selenophosphonium heterocycles (aside from the compounds presented in Chapter 3) have been reported by Tristram Chivers *et al.* and Paul Ragogna *et al.* respectively (Scheme 4.4).[4,5]

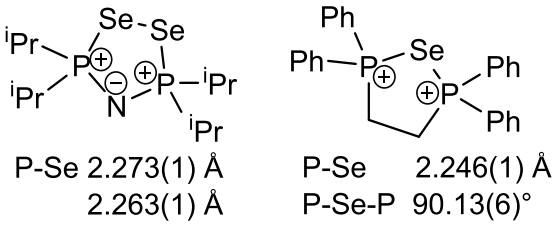

Scheme 4.4: Cyclic selenophosphonium cations by T. Chivers[4] (left) and P. Ragogna[5] (right).

They reported slightly longer bond length for the P-Se bond and observed close to tetrahedral arrangements on the phosphorus atoms. P. Ragogna *et al.* report a P-Se-P angle of almost 90°.

Although attempts to reproduce crystalline material of **4.3**OTf were unsuccessful, they led to the discovery of **4.4**OTf. This singular result implies a potential for cations **1.4,** or selenophosphonium cations in general, to be used in small molecule activation and should therefore be considered a starting point for future investigations in that direction.

A Cubic Silver Cluster – 4.4OTf

The here presented cationic silver cluster (**4.4**OTf) has been discovered in an attempt to reproduce the above presented cation **4.3** without any interfering byproducts. For this purpose, diisopropyl-chloro-phosphine-selenide was dissolved in acetonitrile and one equivalent of silver triflate was added in order to abstract the halide. Surprisingly no silver chloride precipitated upon dissolving the silver triflate. Instead, after standing for four days, protected from light, colourless crystals formed. The crystals were poorly soluble in fresh solvent. However, a $^{31}P\{^{1}H\}$ NMR spectrum was obtained, showing a singlet peak at 74.5 ppm with Se satellite signals ($^{1}J_{PSe}$ = 530 Hz). Another crystal was used for structure determination by single crystal x-ray diffraction, revealing the structure of compound **4.4**OTf (Figure 4.4).

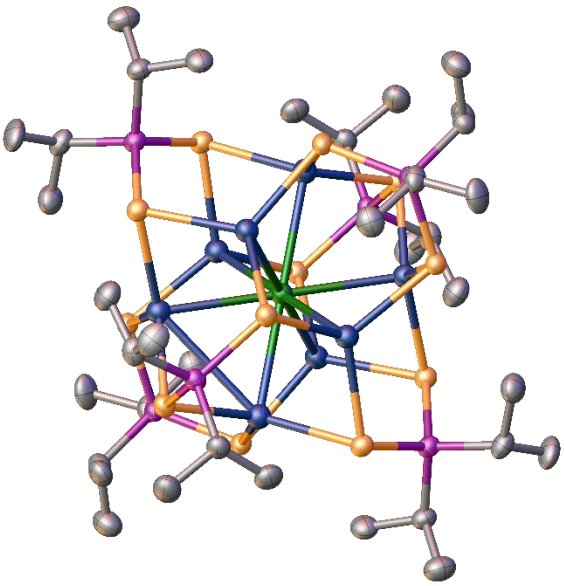

*Figure 4.4: Solid state structure of **4.4**, hydrogen atoms and triflate anion are omitted for clarity, thermal ellipsoids are drawn at 50 % probability level.*

In the solid state, the cationic cluster and a triflate anion are well separated. The triflate anion is highly disordered and could not be modeled successfully. However, its presence has been confirmed by $^{19}F\{^{1}H\}$ NMR spectroscopy. The cationic cluster consists of a cubic arrangement of silver atoms with a chlorine atom in the center of this cube.

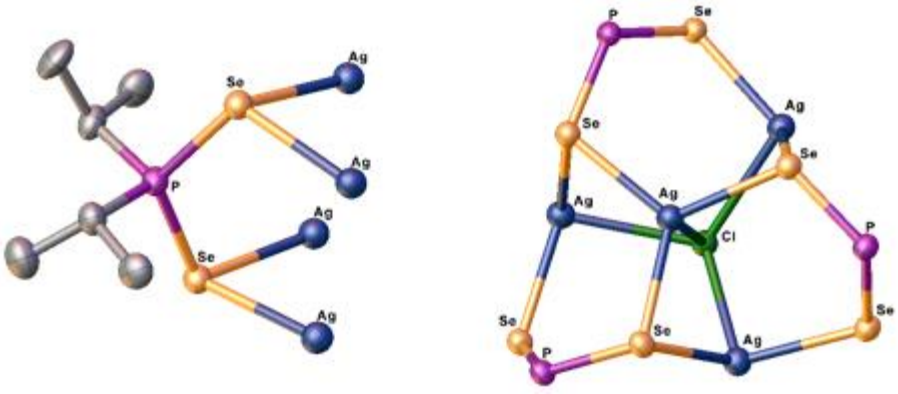

*Figure 4.5: Ligand of **4.4**OTf (left) (hydrogen atoms are omitted for clarity) and environment of an Ag atom in **4.4**OTf (right), thermal ellipsoids are drawn at 50 % probability level.*

An $^{i}Pr_2PSe_2^-$ ligand sits on top of each face of the cube (Figure 4.5), each Se atom coordinates to two silver atoms over each edge of the cube. Selected structural features are shown in Table 4.4.

*Table 4.4: Selected structural parameters of **4.4**.*

Distances	
Ag-Ag	3.323(1) Å
Se-Ag	2.690(1) Å
P-Se	2.193(2) Å
Ag-Cl	2.875(1) Å
Angles	
Ag-Se-Ag	77.0(1)°
Se-P-Se	118.3(1)°
Ag-Ag-Ag	89.9(1)°

Similar clusters, not of silver cations but Cu(I) cations, have been reported by C.W. Liu and B. A. Trofimov *et al.* in 2012.[6] The Cu-Cu, Se-Cu and Cu-Cl distances reported in their work are all shorter than the respective distances in **4.4**, which is consistent with the small radius of the Cu(I) ions. However, their P-Se bond length (2.191(3) Å) as well as the Cu-Cu-Cu (89.25(5)°-90.88(5)°), and Se-P-Se (119.2°-119.8°) angles are in good agreement with the respective values in cation **4.4**. The Cu-Se-Cu angles (82.00(5)°-83.36(5)°) are larger than the Ag-Se-Ag angles in **4.4**, which is consistent with the shorter Cu-Se bond.[6]

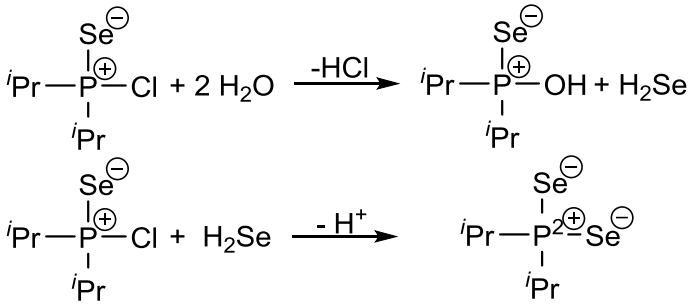

*Scheme 4.5: Proposed mechanism for the formation of the ligand in **4.4**OTf.*

Overall, this cubic cluster of silver atoms with its phosphorus-selenium ligand was a surprising result. The formation of this compound is speculated to have been initiated by contamination with moisture, leading to the *in-situ* generation of H_2Se, which in turn reacted with the starting material to form the $(R_2PSe_2)^-$ ligand (Scheme 4.5). The self-assembly of the cubic cluster of silver atoms held together by this ligand is what makes this compound interesting.

A Lewis Base stabilised OPS cation – 4.5OTf

The here presented OPS^+ cation (**4.5**) was the byproduct of a project which attempted to synthesise phosphorus-sulfur cations by abstracting chloride anions from $SPCl_3$. Specifically, $SPCl_3$, three equivalents of 4-dimethylaminopyridine and three equivalents of trimethylsilyltriflate were dissolved in acetonitrile. Crystals of **4.5**OTf (Figure 4.6) were discovered after four months of attempting to crystallise the reaction products by vapor diffusion of diethyl ether into the reaction solution. The introduction of the oxygen atom on the phosphorus is likely due to contamination with moisture over the four months' time. Cation **4.5** is the first of its kind ever discovered. However, similar PS_2^+ cations, PS_2Pyr_2Br[7], PS_2Pyr_2I[7] and PS_2DMAP_2OTf[8] have been reported previously.

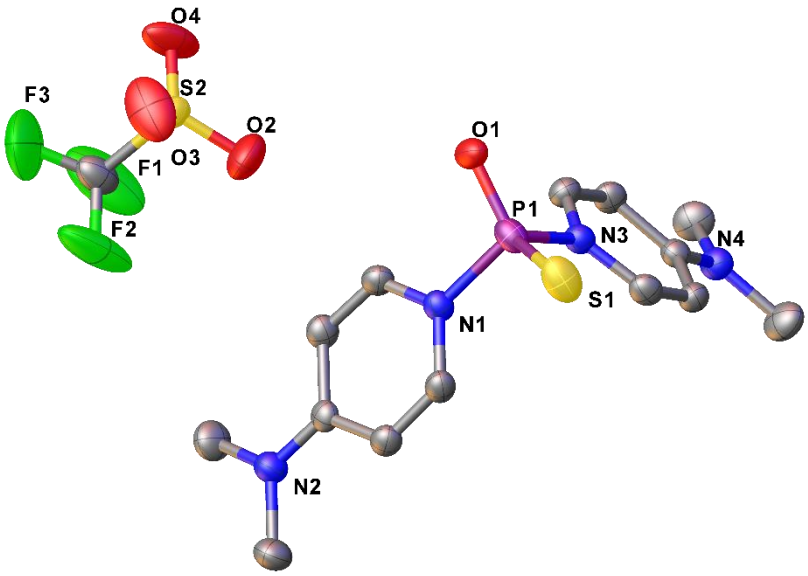

*Figure 4.6: Solid state structure of **4.5**OTf, hydrogen atoms are omitted for clarity, thermal ellipsoids are drawn at 50 % probability level.*

4.5OTf crystallised in the space group P-1 with cation and anion well separated. Selected structural features of **4.5**OTf in comparison to PS_2Pyr_2Br[7] and PS_2DMAP_2OTf[8] are summarized in Table 4.5. The P-S bond is a bit shorter than the P-S bonds in the comparable $PS_2Pyr_2^+$ and $PS_2DMAP_2^+$. The P-N distances are overall in a similar range within the sum of the covalent radii (1.11 Å + 0.71 Å = 1.82 Å)[9] with the exception of one of the P-N bonds in $PS_2Pyr_2^+$. The P-O distance in 4.5 is much shorter than the sum of the covalent radii (1.11 Å + 0.63 Å = 1.74 Å).[9]

*Table 4.5 Selected structural parameter of **4.5OTf** in comparison to PS_2^+ cations.*

Distances	**4.5**OTf	**PS_2Pyr_2Br**[7]	**PS_2DMAP_2OTf**[8]
P-O	1.503(3) Å	n.a.	n.a.
P-S	1.902(1) Å	1.919(2) Å 1.910(2) Å	1.9309(8) Å 1.9321(8) Å
P-N	1.773(3) Å	1.874(13) Å	1.782(2) Å

	1.758(3) Å	1.768(14) Å	1.798(2) Å
Angles			
O-P-S / S-P-S	124.0(1) °	123.75(9) °	124.09(4) °
N-P-N	98.8(1) °	94.2(2) °	96.77(8) °

The O-P-S angle of **4.5** is comparable to the S-P-S angle of $PS_2DMAP_2^+$, which is only slightly larger than the S-P-S angle of PS_2Pyr_2Br. The N-P-N angle is largest in **4.5** and smallest in $PS_2Pyr_2^+$, leading overall to a configuration that lies between a distorted tetrahedral and a seesaw arrangement around the P atom.

Overall, **4.5**OTf is a unique new compound which consists of two different chalcogen atoms combined with phosphorus to form a new phosphorus chalcogen cation. While a reliable synthetic route for this new cation has yet to be developed, the discovery and structural investigation presented here are proof that this is an attainable goal.

References

[1] C. Q. Nguyen, A. Adeogun, M. Afzaal, M. a Malik, P. O'Brien, *Chem. Commun.* **2006**, *274*, 2179.

[2] P. G. Jones, C. Kienitz, C. Thöne, *Zeitschrift für Krist. - Cryst. Mater.* **1994**, *209*, DOI 10.1524/zkri.1994.209.1.82.

[3] S. Yogendra, S. S. Chitnis, F. Hennersdorf, M. Bodensteiner, R. Fischer, N. Burford, J. J. Weigand, *Inorg. Chem.* **2016**, *55*, 1854–1860.

[4] J. Konu, T. Chivers, H. M. Tuononen, *Inorg. Chem.* **2006**, *45*, 10678–10687.

[5] J. W. Dube, M. M. Hänninen, J. L. Dutton, H. M. Tuononen, P. J. Ragogna, *Inorg. Chem.* **2012**, *51*, 8897–8903.

[6] P.-K. Liao, D.-R. Shi, J.-H. Liao, C. W. Liu, A. V. Artem'ev, V. A. Kuimov, N. K. Gusarova, B. A. Trofimov, *Eur. J. Inorg. Chem.* **2012**, *2012*, 4921–4929.

[7] M. Meisel, P. Lönnecke, A.-R. Grimmer, D. Wulff-Molder, *Angew. Chem. Int. Ed.* **1997**, *36*, 1869–1870.

[8] F. D. Henne, F. A. Watt, K. Schwedtmann, F. Hennersdorf, M. Kokoschka, J. J. Weigand, *Chem. Commun.* **2016**, *52*, 2023–2026.

[9] P. Pyykkö, M. Atsumi, *Chem. Eur. J.* **2009**, *15*, 186–197.

Chapter 5: Experimental Details

General Remarks on Experimental Methods

Reactions were performed under an atmosphere of dry nitrogen, either in an MBraun glove box or using standard schlenk procedures.

Reactions in the glove box were carried out in screwcap vials at ambient temperature. When heating was necessary, the reaction mixtures were filled into thick walled glass tubes (reaction bombs) with PTFE screwcaps within the glove box. The sealed glass tubes were then transferred out and heated in an oil bath. After cooling back down to ambient temperature, the tubes were cleaned and transferred back into the glove box, where subsequent treatment, such as filtering etc. took place.

All glassware and heat resistant equipment used for schlenk procedures or in the glove box was dried at 200 °C for at least several hours and evacuated on the schlenk line or in the glove-box antechamber. Heat sensitive equipment, e.g. plastic screwcaps, was generally dried at 60 °C and evacuated in the glove box port for several hours before use.

Reagents and Solvents

All reagents and solvents were purchased from Sigma Aldrich, Alfa Aesar, Strem Chemicals Inc., Fisher Scientific or taken from the inventory of the Burford research group and used without further purification unless otherwise stated.

Anhydrous acetonitrile was purchased from Sigma Aldrich© and stored over dry 3 Å molecular sieves for at least two days before use.

Dichloromethane was dried stirred over calcium hydride, then distilled and subsequently stored over 4 Å molecular sieves.

Diethylether and hexanes (mixture of isomers) was dried over sodium using benzophenone as a colorimetric indicator. Once the blue color indicated dryness the solvent was distilled and subsequently stored over 4 Å molecular sieves.

Molecular sieves were dried at over 300 °C under a dynamic vacuum for two to three days.

Analytical Methods

NMR spectra were measured on a 300 MHz (^{1}H, ^{31}P, ^{13}C, ^{19}F) or a Bruker Avance 360 MHz (^{1}H, ^{31}P, ^{13}C, ^{77}Se). Deuterated solvents for NMR spectroscopy were stored over molecular sieves for at least two days prior to use. NMR spectra of reaction mixtures were measured using a capillary of deuterated acetone inside the sample tube in order to provide a deuterium signal for the lock.

Simulations of NMR spectra were carried out with the gNMR software.[1]

Crystallographic measurements were performed by Prof. Dr. Konstantin Karaghiosoff at Ludwig-Maximilians-University Munich, Germany, using Oxford Xcalibur 3 diffractometer.

The structures were solved and refined using the ShelX programs[2] in the Olex2[3] interface.

IR-Spectroscopy:

IR spectra were recorded on a Thermo Scientific Nicolet IR200 IR spectrometer. In order to prepare the IR sample, a small amount of the respective substance was mixed with hydrocarbon oil and placed between two NaCl plates under an atmosphere of dry N_2 in a glove box. These plates and the hydrocarbon oil offered sufficient protection to take the sample out of the glove box and measure the IR spectrum within a few minutes. However the absorption by the NaCl plates restricts the spectrum to > 650 cm^{-1}.

Elemental Analysis:

Elemental Analysis was performed by Canadian Microanalytical Service Ltd. (http://canmicro.com/).

Melting Points:

Melting points were measured using a Gallenkamp Melting Point Apparatus.

Experiments of Chapter 1: Reactions of Phosphinophosphonium Cations with S_8 and Se

Synthesis of Phosphinophosphonium Cations (1.1($R_3R'_2$)OTf)

The phosphino phosphonium triflate salts were synthesised from the respective trialkyl- (aryl-) phosphine and dialkyl- (diaryl-) chlorophosphine following a previously established procedure (Scheme 5.1).[4,5]

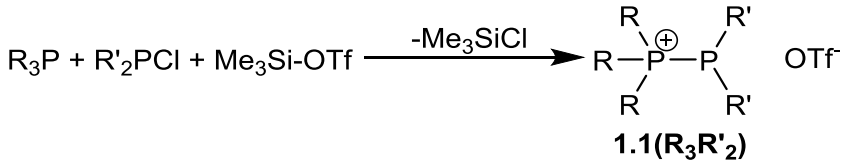

*Scheme 5.1: Synthesis of compounds **1.1**OTf.*

The products were identified by $^{31}P\{^{1}H\}$ NMR spectroscopy as shown in Table 5.1.

Table 5.1: $^{31}P\{^{1}H\}$ NMR data of phosphino phosphonium cations.

Compound	δ (R_3P-) [ppm]	δ (R'_2P-) [ppm]	$^{1}J_{PP}$ [Hz]
1(Me_3Me_2)	17.6	-59.3	276
1(Me_3 $^{i}Pr_2$)	12.1	1.3	325
1(Me_3Ph_2)	15.5	-23.5	294
1(Et_3Et_2)	30.2	-41.5	304
1($^{i}Pr_3Me_2$)	36.2	-54.8	329
1($^{i}Pr_3Et_2$)	38.0	-35.0	335
1($^{i}Pr_3$ $^{i}Pr_2$)	40.5	-0.8	381
1($^{i}Pr_3Cy_2$)	41.1	-8.7	387
1($^{i}Pr_3Ph_2$)	38.3	-26.6	356
1(Cy_3 $^{i}Pr_2$)	29.8	-4.5	386
1(Cy_3Ph_2)	25.3	-22.4	361
1(Ph_3Ph_2)	16.0	-12.6	338
1(Ph_3 $^{i}Pr_2$)	17.8	-6.6	348

General Procedure of the Reactions of Phosphinophosphonium Cations with Chalcogens

This is the basic procedure followed in all the reactions. Details such as stoichiometry, reaction time and temperature for each reaction can be found within the captions of the $^{31}P\{^{1}H\}$ NMR spectra presented below..

The phosphino-phosphonium triflate (**1.1**OTf) was dissolved in acetonitrile or dichloromethane at ambient temperature in a glove box with an atmosphere of dry nitrogen. To this solution, the respective chalcogen was added. The resulting mixture was stirred for the specified amount of time. The mixtures were analysed by $^{31}P\{^{1}H\}$ NMR spectroscopy, for which a small amount of the mixture was pipetted into an NMR sample tube alongside with a glass capillary filled with deuterated acetone. The spectra, along with details of each experiment, such as solvent, reaction time and temperature, are shown in Appendix I.

In order to purify/crystallise the products, the reaction mixtures were layered with diethlyether or hexanes and stored at -35 °C until crystallisation or precipitation occurred. Isolated solids were also investigated by $^{31}P\{^{1}H\}$ NMR spectroscopy.

Detailed procedures for cleanly isolated products can be found below.

Synthesis of 1.2(Me_3Me_2)OTf

Grey selenium (45 mg, 0.58 mmol, 1.0 eqv.) was added to a solution of Me_3PPMe_2OTf in dichloromethane and stirred overnight. During that time the mixture changed from a dark grey suspension to a greyish white suspension. The solvent was removed under reduced pressure and the resulting solid redissolved in acetonitrile. Insoluble residues (unreacted selenium) were filtered off and the solvent removed under reduced pressure.

A crystal suitable for x-ray diffraction was obtained from a different experiment by vapour diffusion of diethyl ether into a solution of **1.2(Me_3Me_2)**OTf in acetonitrile. The identity of the compound was confirmed by $^{31}P\{^{1}H\}$ NMR spectroscopy.

Yield: 152.8 mg (0.42 mmol, 72.1 %) colourless powder

Since according to the $^{31}P\{^{1}H\}$ NMR spectrum the product was only approx. 95 % pure, melting point measurement, IR spectroscopy and elemental analysis were not performed.

$^{31}P\{^{1}H\}$ NMR (121.6 MHz, DCM-d2): δ[ppm] = 17.6 d $^{1}J_{PSe}$ = 382 Hz, 14.7 d $^{1}J_{PP}$ = 68 Hz

$^{19}F\{^{1}H\}$ NMR (282.5 MHz, DCM-d2): δ[ppm] = -79.3 s

^{1}H NMR (300.3 MHz, DCM-d2): δ[ppm] = 2.33 (6H) dd $^{2}J_{HP}$ = 13.4 Hz $^{3}J_{HP}$ = 8.6 Hz, 2.04 (9H) dd $^{1}J_{HP}$ = 13.9 Hz $^{2}J_{HP}$ = 6.9 Hz

$^{13}C\{^{1}H\}$ NMR (75.5 MHz, DCM-d2): δ[ppm] = 18.7 dd $^{1}J_{CP}$ = 41 Hz $^{2}J_{CP}$ = 11 Hz, 5.7 dd $^{1}J_{CP}$ = 43 Hz $^{2}J_{CP}$ = 3 Hz

Synthesis of 1.5(^{i}*Pr$_3$Ph$_2$*)OTf

^{i}Pr$_3$PPPh$_2$OTf (1.0 mmol, 495 mg) was dissolved in dichloromethane (ca. 3 mL), to this colourless solution sulfur (1.0 mmol, 32 mg) was added. The mixture was stirred overnight and monitored by ^{31}P{^{1}H}-NMR spectroscopy. Then the reaction mixture was filtered, layered with diethyl ether (1-2 mL) and stored at -35 °C for crystallisation. After several days, colourless crystals of **1.5(^{i}*Pr$_3$Ph$_2$*)** formed. The solution was decanted and the crystals left to dry under N_2. Selected crystals were used for structure determination by XRD.

^{31}P{^{1}H} NMR (121.6 MHz, DCM-d2): δ[ppm] = 41.4 d , 34.3 d J_{PP} = 103 Hz;

^{19}F{^{1}H} NMR (282.5 MHz, DCM-d2): δ[ppm] = -78.8 s;

^{1}H NMR (300.3 MHz, DCM-d2): δ[ppm] = 8.4 – 8.3 m, 7.8 – 7.7 m, 3.3 m, 1.5 – 1.3 m;

^{13}C{^{1}H} NMR (75.5 MHz, DCM-d2): δ[ppm] = 135.1 d J_{CP} = 3.2 Hz, 133.7 d J_{CP} = 11.4 Hz, 130.6 J_{CP} = 13.7 Hz, 127.1 dd $^{1}J_{CP}$ = 74.5 Hz $^{2}J_{CP}$ = 12.6 Hz, 25.2 d $^{1}J_{CP}$ = 23.0 Hz, 18.5 d $^{2}J_{CP}$ = 4.0 Hz;

MP: 123 °C – 127 °C;

IR [cm^{-1}]: 3151(w), 2922(s), 2728(m), 2664(m), 2360(w), 2328(w), 1457(s), 1377(s), 1275(m), 1222(m), 1152(m), 1086 (m), 1029(m), 929(w), 754(s), 743(s), 719(s), 698(m), 684(m), 668(m);

Synthesis of 1.5(^{i}Pr$_3$^{i}Pr$_2$)OTf

To a solution of ^{i}Pr$_3$PP^{i}Pr$_2$OTf (1.0 mmol, 427 mg) in acetonitrile (2-3 mL), sulfur (2.0 mmol, 64 mg) was added and the mixture was stirred overnight. Subsequently insoluble parts were filtered off, and the solution was layered with diethyl ether and stored at -35° C. After one week more diethyl ether was added and after another week the product crystallised in the form of small needles. The supernatant was decanted and selected crystals were used for X-Ray diffraction.

^{31}P{^{1}H} NMR (121.6 MHz, MeCN-d3): δ[ppm] = 86.4 d, 38.7 d $^{1}J_{PP}$ = 151 Hz;

Since by ^{31}P-NMR spectroscopy the product still appeared impure (impurities included **7(^{i}Pr$_3$^{i}Pr$_2$)**) after crystallisation no further analytics were obtained.

Synthesis of 1.7($Me_3{}^iPr_2$)OTf

Me_3PPiPr_2OTf (1.0 mmol, 342 mg) and sulfur (2.0 mmol, 64 mg) were mixed in acetonitrile (2-3 mL). The mixture was stirred for three days at room temperature and subsequently for another day at 50 - 60 °C. Afterwards the mixture was filtered and the solution layered with diethyl ether, upon which crystals started to form. To ensure complete crystallisation of the product, the mixture was left at -35 °C for three days before the product was collected by suction filtration. Selected crystals were used for structure determination by XRD.

Yield: 107.4 mg, 0.26 mmol, 26 %

$^{31}P\{^1H\}$ NMR (121.6 MHz, DCM-d2): δ[ppm] = 116.7 d J_{PP} = 11 Hz, 57.2 d J_{pp} = 11 Hz;

$^{19}F\{^1H\}$ NMR (282.5 MHz, DCM-d2): δ[ppm] = -79.0 s;

^1H NMR (300.3 MHz, DCM-d2): δ[ppm] = 2.60 – 2.44 m, 2.48 d J_{HP} = 13.7 Hz, 1.40 – 1.30 m;

$^{13}C\{^1H\}$ NMR (75.5 MHz, DCM-d2): δ[ppm] = 35.6 d J_{CP} = 44.0 Hz, 16.4 – 15.4 m;

MP: 135 °C - 137 °C;

IR [cm^{-1}]: 3869(m), 3853(m), 3838(m), 3820(m), 3801(m), 3744(w), 2927(s), 2726(m), 2677(w), 2360(w), 2338(w), 1457(s), 1376(s), 1298(m), 1155(m), 1030(m), 965(m), 870(m), 766(s); 757(s), 722(s), 668(s);

Experiments of Chapter 2: Reversible Oxidative Se-Se Coupling of Phosphine Selenides by $Ph_3Sb(OTf)_2$

This subchapter has been published as supporting information for the publication of Chapter 2.[6] Therefore the formatting is inconsistent with the rest of the thesis to comply with the publishers guidelines.

Synthesis of Bis-trimethylphosphonium-diselenide bis-triflate, 2.2(Me)OTf_2

Trimethyl-phosphine selenide (244.3 mg, 1.58 mmol, 2 eqv.) were dissolved in dry acetonitrile (ca. 2 mL). To this solution triphenyl-antimony bistriflate (513 mg, 0.79 mmol, 1 eqv.) was added. The resulting yellow solution was layered with dry diethyl ether (ca. 1 mL) and stored at -35 °C. Crystals began forming within a few hours, but the solution was left overnight to ensure complete precipitation/crystallisation of the product. Finally the solution was decanted and the product was washed with dry diethyl ether and subsequently dried under reduced pressure for approx. 1h yielding 382 mg (0.63 mmol, 79.7 %) yellow needle like crystals, of which the following analytical data was obtained.

Single crystals for structure determination by XRD were obtained by vapour diffusion of diethyl ether into a solution of **2.2(Me)** in acetonitrile over the course of four days.

m.p. 160 - 162°C; ^{1}H NMR (300.3 MHz, [D_3]MeCN): δ [ppm] = 2.35 (d, J(H,P) = 14 Hz); ^{13}C{^{1}H} NMR (75.5 MHz, [D_3]MeCN): δ [ppm] = 14.4 (d, J(C,P) = 44 Hz); ^{31}P{^{1}H} NMR (121.6 MHz, [D_3]MeCN): δ [ppm] = 40.4 (s, ^{1}J(P,Se) = 408 Hz); ^{77}Se{^{1}H} NMR (68.8 MHz, [D_3]MeCN): δ [ppm] = 320 (d); ^{19}F{^{1}H} NMR (282.5 MHz, [D_3]MeCN): δ [ppm] = -79.3 (s); IR (Nujol/NaCl plates) 2923(s), 1455 (s), 1377 (s), 1260 (s), 1159 (s), 1031(s), 947 (s), 858 (m), 757 (w), 728(w), 638 (m), 572(m), 515(w) cm^{-1}; elemental analysis could not be obtained, because the sample decomposed under vacuum, indicated by a colour change to red. The resulting EA data did not correspond to the original compound.

Synthesis of Bis-triisopropylphosphonium-diselenide bis-triflate, 2.2(^{i}Pr)OTf$_2$

Triisopropyl-phosphine selenide (519.7 mg, 2.17 mmol, 2 eqv.) was dissolved in dry acetonitrile (ca. 3 mL) forming a colourless solution. Then triphenyl-antimony bistriflate (1.06 mmol, 707.4 mg, 1 eqv.) was added upon which the solution turned orange. In order to completely dissolve the triphenyl-antimony bistriflate more dry acetonitrile (ca. 2 mL) was added before layering the solution with dry diethyl ether (ca. 3 mL) and storing it at -35 °C. Overnight a red solid began to precipitate, more diethyl ether (ca. 2-3 mL) was added to ensure complete precipitation of the product over another night at -35 °C. Finally the residual now yellow solution was decanted and the remaining product was washed with dry diethyl ether. After evaporation of the residual ether the yield amounted to 649 mg of red solid.

Single crystals for structure determination by XRD were obtained by vapour diffusion of diethyl ether into a solution of **2.2(^{i}Pr)** in acetonitrile over the course of five days.

m.p. 146 °C - 154 °C; ^{1}H NMR (300.3 MHz, [D$_3$]MeCN): δ [ppm] = 1.34 (dd J = 18 Hz J = 7 Hz, 36H; CH$_3$), 2.8 (m, 6H, CH); ^{13}C{^{1}H} NMR (90.6 MHz, [D$_3$]MeCN): δ [ppm] =26.2 (d ^{1}J(C,P) = 28 Hz, 17.1 (d ^{2}J(C,P) = 4 Hz); ^{31}P{^{1}H} NMR (121.6 MHz, [D$_3$]MeCN): δ [ppm] = 83.2 (s, $^{1}J(P,Se)$ = 466 Hz); ^{19}F{^{1}H} NMR (282.5 MHz, [D$_3$]MeCN): δ [ppm] = -79.3 (s); IR (Nujol/NaCl plates) 2867 (s), 1457 (s), 1375 (s), 1277 (s), 1153 (s), 1085 (m), 1029 (s), 879 (w), 755 (w), 722 (s), 692 (w), 675 (w) cm^{-1};elemental analysis calcd (%) for $C_{20}H_{42}F_6O_6P_2S_2Se_2$: C 30.94, H 4.45, N 0; found: C 31.38, H 4.45, N <0.3;

Experiments of Chapter 3: New Cyclic Phosphorus-Selenium Cations

Synthesis of starting materials – $R_2P(Se)Cl$

The chlorophosphine was dissolved in dichloromethane and a small excess of grey selenium was added to the solution. The mixture was stirred at room temperature for several days, during which the solution turned yellow. The progress of the reaction was monitored by $^{31}P\{^1H\}$ NMR spectroscopy. Upon completion of the reaction, excess selenium was filtered off and the solvent was removed under reduced pressure (2 hours), yielding a yellow oil.

R = Ph

$^{31}P\{^1H\}$ NMR (121.6 MHz, DCM-d2): δ[ppm] = 71.8, $^1J_{PSe}$ = 852 Hz

R = ^{i}Pr

$^{31}P\{^1H\}$ NMR (121.6 MHz, DCM-d2): δ[ppm] = 125.9, $^1J_{PSe}$ = 825 Hz

Synthesis of 3.1a$(Al_2Cl_7)_2$ – $(Ph_2PSe)_2(Al_2Cl_7)_2$

Chlorodiphenylphosphine selenide (4.7 mmol, 1411 mg) was dissolved in dichloromethane, then two equivalents of aluminum trichloride (9.4 mmol, 1256mg) were added to the solution. Within a few minutes the mixture turned from a yellow suspension to an orange solution and then to a yellow solution, the mixture was stirred overnight. Subsequently the almost clear solution was filtered, layered with hexanes and stored at -35 °C to induce crystallisation. Finally, the supernatant was decanted and the so obtained yellow crystals were dried under reduced pressure.

Crystals suitable for XRD were obtained from a solution of the product in dichloromethane layered with hexanes and stored at -35 °C for one week, in a separate experiment. The identity of the product was confirmed by $^{31}P\{^1H\}$-NMR spectroscopy.

Yield: 1.45 mmol, 1614 mg, 62 %

$^{31}P\{^1H\}$ NMR (121.6 MHz, DCM-d2): δ[ppm] = -10.5 s, J_{PSe} = 263.3 Hz

$^{77}Se\{^1H\}$ NMR (68.7 MHz, DCM-d2): δ[ppm] = 633.2 t. J_{SeP} = 263.6 Hz

^{27}Al NMR (93.9 DCM-d2): δ[ppm] = 103 broad s

^1H NMR (300.3 MHz, DCM-d2): δ[ppm] = 7.9 to 8.2 m

MP: 122 °C - 128 °C

Synthesis of 3.1b$(Al_2Cl_7)_2$ – $(^iPr_2PSe)_2(Al_2Cl_7)_2$

Chlorodiisopropylphosphine selenide (3.8 mmol, 885 mg) was dissolved in dichloromethane, then two equivalents of aluminum trichloride (7.6 mmol, 1019 mg) were added to the solution. Within a few minutes the mixture turned from a yellow suspension to an orange solution and then to a yellow solution, the mixture was stirred overnight. Subsequently, the almost clear solution was filtered, layered with hexanes and stored at -35 °C to induce crystallisation. Finally, the supernatant was decanted and a few crystals were selected for structure determination by XRD. The remainder of the crystals were dried under N_2 which rapidly led to desolvation yielding a yellowish powder.

Yield: 0.42 mmol, 423 mg, 22 %

$^{31}P\{^1H\}$ NMR (145.8 MHz, DCM-d2): δ[ppm] = 58.5 s, J_{PSe} = 248.7 Hz

$^{77}Se\{^1H\}$ NMR (68.7 MHz, DCM-d2): δ[ppm] = 201 t, J_{PSe} = 246 Hz

^{27}Al NMR (93.9 MHz, DCM-d2): δ[ppm] = 104 ppm (broad singlet)

^1H NMR (300.3 MHz, DCM-d2): δ[ppm] = 3.56 – 3.39 m, 1.72 dd *J* = 28.1 Hz *J* = 6.9 Hz

$^{13}C\{^1H\}$ NMR (75.5 MHz, DCM-d2): δ[ppm] = 35.6 m, 18.4 m

EA: found (calc. for $C_{12}H_{28}Al_4Cl_{14}P_2Se_2$): C 14.18 % (14.46 %), H 2.87 % (2.83 %), N <0.3 % (0 %)

MP: 74 °C - 80 °C

Discovery of 3.2 – $(Ph_2PSe)_2CH_2(AlCl_4)_2$

Compound 3.1a$(Al_2CL_7)_2$ and two equivalents of $SbPH_3$ were dissolved in dichloromethane, resulting in a clear yellow solution. The solution was stirred for approximately 20 minutes before the result was investigated by $^{31}P\{^1H\}$ NMR spectroscopy. The spectrum indicated complete consumption of the starting material, but the products could not be conclusively identified. The product mixture appeared to contain $Ph_2P\text{-}PPh_2\text{-}PPh_2^+$ (Chapter 3). Upon standing for about six weeks, most of the solvent evaporated, leaving behind a red residue and a crystal of **3.2$(AlCl_4)_2$** which was identified by single crystal x-ray diffraction.

Synthesis of 3.3 – $(Ph_2P)_2Se_3)(Al_2Cl_7)_2$

Compound **3.1a$(Al_2Cl_7)_2$**, $(Ph_2PSe)_2(Al_2Cl_7)_2$, and one equivalent of grey selenium were mixed in a glass tube and heated to 140 °C (oil bath temperature) overnight. The melt turned dark red and did not entirely solidify upon cooling to room temperature. The resulting dark red very viscous sticky substance was identified as cation **3.3** by $^{31}P\{^1H\}$ NMR spectroscopy. Upon storage in a freezer (-35 °C) it solidified to a glass-like solid, Attempts to crystallize the products from a solution in dichloromethane by various methods failed.

$^{31}P\{^1H\}$ NMR (121.6 MHz, DCM-d2): δ[ppm] = 92.1 s

$^{77}Se\{^1H\}$ NMR (95.5 MHz, DCM-d2): δ[ppm] = 531 d $^1J_{PSe}$ = 414 Hz, 426 t $^1J_{PSe}$ = 412 Hz

^1H NMR (300.3 MHz, DCM-d2): δ[ppm] = 8.3 – 7.6 mult.

Experiments of Chapter 4: Unexpected Discoveries

Discovery of 4.1

Grey selenium (2.5 mmol, 197 mg) was added to a solution of **1.1(Me$_3$Me$_2$)**OTf (1.0 mmol, 286 mg) in acetonitrile (ca. 3 mL). The solution was heated to 64 °C – 75 °C overnight. Subsequently, unreacted selenium was filtered off and washed with acetonitrile (2 x 1 mL). The solution was layered with diethyl ether and stored at -35 °C. After six days the solvent was evaporated under low pressure, the solid residue was redissolved in acetonitrile and crystallised by vapour diffusion of diethyl ether into the solution. The resulting crystal was identified as **4.1** by single crystal x-ray diffraction.

Discovery of 4.2

Grey selenium (0.25 mmol, 20 mg) was added to a solution of **1.1(Me$_3$^{i}Pr$_2$)**OTf (0.25 mmol, 86 mg) in acetonitrile (ca. 3 mL). The mixture was stirred at 58 °C for half a day. After standing at RT for approx. four weeks, crystals of **4.2** formed. They were identified by single crystal x-ray diffraction.

Discovery of 4.3OTf

Grey selenium (2.0 mmol, 158 mg) was added to a solution of **1.1(Ph$_3$^{i}Pr$_2$)**OTf (1.0 mmol, 528 mg) in acetonitrile (2 – 3 mL). The solution was stirred over a weekend. Eventually the solution was filtered and a crystallisation attempt was made by layering the solution with diethyl ether and storing at -35 °C. Over the course of several days, more diethyl ether was added until colourless crystals formed. The crystals were identified as **4.3**OTf by single crystal x-ray diffraction.

Discovery of 4.4OTf

Diisopropylchlorophosphine selenide and silver triflate were dissolved in acetonitrile. The solution was left standing for four days, protected from light. During this time, two colourless crystals formed which were identified as **4.4**OTf by single crystal x-ray diffraction.

A second crystal was attempted to dissolve in fresh solvent for NMR spectroscopy but the solubility was poor.

^{31}P{^{1}H} NMR (121.6 MHz, MeCN-d3): δ[ppm] = 74.5 s, J_{PSe} = 532.9 Hz

^{19}F{^{1}H} NMR (282.5 MHz, MeCN-d3): δ[ppm] = -79.4 s

^{1}H NMR (300.3 MHz, MeCN-d3): δ[ppm] = 2.45 – 2.57 m, 1.33 *J* = 19.9 Hz *J* = 6.9 Hz

Discovery of 4.5OTf

4-dimethylaminopyridine (0.75 mmol, 92 mg), $SPCl_3$ (0.25 mmol, 25.4 µL) and trimethylsilyl triflate (0.75 mmol, 135.5 µL) were dissolved in acetonitrile. The solution was stirred overnight before the solvent was removed under reduced pressure. The resulting residue was crystallised by vapour diffusion of diethyl ether into an acetonitrile solution. The resulting crystal was identified as **4.5**OTf by single crystal x-ray diffraction.

References

[1] P. H. M. Budzelaar, **2006**.

[2] G. M. Sheldrick, *Acta Crystallogr. Sect. A Found. Crystallogr.* **2008**, *64*, 112–122.

[3] O. V. Dolomanov, L. J. Bourhis, R. J. Gildea, J. A. K. Howard, H. Puschmann, *J. Appl. Crystallogr.* **2009**, *42*, 339–341.

[4] S. S. Chitnis, E. MacDonald, N. Burford, U. Werner-Zwanziger, R. McDonald, *Chem. Commun.* **2012**, *48*, 7359.

[5] N. Burford, P. J. Ragogna, R. McDonald, M. J. Ferguson, *J. Am. Chem. Soc.* **2003**, *125*, 14404–14410.

[6] M. J. Poller, N. Burford, K. Karaghiosoff, *Chem. Eur. J.* **2018**, *24*, 85–88.

Appendix I: Supporting Information for Chapter 1

This Appendix contains the supporting information for Chapter 1, excluding experimental procedures, which are presented in Chapter 5.

$^{31}P\{^{1}H\}$ NMR spectra of Reactions of Phosphino-Phosphonium Cations with Selenium

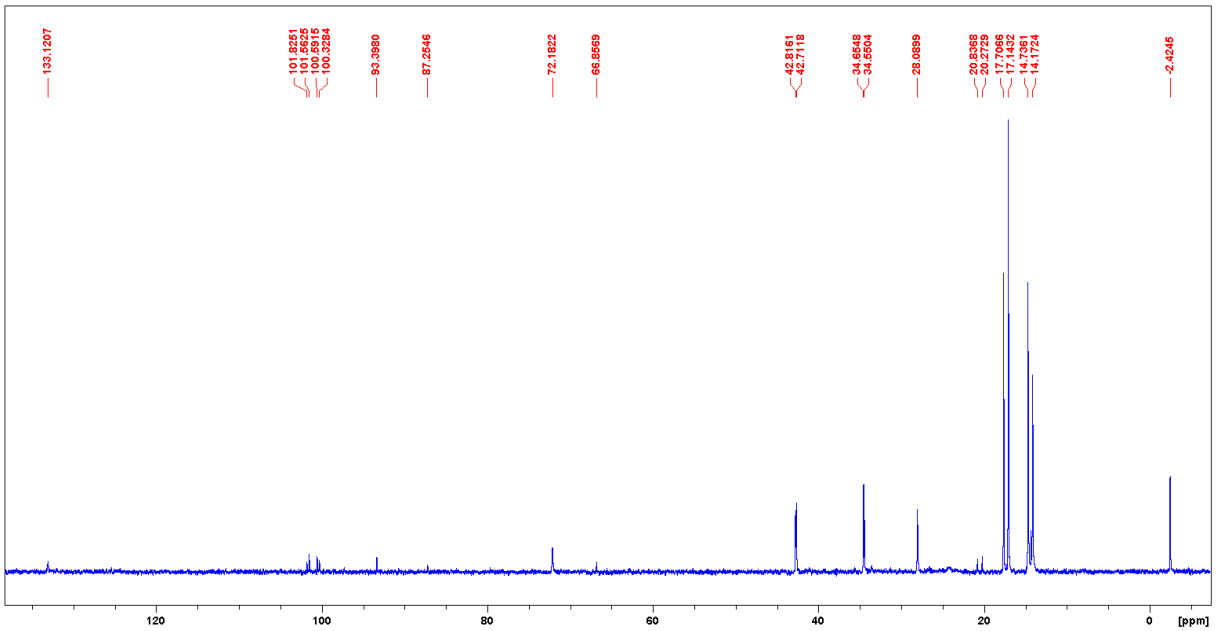

*Figure AI.1: $^{31}P\{^{1}H\}$ NMR spectrum of **1.1(Me$_3$Me$_2$)**OTf + 2 Se in MeCN, 63-65°C, 1 h.*

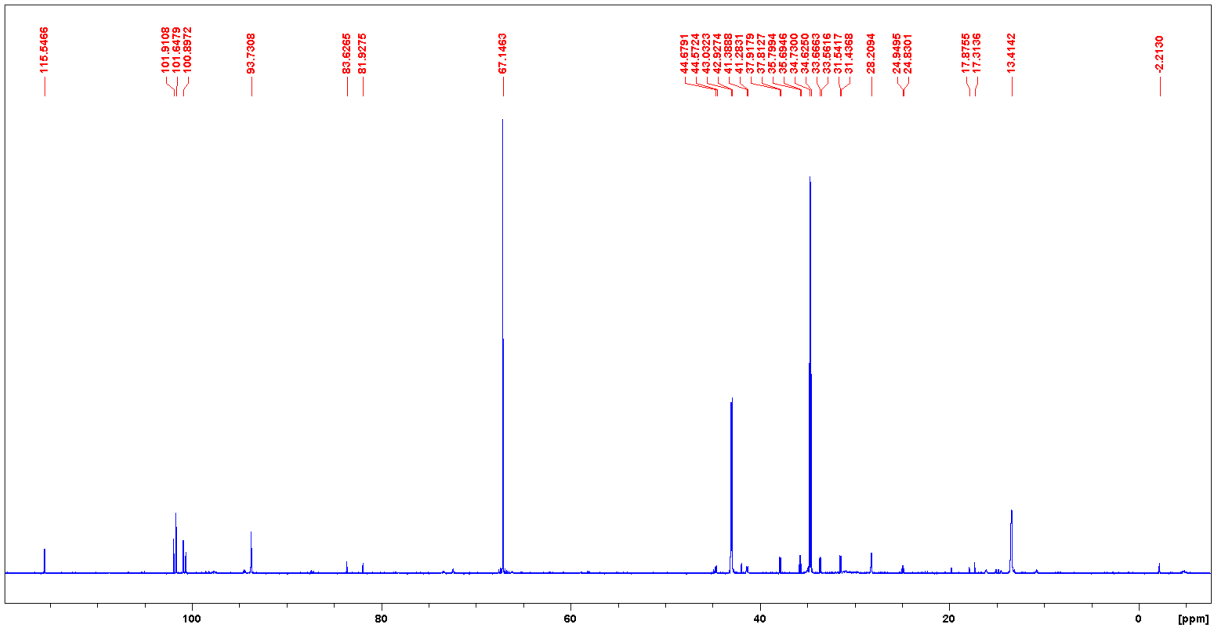

*Figure AI.2: $^{31}P\{^{1}H\}$ NMR spectrum of **1.1(Me$_3$Me$_2$)**OTf + 2 Se in MeCN, 66°C, 2.5 d.*

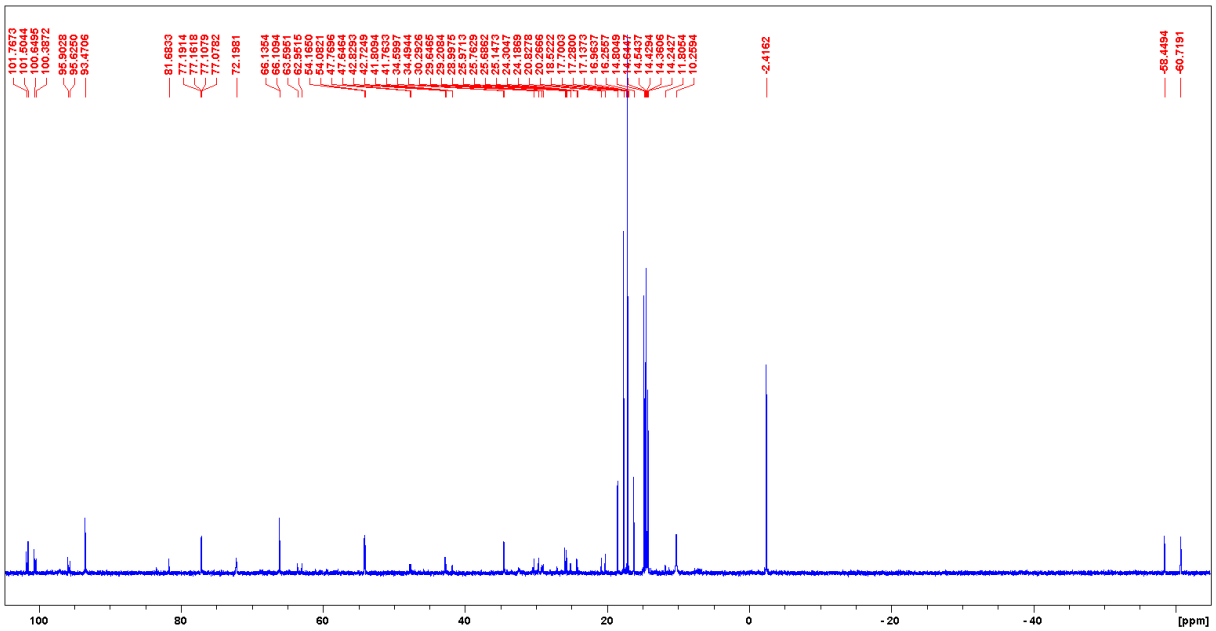

*Figure AI.3: $^{31}P\{^{1}H\}$ NMR spectrum of **1.1(Me$_3$Me$_2$)**OTf + 1 Se in MeCN, 64 °C, overnight.*

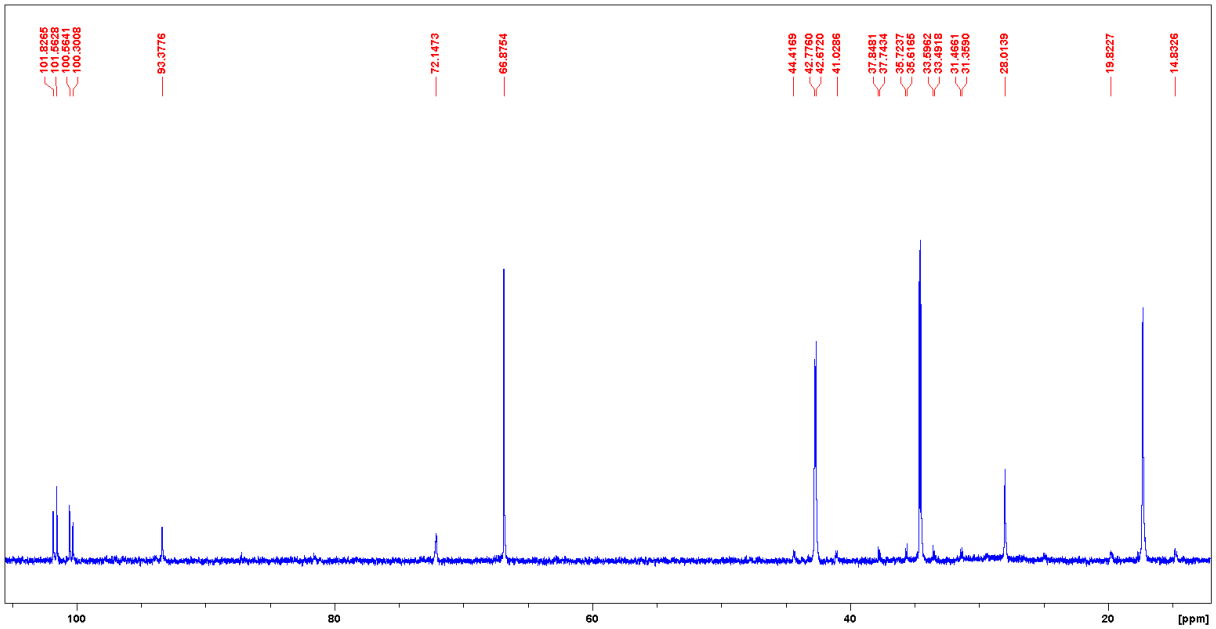

*Figure AI.4: $^{31}P\{^{1}H\}$ NMR spectrum of **1.1(Me$_3$Me$_2$)**OTf + 5 Se in MeCN, 65 °C, 2 d.*

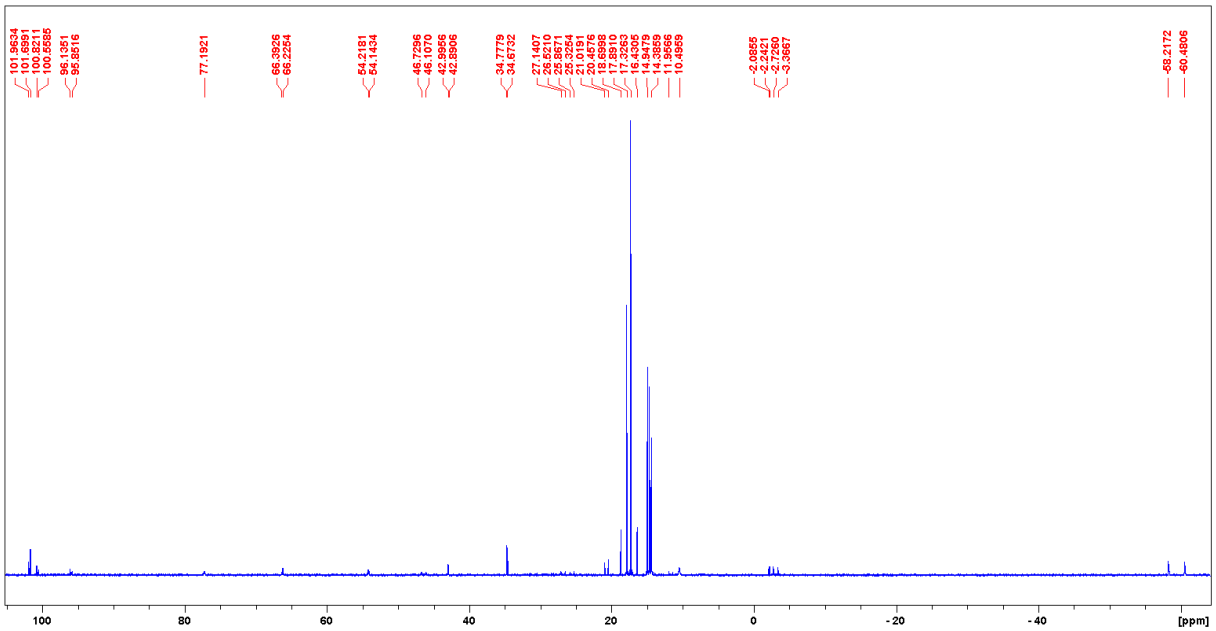

*Figure AI.5: $^{31}P\{^{1}H\}$ NMR spectrum of **1.1(Me$_3$Me$_2$)**OTf + 1 Se in MeCN, 60 °C, overnight.*

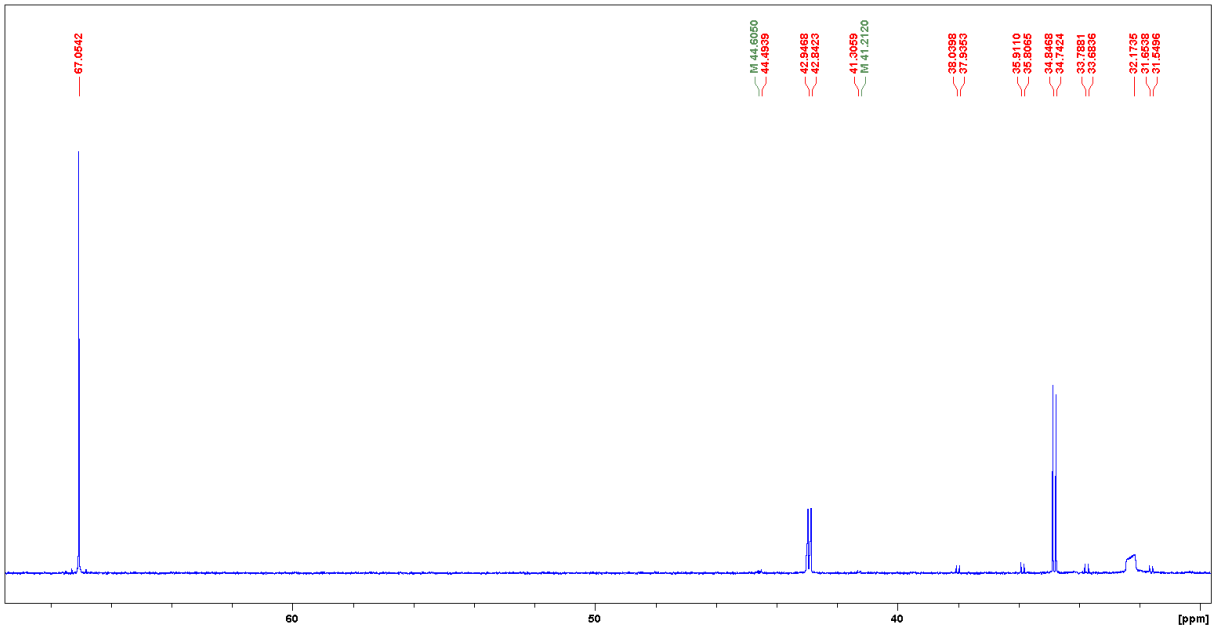

*Figure AI.6: $^{31}P\{^{1}H\}$ NMR spectrum of **1.1(Me$_3$Me$_2$)**OTf + 2.5 Se in MeCN, 64-75 °C, overnight*

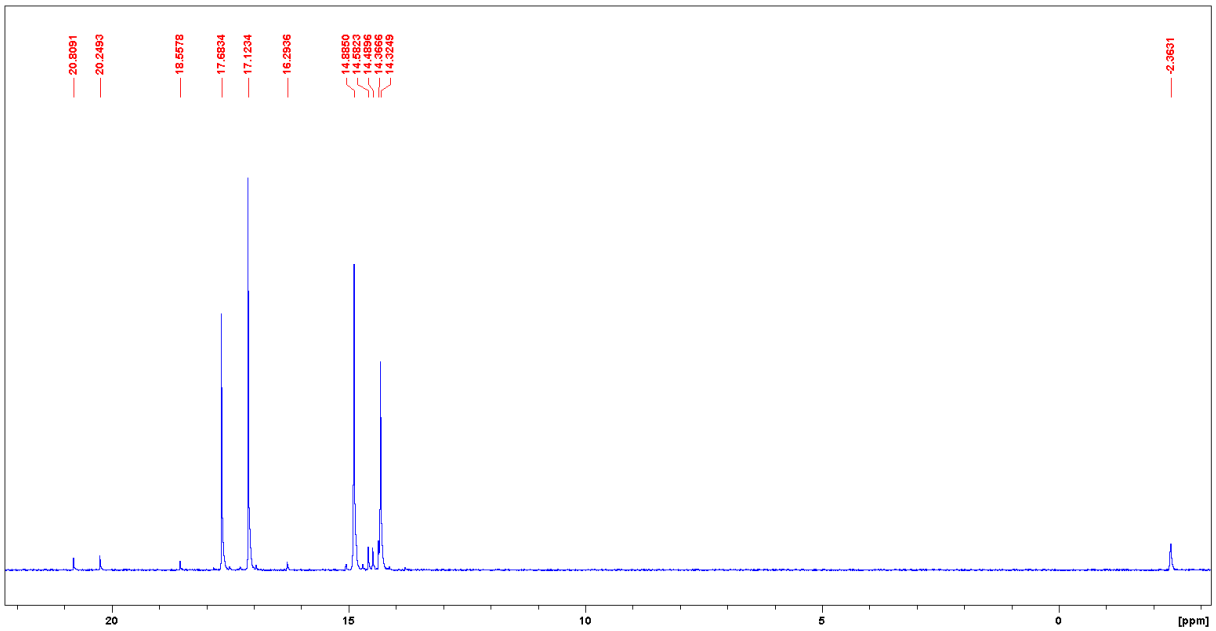

*Figure AI.7: $^{31}P\{^{1}H\}$ NMR spectrum of **1.1(Me$_3$Me$_2$)**OTf + 1 Se in DCM, RT, overnight*

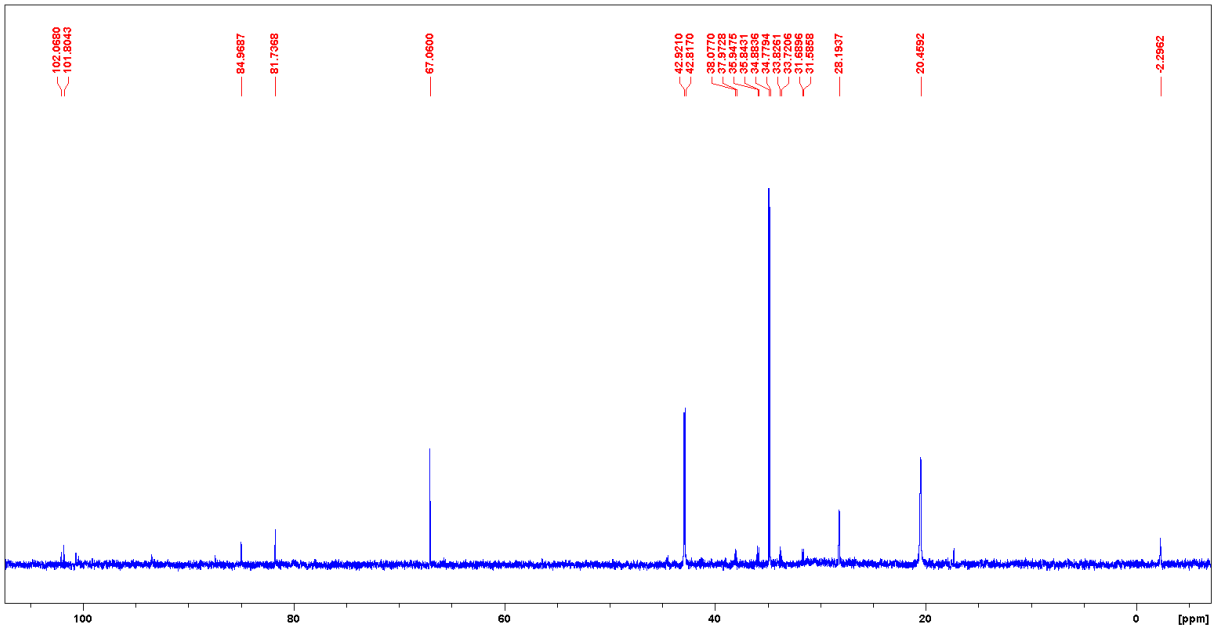

*Figure AI.8: $^{31}P\{^{1}H\}$ NMR spectrum of **1.1(Me$_3$Me$_2$)**OTf + 2 Se in MeCN, 54-70 °C, overnight.*

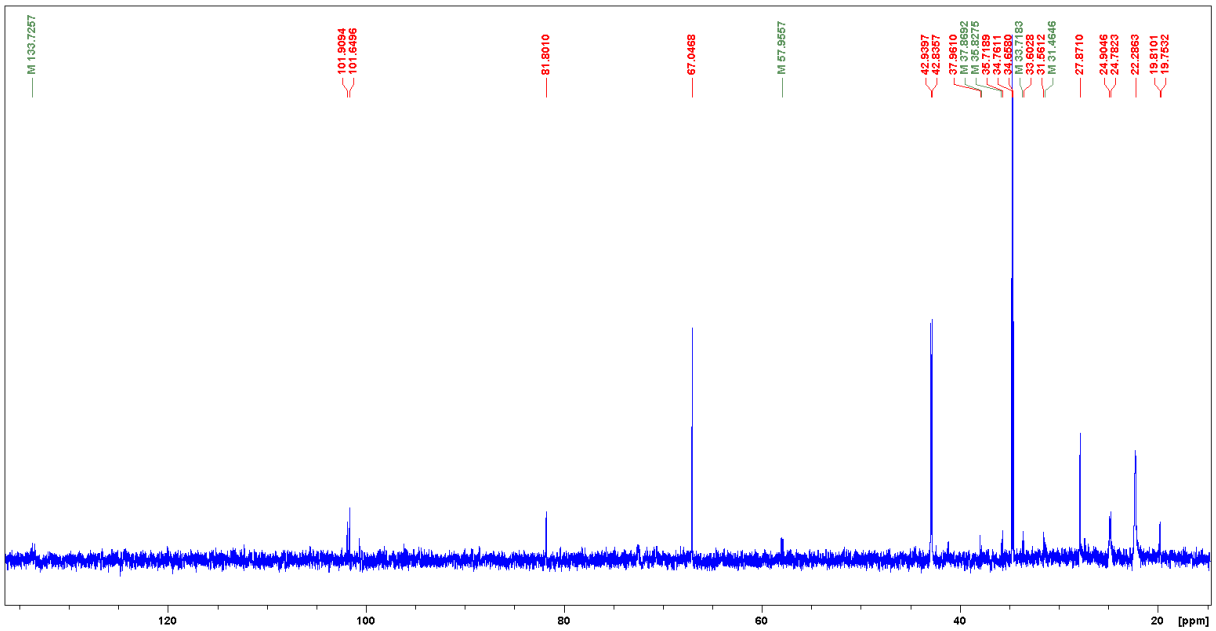

*Figure AI.9: $^{31}P\{^{1}H\}$ NMR spectrum of **1.1(Me$_3$Me$_2$)**OTf + 4 Se in MeCN, 60-70 °C, 2 d.*

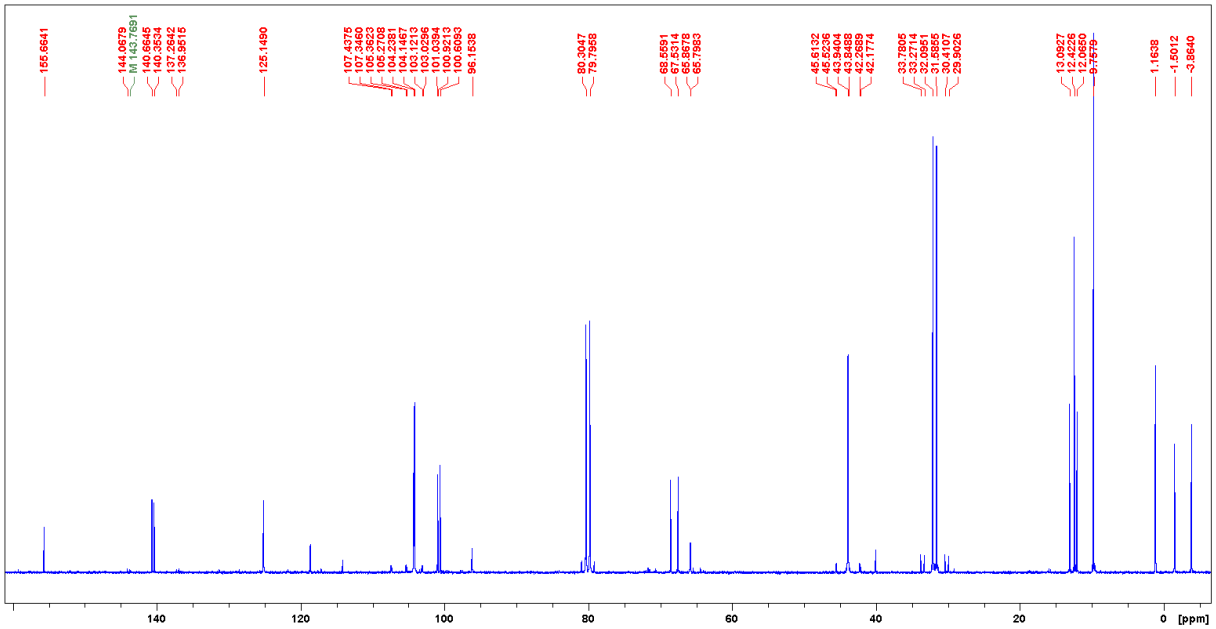

*Figure AI.10: $^{31}P\{^{1}H\}$ NMR spectrum of **1.1(Me$_3$^{i}Pr$_2$)**OTf + 1 Se in DCM, RT, 8 d.*

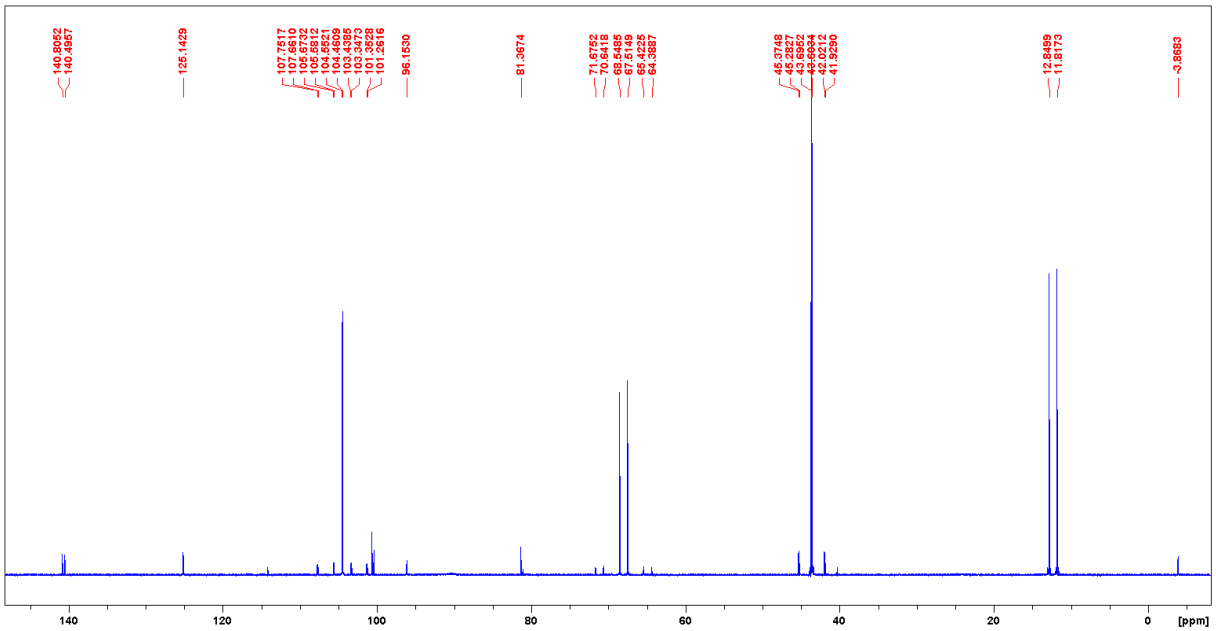

*Figure AI.11: $^{31}P\{^{1}H\}$ NMR spectrum of **1.1(Me$_3$^{i}Pr$_2$)**OTf + 2 Se in DCM, RT, 8 d.*

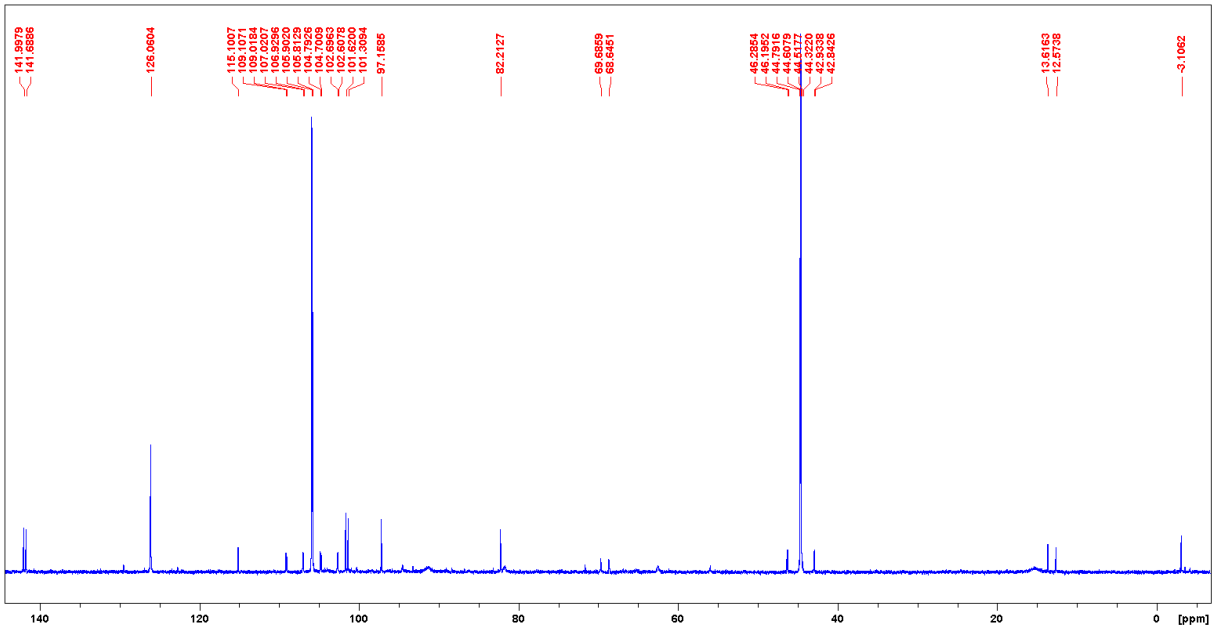

*Figure AI.12: $^{31}P\{^{1}H\}$ NMR spectrum of **1.1(Me$_3$^{i}Pr$_2$)**OTf + 1 Se in MeCN, 69 °C, overnight.*

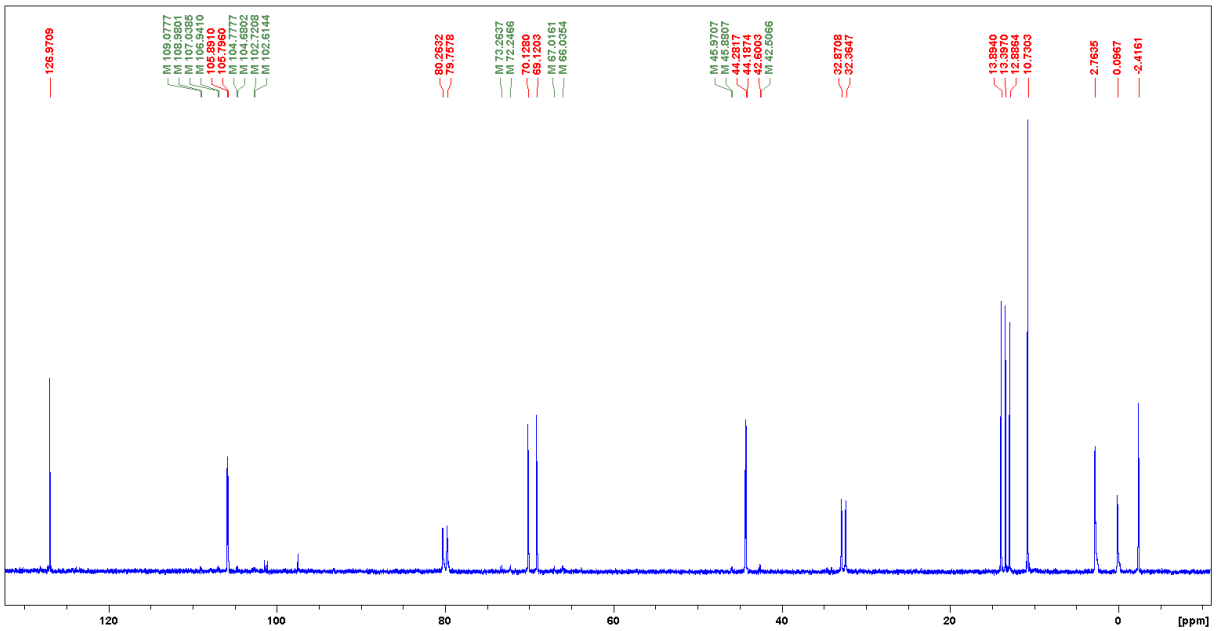

*Figure AI.13: $^{31}P\{^{1}H\}$ NMR spectrum of **1.1(Me$_3$^{i}Pr$_2$)**OTf + 1 Se in MeCN, 58 °C, 6 h.*

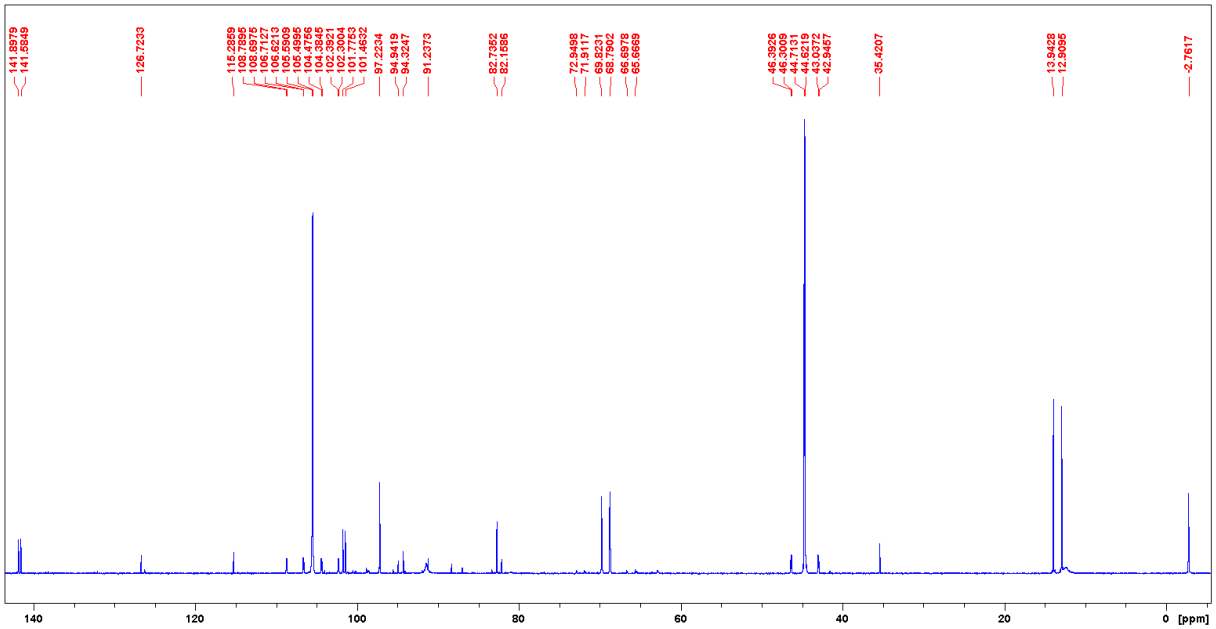

*Figure AI.14: $^{31}P\{^{1}H\}$ NMR spectrum of **1.1(Me$_3$^{i}Pr$_2$)**OTf + 2 Se in MeCN, 58 °C, overnight.*

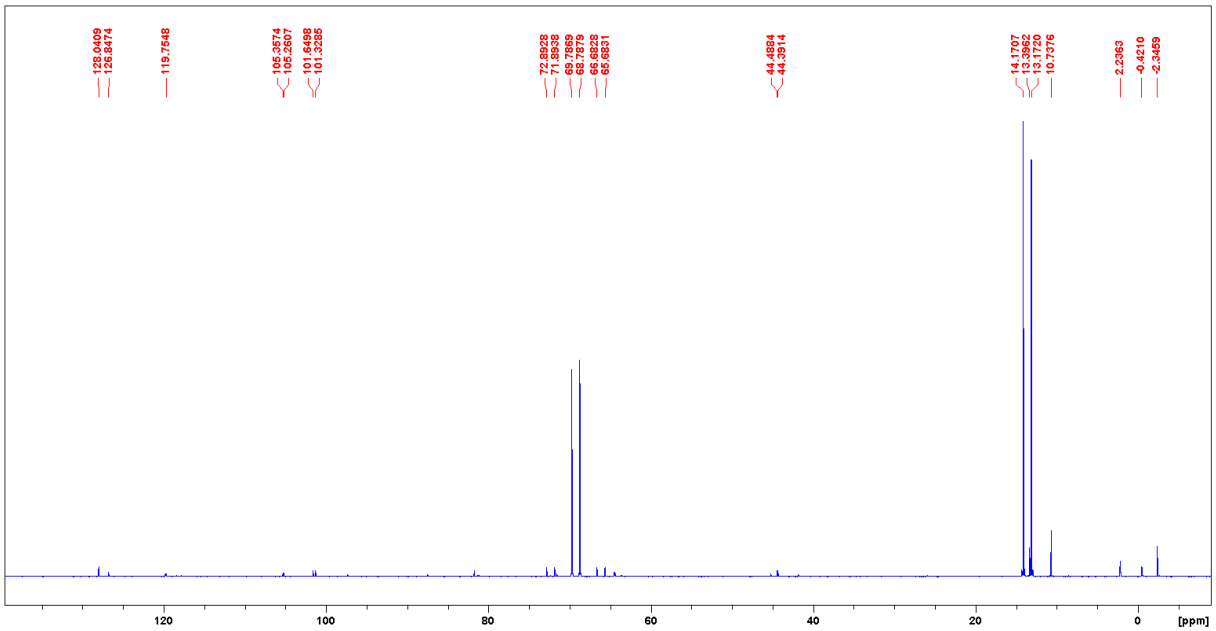

*Figure AI.15: $^{31}P\{^{1}H\}$ NMR spectrum of **1.1(Me$_3$^{i}Pr$_2$)**OTf + 1 Se in MeCN, RT, overnight.*

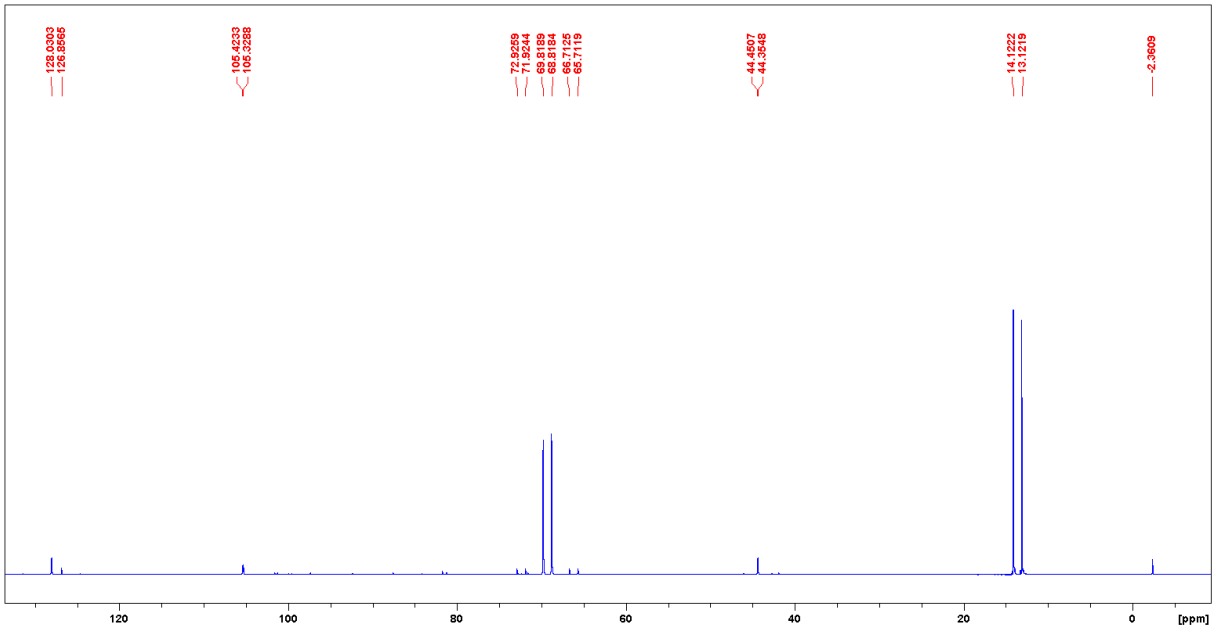

*Figure AI.16: $^{31}P\{^{1}H\}$ NMR spectrum of **1.1(Me$_3$^{i}Pr$_2$)**OTf + 2 Se in MeCN, RT, overnight.*

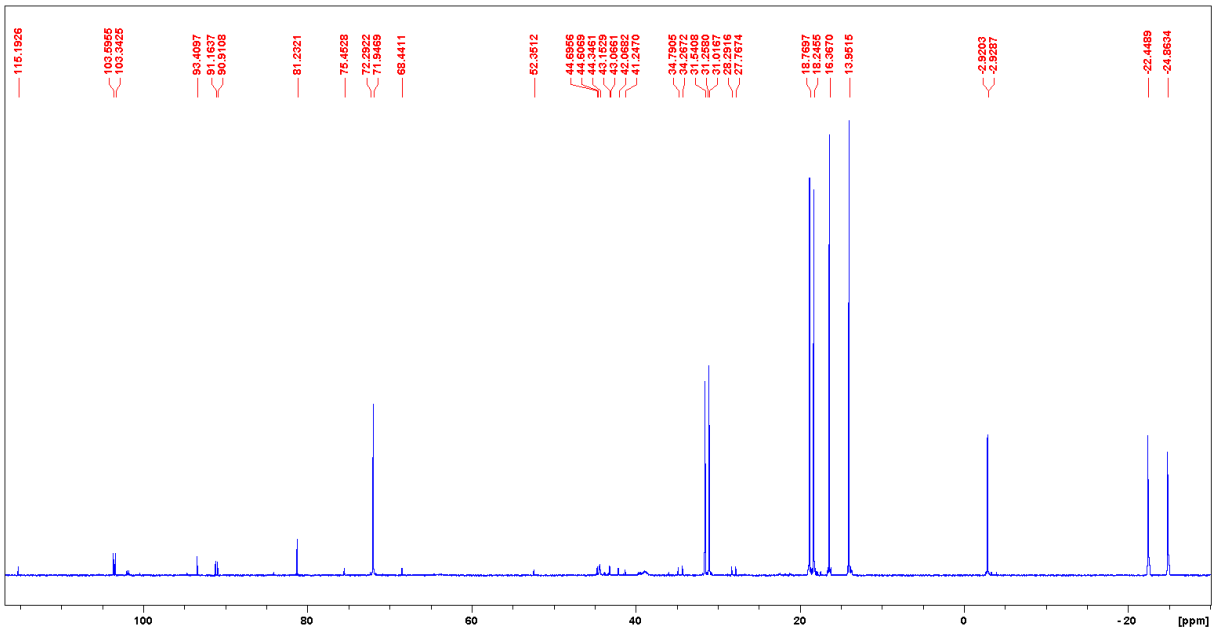

*Figure AI.17: $^{31}P\{^{1}H\}$ NMR spectrum of **1.1(Me$_3$Ph$_2$)**OTf + 1 Se in DCM, RT, 4 h.*

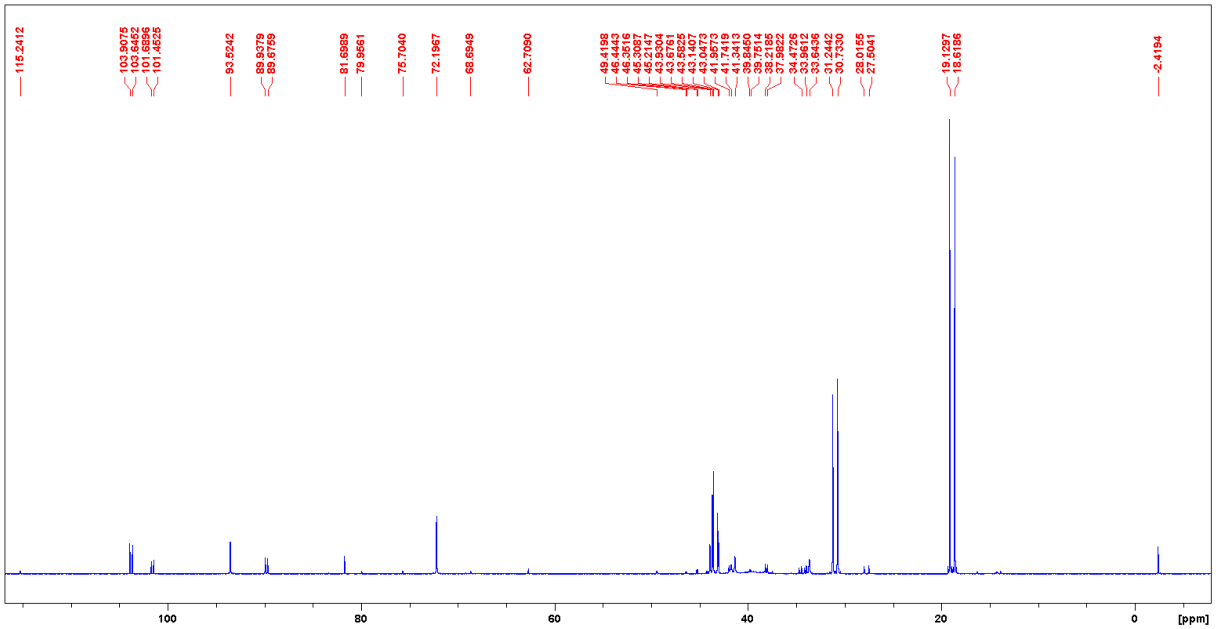

*Figure AI.18: $^{31}P\{^{1}H\}$ NMR spectrum of **1.1(Me$_3$Ph$_2$)**OTf + 2 Se in MeCN, RT, 2 d.*

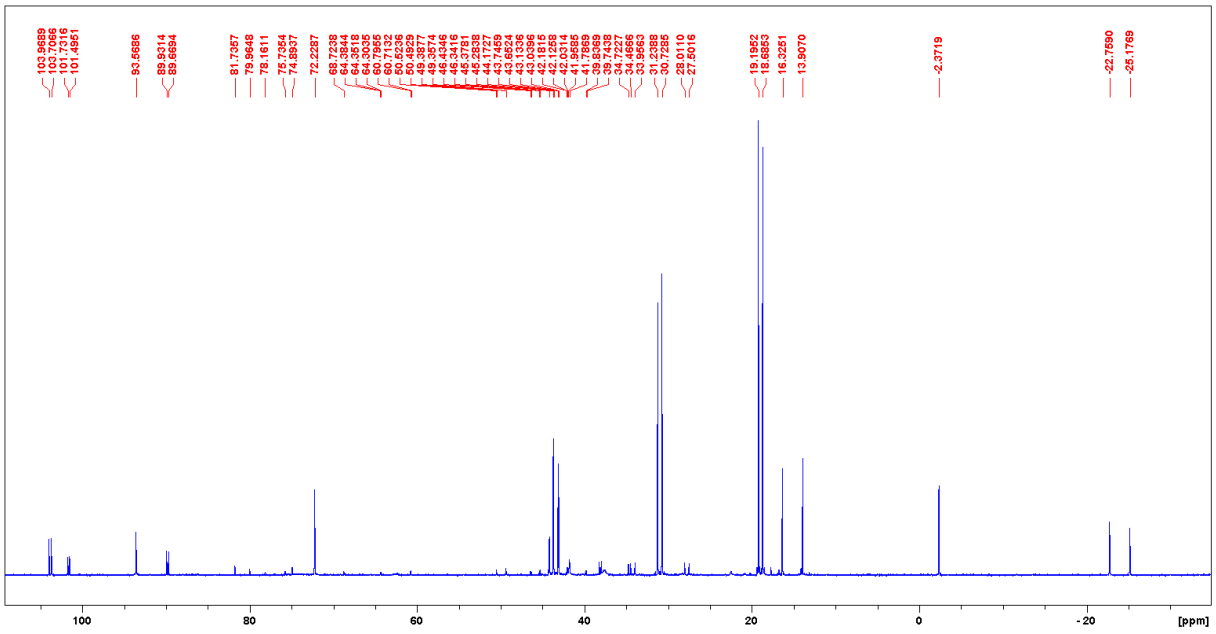

*Figure AI.19: $^{31}P\{^{1}H\}$ NMR spectrum of **1.1(Me$_3$Ph$_2$)**OTf + 1 Se in MeCN, RT, overnight.*

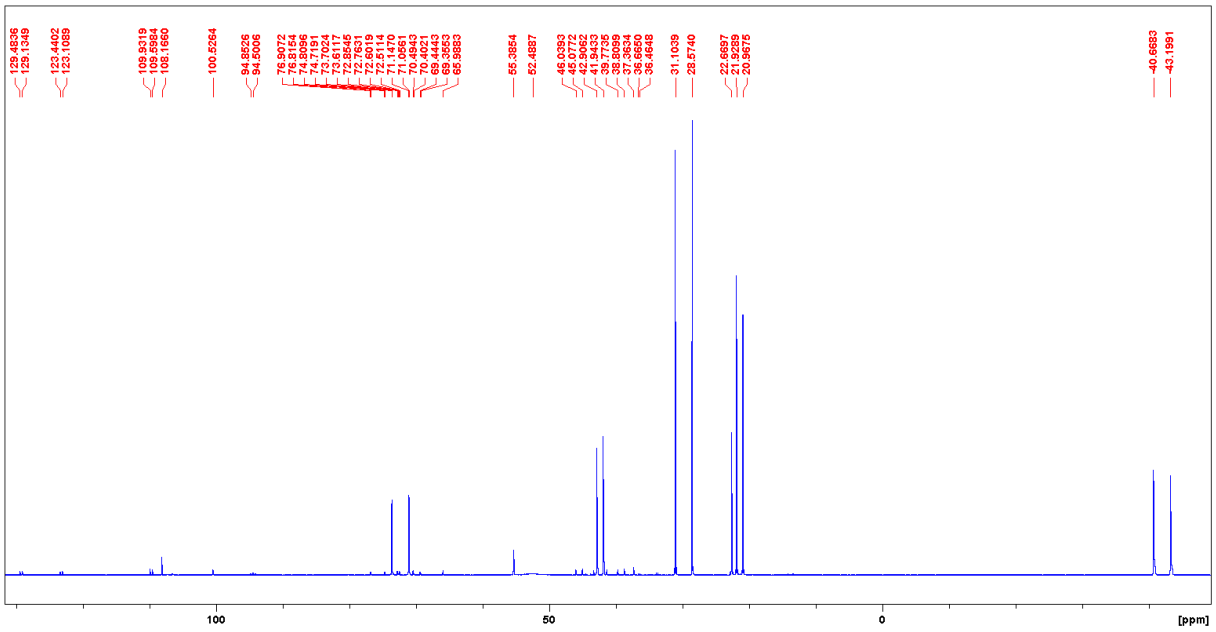

*Figure AI.20: $^{31}P\{^{1}H\}$ NMR spectrum of **1.1(Et$_3$Et$_2$)**OTf + 1 Se in DCM, RT, overnight.*

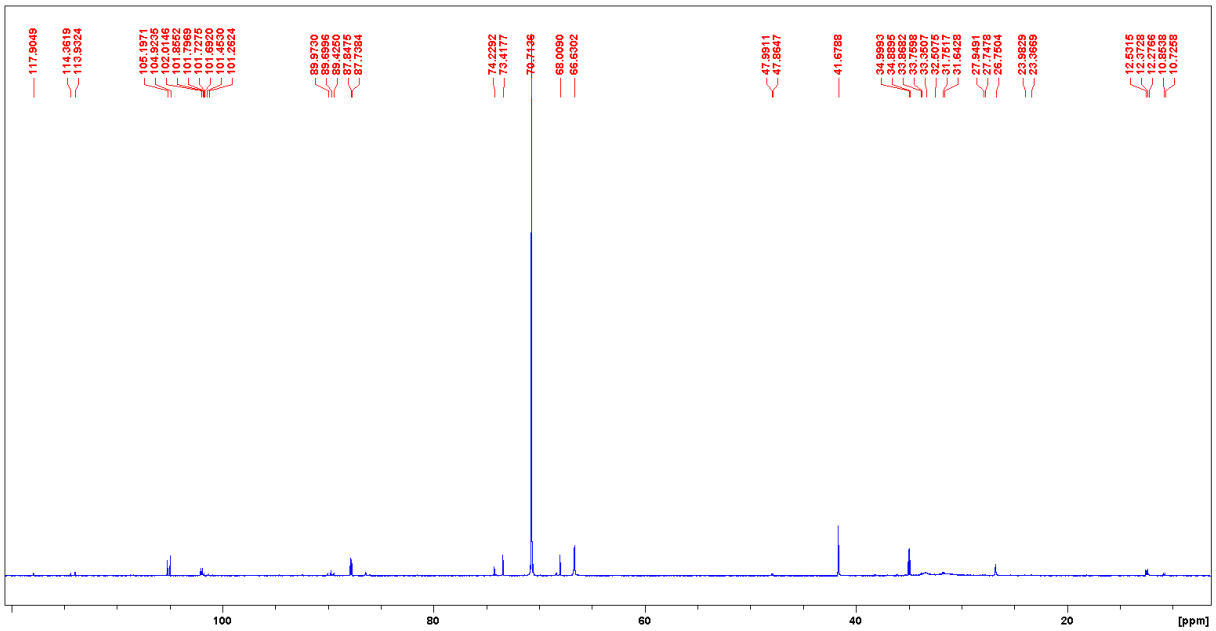

*Figure AI.21: $^{31}P\{^{1}H\}$ NMR spectrum of **1.1(^{i}Pr$_3$Me$_2$)**OTf + 2 Se in MeCN, 59 °C, overnight.*

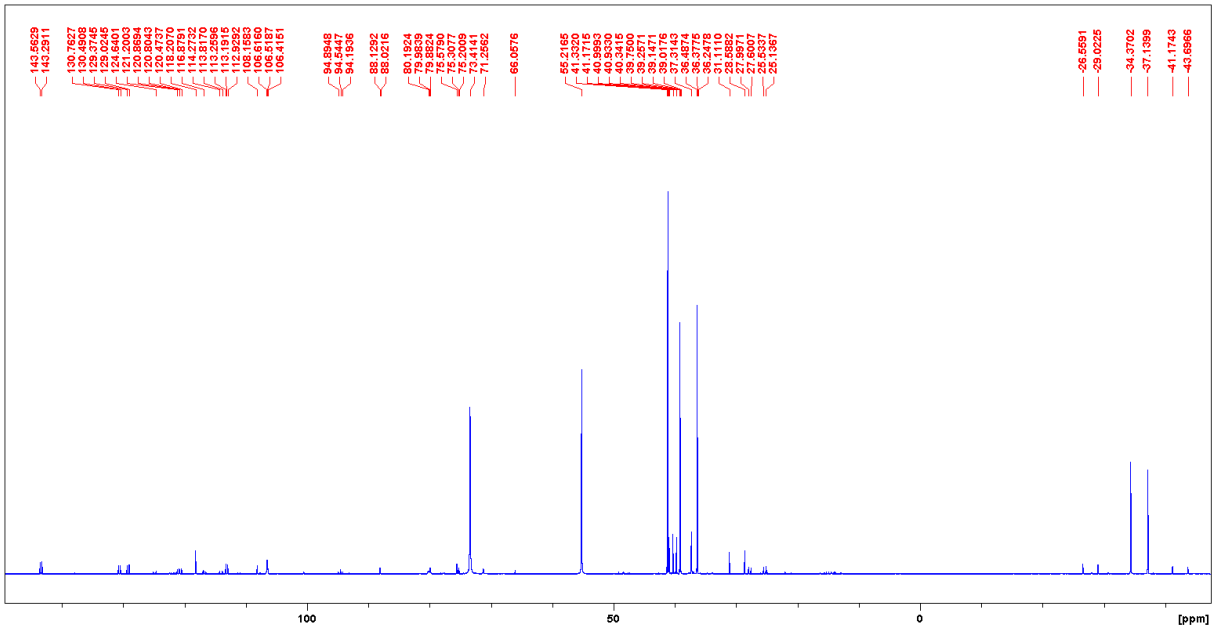

*Figure AI.22: $^{31}P\{^{1}H\}$ NMR spectrum of **1.1(^{i}Pr$_3$Et$_2$)**OTf + 1 Se in DCM, RT, overnight.*

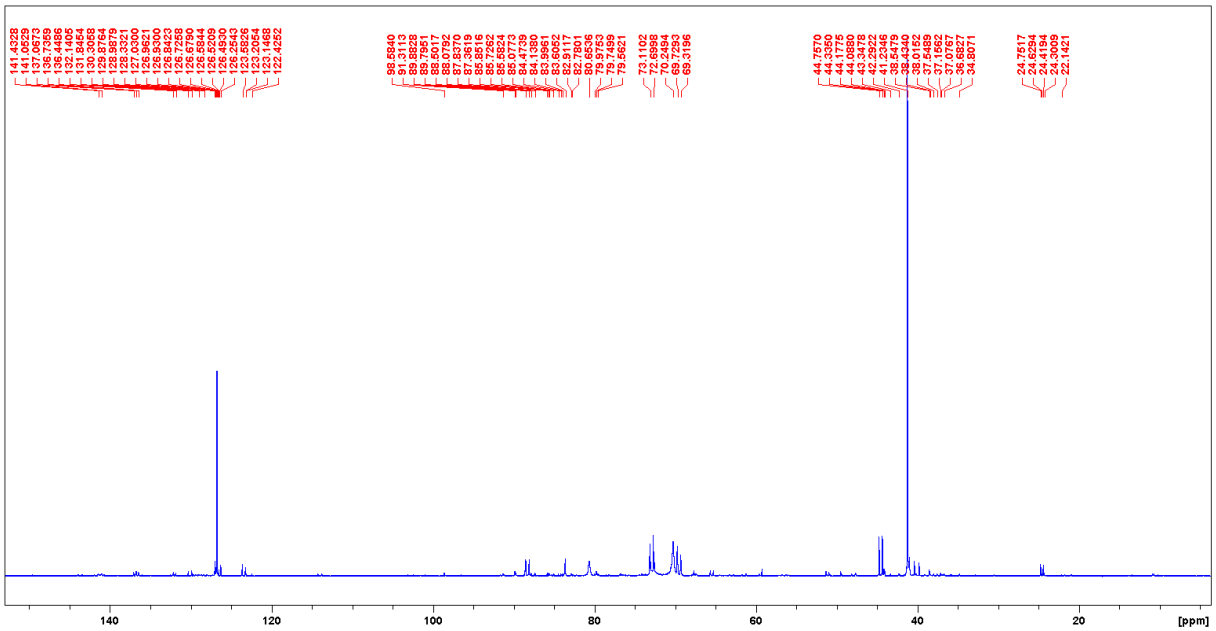

*Figure AI.23: $^{31}P\{^{1}H\}$ NMR spectrum of **1.1(${}^{i}Pr_3{}^{i}Pr_2$)**OTf + 1 Se in MeCN, 67 °C, 3 d.*

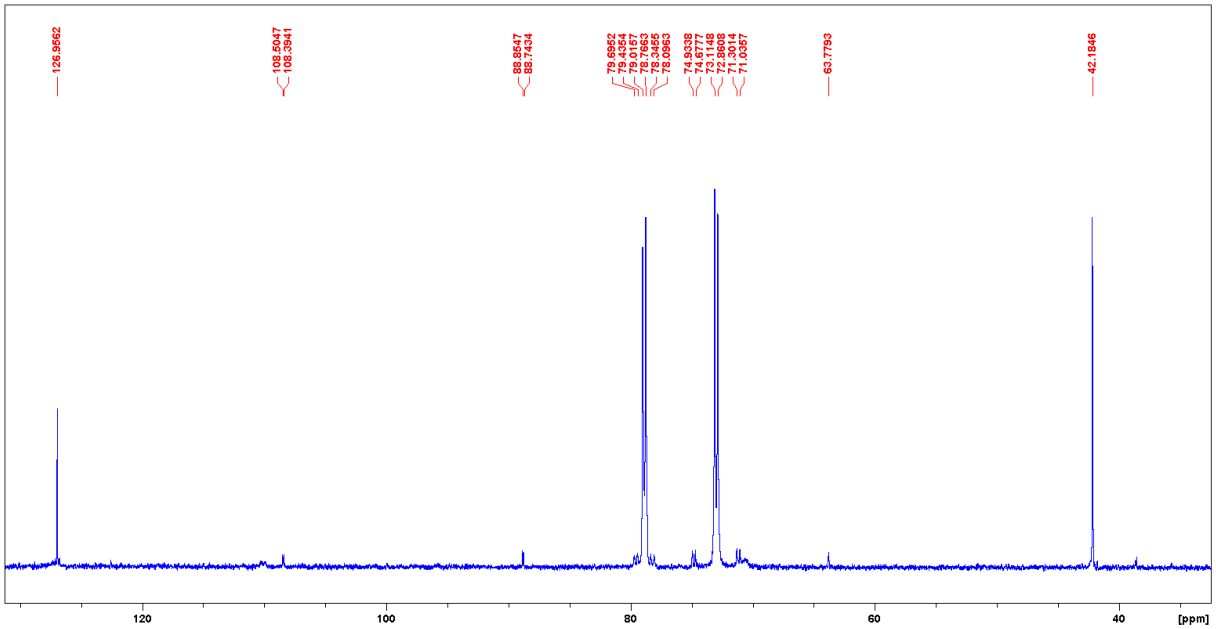

*Figure AI.24: $^{31}P\{^{1}H\}$ NMR spectrum of **1.1(${}^{i}Pr_3{}^{i}Pr_2$)**OTf + 1 Se in MeCN, 59 °C, 3.5 h.*

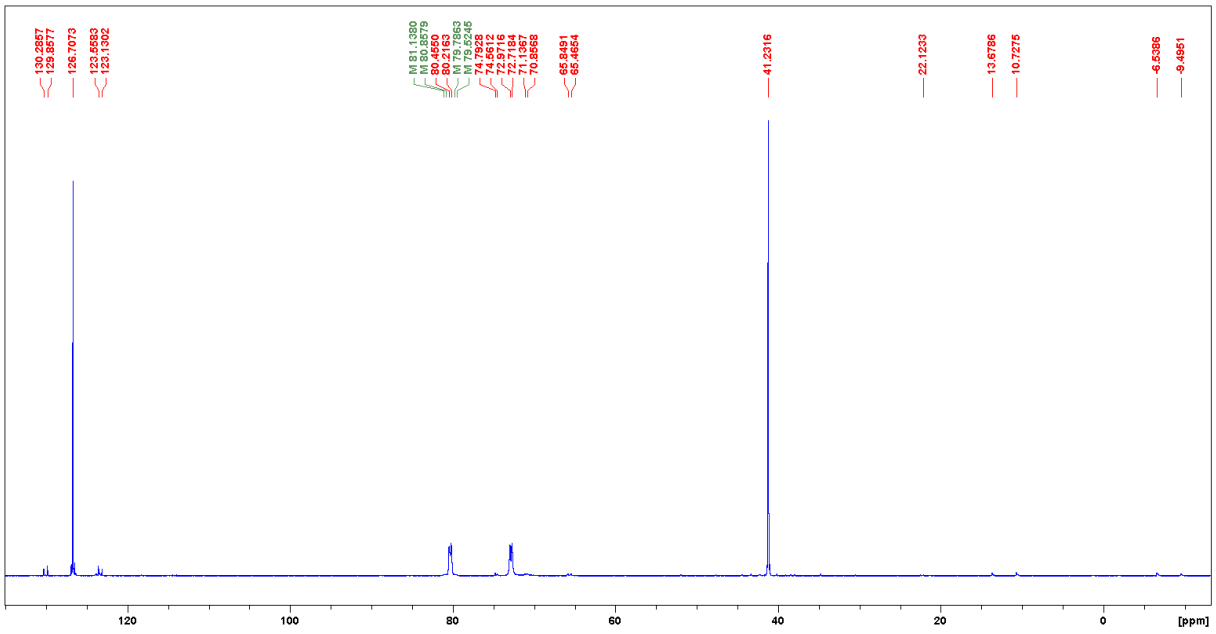

*Figure AI.25: $^{31}P\{^{1}H\}$ NMR spectrum of **1.1(^{i}Pr$_3$^{i}Pr$_2$)**OTf + 1 Se in DCM, RT, 5 d.*

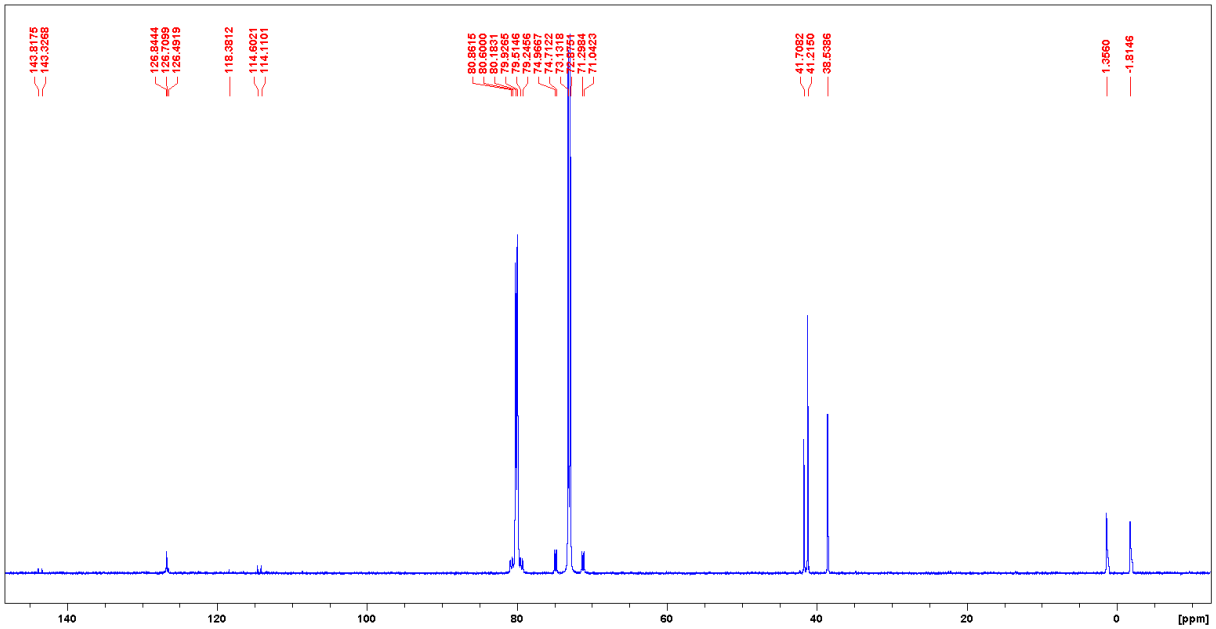

*Figure AI.26: $^{31}P\{^{1}H\}$ NMR spectrum of **1.1(^{i}Pr$_3$^{i}Pr$_2$)**OTf + 1 Se in DCM, RT, 2 h.*

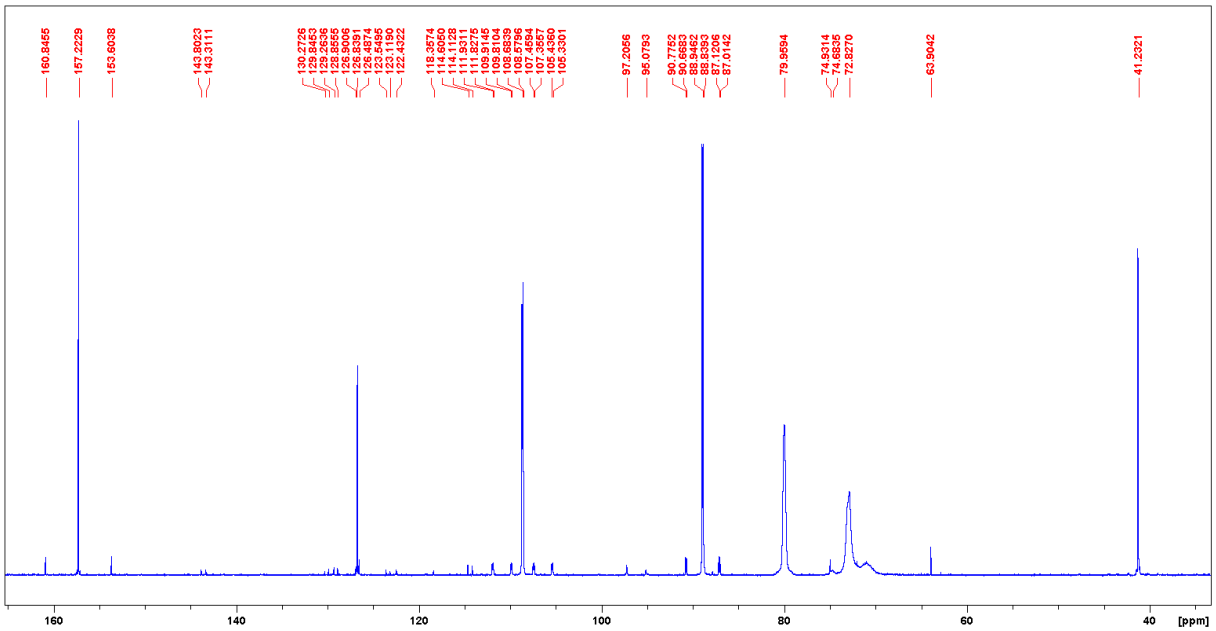

*Figure AI.27: $^{31}P\{^{1}H\}$ NMR spectrum of **1.1(${}^{i}Pr_3{}^{i}Pr_2$)**OTf + 2 Se in DCM, RT, 4 h.*

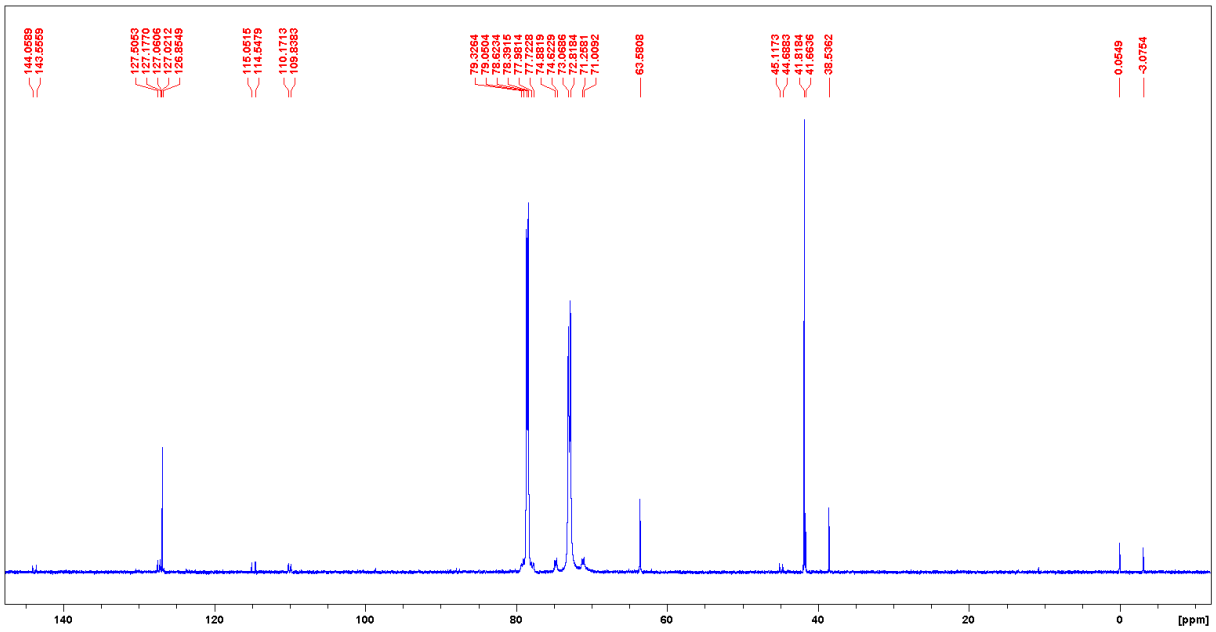

*Figure AI.28: $^{31}P\{^{1}H\}$ NMR spectrum of **1.1(${}^{i}Pr_3{}^{i}Pr_2$)**OTf + 1 Se in MeCN, RT, overnight.*

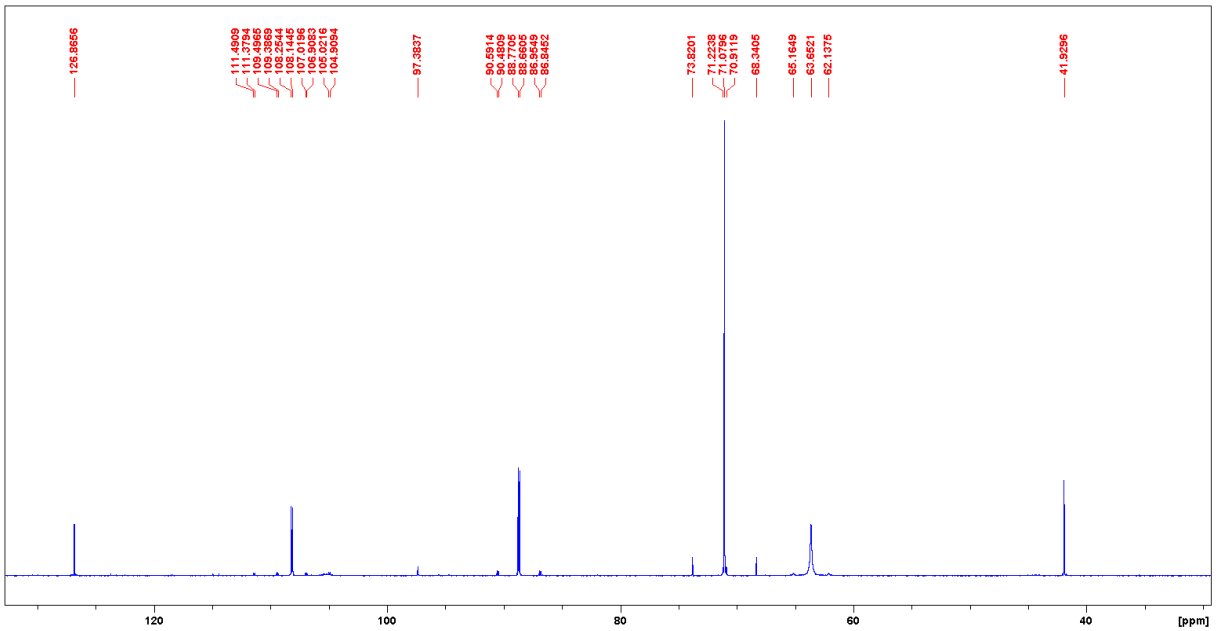

*Figure AI.29: $^{31}P\{^{1}H\}$ NMR spectrum of **1.1(^{i}Pr$_3$^{i}Pr$_2$)**OTf + 2 Se in MeCN, RT, overnight.*

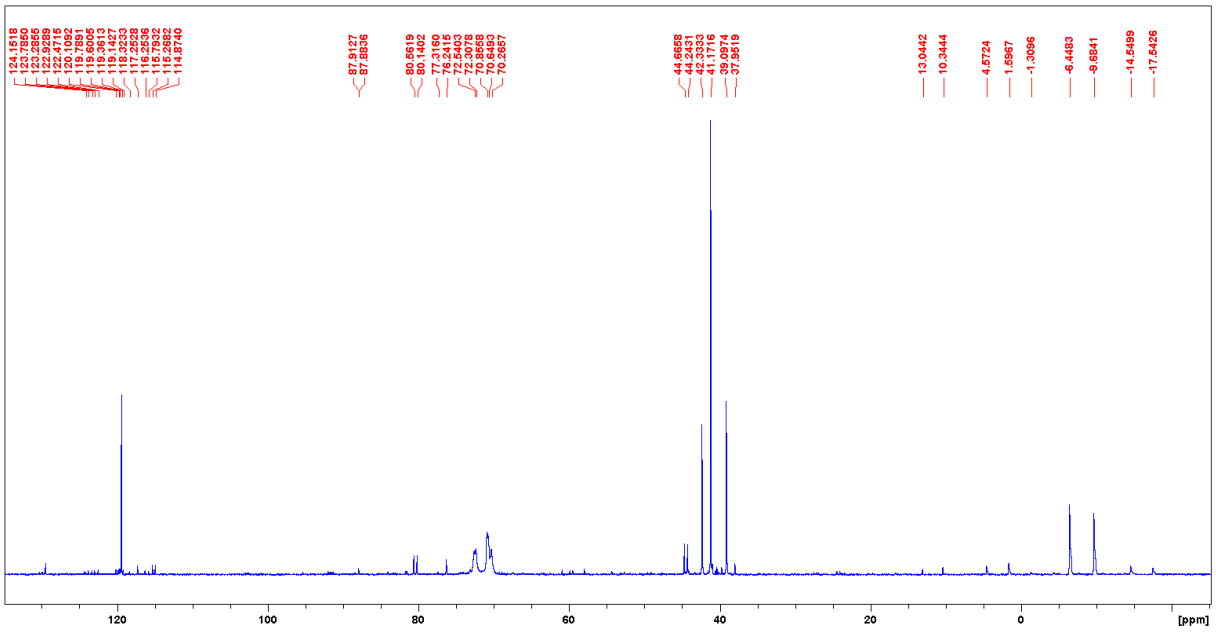

*Figure AI.30: $^{31}P\{^{1}H\}$ NMR spectrum of **1.1(^{i}Pr$_3$Cy$_2$)**OTf + 1 Se in MeCN, 67 °C, overnight.*

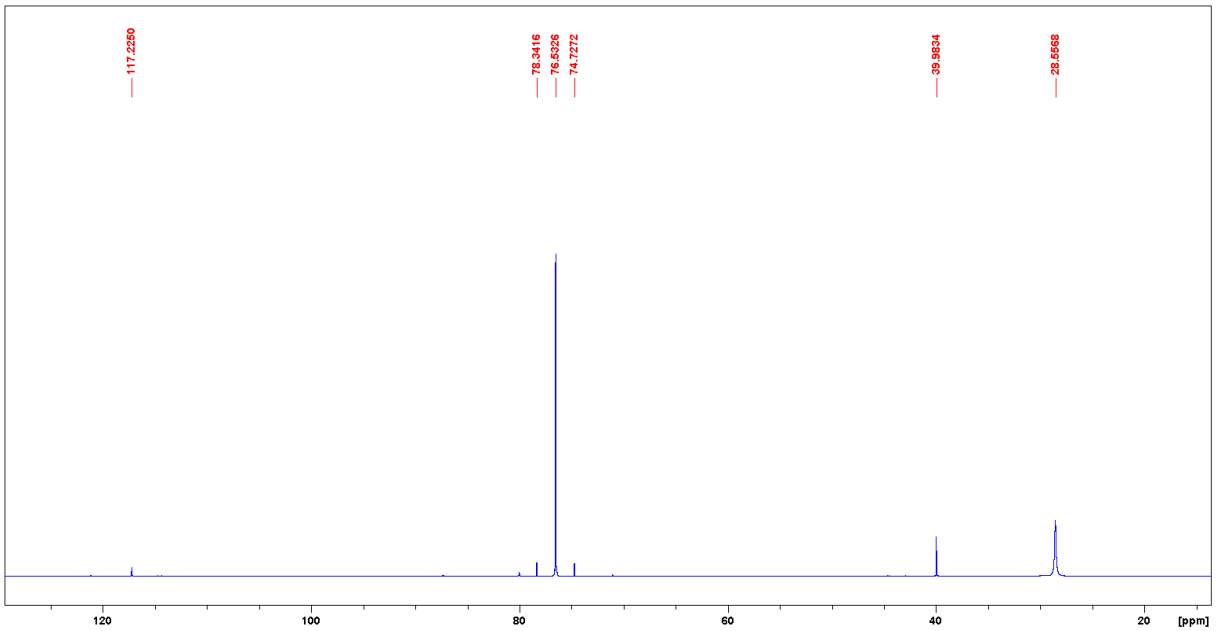

*Figure AI.31: $^{31}P\{^{1}H\}$ NMR spectrum of **1.1($^{i}Pr_3Ph_2$)**OTf + 1 Se in DCM, RT, overnight.*

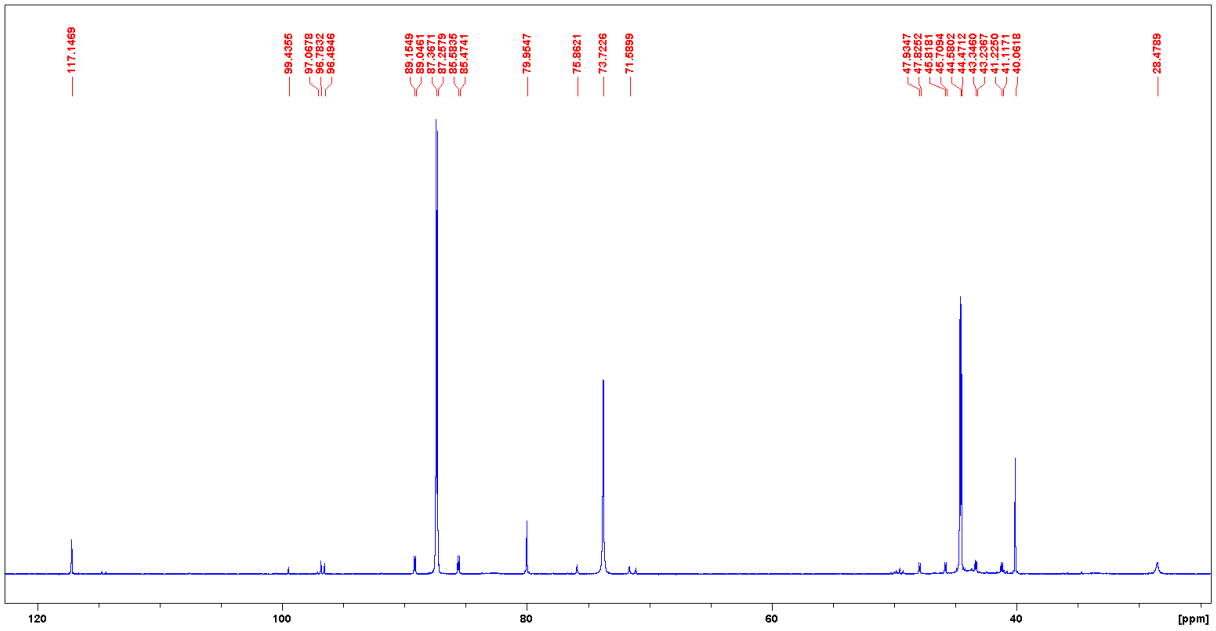

*Figure AI.32: $^{31}P\{^{1}H\}$ NMR spectrum of **1.1($^{i}Pr_3Ph_2$)**OTf + 2 Se in DCM, RT, overnight.*

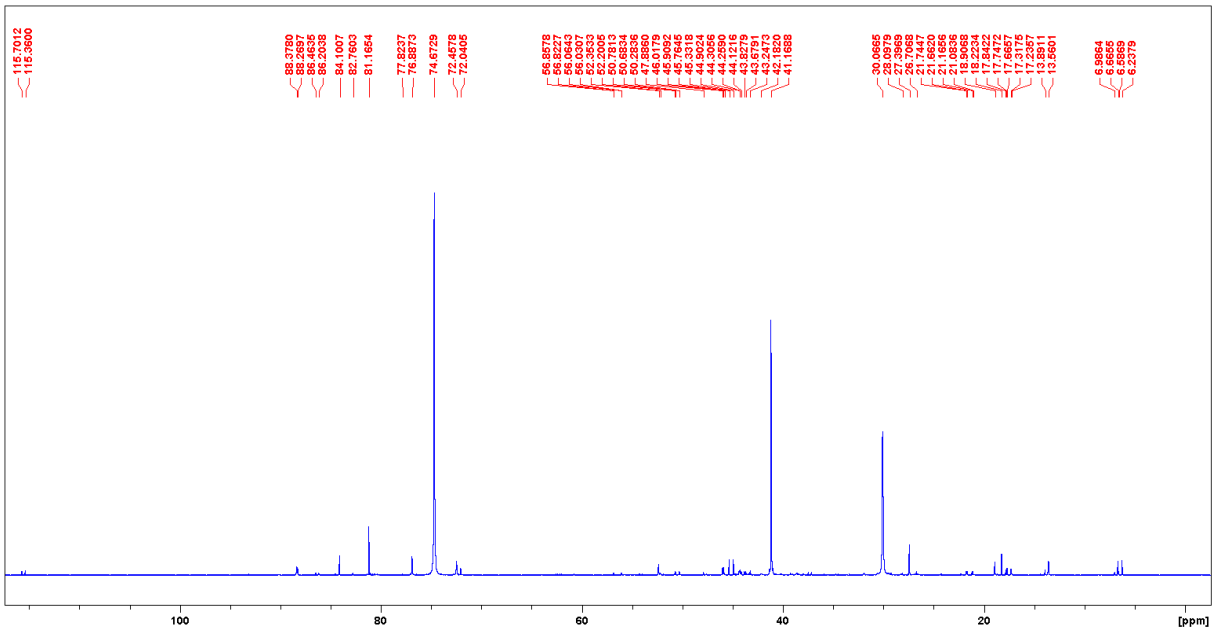

*Figure AI.33: $^{31}P\{^{1}H\}$ NMR spectrum of **1.1(^{i}Pr$_3$Ph$_2$)**OTf + 1 Se in MeCN, 69 °C, overnight.*

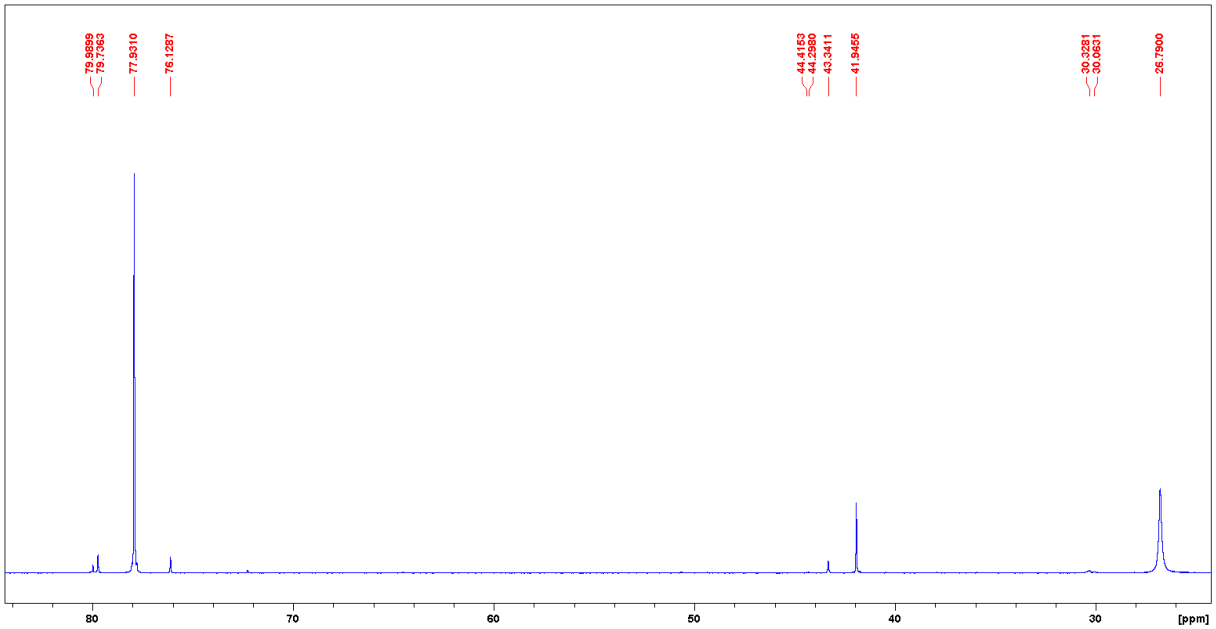

*Figure AI.34: $^{31}P\{^{1}H\}$ NMR spectrum of **1.1(^{i}Pr$_3$Ph$_2$)**OTf + 1 Se in MeCN, RT, overnight.*

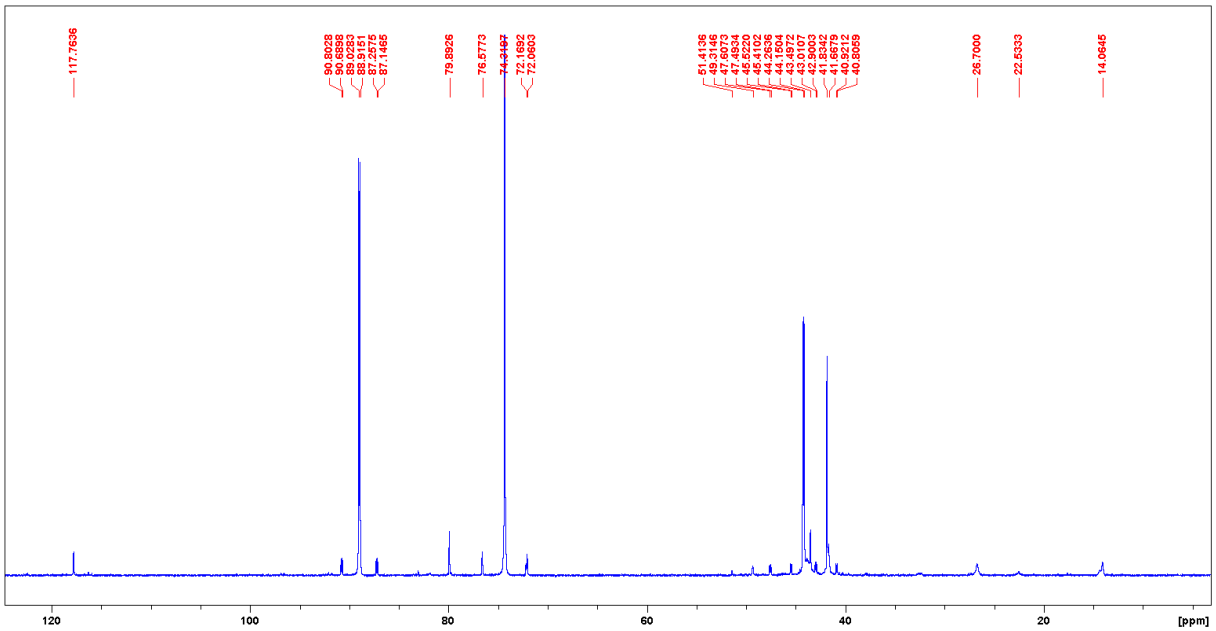

*Figure AI.35: $^{31}P\{^{1}H\}$ NMR spectrum of **1.1(^{i}Pr$_3$Ph$_2$)**OTf + 2 Se in MeCN, RT, overnight.*

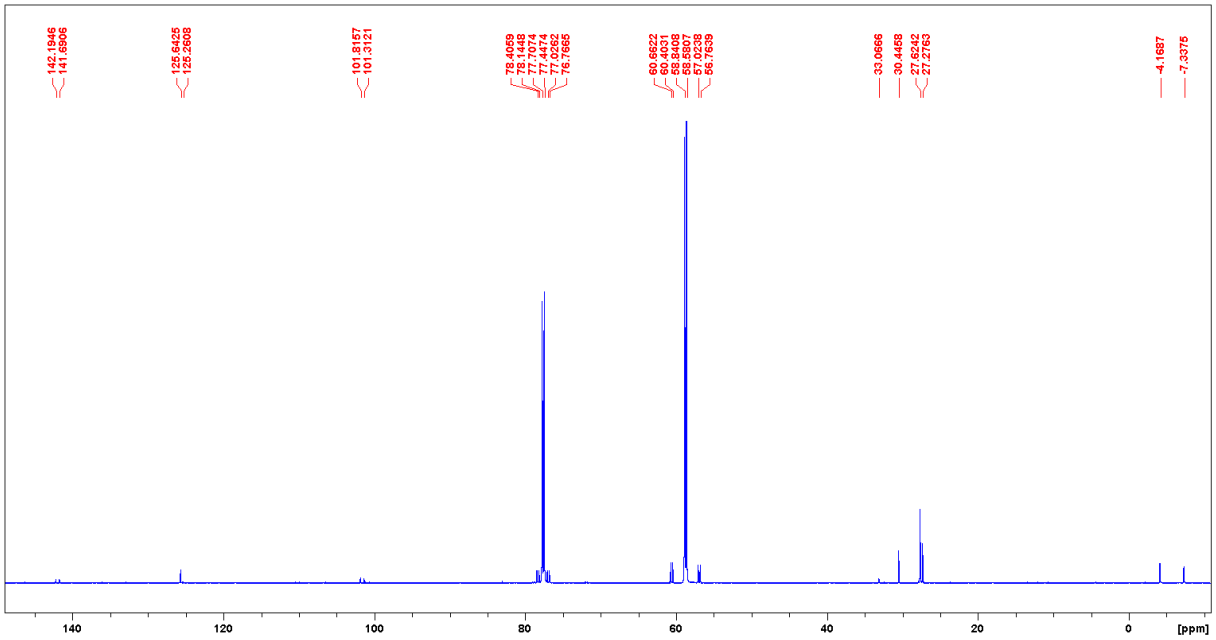

*Figure AI.36: $^{31}P\{^{1}H\}$ NMR spectrum of **1.1(Cy$_3$^{i}Pr$_2$)**OTf + 1 Se in DCM, RT, overnight.*

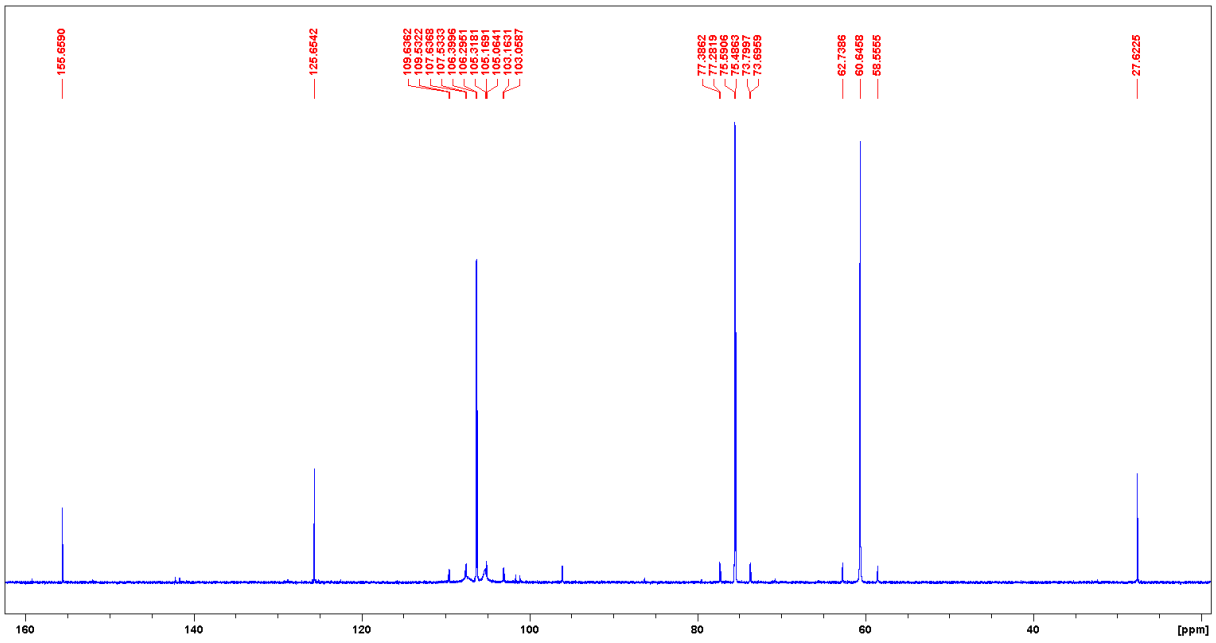

*Figure AI.37: $^{31}P\{^{1}H\}$ NMR spectrum of **1.1(Cy$_3$^{i}Pr$_2$)**OTf + 2.5 Se in DCM, RT, overnight.*

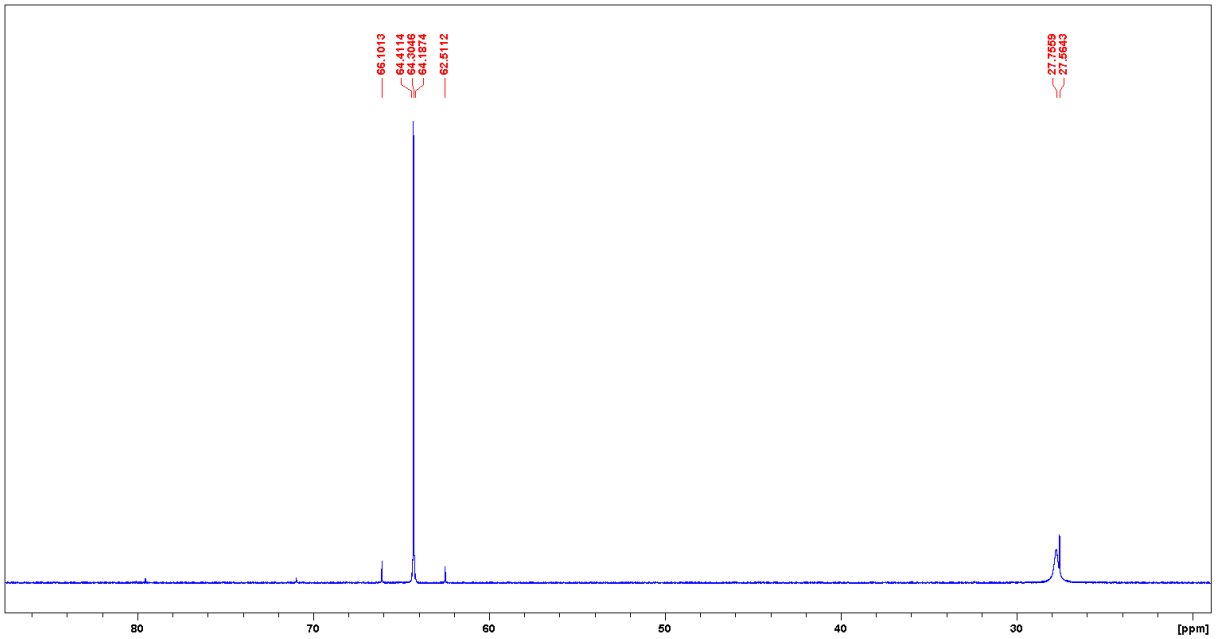

*Figure AI.38: $^{31}P\{^{1}H\}$ NMR spectrum of **1.1(Cy$_3$Ph$_2$)**OTf + 1 Se in DCM, RT, overnight.*

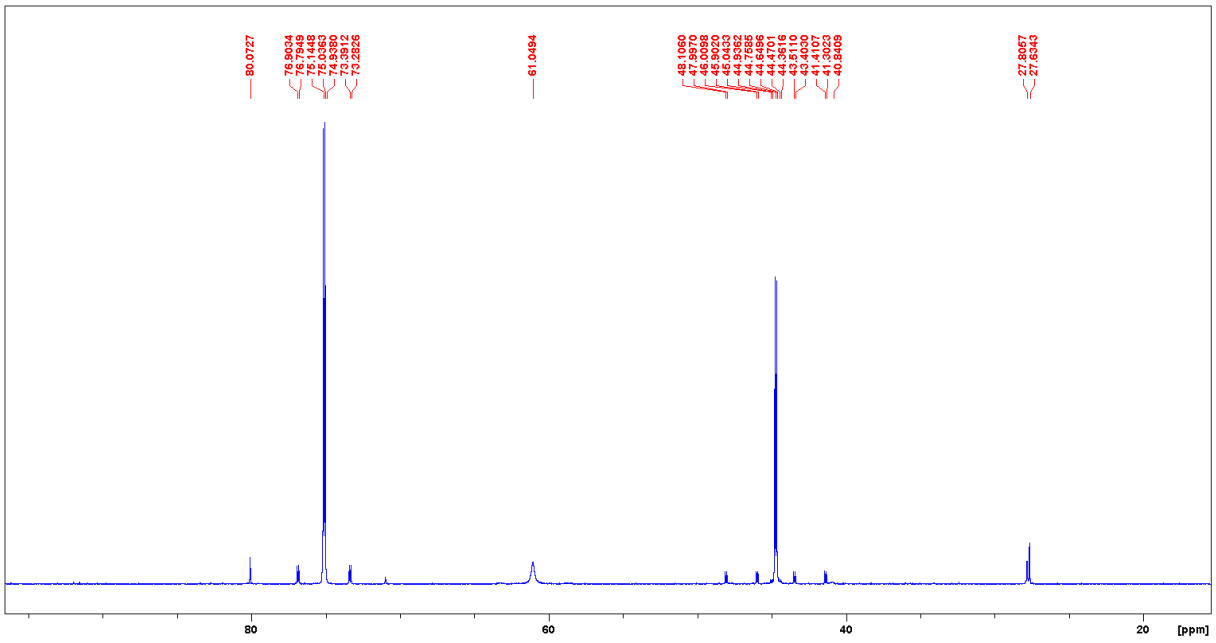

*Figure AI.39: $^{31}P\{^{1}H\}$ NMR spectrum of **1.1(Cy$_3$Ph$_2$)**OTf + 2 Se in DCM, RT, overnight.*

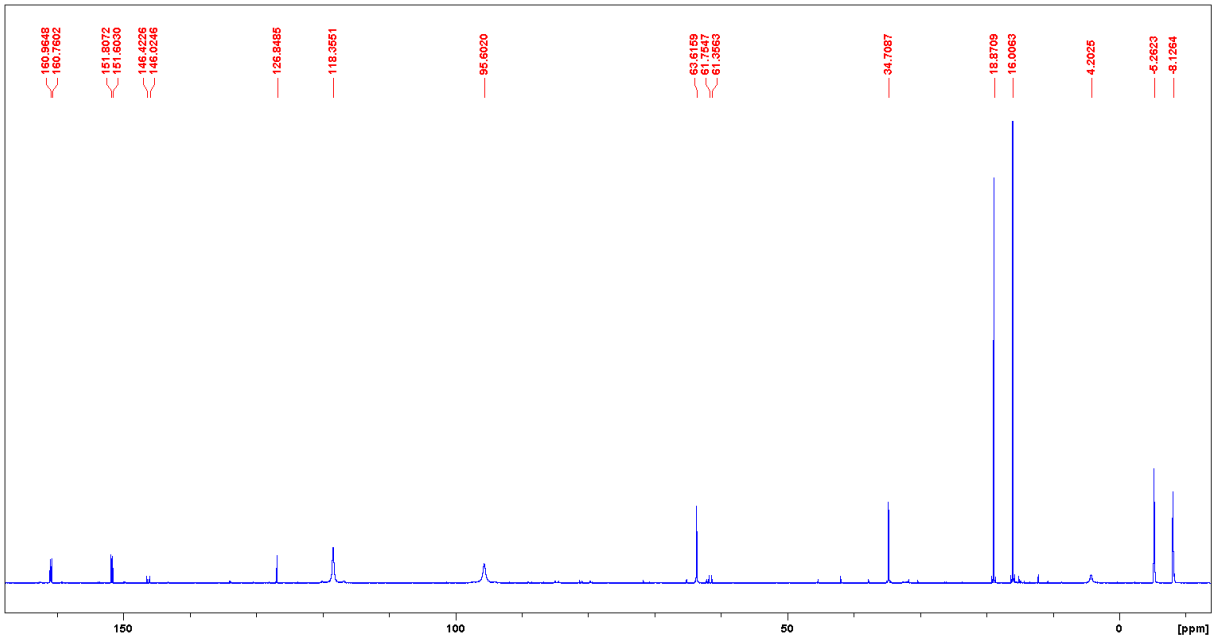

*Figure AI.40: $^{31}P\{^{1}H\}$ NMR spectrum of **1.1(Ph$_3$^{i}Pr$_2$)**OTf + 1 Se in MeCN, RT, 4 h.*

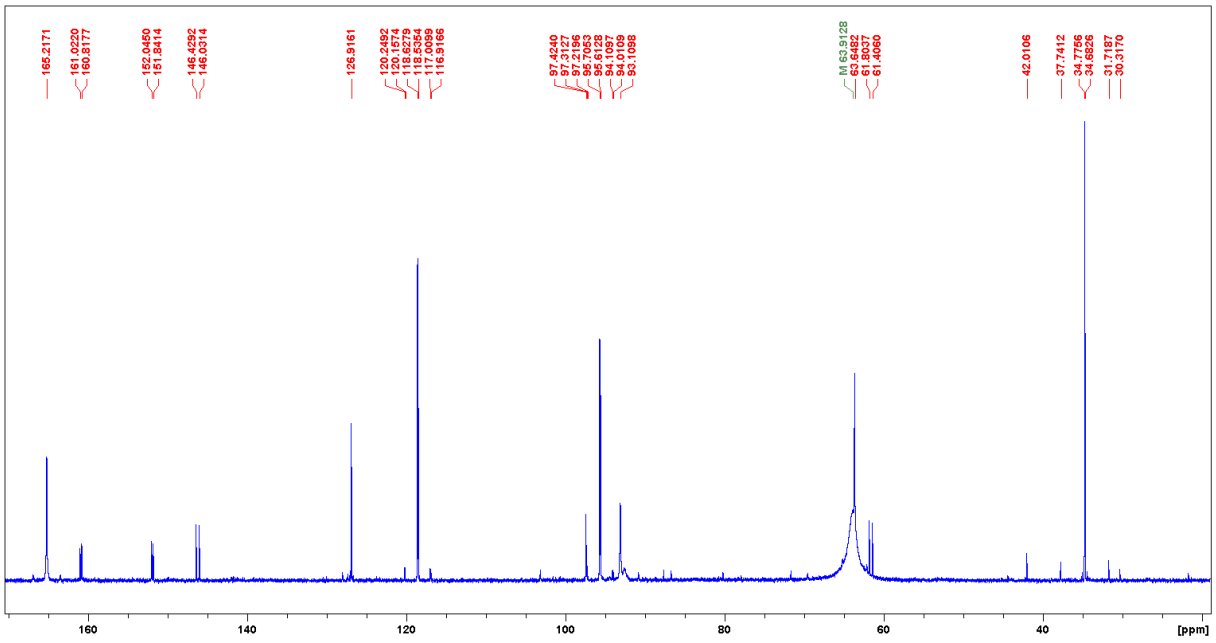

*Figure AI.41: $^{31}P\{^{1}H\}$ NMR spectrum of **1.1(Ph$_3$^{i}Pr$_2$)**OTf + 2 Se in MeCN, RT, 4 h.*

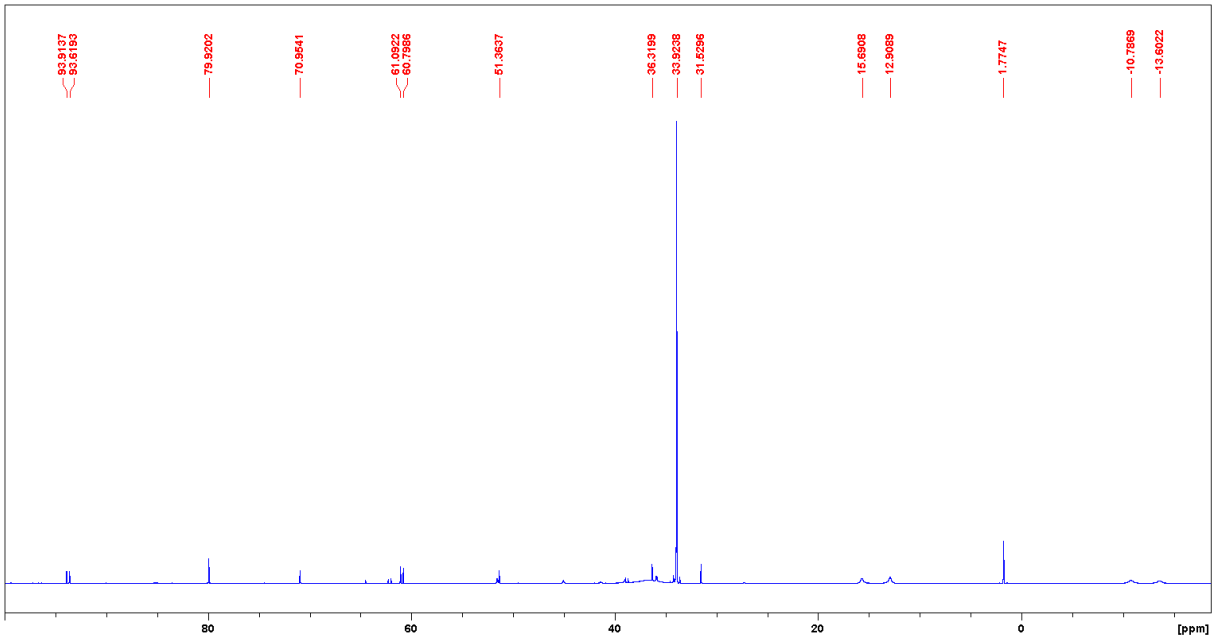

*Figure AI:42: $^{31}P\{^{1}H\}$ NMR spectrum of **1.1(Ph$_3$Ph$_2$)**OTf + 1 Se in DCM, RT, 3 d.*

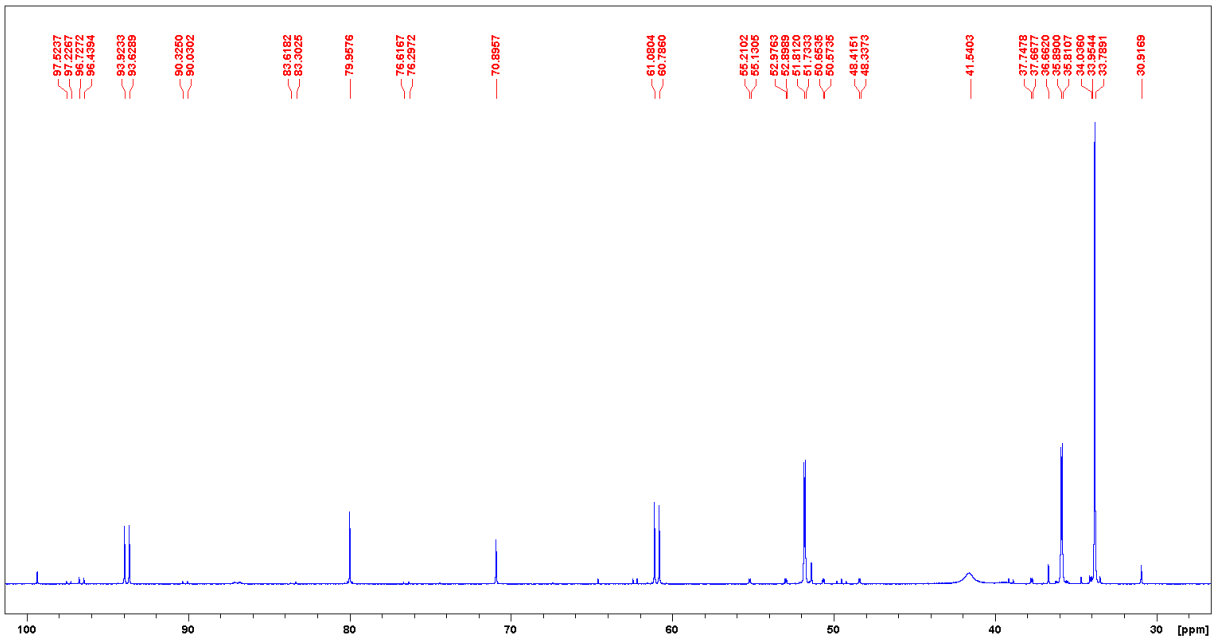

*Figure AI.43: $^{31}P\{^{1}H\}$ NMR spectrum of **1.1(Ph$_3$Ph$_2$)**OTf + 2 Se in DCM, RT, 3 d.*

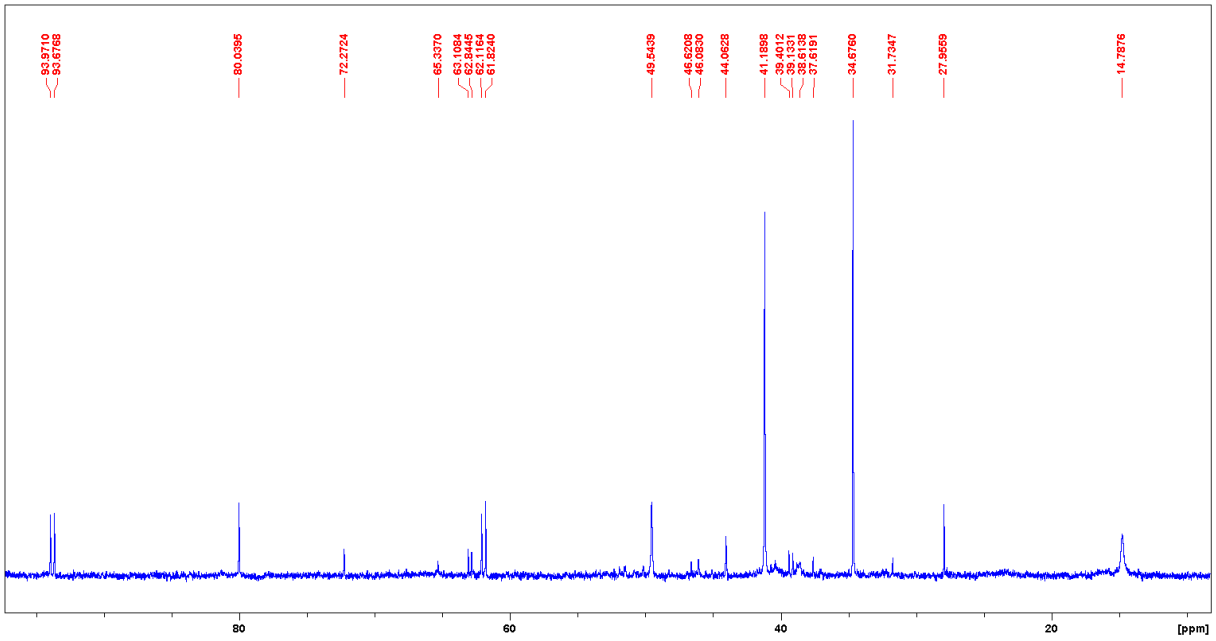

*Figure AI.44: $^{31}P\{^{1}H\}$ NMR spectrum of **1.1(Ph$_3$Ph$_2$)**OTf + 2 Se in MeCN, RT, 10 d.*

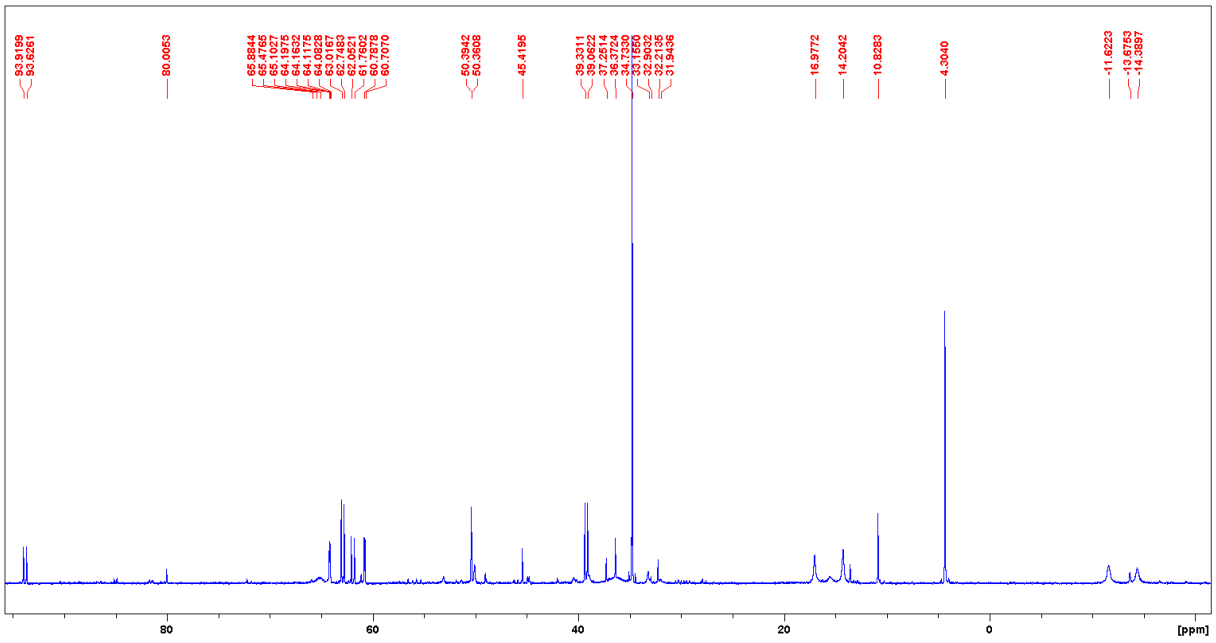

*Figure AI.45: $^{31}P\{^{1}H\}$ NMR spectrum of **1.1(Ph$_3$Ph$_2$)**OTf + 1 Se in MeCN, RT, overnight.*

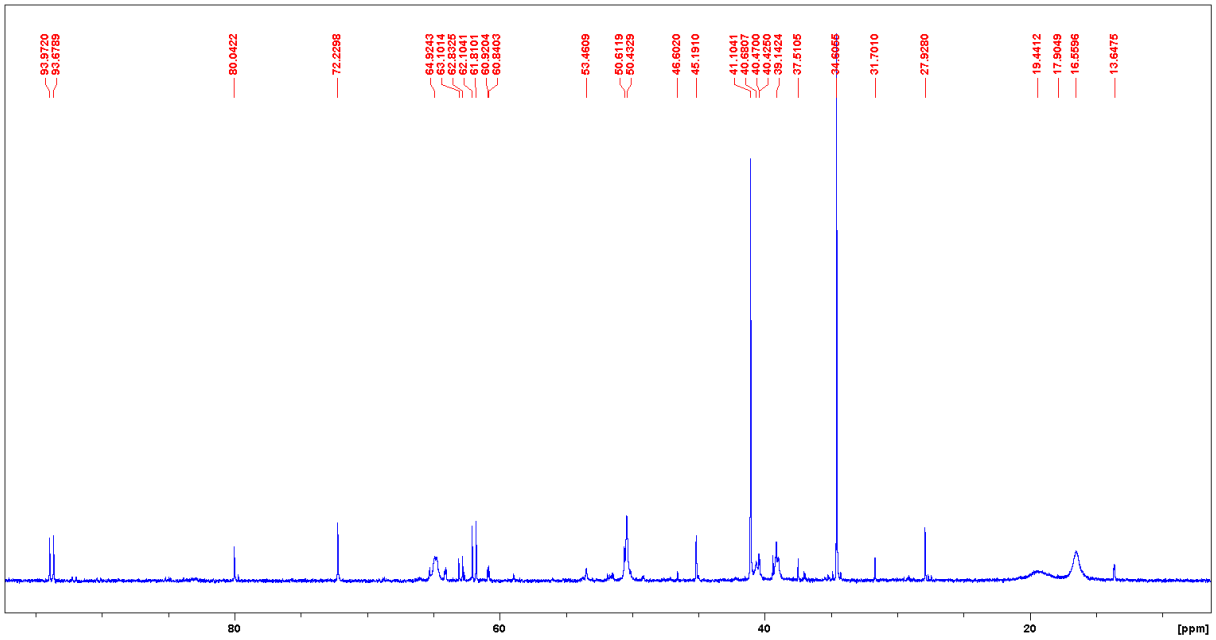

*Figure AI:46: $^{31}P\{^{1}H\}$ NMR spectrum of **1.1(Ph$_3$Ph$_2$)**OTf + 2 Se in MeCN, RT, overnight.*

$^{31}P\{^{1}H\}$ NMR spectra of Reactions of Phosphino-Phosphonium Cations with Sulfur

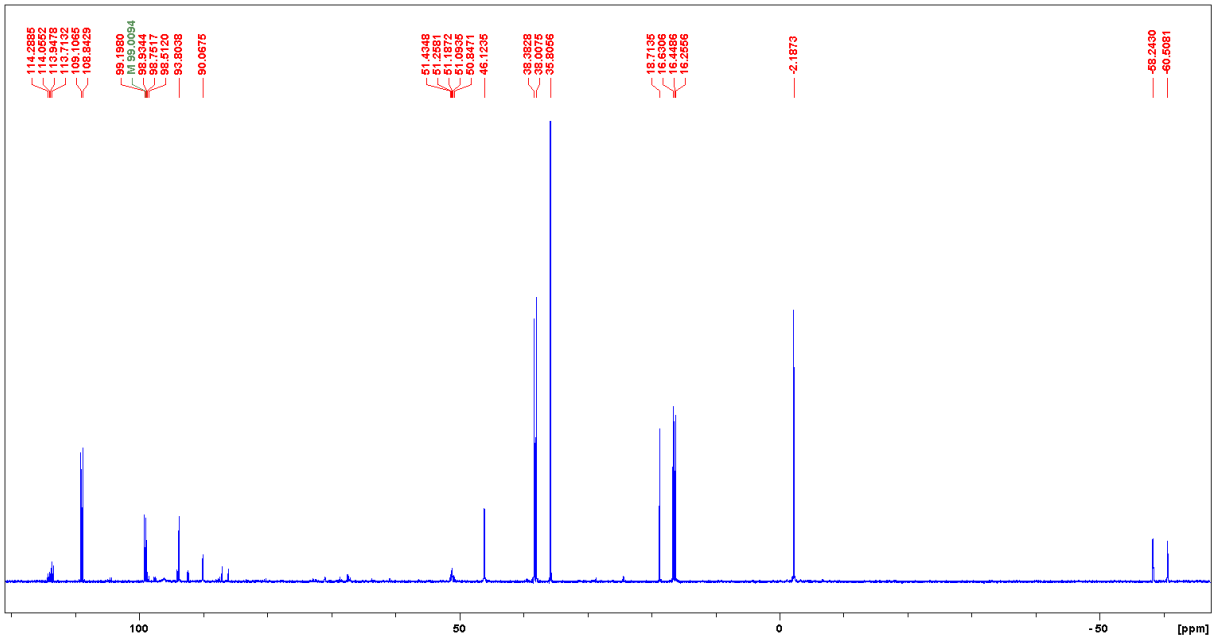

*Figure AI.47: $^{31}P\{^{1}H\}$ NMR spectrum of **1.1(Me$_3$Me$_2$)**OTf + 1 S in DCM, RT, 3 d; then MeCN, 67 °C, 1 d.*

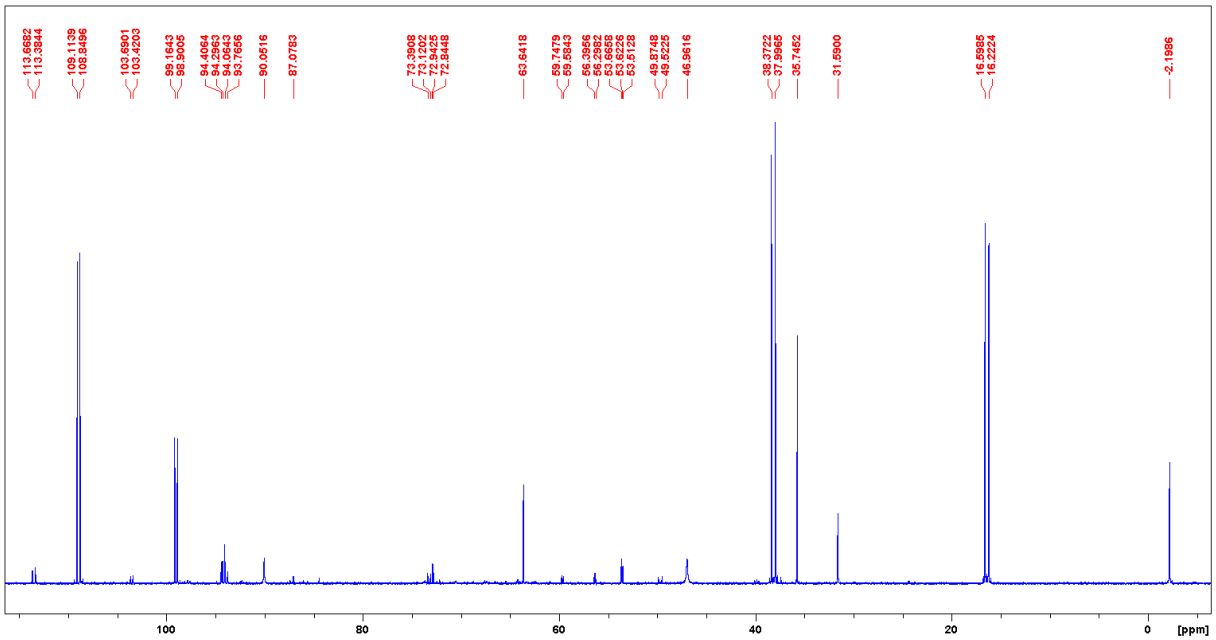

*Figure AI.48: $^{31}P\{^{1}H\}$ NMR spectrum of **1.1(Me$_3$Me$_2$)**OTf + 2 S in DCM, RT, 3 d; then MeCN, 68 °C, 4 d.*

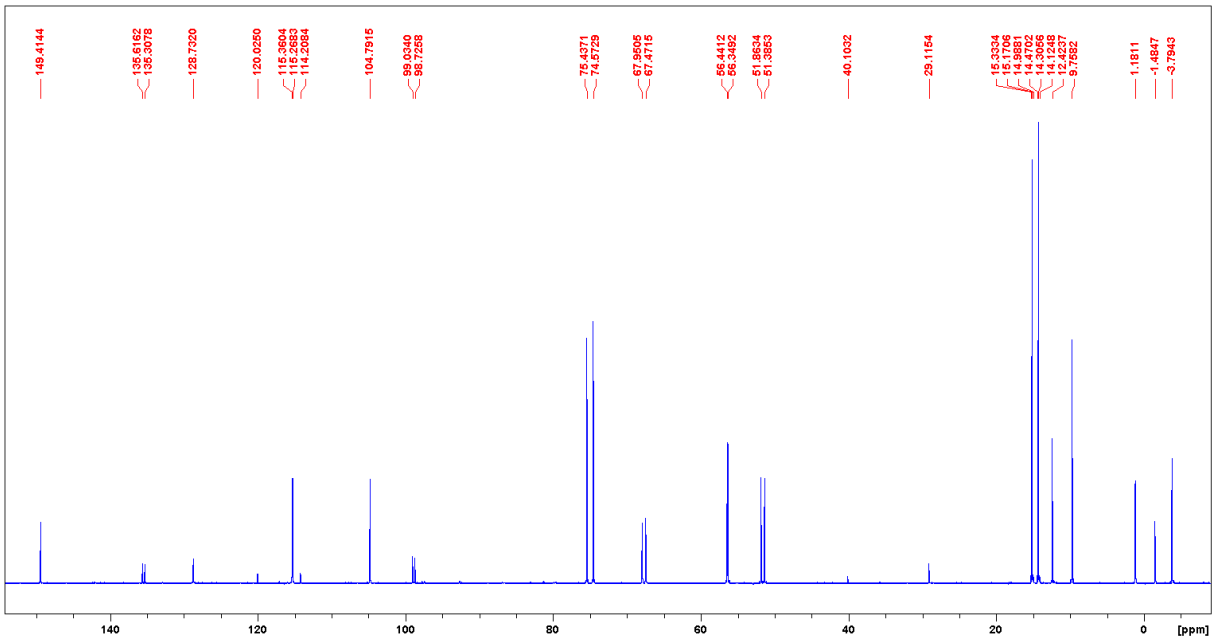

*Figure AI.49: $^{31}P\{^{1}H\}$ NMR spectrum of **1.1(Me$_3$^{i}Pr$_2$)**OTf + 1 S in DCM, RT, 7 d.*

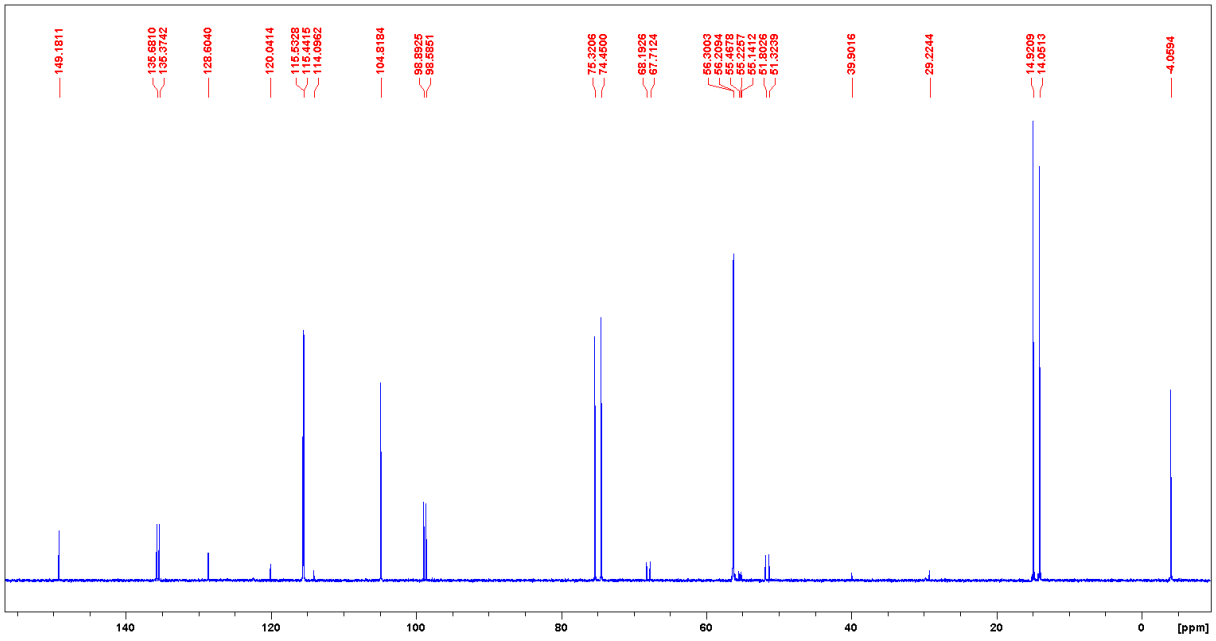

*Figure AI.50: $^{31}P\{^{1}H\}$ NMR spectrum of **1.1(Me$_3$^{i}Pr$_2$)**OTf + 2 S in DCM, RT, 7 d.*

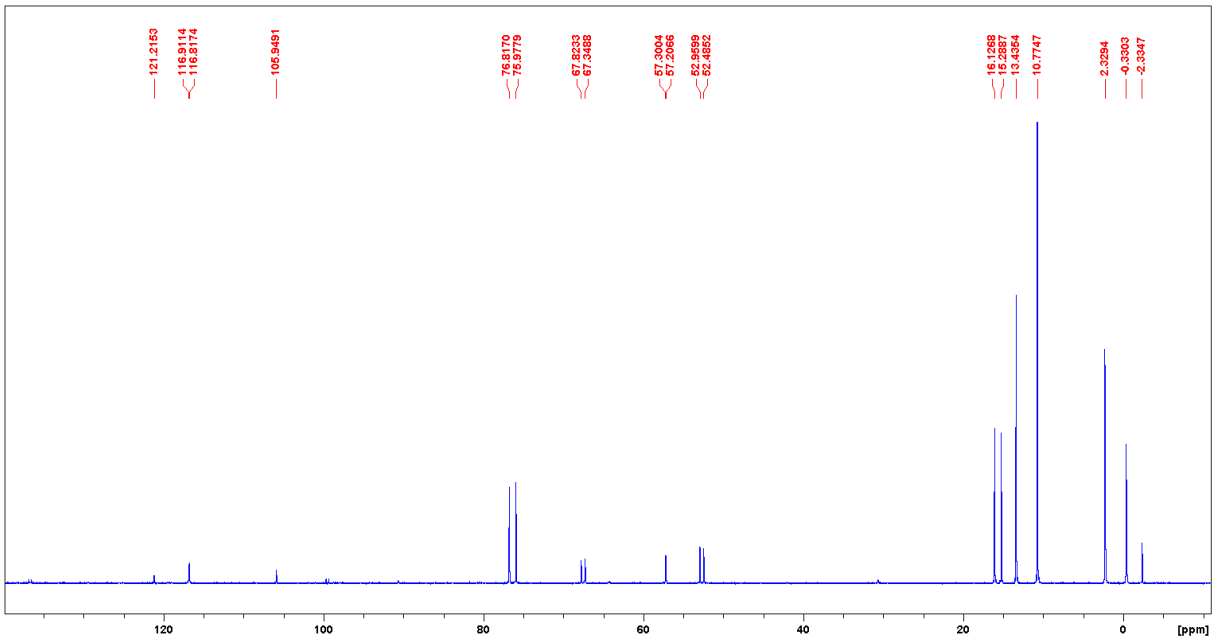

*Figure AI.51: $^{31}P\{^{1}H\}$ NMR spectrum of **1.1(Me$_3$^{i}Pr$_2$)**OTf + 1 S in MeCN, RT, overnight.*

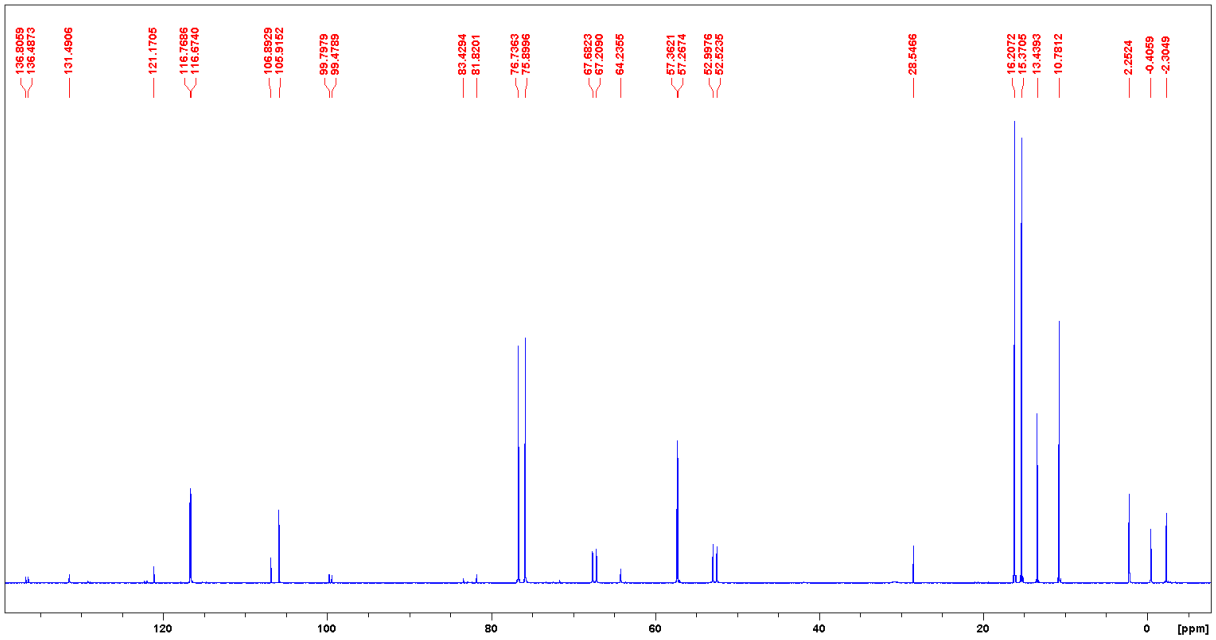

*Figure AI.52: $^{31}P\{^{1}H\}$ NMR spectrum of **1.1(Me$_3$^{i}Pr$_2$)**OTf + 1 S in MeCN, RT, 5 d.*

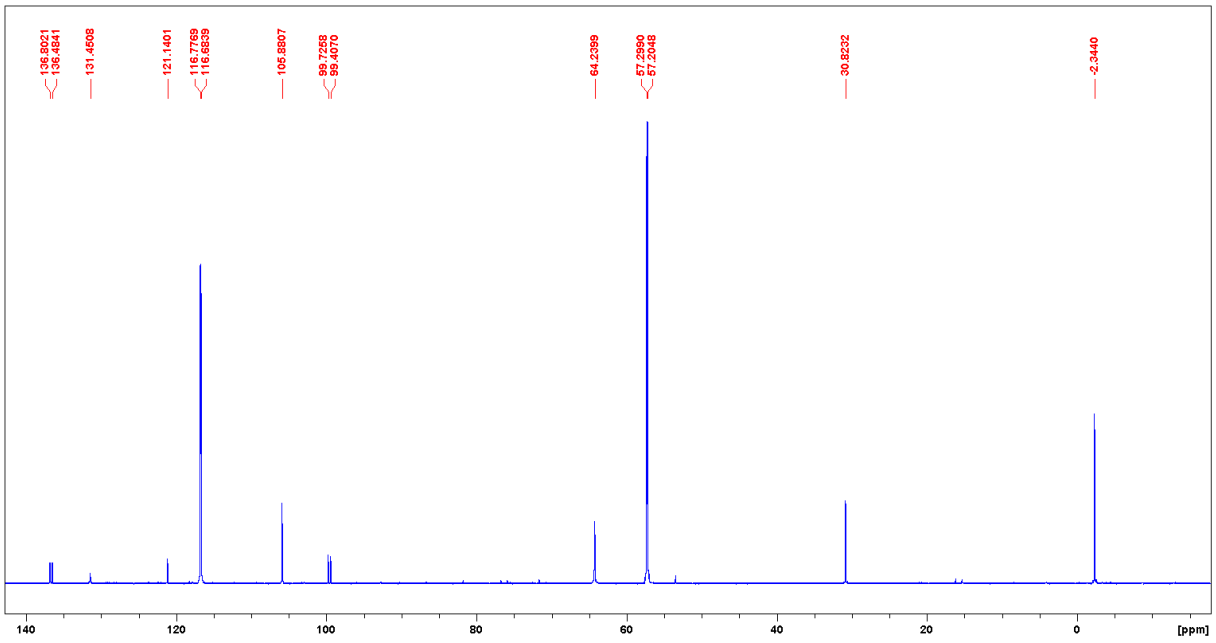

*Figure AI.53: $^{31}P\{^{1}H\}$ NMR spectrum of **1.1(Me$_3$^{i}Pr$_2$)**OTf + 2 S in MeCN, RT, 5 d; 50-60 °C, 2 d.*

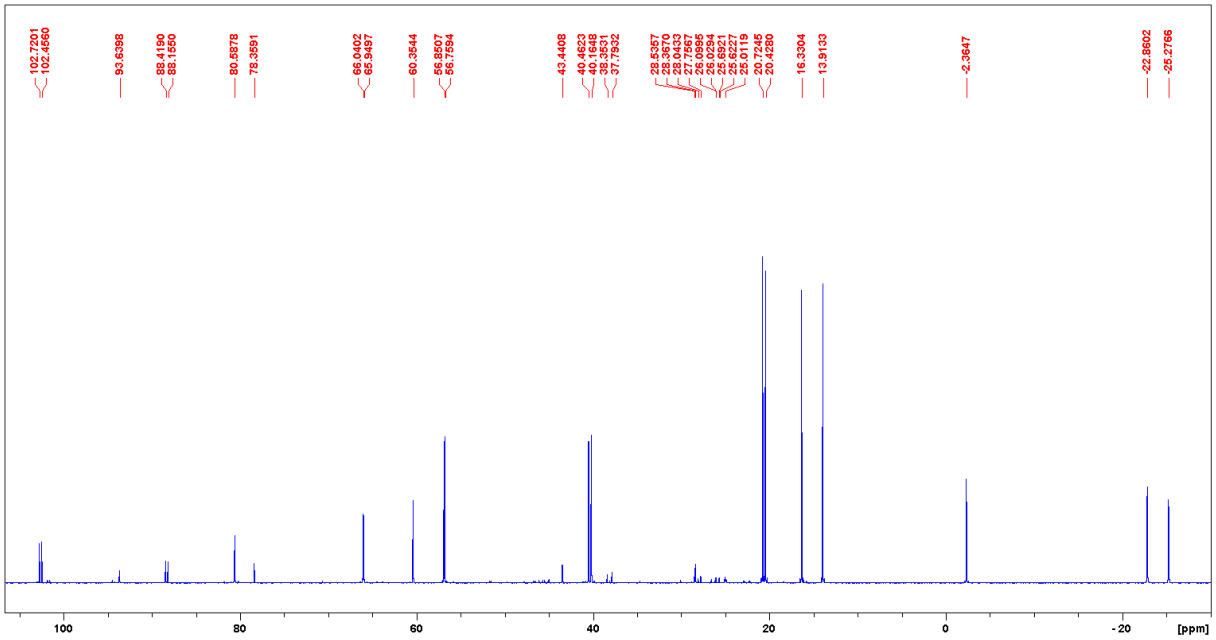

*Figure AI.54: $^{31}P\{^{1}H\}$ NMR spectrum of **1.1(Me$_3$Ph$_2$)**OTf + 1 S in MeCN, RT, overnight; 40-60 °C, overnight.*

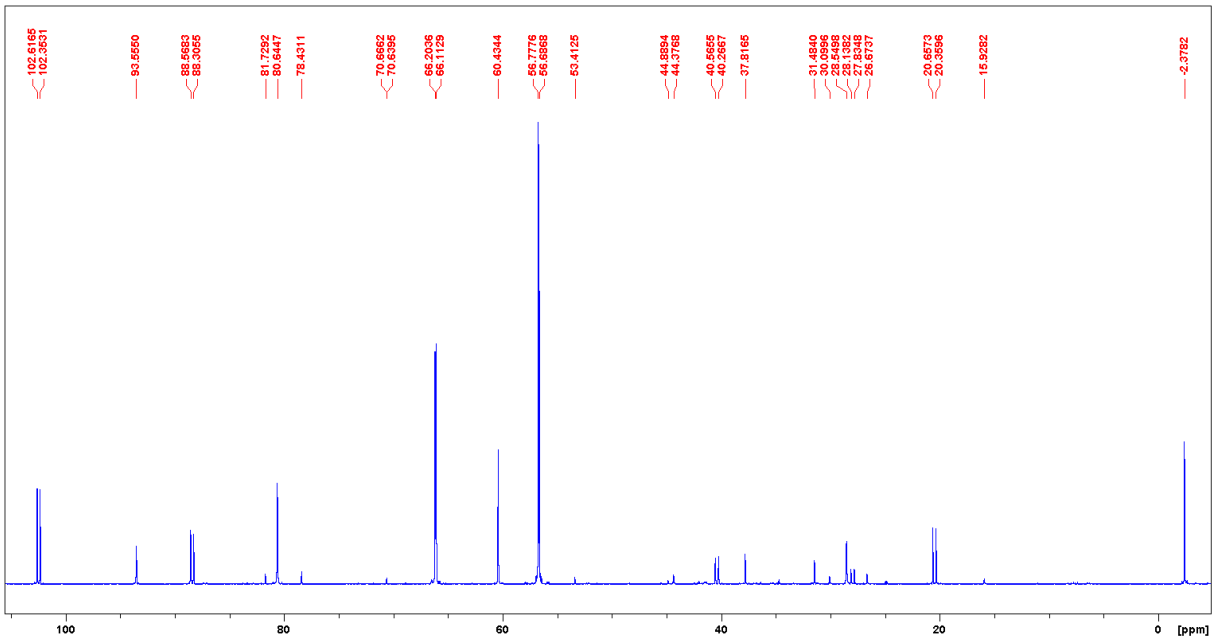

*Figure AI.55: $^{31}P\{^{1}H\}$ NMR spectrum of **1.1(Me$_3$Ph$_2$)**OTf + 2 S in MeCN, 60-70 °C, 2 d.*

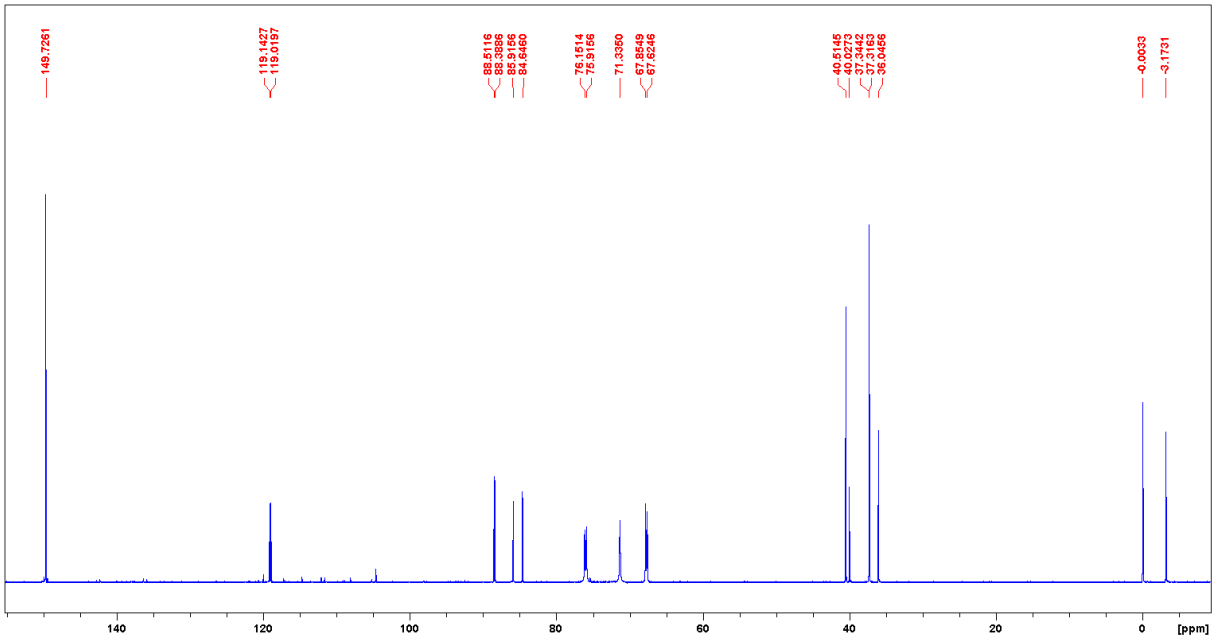

*Figure AI.56: $^{31}P\{^{1}H\}$ NMR spectrum of **1.1(^{i}Pr$_3$^{i}Pr$_2$)**OTf + 1 S in DCM, RT, 3 d.*

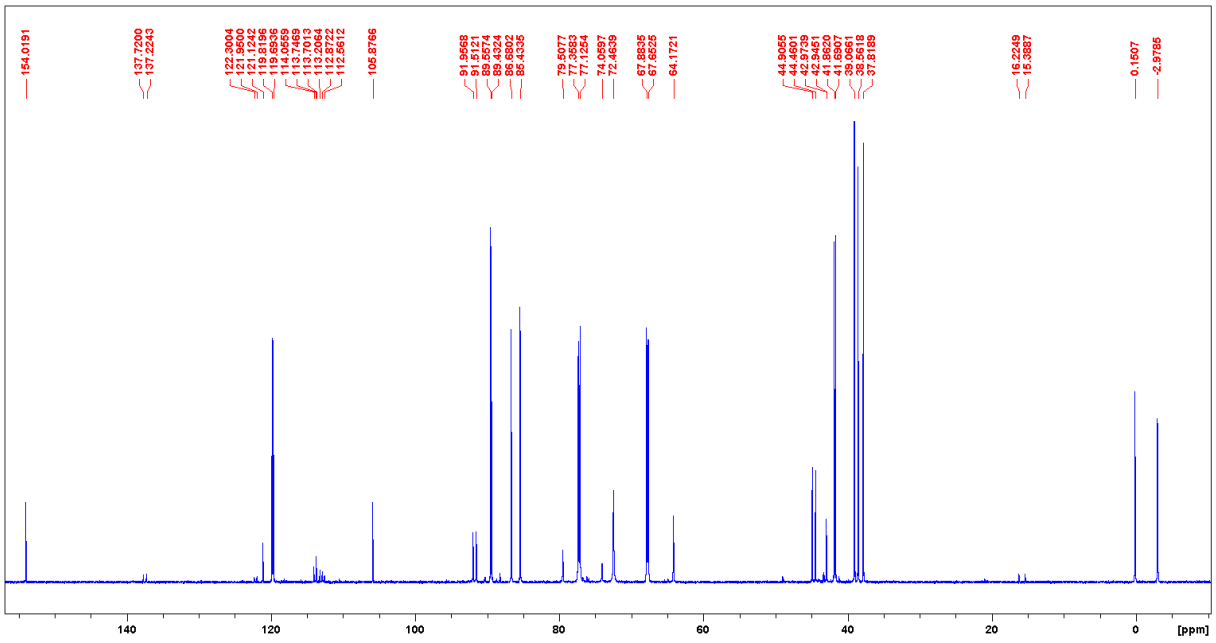

*Figure AI.57: $^{31}P\{^{1}H\}$ NMR spectrum of **1.1(^{i}Pr$_3$^{i}Pr$_2$)**OTf + 1 S in MeCN, RT, overnight.*

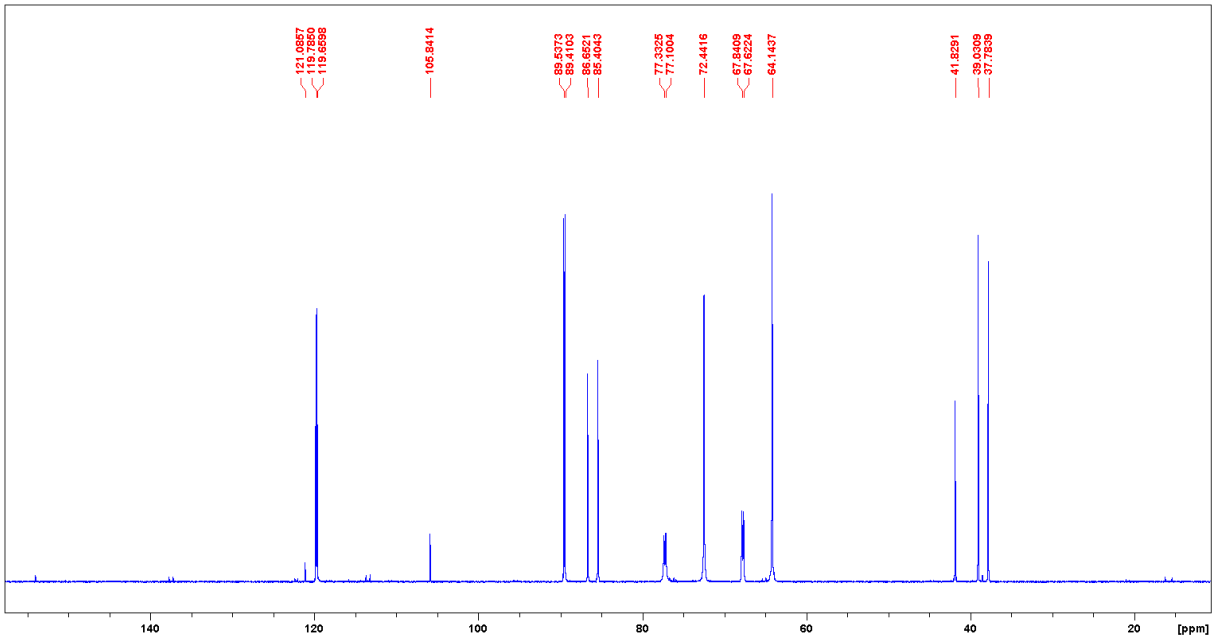

*Figure AI.58: $^{31}P\{^{1}H\}$ NMR spectrum of **1.1(^{i}Pr$_3$^{i}Pr$_2$)**OTf + 2 S in MeCN, RT, overnight.*

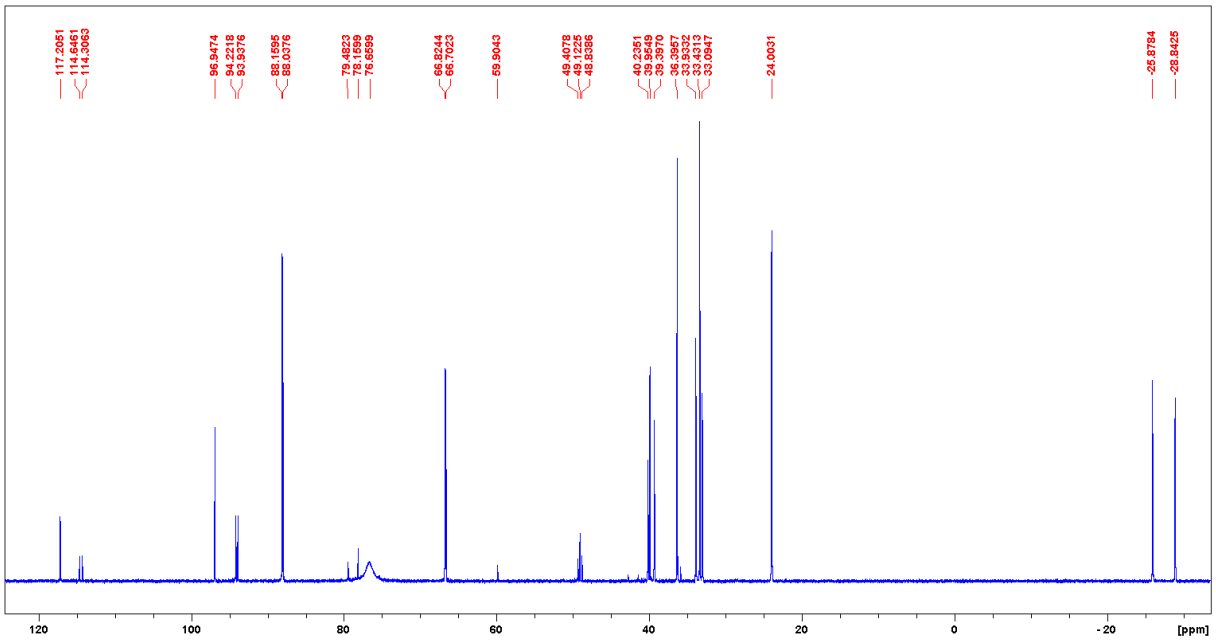

*Figure AI.59: $^{31}P\{^{1}H\}$ NMR spectrum of **1.1(^{i}Pr$_3$Ph$_2$)**OTf + 1 S in DCM, RT, overnight.*

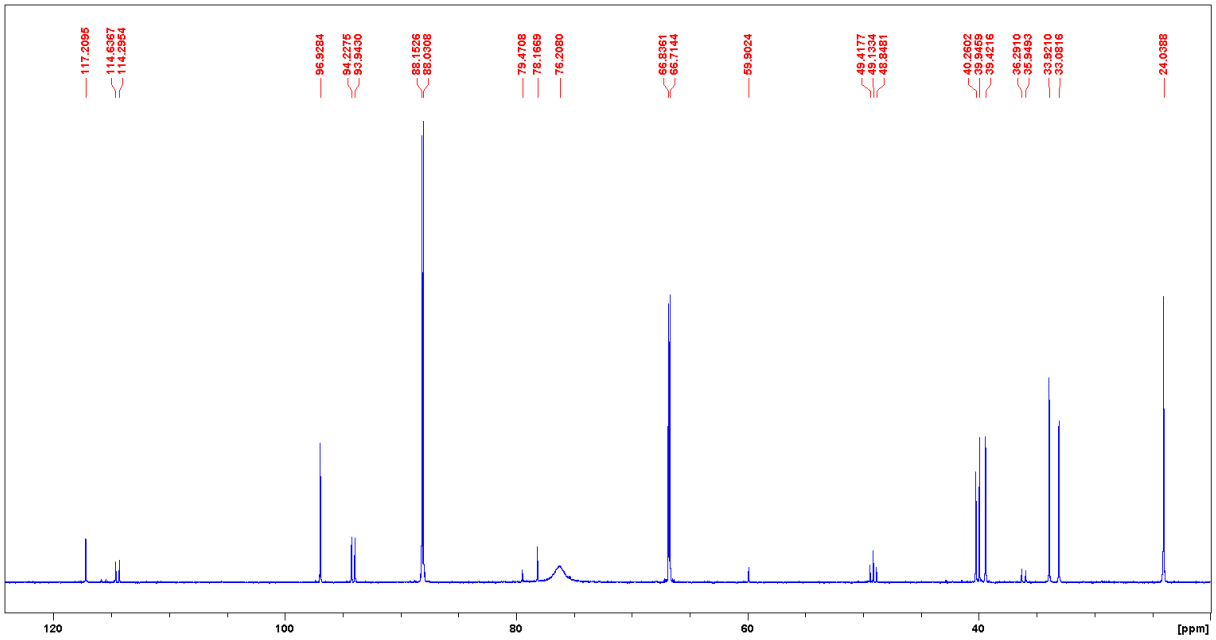

*Figure AI.60: $^{31}P\{^{1}H\}$ NMR spectrum of **1.1(^{i}Pr$_3$Ph$_2$)**OTf + 2 S in DCM, RT, overnight.*

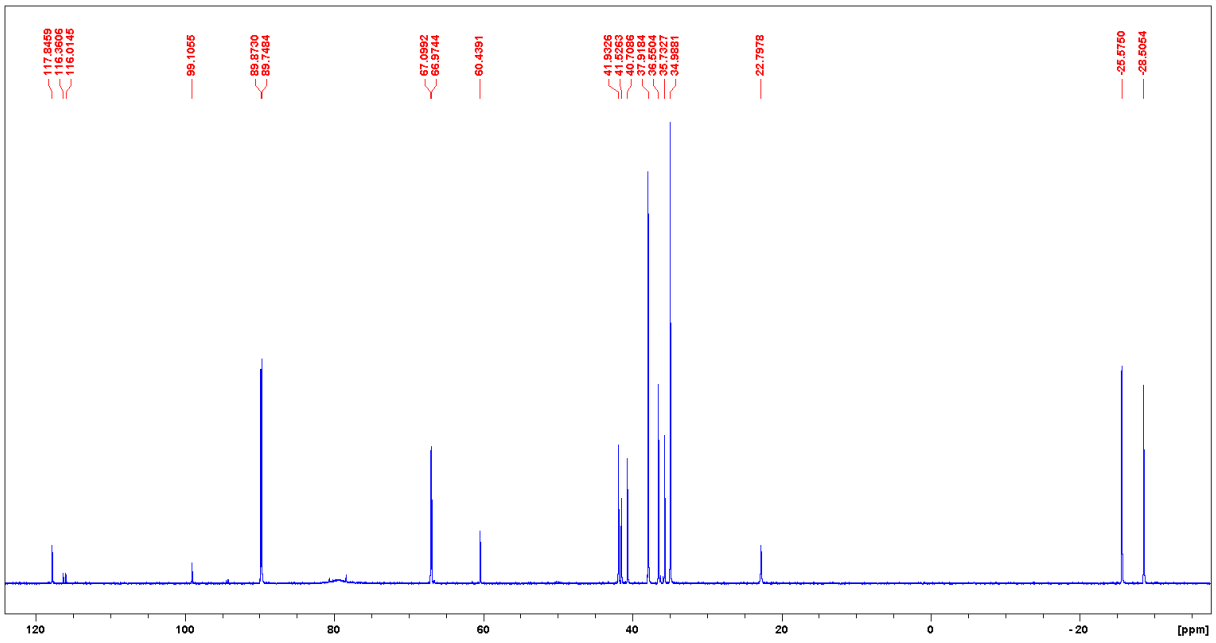

*Figure AI.61: $^{31}P\{^{1}H\}$ NMR spectrum of **1.1(^{i}Pr$_3$Ph$_2$)**OTf + 1 S in MeCN, RT, overnight.*

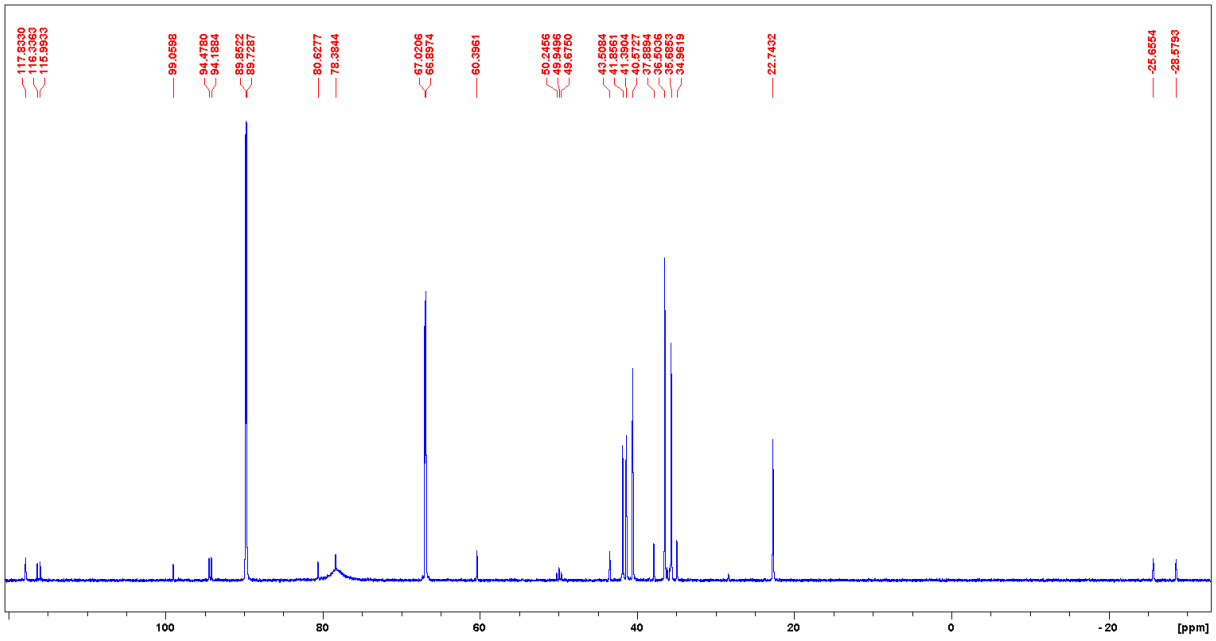

*Figure AI.62: $^{31}P\{^{1}H\}$ NMR spectrum of **1.1(^{i}Pr$_3$Ph$_2$)**OTf + 2 S in MeCN, RT, overnight.*

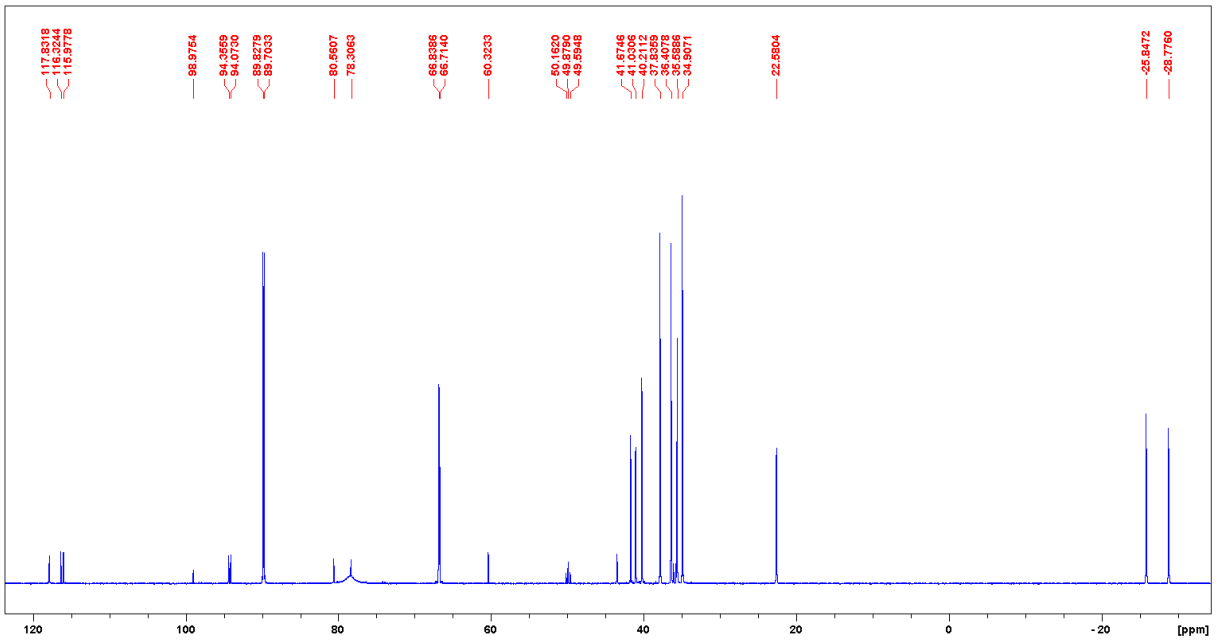

*Figure AI.63: $^{31}P\{^{1}H\}$ NMR spectrum of **1.1(^{i}Pr$_3$Ph$_2$)**OTf + 1 S in MeCN, RT, overnight.*

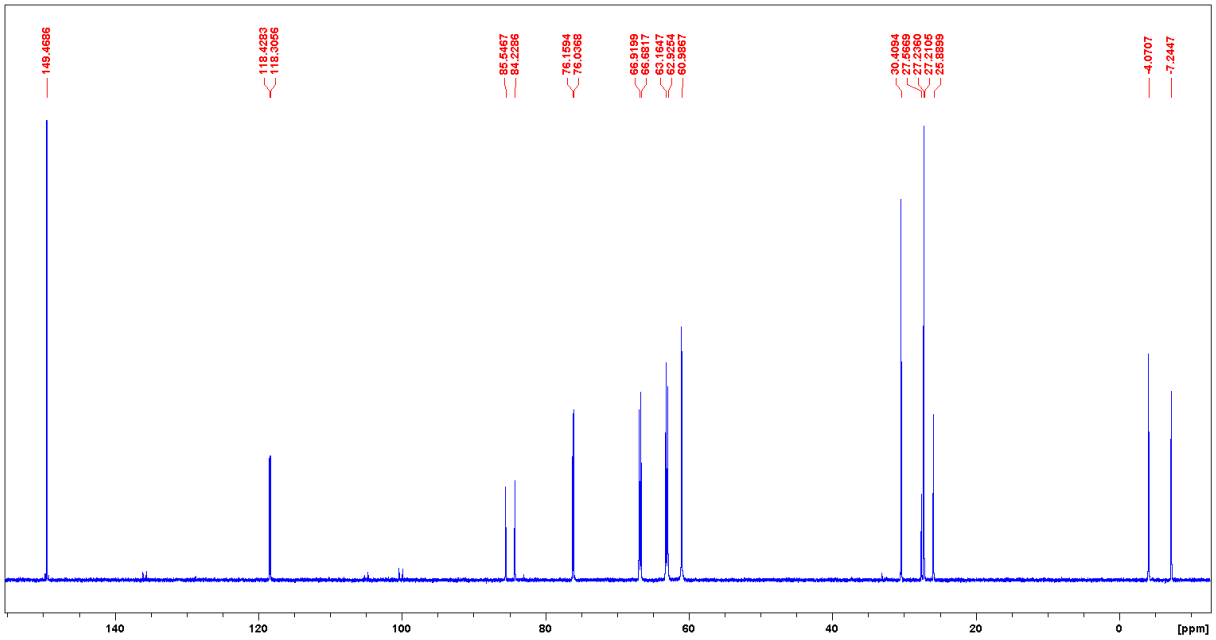

*Figure AI.64: $^{31}P\{^{1}H\}$ NMR spectrum of **1.1(Cy$_3$^{i}Pr$_2$)**OTf + 1 S in DCM, RT, overnight.*

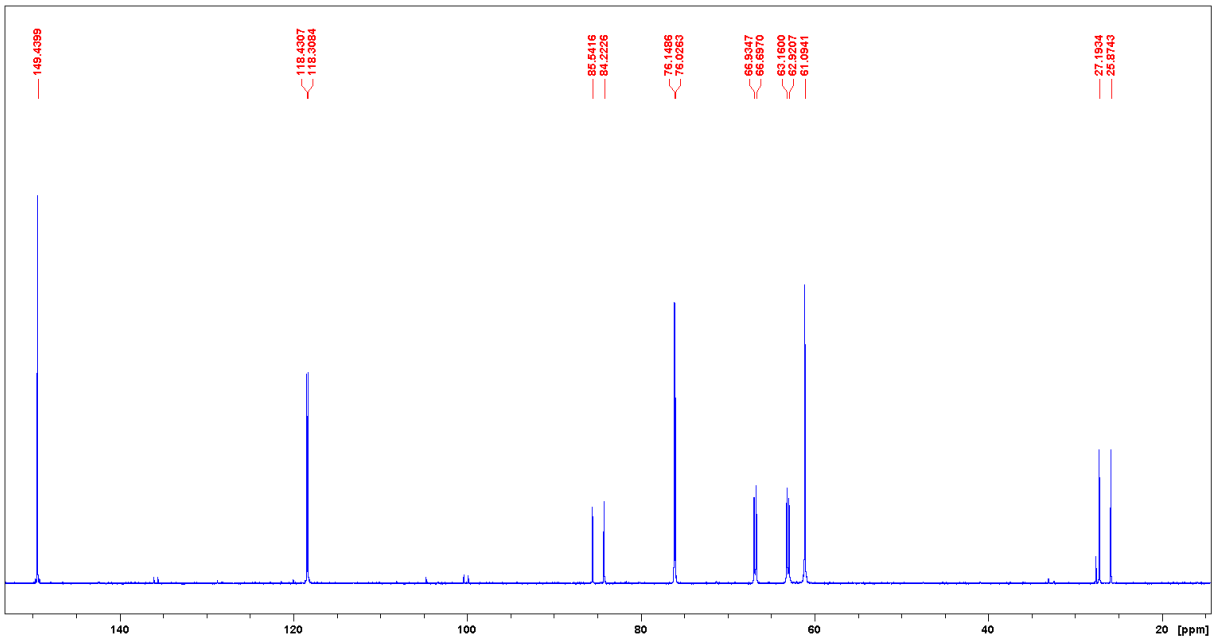

*Figure AI.65: $^{31}P\{^{1}H\}$ NMR spectrum of **1.1(Cy$_3$^{i}Pr$_2$)**OTf + 2 S in DCM, RT, overnight.*

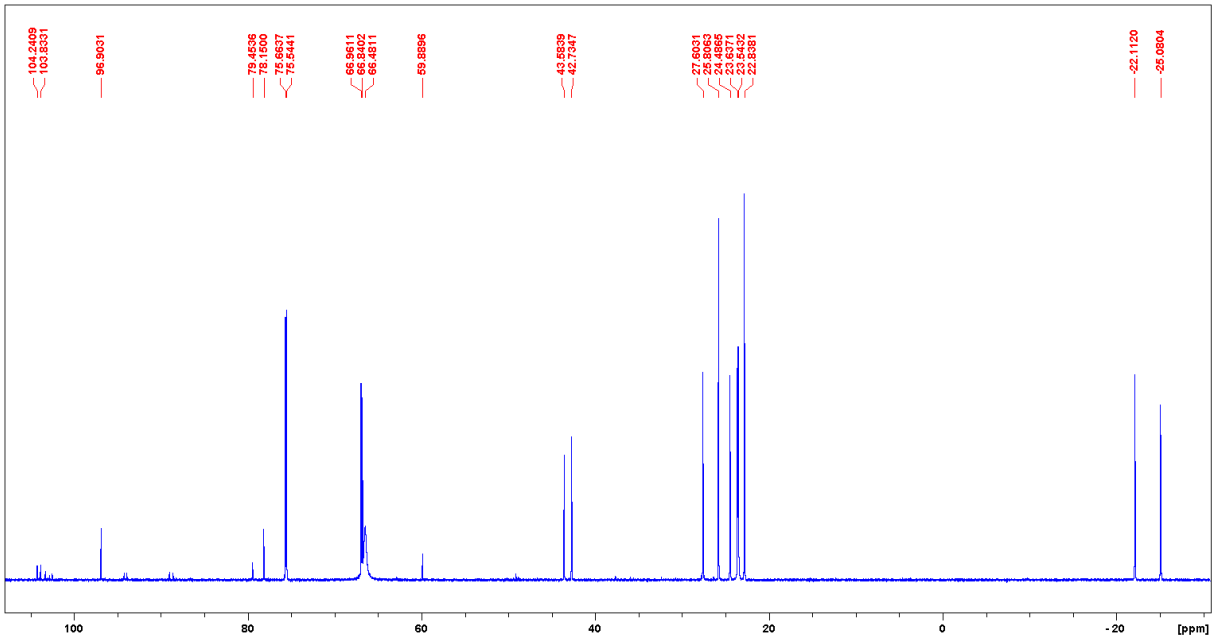

*Figure AI.66: $^{31}P\{^{1}H\}$ NMR spectrum of **1.1(Cy$_3$Ph$_2$)**OTf + 1 S in DCM, RT, 2 d.*

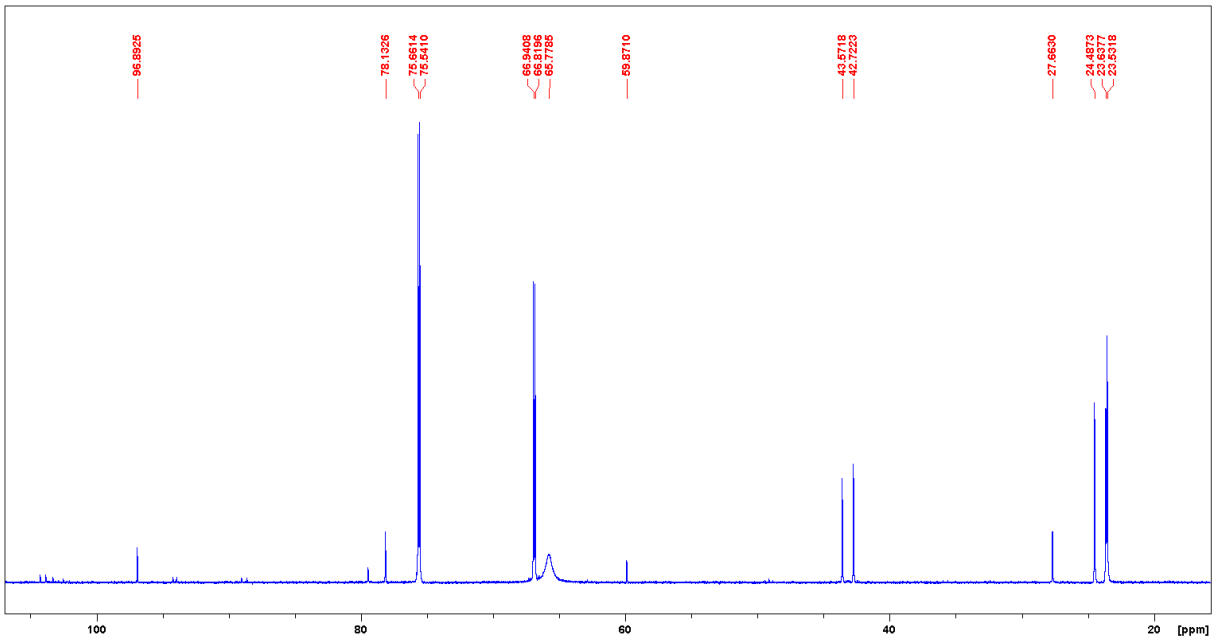

*Figure AI.67: $^{31}P\{^{1}H\}$ NMR spectrum of **1.1(Cy$_3$Ph$_2$)**OTf + 2 S in DCM, RT, 2 d.*

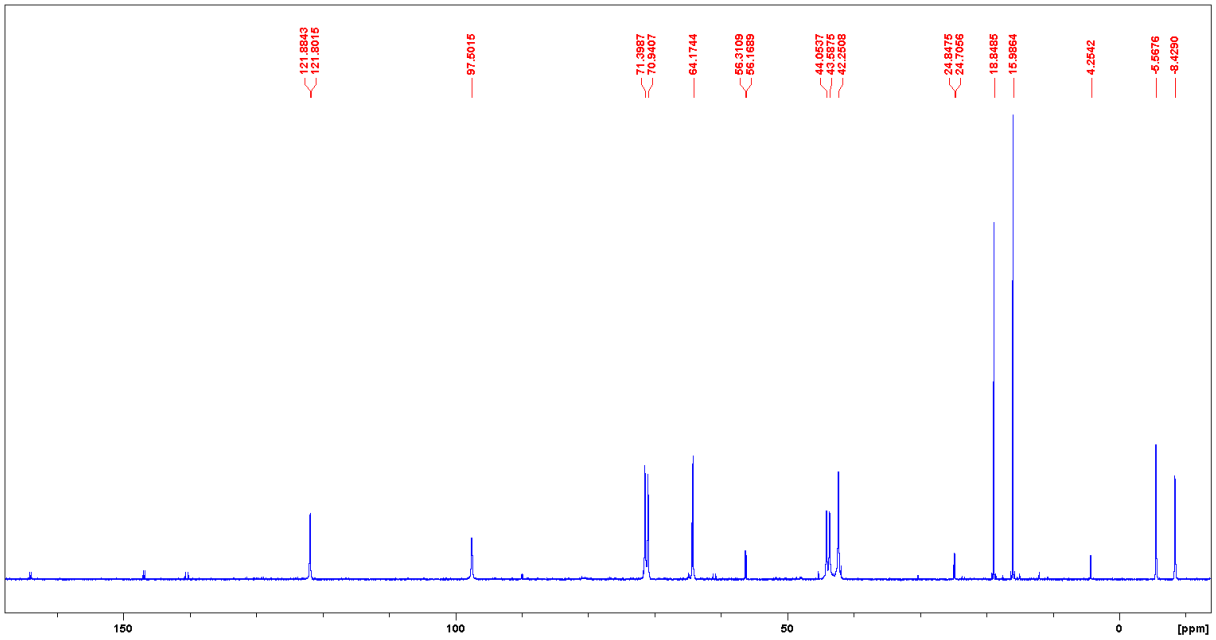

*Figure AI.68: $^{31}P\{^{1}H\}$ NMR spectrum of **1.1(Ph$_3$^{i}Pr$_2$)**OTf + 1 S in MeCN, RT, 4 d, then 50 °C, 2 h; Ph$_3$PS percipitated from the solution.*

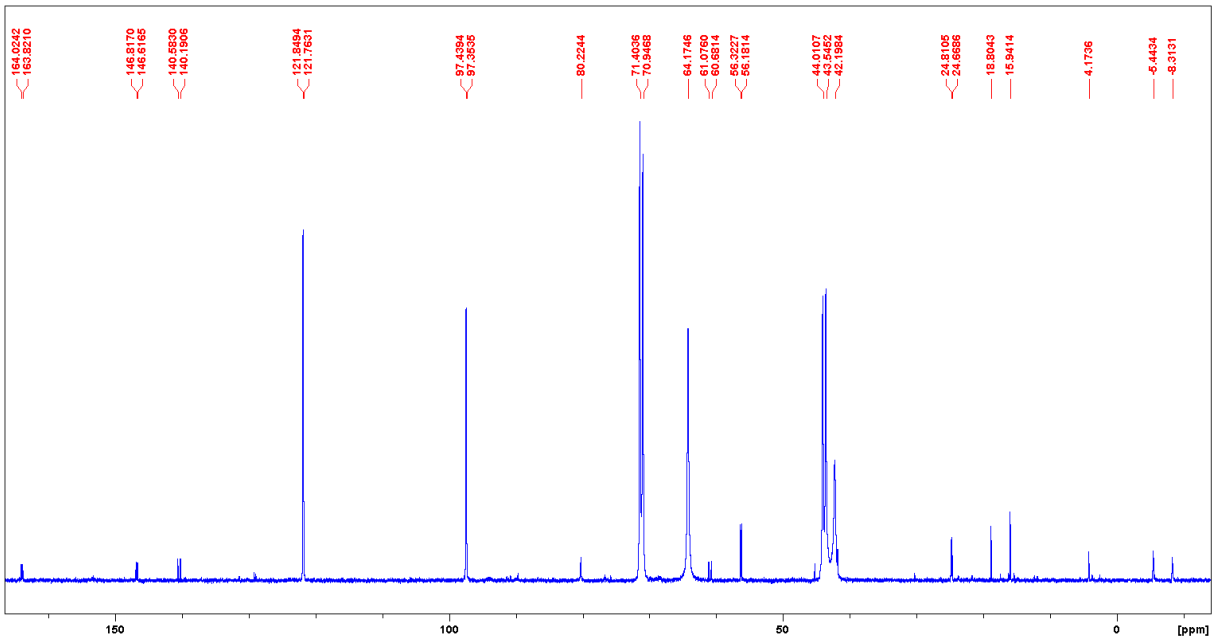

*Figure AI.69: $^{31}P\{^{1}H\}$ NMR spectrum of **1.1(Ph$_3$^{i}Pr$_2$)**OTf + 2 S in MeCN, RT, 3 d.*

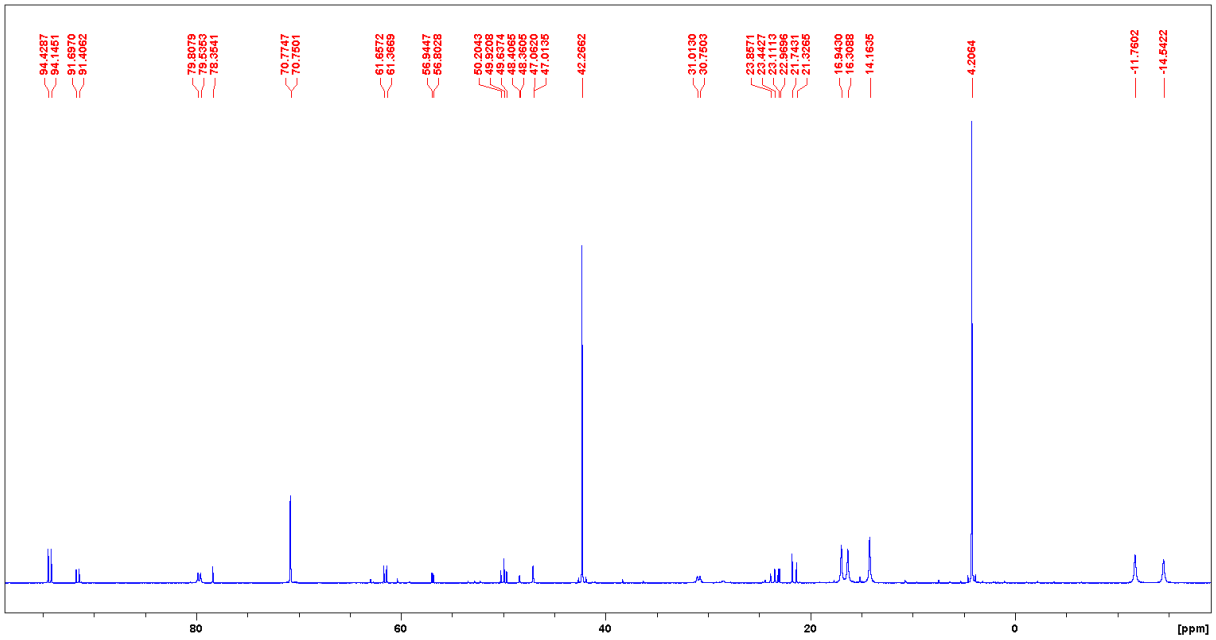

*Figure AI.70: $^{31}P\{^{1}H\}$ NMR spectrum of **1.1(Ph$_3$Ph$_2$)**OTf + 1 S in MeCN, RT, overnight.*

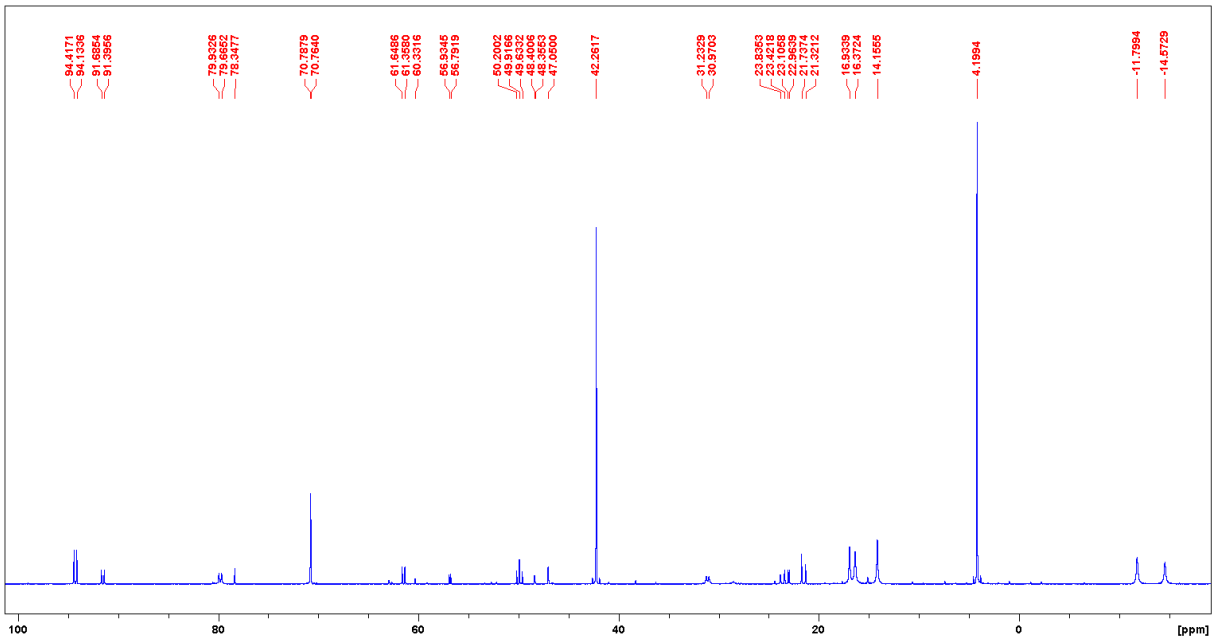

*Figure AI.71: $^{31}P\{^{1}H\}$ NMR spectrum of **1.1(Ph$_3$Ph$_2$)**OTf + 1 S in MeCN, RT, overnight.*

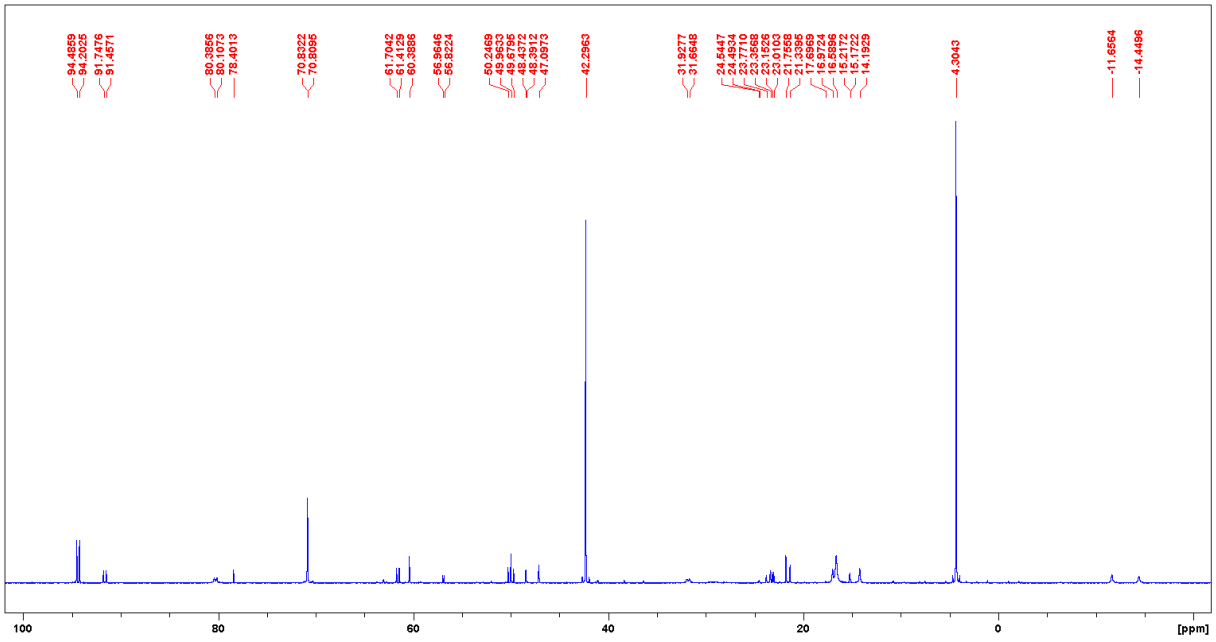

*Figure AI.72: $^{31}P\{^{1}H\}$ NMR spectrum of **1.1(Ph$_3$Ph$_2$)**OTf + 2 S in MeCN, RT, overnight.*

Structure Determination – X-Ray diffraction

Structure of trimethylphosphine selenide

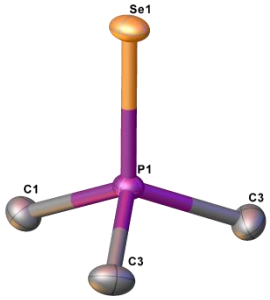

Figure AI.73: Solid state structure of Me_3PSe, hydrogen atoms are omitted for clarity, thermal ellipsoids are drawn at 50 % probability level.

The structure of Me_3PSe was obtained in an attempt to crystallise **2(Me_3Me_2)** from an acetonitrile solution by layering it with diethyl ether. A structure of Me_3PSe was previously reported by J. B. Robert *et al.* in 1980.[6] However, since the .cif file, which J. B. Robert *et al.* provided to the CCDC, did not contain a list of bonds with estimated standard deviations, we decided to provide our own structural data as reference. The structures do not differ much, both crystallised in the $P2_1/m$ space group, in which two of the carbon atoms are symmetrically equivalent. Table AI.1 provides an overview of the structural details.

Table AI.1: Bond distances and Angles in Me_3PSe reported by J. B. Robert et al. and observed by us.

	J. B. Robert *et al.* [6]	Our structure
Bonds		
P-Se	2.111(3) Å	2.1130(11) Å
P-C1	1.787(13) Å	1.796(4) Å
P-C3	1.784(16) Å	1.800(4) Å
Angles		
Se-P-C3	112.86(4)°	112.63(12)°
Se-P-C1	113.28(5)°	113.15(16)°
C3-P-C3	107.44(6)°	106.8(3)°
C1-P-C3	104.86(5)°	105.52(14)°

Crystallographic Data – Tables

Table AI.2: Crystallographic Data for compounds of Chapter 1.

	Me_3PSe	**1.2(Me_3Me_2)OTf**
CCDC Number	1813378	1813379
Empirical formula	C_3H_9PSe	$C_6H_{15}F_3O_3P_2SSe$
Formula weight	155.03	365.14
Temperature/K	173	173
Crystal system	monoclinic	orthorhombic
Space group	$P2_1/m$	Pnma
a/Å	6.4103(6)	12.5509(4)
b/Å	7.7660(8)	9.2217(3)
c/Å	6.5044(7)	11.6991(4)
α/°	90	90
β/°	91.026(9)	90
γ/°	90	90
Volume/$Å^3$	323.75(6)	1354.06(7)
Z	2	4
$\rho_{calc}g/cm^3$	1.590	1.791
μ/mm^{-1}	5.906	3.188
F(000)	152.0	728.0
Crystal size/mm^3	0.289 × 0.177 × 0.12	0.4 × 0.4 × 0.35
Radiation	MoKα (λ = 0.71073)	MoKα (λ = 0.71073)
2Θ range for data collection/°	8.85 to 64.69	8.594 to 64.704
Index ranges	-5 ≤ h ≤ 9, -7 ≤ k ≤ 11, -9 ≤ l ≤ 8	-18 ≤ h ≤ 18, -13 ≤ k ≤ 13, -17 ≤ l ≤ 17
Reflections collected	1816	27000
Independent reflections	1111 [R_{int} = 0.0267, R_{sigma} = 0.0544]	2458 [R_{int} = 0.0485, R_{sigma} = 0.0243]
Data/restraints/parameters	1111/0/30	2458/0/111
Goodness-of-fit on F^2	1.032	1.045
Final R indexes [I>=2σ (I)]	R_1 = 0.0400, wR_2 = 0.0793	R_1 = 0.0287, wR_2 = 0.0654
Final R indexes [all data]	R_1 = 0.0574, wR_2 = 0.0866	R_1 = 0.0406, wR_2 = 0.0706
Largest diff. peak/hole / e $Å^{-3}$	0.54/-0.60	0.47/-0.48

	1.5(^{i}Pr$_3$^{i}Pr$_2$)OTf	**1.5(^{i}Pr$_3$Ph$_2$)OTf**
CCDC Number	1813380	1813381
Empirical formula	$C_{16}H_{35}F_3O_3P_2S_2$	$C_{22}H_{31}F_3O_3P_2S_2$
Formula weight	458.50	526.53
Temperature/K	173	123
Crystal system	orthorhombic	monoclinic
Space group	$P2_12_12_1$	$P2_1/c$
a/Å	12.6606(4)	14.8752(5)
b/Å	13.1243(5)	9.4386(3)
c/Å	13.7917(7)	17.8969(5)
α/°	90	90
β/°	90	96.160(3)
γ/°	90	90
Volume/Å^3	2291.65(16)	2498.24(14)
Z	4	4
ρ_{calc}g/cm^3	1.329	1.400
μ/mm^{-1}	0.409	0.386
F(000)	976.0	1104.0
Crystal size/mm^3	0.3 × 0.15 × 0.03	0.459 × 0.38 × 0.292
Radiation	MoKα (λ = 0.71073)	MoKα (λ = 0.71073)
2Θ range for data collection/°	8.574 to 61.078	8.636 to 61.148
Index ranges	-17 ≤ h ≤ 17, -18 ≤ k ≤ 16, -18 ≤ l ≤ 18	-19 ≤ h ≤ 20, -12 ≤ k ≤ 12, -24 ≤ l ≤ 23
Reflections collected	20920	21408
Independent reflections	6395 [R_{int} = 0.0631, R_{sigma} = 0.0773]	6881 [R_{int} = 0.0398, R_{sigma} = 0.0461]
Data/restraints/parameters	6395/0/245	6881/0/295
Goodness-of-fit on F^2	1.028	1.023
Final R indexes [I>=2σ (I)]	R_1 = 0.0539, wR_2 = 0.1118	R_1 = 0.0401, wR_2 = 0.0875
Final R indexes [all data]	R_1 = 0.0951, wR_2 = 0.1313	R_1 = 0.0612, wR_2 = 0.1002
Largest diff. peak/hole / e Å^{-3}	0.51/-0.28	0.41/-0.36

	1.5($Cy_3{}^iPr_2$)OTf	**1.7($Me_3{}^iPr_2$)OTf**
CCDC Number	n.a.	1813382
Empirical formula	$C_{25}H_{47}F_3O_3P_2S_2$	$C_{10}H_{23}F_3O_3P_2S_3$
Formula weight	578.68	406.40
Temperature/K	143	173
Crystal system	monoclinic	monoclinic
Space group	$P2_1/c$	I2/a
a/Å	10.4379(4)	18.5955(10)
b/Å	10.2481(4)	8.4399(4)
c/Å	27.6352(11)	24.4141(12)
α/°	90	90
β/°	94.735(4)	102.423(5)
γ/°	90	90
Volume/Å^3	2946.0(2)	3741.9(3)
Z	4	8
ρ_{calc}g/cm^3	1.305	1.443
μ/mm^{-1}	0.333	0.598
F(000)	1240.0	1696.0
Crystal size/mm^3	0.35 × 0.25 × 0.1	0.4 × 0.15 × 0.02
Radiation	MoKα (λ = 0.71073)	MoKα (λ = 0.71073)
2Θ range for data collection/°	8.37 to 61.012	8.392 to 64.398
Index ranges	-14 ≤ h ≤ 13, -14 ≤ k ≤ 13, -38 ≤ l ≤ 38	-22 ≤ h ≤ 27, -12 ≤ k ≤ 12, -36 ≤ l ≤ 35
Reflections collected	28290	19841
Independent reflections	8092 [R_{int} = 0.0574, R_{sigma} = 0.0579]	6204 [R_{int} = 0.0680, R_{sigma} = 0.0870]
Data/restraints/parameters	8092/0/393	6204/0/197
Goodness-of-fit on F^2	1.044	1.011
Final R indexes [I>=2σ (I)]	R_1 = 0.0578, wR_2 = 0.1403	R_1 = 0.0628, wR_2 = 0.1335
Final R indexes [all data]	R_1 = 0.0827, wR_2 = 0.1597	R_1 = 0.1295, wR_2 = 0.1643
Largest diff. peak/hole / e Å^{-3}	0.99/-0.39	1.13/-0.65

References

[1] G. M. Sheldrick, *Acta Crystallogr. Sect. A Found. Crystallogr.* **2008**, *64*, 112–122.

[2] O. V. Dolomanov, L. J. Bourhis, R. J. Gildea, J. A. K. Howard, H. Puschmann, *J. Appl. Crystallogr.* **2009**, *42*, 339–341.

[3] S. S. Chitnis, E. MacDonald, N. Burford, U. Werner-Zwanziger, R. McDonald, *Chem. Commun.* **2012**, *48*, 7359.

[4] N. Burford, P. J. Ragogna, R. McDonald, M. J. Ferguson, *J. Am. Chem. Soc.* **2003**, *125*, 14404–14410.

[5] J. J. Weigand, N. Burford, D. Mahnke, A. Decken, *Inorg. Chem.* **2007**, *46*, 7689–7691.

[6] A. Cogne, A. Grand, J. Laugier, J. B. Robert, L. Wiesenfeld, *J. Am. Chem. Soc.* **1980**, *102*, 2238–2242.

Appendix II: Supporting Information for Chapter 2

This Appendix shows the supporting information for Chapter 2 as it was published, excluding synthetic details, which are instead presented in Chapter 5.

NMR Spectroscopy

NMR spectra were measured on Bruker Avance 300 MHz (^{1}H, ^{31}P, ^{13}C, ^{19}F) or a Bruker Avance 360 MHz (^{31}P, ^{77}Se, all low temperature experiments) instrument. All spectra were recorded at a temperature of 298 K unless stated otherwise.

NMR solvents were dried over molecular sieves (3 Å for acetonitrile, 4 Å for dichloromethane) for at least one day before use.

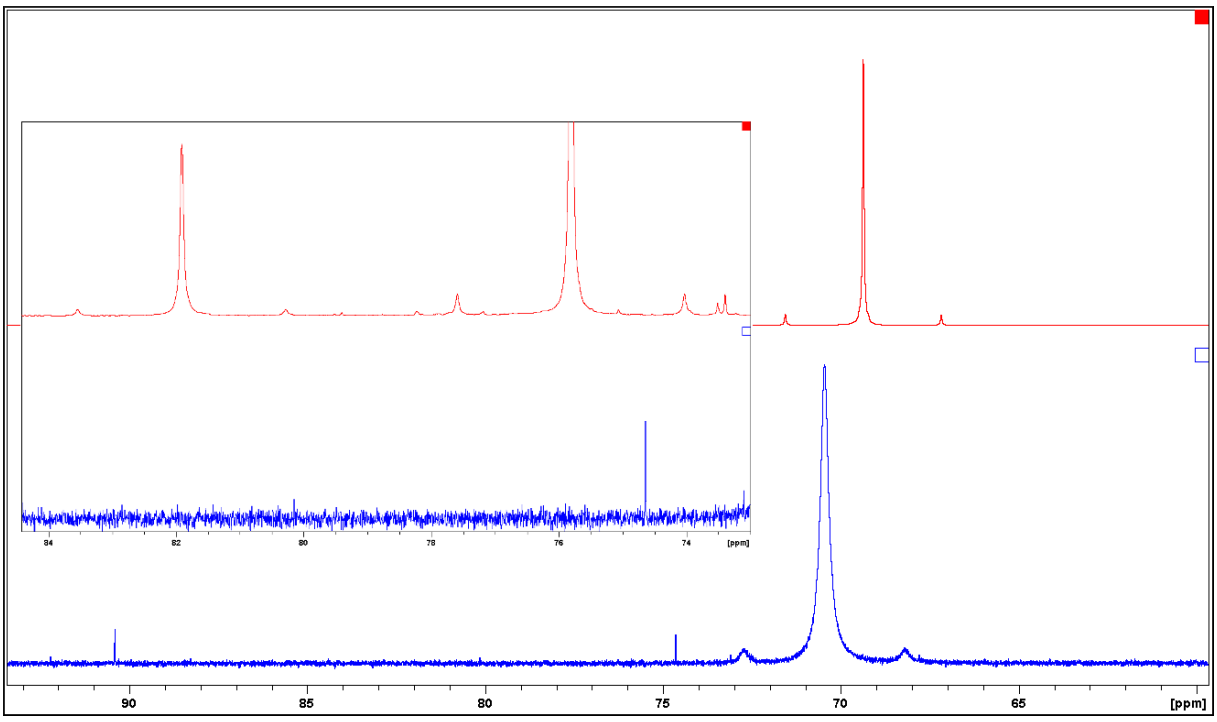

Figure AII.1: $^{31}P\{^{1}H\}$ NMR of 2 $^{i}Pr_3PSe$ + Ph_3SbOTf_2 at 298 K (bottom) and at 187 K (top) with enlargement of the area between 73 ppm and 84 ppm.

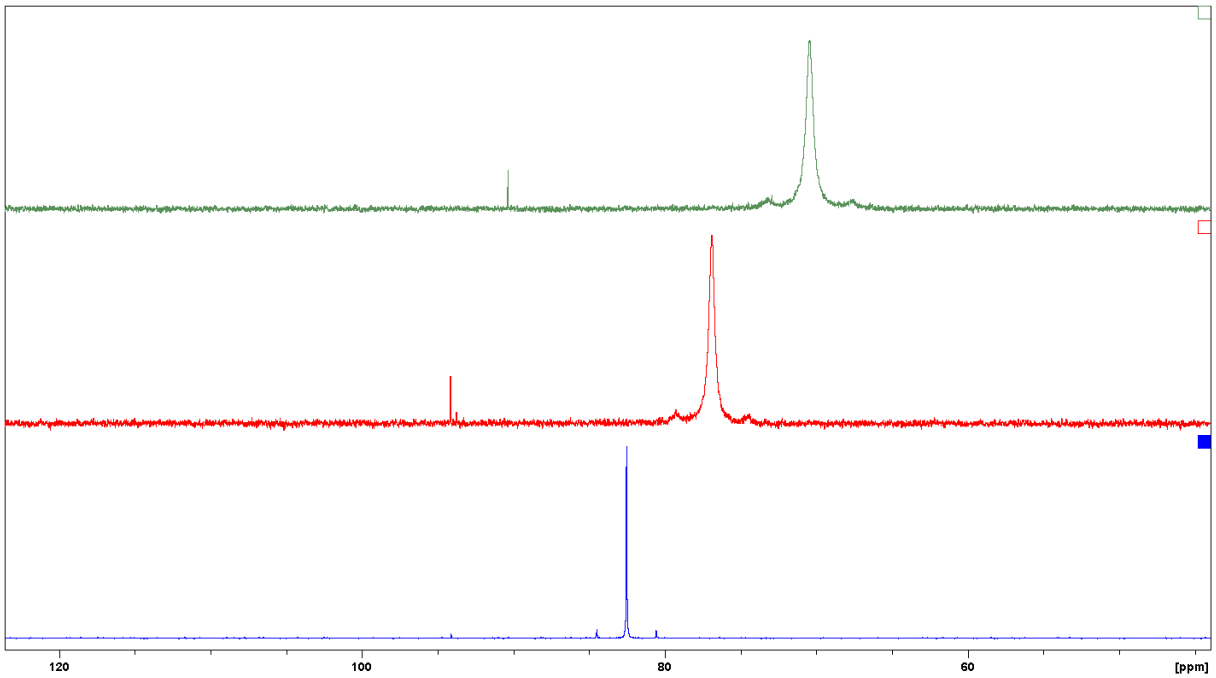

*Figure AII.2: NMR of compound **2.2(^{i}Pr)** (bottom) and **2.2(^{i}Pr)** + Ph_3Sb (middle) in MeCN-d3 and **2.2(^{i}Pr)** + Ph_3Sb in DCM-d2 (top).*

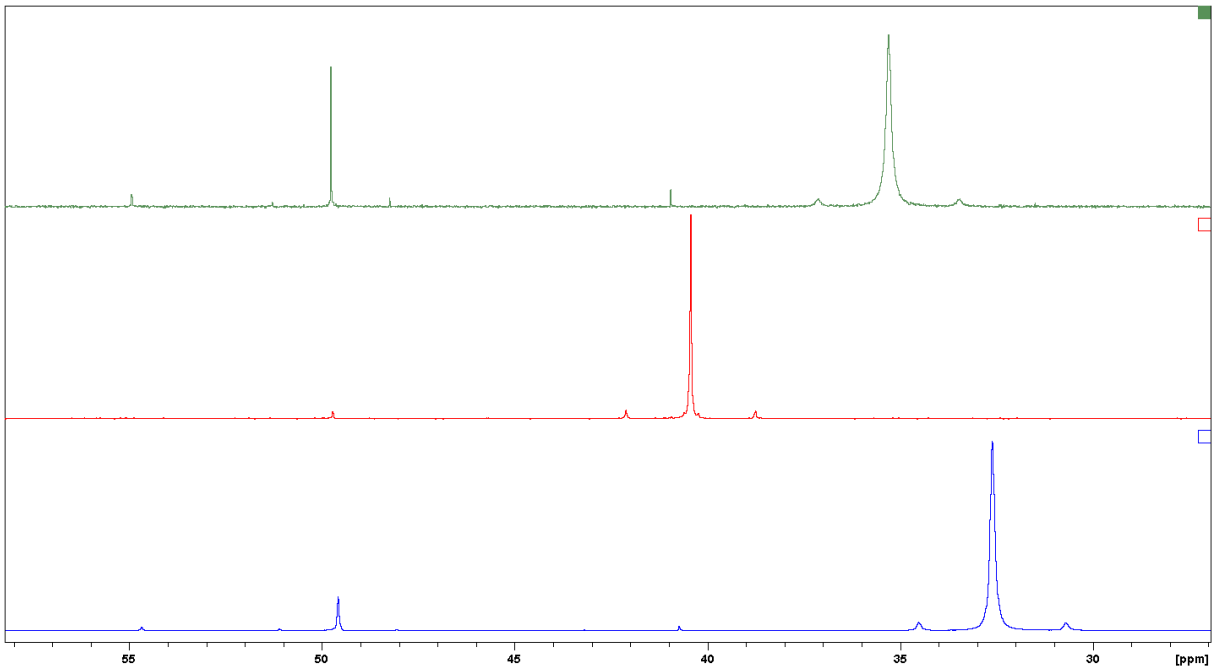

*Figure AII.3: NMR of compound **2.1(Me_3PSe)** (bottom) formed during the synthesis of **2.2(Me)** (middle) and **2.2(Me)** + Ph3Sb (top) in MeCN-d3, the peak at 50 ppm is presumably $Me_3PSePMe_3^{2+}$ (based on ^{31}P and ^{77}Se NMR) which is encountered in most samples of **2.2(Me)** but could not be isolated.*

Crystallographic Information

XRD data collection for **2.2(Me)** was performed by Dr. Brian Patrick at the University of British Columbia (Vancouver) using a Bruker APEX-II CCD. The data for **2.2(^{i}Pr)** was collected by Prof. Dr. Konstantin Karaghiosoff at the Ludwig-Maximilians-University Munich using an Oxford Xcalibur 3 diffractometer. The structures were solved and refined using the ShelX programs[1] in the Olex2[2] interface.

*Table AII.1: Crystallographic data for compounds **2.2(Me)**OTf_2 and **2.2(^{i}Pr)**OTf_2.*

	2.2(Me)OTf_2	**2.2(^{i}Pr)**OTf_2
CCDC Number	1555001	1555002
Empirical formula	$C_8H_{18}F_6O_6P_2S_2Se_2$	$C_{20}H_{42}F_6O_6P_2S_2Se_2$
Formula weight	608.20	776.51
Temperature/K	296.15	123
Crystal system	monoclinic	monoclinic
Space group	C2/c	$P2_1/c$
a/Å	16.0321(12)	8.7470(3)
b/Å	13.1043(10)	8.9002(3)
c/Å	12.0448(9)	20.6210(6)
α/°	90	90
β/°	127.1600(10)	99.683(3)
γ/°	90	90
Volume/Å^3	2016.7(3)	1582.48(9)
Z	4	2
ρ_{calc}g/cm^3	2.003	1.630
μ/mm^{-1}	4.108	2.637
F(000)	1192.0	788.0
Crystal size/mm^3	0.2 × 0.19 × 0.17	0.3 × 0.2 × 0.06
Radiation	MoKα (λ = 0.71073)	MoKα (λ = 0.71073)
2Θ range for data collection/°	4.452 to 60.066	8.362 to 64.844
Index ranges	-22 ≤ h ≤ 22, -18 ≤ k ≤ 18, -16 ≤ l ≤ 16	-12 ≤ h ≤ 12, -13 ≤ k ≤ 13, -24 ≤ l ≤ 30
Reflections collected	12944	18073
Independent reflections	2953 [R_{int} = 0.0272, R_{sigma} = 0.0219]	5291 [R_{int} = 0.0368, R_{sigma} = 0.0387]
Data/restraints/parameters	2953/0/121	5291/0/178
Goodness-of-fit on F^2	1.035	1.011
Final R indexes [I>=2σ (I)]	R_1 = 0.0173, wR_2 = 0.0411	R_1 = 0.0323, wR_2 = 0.0671
Final R indexes [all data]	R_1 = 0.0205, wR_2 = 0.0421	R_1 = 0.0453, wR_2 = 0.0726
Largest diff. peak/hole / e Å^{-3}	0.47/-0.31	0.45/-0.47

References

[1] G. M. Sheldrick, *Acta Crystallogr. Sect. A Found. Crystallogr.* **2008**, *64*, 112–122.

[2] O. V. Dolomanov, L. J. Bourhis, R. J. Gildea, J. A. K. Howard, H. Puschmann, *J. Appl. Crystallogr.* **2009**, *42*, 339–341.

Appendix III: Supporting Information for Chapter 3

Crystallographic Information

Data collection was performed by Prof. Dr. Konstantin Karaghiosoff at the Ludwig-Maximilians-University Munich using an Oxford Xcalibur 3 diffractometer with a Spellman generator (50 kV, 40 mA) and Kappa CCD detector operating with Mo-Kα radiation (λ = 0.71073 Å)

The structures were solved and refined using the ShelX programs[23] in the Olex2[24] interface.

Table AIII.1: Crystallographic information for compounds of Chapter 3.

	3.1a(Al_2Cl_7)$_2$	**3.1b(Al_2Cl_7)$_2$**
CCDC Number	n.a.	n.a.
Empirical formula	$C_{24}H_{20}Al_4Cl_{14}P_2Se_2$	$C_{12}H_{28}Al_4Cl_{14}P_2Se_2$
Formula weight	1132.48	996.42
Temperature/K	133	143
Crystal system	monoclinic	orthorhombic
Space group	$P2_1/n$	$P2_12_12_1$
a/Å	11.9961(2)	10.2846(3)
b/Å	20.4284(3)	18.8915(5)
c/Å	17.7409(3)	38.8332(14)
α/°	90	90
β/°	91.3920(10)	90
γ/°	90	90
Volume/Å^3	4346.32(12)	7545.0(4)
Z	4	8
ρ_{calc}g/cm^3	1.731	1.754
μ/mm^{-1}	2.737	3.139
F(000)	2208.0	3904.0
Crystal size/mm^3	0.384 × 0.255 × 0.069	0.15 × 0.1 × 0.03
Radiation	MoKα (λ = 0.71073)	MoKα (λ = 0.71073)
2Θ range for data collection/°	8.298 to 64.852	8.332 to 54.2
Index ranges	-18 ≤ h ≤ 18, -30 ≤ k ≤ 30, -26 ≤ l ≤ 26	-13 ≤ h ≤ 11, -24 ≤ k ≤ 20, -45 ≤ l ≤ 49
Reflections collected	92075	66604
Independent reflections	14836 [R_{int} = 0.0481, R_{sigma} = 0.0354]	16548 [R_{int} = 0.0871, R_{sigma} = 0.0896]
Data/restraints/parameters	14836/0/415	16548/0/629
Goodness-of-fit on F^2	1.027	1.134
Final R indexes [I>=2σ (I)]	R_1 = 0.0370, wR_2 = 0.0754	R_1 = 0.0707, wR_2 = 0.1419
Final R indexes [all data]	R_1 = 0.0649, wR_2 = 0.0876	R_1 = 0.1056, wR_2 = 0.1540
Largest diff. peak/hole / e Å^{-3}	0.90/-0.63	1.24/-0.93

Flack parameter	0.003(5)

Compound	**3.2(AlCl$_4$)$_2$**
CCDC Number	n.a.
Empirical formula	$C_{25}H_{22}Al_2Cl_8P_2Se_2$
Formula weight	879.84
Temperature/K	143
Crystal system	triclinic
Space group	P-1
a/Å	9.2754(7)
b/Å	13.7880(12)
c/Å	15.4334(12)
α/°	67.595(8)
β/°	76.432(6)
γ/°	80.475(7)
Volume/Å^3	1767.5(3)
Z	2
ρ_{calc}g/cm^3	1.653
μ/mm^{-1}	2.854
F(000)	864.0
Crystal size/mm^3	0.3 × 0.04 × 0.03
Radiation	MoKα (λ = 0.71073)
2Θ range for data collection/°	8.346 to 57.608
Index ranges	-11 ≤ h ≤ 11, -18 ≤ k ≤ 17, -20 ≤ l ≤ 20
Reflections collected	14241
Independent reflections	7963 [R_{int} = 0.0534, R_{sigma} = 0.1143]
Data/restraints/parameters	7963/0/352
Goodness-of-fit on F^2	1.018
Final R indexes [I>=2σ (I)]	R_1 = 0.0668, wR_2 = 0.1345
Final R indexes [all data]	R_1 = 0.1282, wR_2 = 0.1665
Largest diff. peak/hole / e Å^{-3}	1.41/-0.64

NMR Spectra

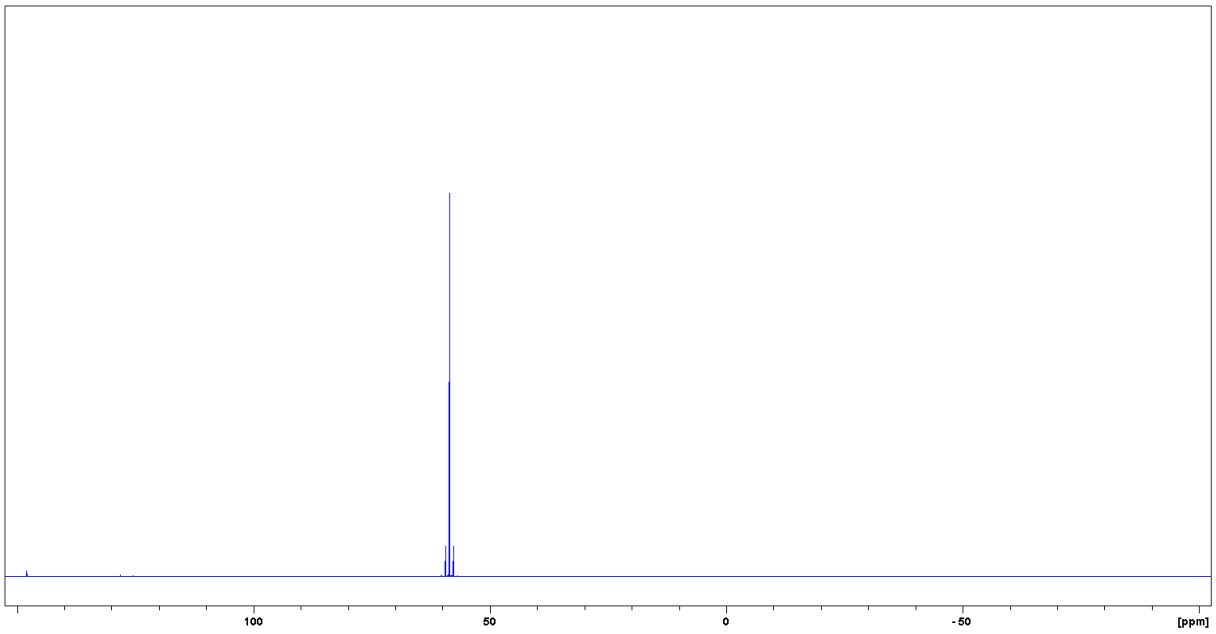

*Figure AIII.1: $^{31}P\{^{1}H\}$ NMR spectrum of **3.1b**.*

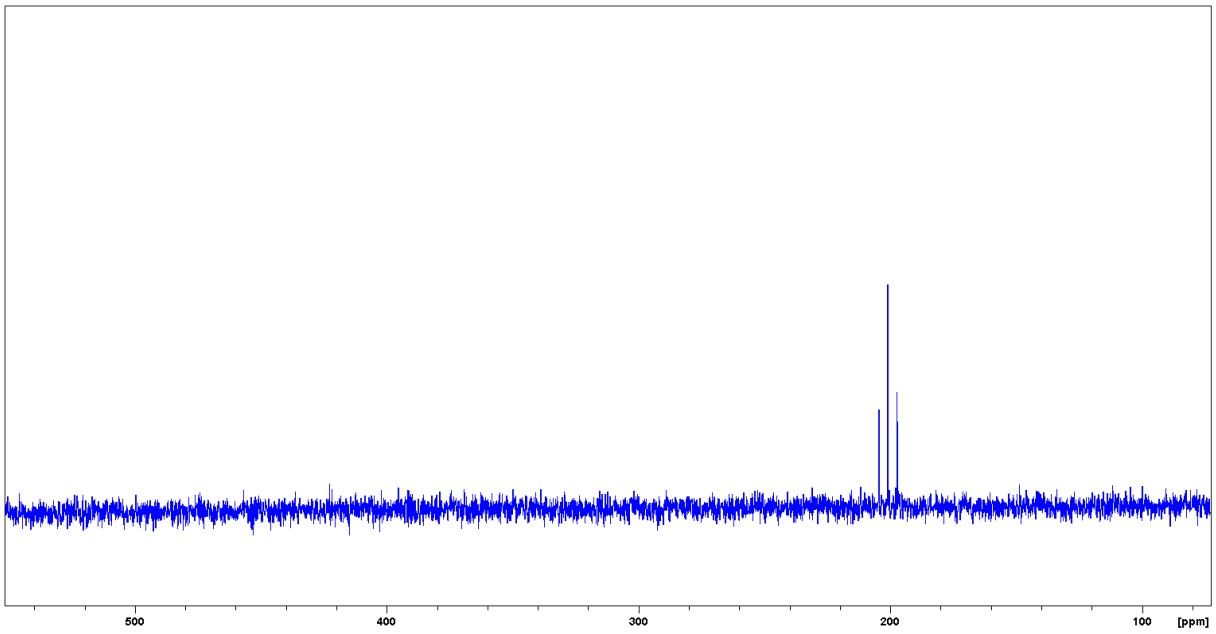

*Figure AIII.2: $^{77}Se\{^{1}H\}$ NMR spectrum of **3.1b**.*

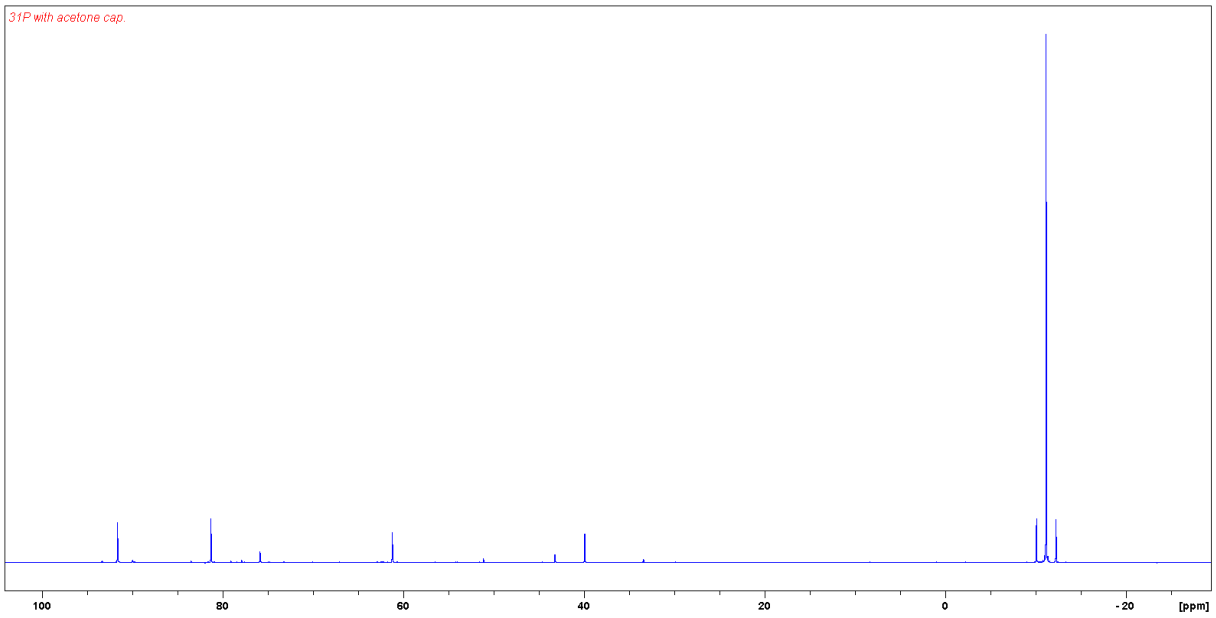

*Figure AIII.3: $^{31}P\{^{1}H\}$ NMR spectrum of the reaction mixture for the synthesis of **3.1a**, showing mainly **3.1a** at -11 ppm, the starting material which has a chemical shift of 72 ppm is not present anymore.*

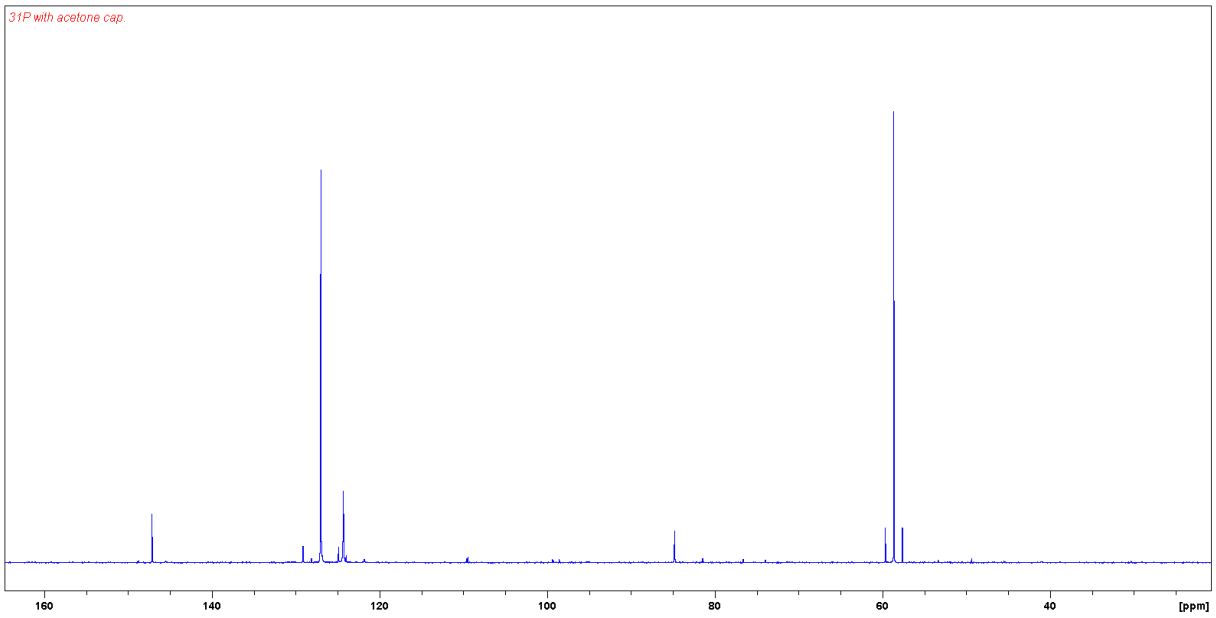

*Figure AIII.4: $^{31}P\{^{1}H\}$ NMR spectrum of the reaction mixture for the synthesis of **3.1b**, showing the presumed $^{i}Pr_2P(Se)Cl – AlCl_3$ adduct at 127 ppm and **3.1b** at 59 ppm.*

Appendix IV: Supporting Information for Chapter 4

Crystallographic Information for Compounds of Chapter 4

	4.1	**4.2**
CCDC Number	n.a.	n.a.
Empirical formula	$C_4H_{12}P_2Se_4$	$C_{12}H_{28}OP_2Se_2$
Formula weight	437.92	408.20
Temperature/K	173	100.0
Crystal system	monoclinic	monoclinic
Space group	I2/a	$P2_1/a$
a/Å	11.5758(10)	13.2791(7)
b/Å	6.4718(6)	9.7922(5)
c/Å	17.2223(13)	14.2691(7)
α/°	90	90
β/°	107.006(8)	108.9126(15)
γ/°	90	90
Volume/Å^3	1233.82(19)	1755.27(16)
Z	4	4
ρ_{calc}g/cm^3	2.357	1.545
μ/mm^{-1}	12.097	4.382
F(000)	808.0	824.0
Crystal size/mm^3	0.383 × 0.267 × 0.046	0.1 × 0.09 × 0.06
Radiation	MoKα (λ = 0.71073)	MoKα (λ = 0.71073)
2Θ range for data collection/°	9.404 to 64.31	3.018 to 54.988
Index ranges	-16 ≤ h ≤ 16, -9 ≤ k ≤ 7, -25 ≤ l ≤ 25	-17 ≤ h ≤ 17, -12 ≤ k ≤ 12, -18 ≤ l ≤ 17
Reflections collected	6296	33750
Independent reflections	2039 [R_{int} = 0.0813, R_{sigma} = 0.0876]	4039 [R_{int} = 0.0443, R_{sigma} = 0.0238]
Data/restraints/parameters	2039/0/48	4039/0/162
Goodness-of-fit on F^2	1.140	1.235
Final R indexes [I>=2σ (I)]	R_1 = 0.0758, wR_2 = 0.2256	R_1 = 0.0225, wR_2 = 0.0703
Final R indexes [all data]	R_1 = 0.1007, wR_2 = 0.2476	R_1 = 0.0292, wR_2 = 0.0936
Largest diff. peak/hole / e Å^{-3}	2.31/-1.76	0.44/-0.75

	4.3OTf	**4.4**OTf
CCDC Number	n.a.	n.a.
Empirical formula	$C_{11}H_{20}F_3N_2O_3PSSe$	$C_{19}H_{84}F_3SO_3P_6Se_{12}Ag_8Cl$
Formula weight	427.28	117.87
Temperature/K	173	293(2)
Crystal system	monoclinic	trigonal
Space group	P2/n	R-3
a/Å	10.3699(3)	17.2699(15)
b/Å	7.8217(3)	17.2699(15)
c/Å	22.2846(9)	22.3357(18)
α/°	90	90
β/°	93.849(3)	90
γ/°	90	120
Volume/Å^3	1803.43(11)	5769.1(11)
Z	4	72
ρ_{calc}g/cm^3	1.574	2.443
μ/mm^{-1}	2.325	7.915
F(000)	864.0	3989.0
Crystal size/mm^3	0.25 × 0.15 × 0.05	
Radiation	MoKα (λ = 0.71073)	MoKα (λ = 0.71073)
2Θ range for data collection/°	8.366 to 64.714	9.112 to 64.824
Index ranges	-15 ≤ h ≤ 14, -11 ≤ k ≤ 11, -33 ≤ l ≤ 31	-24 ≤ h ≤ 24, -25 ≤ k ≤ 25, -33 ≤ l ≤ 33
Reflections collected	36978	40731
Independent reflections	6147 [R_{int} = 0.0653, R_{sigma} = 0.0503]	4373 [R_{int} = 0.0983, R_{sigma} = 0.0549]
Data/restraints/parameters	6147/0/212	4373/0/160
Goodness-of-fit on F^2	1.021	0.931
Final R indexes [I>=2σ (I)]	R_1 = 0.0498, wR_2 = 0.1112	R_1 = 0.0576, wR_2 = 0.1553
Final R indexes [all data]	R_1 = 0.0981, wR_2 = 0.1340	R_1 = 0.0960, wR_2 = 0.1872
Largest diff. peak/hole / e Å^{-3}	0.65/-0.70	2.58/-1.78

	4.5OTf
CCDC Number	n.a.
Empirical formula	$C_{15}H_{20}F_3N_4O_4PS_2$
Formula weight	472.44
Temperature/K	173
Crystal system	triclinic
Space group	P-1
a/Å	8.1647(4)
b/Å	9.8399(6)
c/Å	13.6169(7)
α/°	70.067(5)
β/°	80.091(4)
γ/°	85.474(4)
Volume/Å^3	1012.86(10)
Z	2
ρ_{calc}g/cm^3	1.549
μ/mm^{-1}	0.399
F(000)	488.0
Crystal size/mm^3	0.25 x 0.10 x 0.04
Radiation	MoKα (λ = 0.71073)
2Θ range for data collection/°	8.796 to 64.796
Index ranges	-11 ≤ h ≤ 11, -14 ≤ k ≤ 14, -19 ≤ l ≤ 20
Reflections collected	21395
Independent reflections	6716 [R_{int} = 0.0652, R_{sigma} = 0.0870]
Data/restraints/parameters	6716/0/266
Goodness-of-fit on F^2	1.035
Final R indexes [I>=2σ (I)]	R_1 = 0.0738, wR_2 = 0.1678
Final R indexes [all data]	R_1 = 0.1439, wR_2 = 0.2117
Largest diff. peak/hole / e Å^{-3}	1.04/-0.49

NMR Spectra of Compound 4.4OTf

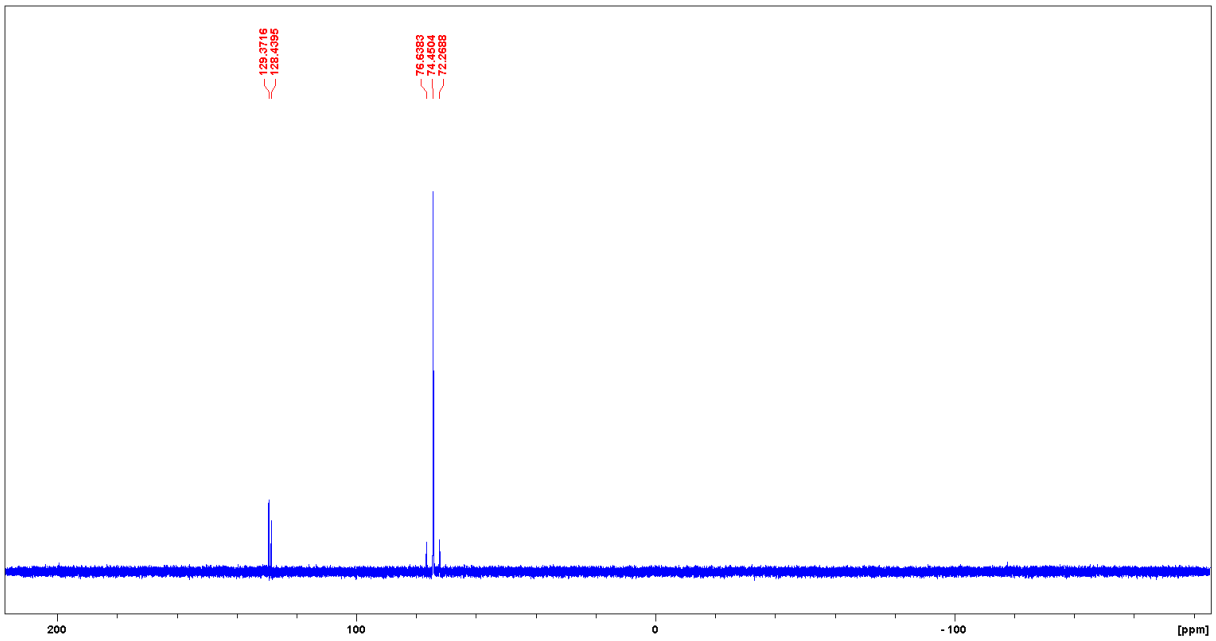

*Figure AIV.1: $^{31}P\{^{1}H\}$ NMR Spectrum of **4.4**OTf (74.5 ppm $^{1}J_{PSe}$ = 531 Hz), the signal at 128 and 129 ppm is unidentified.*

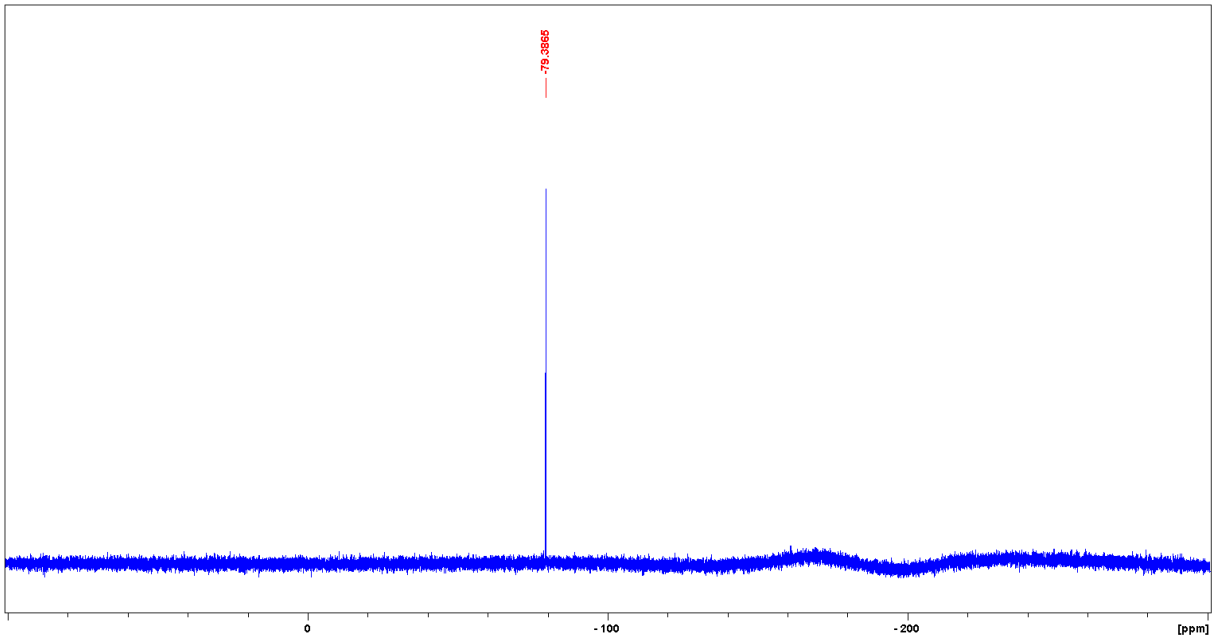

*Figure AIV.2: $^{19}F\{^{1}H\}$ NMR Spectrum of **4.4**OTf (-79.4 ppm).*